©[2014]

Cristina Ochoa Cardona

ALL RIGHTS RESERVED

HOMOLOGOUS RECOMBINATION SITES DURING *DROSOPHILA* FEMALE MEIOSIS AND THE ROLE OF THE *DROSOPHILA* INO80 COMPLEX IN MEIOTIC RECOMBINATION

By

CRISTINA OCHOA CARDONA

A Dissertation submitted to the

Graduate School-New Brunswick

And

The Graduate School of Biomedical Sciences

Rutgers, The State University of New Jersey

In partial fulfillment of the requirements

For the degree of

Doctor of Philosophy

Graduate Program in Cell and Developmental Biology

Written under the direction of

Thomas Kusch

And approved by

_____

_____

_____

_____

New Brunswick, New Jersey

October, 2014

ABSTRACT OF THE DISSERTATION

Homologous Recombination Sites During *Drosophila* Female Meiosis And The Role Of The *Drosophila* Ino80 Complex In Meiotic Recombination

By CRISTINA OCHOA CARDONA

Dissertation Director:

Thomas Kusch

DNA Double Strand breaks (DSBs) are one of the most lethal types of genomic damage. Irregularities in the repairs of DSBs can lead to chromosomal aberrations, such as deletions, translocations, and inversions that ultimately are responsible for cancer, infertility, and birth defects. Cells have several conserved and controlled DNA repair pathways, in which a plethora of factors must be activated and recruited to the break. Moreover, eukaryotes must also locally and transiently modify chromatin to allow access of repair factors. Very little is known about chromatin remodeling during DSB processing in higher eukaryotes, partially due to the lack of suitable study models.

Here I used *Drosophila* female meiosis as the model and show the development of a marker and fixation protocol that enables the labeling and following of DSB sites during recombinational repair. Moreover, I provide evidence that early and late repair sites correspond to non-crossovers (NCO) and crossovers (CO), respectively. In the next part of this study, I provide novel evidence that: 1) COs persist longer than NCOs and are mobilized to the nuclear periphery, 2) movement of COs to the periphery is

developmentally controlled, depends on ATR, and occurs during mid-pachytene when NCOs are repaired, 3) any persisting DSB can form MRN foci that are mobilized to the periphery from mid-pachytene on.

Furthermore, I focus on the role of dINO80, an ATP-dependent chromatin remodeler, during meiotic recombination. To date it has never been shown that INO80 has a role in meiosis or whether it functions in early recognition steps. Here I show that Ino80, the catalytic subunit of the INO80 complex, interacts in a damage dependent fashion with components of the MRN complex, and that Ino80 is required for the recognition of the majority of meiotic DSBs. Furthermore this study suggests that the ATP-dependent remodeling function of dIno80 is crucial for its role in recognition of meiotic DSBs. *Drosophila* female meiosis in conjunction with the developed techniques in this study provide a powerful system to study the dynamics of meiotic DSB sites and to spatially and temporally dissect the role of chromatin modifying complexes in DSB repair.

ACKNOWLEGMENT

This dissertation represents the effort of many years of work and would not have been possible without the support and cooperation of many people who deserve my acknowledgment.

I would like to gratefully and sincerely thank Dr. Thomas Kusch for all the time, advice and guidance -- for helping me to develop my background in cell and developmental biology and the honor to experience research and its practical applications beyond the textbooks. I am grateful for all his efforts and for the opportunity he gave me to work in this project.

I like to express my deepest gratitude to Dr. Richard Padgett, for the opportunity to complete my dissertation, and for his support, advice, and guidance. This dissertation and its defense could not have been possible without him.

I would also gratefully thank my committee members, Dr. Sunita Gupta Kramer, Dr. Nancy C. Walworth, Dr. Kim S. McKim, Dr. Marc Gartenberg, who gladly accepted to participate in my thesis defense committee. I am thankful for their constructive comments and advise.

I would like to thank former members of the Kusch lab (Kyoung-Han Choi**,** Grace Chen, Amanda Mei and Camtu Nguyen) for their help and support and Frank Macabenta for his comments on this Manuscript.

I would like to thank my family, especially my mother who raised me with consistent love and patience. They were always supporting me and encouraging me, and had faith in me during all this time. Thank you everyone, for always being there and for giving me your unconditional love and support.

To my son Michael -- God has blessed me with such a wonderful son. You are the reason I keep going strong; with your unconditional love, there is nothing in the world I cannot achieve.

Finally, I would like to thank my husband, Richard Cardona. I would like to express my profound gratitude from the bottom of my heart for his love and continuous support during all these years. Thank you for your dedication to help me achieve this milestone in my life.

Table of Contents

I. INTRODUCTION

1. DNA Double Strand Breaks.

DNA Double Strand Breaks (DSBs) are one of the most harmful; DNA lesions, where the phosphoribosyl backbones of both DNA strands are broken simultaneously. DSBs occur as a consequence of exposure to exogenous and endogenous agents, or as byproducts of genomic rearrangements within the cell. DSBs can also be generated during replication, when DNA lesions are encountered by the replication machinery (Arnaudeau, Lundin et al. 2001). Exogenous agents that cause DSBs include: ionizing radiation, chemicals like methyl methanesulfonate and temozolomide that attach alkyl groups to DNA bases (Ciccia and Elledge 2010), or topoisomerase inhibitors that can introduce DSBs by preventing the resealing process during DNA unwinding (Froelich-Ammon and Osheroff 1995). Endogenously-generated DSBs are the result of metabolic byproducts, such as free oxygen radicals or nitrogen species (Ciccia and Elledge 2010). In addition, endogenous DSBs can also be the byproduct of physical stress generated by collapsed replication forks and when dicentric or catenated chromosomes are pulled to opposite poles during mitosis (Acilan, Potter et al. 2007; Sinha and Peterson 2009). DSBs are also made on purpose by the cell during genomic rearrangement processes, such as yeast mating type switch, variable (diversity) join V[D]J recombination, class-switching recombination, and meiotic recombination (Sinha and Peterson 2009).

Non-repair or misrepair of DSBs can result in a large number of defects. Firstly, failures in the repair process can result in the loss of genetic information, generating chromosomal fragments or chromosomal translocations that are ultimately responsible for miscarriages, infertility, birth defects, and cancer (Richardson and Jasin 2000; Khanna and Jackson 2001). Secondly, misrepair of DSBs can cause defects in the development of the immune system, due to the fact that V(D)J recombination is required for the generation of a wide number of unique antibodies (Hiom 2010). Thirdly, malfunction in the repair pathway can result in neurological disorders. Neurons need high levels of oxygen, which are obtained via mitochondrial respiration; as a result, they are exposed to high levels of oxidative stress and need to efficiently repair damage caused by these free oxygen radicals (Jackson and Bartek 2009; Ciccia and Elledge 2010). Neuronal tissues also have low regeneration capacities and thus need to quickly overcome DNA damage (Jackson and Bartek 2009; Ciccia and Elledge 2010). Due to the high importance of prompt DSB repair, eukaryotes from yeast to humans have evolved two main conserved pathways for repair of DSBs: Non Homologous End Joining (NHEJ), and Homologous Recombination (HR).

1.1. Non-Homologous End Joining

Non Homologous End Joining (NHEJ) is the predominant form of DNA repair in G1 phase of the cell cycle. This process can be error-prone, due to the fact that the

break is just fixed by re-joining the two ends without considering the sequence fidelity at the break (see figure1) (Hiom 2010; Mladenov and Iliakis 2011). In this pathway, there could also be loss of nucleotides or alteration of nucleotides around the break (Hiom 2010). The main sensor of the break is the heterodimeric Ku70/80 complex, which binds to the DNA, tethering the two broken ends and activating processing factors such as DNA-dependent protein kinase (DNA-PKcs) (Hefferin and Tomkinson 2005; Ciccia and Elledge 2010; Hiom 2010). Once DNA PKcs are bound to the DNA, they phosphorylate themselves and then allow the binding of ligases (lig4/liflin yeast, ligase IV/XRCC4 in mammals) that will rejoin the two broken ends (Hefferin and Tomkinson 2005; Ciccia and Elledge 2010; Hiom 2010). In some cases during NHEJ, endonucleases such as Artemis from mammals seem to function at the DNA ends already bound by DNA-PKcs. It is thought that their main function is in the processing of ends when needed. Pawelczak and Turchi showed that Artemis can trim overhangs and cleave hairpins at the transition between double and single-stranded DNA before religation (Pawelczak and Turchi 2010).

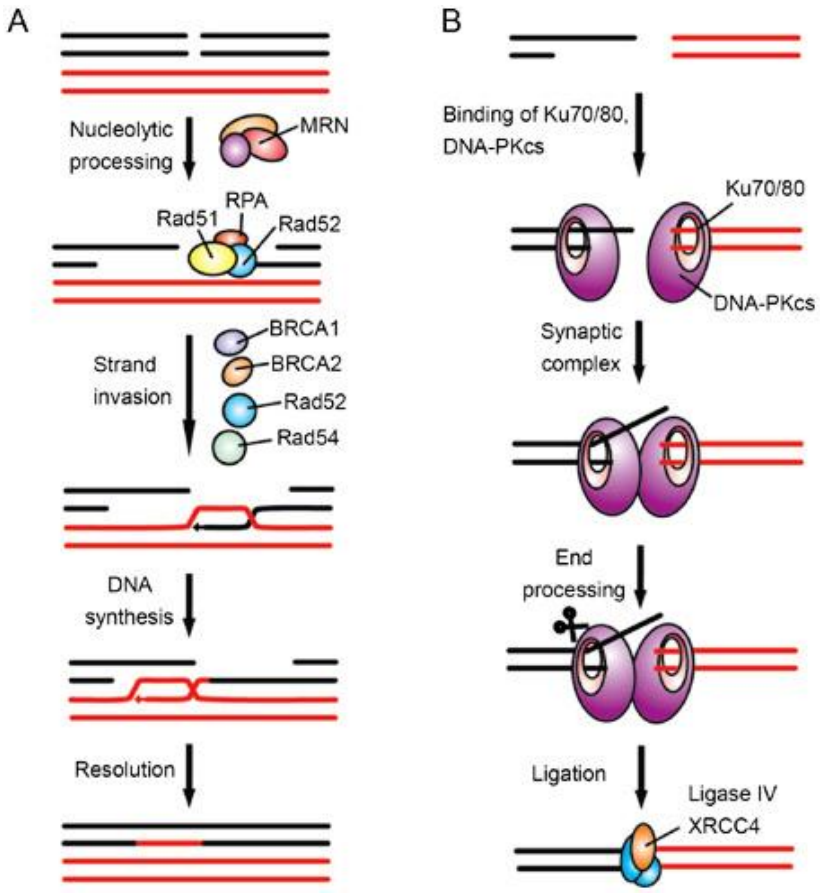

Figure 1: Overview of homologous recombination (HR) and non-homologous end joining (NHEJ). (A) shows the main events and factors during HR. The MRN complex recognizes the DSB, and then there is nucleolytic processing or end resection in order to create a 3' overhang that will invade the homolog. RPA binds to the overhangs followed by strand invasion by the recombinase Rad51 with the help of the mediators Rad52, Rad54, BRCA1, and BRCA2. The final steps in HR are the formation of intermediate structures and their resolution. (B) Shows NHEJ. KU70/Ku80 recognizes the break, and then DNA-PKcs are activated and bind to the DSB. If required, the ends are resected and finally ligated by Ligase4 (Weterings and Chen 2008).

1.2. Homologous Recombination

Homologous recombination (HR) is the most accurate form of DNA damage repair, due to the fact that it uses a homologous sequence elsewhere in the genome as a template to copy from and repair the break (see figure1). During HR the sister chromatid or the homologous chromosome are used as the template. It occurs mainly in the S and G2 phases of the cell cycle, possibly due to the fact that both sister chromatids are present. In germ cells, meiotic double strand breaks are repaired by HR during pachytene of meiosis I, when both homologous chromosomes pair up and exchange genetic material (recombination). In somatic cells, HR repairs DNA breaks that occur after environmental stress and in the recovery of stalled or broken replication forks (Da Ines, Degroote et al. 2013). The repair of these DSB by HR generates two types of recombinant molecules, crossover (CO) and gene conversion without cross-over (NCO) (Youds and Boulton 2011). CO result from reciprocal exchanges of genetic information between homologous and NCOs result from a unidirectional transfer of information from a donor to an acceptor (Chen, Cooper et al. 2007; Youds and Boulton 2011). It also should be noted that NCOs are usually the outcome of most of the somatic HR unless it is the immune system (O'Driscoll and Jeggo 2006).

Due to the fact that my studies focus on DNA repair during meiotic recombination, the following pages first, provide a description of HR in mammals and *Drosophila melanogaster,* two organisms with highly-conserved mechanisms

and factors, and yeast, where most of the mechanisms and factors were studied initially. Then a later section will focus on meiosis as a specialized form of HR.

1.2.1. Recognition of DSBs during homologous recombination

The MRN (MRX in yeast) complex composed of Mre11, Rad50 and Nbs1 (Xrs2 in yeast) is considered the main sensor of DSBs that are repaired through HR (van den Bosch, Bree et al. 2003; Williams, Lees-Miller et al. 2010). This complex activates repair and checkpoint signaling pathways, mainly by the activation of Ataxia telangiectasia mutated (ATM) and ataxia telangiectasia and Rad3 related (ATR) serine-threonine kinases that phosphorylate themselves and many other downstream effectors key to the repair of DSBs (Girard, Riballo et al. 2002; Uziel, Lerenthal et al. 2003; Lee and Paull 2005; Paull and Lee 2005). The MRN complex not only activates ATM/ATR, but also binds to the DNA, tethering the two ends of the break and keeping them together (de Jager, van Noort et al. 2001; Williams, Moncalian et al. 2008). The complex is also involved in processing of the DNA ends to create a 3' overhang that will initiate strand invasion, an important step necessary for accurate DSB repair (Paull and Gellert 1998; Trujillo and Sung 2001).

1.2.1.1. Mre11 protein in DSB repair

Mre11 protein is highly conserved amongst eukaryotes; it has an N-terminal

phosphoesterase domain and two C-terminal DNA binding domains (Trujillo, Yuan et al. 1998; van den Bosch, Bree et al. 2003; Lamarche, Orazio et al. 2010). It plays several key functions in the repair of DSBs: 1. It has the capability to bind DNA, and tethers the two ends of the breaks, 2. It has ssDNA 3' to 5' endonuclease and exonuclease activity, as well as hairpin opening activity important for the creation of the 3' overhangs (Paull and Gellert 1998; Trujillo, Yuan et al. 1998; Trujillo and Sung 2001; Rupnik, Lowndes et al. 2010).

1.2.1.2. Rad50 protein in DSB repair

Rad50 is also highly conserved in eukaryotes; it has a globular ABC ATPase domain, composed of an N-terminal walker A and a C-terminal walker B domain, which associate with one another to form an ATP binding region (Rupnik, Lowndes et al. 2010; Williams, Lees-Miller et al. 2010; Stracker and Petrini 2011). The central region of RAD50 is composed of a large coiled-coil structure with Zn-hook in the middle. Each unit of Mre11 binds to one unit of Rad50 at the intersection of Rad50 globular domain and its coil-coil structure, to form what is called the $Mre11_2Rad50_2$ core complex (Rupnik, Lowndes et al. 2010; Williams, Lees-Miller et al. 2010). Rad50's long coil-coil structure helps in the tethering of the DNA ends (Lamarche, Orazio et al. 2010; Williams, Lees-Miller et al. 2010). In yeast, mutations in the Walker A or B globular domains or the Zn-hook result in DNA damage sensitivity and DNA repair defects (Lamarche, Orazio et al. 2010; Rupnik,

Lowndes et al. 2010).

1.2.1.3. NBS1 protein in DSB repair

Nbs1 (Xrs2 in yeast) is the least conserved of the three components of the MRN complex in eukaryotes; however, they all have a FHA and two BRCT repeats in the N-terminus and a binding domain for Mre11 and ATM in the C-terminus (Rupnik, Lowndes et al. 2010; Williams, Lees-Miller et al. 2010). In mammals Nbs1 (as well as Xrs2 in yeast) is in charge of nuclear import of the MRN complex. Interaction of Nbs1 with ATM is key for ATM activation, as well as activation of downstream effectors involved in the repair response pathway (Lee and Paull 2007). Nbs1 is also required for signaling by the ATR pathway (Stiff, Reis et al. 2005). Furthermore, Nbs1 as well as Xrs2 help to regulate Mre11's nuclease activity during meiosis (Williams, Lees-Miller et al. 2010). Studies showed that *Drosophila* Nbs, as its yeast homolog, is important for MRN nuclear import (Ciapponi, Cenci et al. 2006; Gao, Bi et al. 2009).

The components of the MRN complex are structurally related in all eukaryotes; however, functionally the mammalian MRN complex and the *Drosophila* MRN complex seem to be closer than their yeast homolog. Mammalian *mre11, rad50*, and *nbs1* null mutations cause embryonic lethality (Xiao and Weaver 1997; Luo, Yao et al. 1999; Zhu, Petersen et al. 2001). Hypomorphic *mre11* mutations are responsible for ataxia-telangiectasia-like disorder (ATLD) and *nbs1* hypomorphic

mutations lead to Nijmegen breakage syndrome (NBS); both ATLD and NBS are characterized by immunodeficiency, acute predisposition to cancer, developmental defects and at the cellular level by high sensitivity to ionizing radiation and chromosomal instability (van den Bosch, Bree et al. 2003). No genetic disorders have been associated with *rad50* hypomorphic mutations; however, mice with *rad50* hypomorphic mutations show cancer predisposition and developmental defects (Bender, Sikes et al. 2002). In *Drosophila, rad50, mre11*, and *nbs* null mutations are also lethal (Gorski, Romeijn et al. 2004; Oikemus, Queiroz-Machado et al. 2006). Hypomorphic mutations in *mre11, rad50*, and *nbs* embryos lead to developmental defects and at the cellular level to defective chromosomal segregation, chromosomal instability, and high sensitivity to irradiation (Gorski, Romeijn et al. 2004; Oikemus, Queiroz-Machado et al. 2006; Gao, Bi et al. 2009). Also, in mice, the replacement of MRE11 with an allele that does not have nuclease activity is lethal and mutations in the nuclease domain of yeast Mre11 have mild DNA repair defects (Costanzo, Robertson et al. 2001). In contrast to both mammals and *Drosophila, mre11, rad50* and *Xrs2* null mutations in yeast are viable (Errico and Costanzo 2010). This suggests that mammalian and *Drosophila* MRN complexes may share more critical functions for cell viability.

1.2.2. Activation of ATM

The next step in the pathway is the activation of ATM, a member of the phosphatidyl inositol 3-kinase-like family of serine/threonine protein kinases (PIKKs), that is rapidly and specifically activated in response to DNA damage (Bensimon, Aebersold et al. 2011). ATM exists as a dimer that, when activated, phosphorylates itself, becomes a monomer, and activates downstream-acting proteins involved in the DNA damage response pathway and DNA damage-dependent cell cycle checkpoint control (Bakkenist and Kastan 2003; Lee and Paull 2007). It is not completely understood how ATM is activated, but some groups support the view that ATM is activated via interaction with components of the MRN complex. Studies in which human cells with deficiencies in Nbs1 and Mre11 were utilized showed that these two proteins function upstream of ATM (Girard, Riballo et al. 2002; Uziel, Lerenthal et al. 2003; Berkovich, Monnat et al. 2007; Lee and Paull 2007). Stracker *et al.* reached the same conclusion after studying the ATM signaling pathway in cells infected with adenovirus; in these studies, viral proteins degraded the MRN complex and affected ATM signaling (Stracker, Carson et al. 2002; Carson, Schwartz et al. 2003). *In vitro* studies also support these findings; recombinant ATM and MRN proteins interact *in vitro*, and ATM's activity was shown to increase over 200-fold in *in-vitro* assays in the presence of DNA and MRN complex (Paull and Lee 2005). Although these studies strongly support that the MRN complex gets first to the break and activates ATM, another study suggested that ATM can be activated by rapid change in chromatin structure, independent of binding to DNA double strand

breaks (Bakkenist and Kastan 2003). Bakkenist and Kastan showed that ATM can be activated due to exposure to different chemicals such as: chloroquine, histone deacetylase inhibitors, NaCl, or by hypotonic swelling. In this study it was claimed that ATM was activated in the absence of detectable DNA strand breaks due to the fact that ATM substrates that would be phosphorylated at the site of breaks such as H2AX fail to become phosphorylated after the different treatments. These findings suggest that not only the MRN complex but also chromatin structural changes caused by histone hyperacetylation may be sufficient for ATM activation.

ATM is the main mobilizer of the cellular response to DNA damage. It directly or indirectly phosphorylates and activates a large number of proteins involved in cell survival and cell death after DNA damage. During DNA damage ATM is involved in the DNA repair and cell cycle checkpoint control; however it is also involved in the activation of cell death or senescence.

Most ATM functions are conserved among eukaryotes; in yeast, Tel1 have similar functions to their mammalian counterpart ATM. They are involved in DNA damage response and cell cycle check point. The *Drosophila* homolog of ATM, tefu (telomere fusion), also has roles similar to their mammalian counterparts in cell cycle checkpoints and DSB repair. *tefu* mutants are extremely sensitive to ionizing radiation. In addition, *tefu* mutants have defects in G2/M checkpoint at low doses of IR; however, there are no defects in the G2/M checkpoint upon introduction of damage with higher doses of γ-irradiation (Oikemus, Queiroz-Machado et al. 2006).

tefu mutants do not reach adulthood, they die as pupae with a few escapers that are sterile and die at a young age. (Song, Mirey et al. 2004). Recent studies using a temperature sensitive *tefu* mutant confirmed a role for tefu in DNA repair and further suggested that tefu negatively regulates the formation of programmed DSBs during female meiosis (Joyce, Pedersen et al. 2011).

1.2.3. Role of phosphorylation of histone H2A.X during DNA repair

Another key role of ATM and also ATR (ATR is another PIKK activated in response to DNA damage that works later in the repair pathway) is the phosphorylation of the histone variant H2A.X (Rogakou, Pilch et al. 1998; Rogakou, Boon et al. 1999; Paull, Rogakou et al. 2000; Burma, Chen et al. 2001). The canonical histones are H2A, H2B, H3, and H4; these histones are expressed and incorporated into nucleosomes in the S phase. In contrast, histone variants are integrated independent of replication and made throughout the cell cycle and (Henikoff and Ahmad 2005). Different variants of the canonical H2A histone exist. All eukaryotes have H2A.X and H2A.Z-type variants; vertebrates have a variant named macro H2A, and mammals have a specific H2A variant named H2ABBd (Bar-body deficient) (Jin, Cai et al. 2005). In yeast, H2A.X replaces H2A as the canonical histone. *Drosophila melanogaster* has the H2A core histone and only one H2A variant, H2Av, which is a fusion of H2A.X/H2A.Z. In eukaryotes from yeast to humans, H2A.X has a conserved C-terminus SQ motif. The serine within the motif is the residue that gets

phosphorylated after DNA damage (Jin, Cai et al. 2005). The phosphorylated form or H2A.X is referred to as γ-H2A.X or γ-H2Av in flies (Kusch, Florens et al. 2004).

Phosphorylation of HA2.X spreads mega bases away from the break. By using quantitative multiplex ChiP, Shroff *et al.* showed that as quickly as 15 minutes after induction of a DSB phosphorylation of H2A.X spreads about 50 kb away from the break (Shroff, Arbel-Eden et al. 2004). These studies showed that no γ-H2A.X was detected 1-2 Kb away from the break and that γ-H2A.X levels picked at about 2 Kb from the break (Shroff, Arbel-Eden et al. 2004). In contrast to yeast, only about 10% of nucleosomes contain H2A.X in mammals. However, in mammals it is also believed that γ–H2A.X can spread mega-bases away from the break. After exposing hamster CHO cell cultures to ionizing radiation and densitrometic analysis, it was estimated that 1% of H2A.X gets phosphorylated per gray of ionization. Based on these findings it was calculated that about 2 Mb of chromatin seems to be involved per DNA (Rogakou, Pilch et al. 1998; Redon, Pilch et al. 2002). Additionally, immunocytochemical studies done using human cells suggested that γ-H2A.X spreads mega-bases away from the break (Rogakou, Boon et al. 1999).

Phosphorylation of H2AX has some important functions. For instance, γ-H2A.X is essential to maintaining genome stability, mice with a targeted disruption of H2A.X were viable but showed poor cell proliferation, premature entry into senescence, chromosomal abnormalities, sensitivity to ionization radiation and increased nuclear fragmentation (Bassing, Chua et al. 2002). Female mice lacking H2A.X are fertile as

oppose to males whose germs cells are arrested in the pachytene stage of meiosis I and thus are infertile (Celeste, Petersen et al. 2002; Celeste, Fernandez-Capetillo et al. 2003). A large number of studies support the fact that γ-H2A.X is necessary for the proper accumulation of factors to repair sites. The accumulation of recognition and repair factors to DSBs appears as nuclear foci when imaged under a fluorescence microscope. Brca1 and Rad51 are two proteins known to accumulate at damage-induced repair foci in wild type cells. However, after mouse embryonic fibroblasts (MEF) were treated with wortmannin, an inhibitor of protein kinases used to inhibit ATM, not only γ-H2AX, but also Brca1 and Rad51 did not form any detectable foci (Paull, Rogakou et al. 2000). A separate set of studies examined the distribution of Brca1, 53bp1, and Nbs1, factors also known to colocalize with γ-H2AX in irradiation-induced foci. In these studies mouse B cells, lacking H2A.X, showed an impaired formation of Nbs1, 53bp1, and Brca1 foci when the foci distribution was determined by immunofluorescence post-irradiation (Celeste, Petersen et al. 2002).

In yeast, the first damage-specific histone modification identified was phosphorylation of H2A S129 (H2AX S139 in mammalian cells) within the SQ motif. Yeast lacking the H2A.X C-terminal SQ motif are moderately sensitive to DNA damaging agents and have defects in the NHEJ repair pathway, but the HR repair pathway seems to be unaffected (Downs, Lowndes et al. 2000). In accordance with these findings, meiosis is normal in yeast mutants unable to phosphorylate H2A.X (Downs, Lowndes et al. 2000). However, another study failed to observe NHEJ

defects in a similar H2A mutant (Wyatt, Liaw et al. 2003). Interestingly, data from later studies in yeast suggest that upon DNA damage histone H2A can also be phosphorylated in C-terminal residues: T126 and S122 (Harvey, Jackson et al. 2005; Moore, Yazgan et al. 2007). Both phosphorylations were shown to be important for survival in the presence of a number of DNA-damage-inducing agents (Moore, Yazgan et al. 2007), (Harvey, Jackson et al. 2005). Investigators also showed that the role of H2A S122 in DSB repair is distinct from the role of S129 (Moore, Yazgan et al. 2007).

Studies done using *Drosophila* tissue cultured cells and larvae showed that Ser137, located within an SQ motif in the C- terminus of H2Av, gets phosphorylated in response to DNA damage (Madigan, Chotkowski et al. 2002). Phosphorylation of H2Av is rapid; it occurs within 1 minute and was reported to be maximal at 5 minutes in *Drosophila* S2 cells that were γ-irradiated (Madigan, Chotkowski et al. 2002). Removal of γ-H2Av occurs at the nucleosome level; the *Drosophila* Tip60 (dTip60) chromatin-remodeling complex acetylates nucleosomal phospho-H2Av and exchanges it with an unmodified H2Av (Kusch, Florens et al. 2004). Mutations in Tip60 cause accumulation of γ-H2Av; however, it is unknown if breaks are repaired by the time γ-H2Av is exchanged (Ikura, Ogryzko et al. 2000; Kusch, Florens et al. 2004). Recent studies suggest that in the female germ line in flies, γ-H2Av is continuously exchanged in meiotic DSBs even before repair has occurred; this constant exchange requires new phosphorylation by ATM and ATR at the break site (Joyce, Pedersen et al. 2011). In Joyce *et al* study it was proposed that the removal

of γ-H2Av depends on the cessation of ATR or ATM activity; however, it is not completely clear when ATR or ATM activity ceases in oogenesis and if it does after repair is done.

In *Drosophila,* the ability to phosphorylate H2Av seems to be important for genome stability. *Drosophila* null mutations of H2Av are lethal due to the essential role of H2A.Z in all eukaryotes, which was confirmed by amino-acid swap experiments in which residues unique to *Drosophila* H2Av were replaced with equivalently positioned *Drosophila* H2A.1 residues. While the C-terminus without a phosphorylation site was viable, it was found that a small C-terminal domain of H2Av which is buried inside the histone core and not directly involved in interactions with DNA (likely to be a domain involved in protein-protein interactions) was essential (Clarkson, Wells et al. 1999). This domain interacts with Swr1 in yeast, which might explain why its mutation causes the failure of H2Av incorporation and the downstream effects that caused developmental arrest. Thus viability is not conferred by the SQ motif of H2Av and lack of the phosphorylation site is not lethal. However, transgenic constructs in which Ser 137 is changed to alanine fail to fully rescue the lethality of $H2Av^{810}$ null mutants after irradiation (Kotova, Lodhi et al. 2011).

1.2.4. Processing of DSBs

After the recognition of the break and the signaling to ATM, there are a number

of key steps involved in the repair of the break (Mimitou and Symington 2008). First, the ends of the break need to be processed to create a 3' single stranded DNA overhang that will invade the homologous chromosome. Second, stabilization of the ssDNA by association of Replication protein A (RPA) has to occur, followed by the binding of the recombinase Rad51. Association of DNA with Rad51 forms a nucleoprotein filament, also known as presynaptic filament, which looks for a homology region to repair the break. The third step is the formation and resolution of intermediates created during the homology search and the recombination of genome (see figure2).

1.2.4.1. End resection

Recently, the work of several groups has shed light on how the formation of the ssDNA 3' overhang, or end resection process, may occur. These studies suggest that Exo1, a nuclease, and Dna2, a nuclease/helicase, that work together with the helicase, Sgs1 are needed for long-range resection (Zhu, Chung et al. 2008; Paull 2010; Mimitou and Symington 2011). *exo1* mutants have reduced resection, but homologous recombination still occurs (Mimitou and Symington 2008; Zhu, Chung et al. 2008). In addition, *exo1* and *sgs1-dna2* double mutants have very severe resection defects (Mimitou and Symington 2008). Altogether, it has been suggested that Exo1 and Sgs1-Dna2 work in different but redundant pathways (Zhu, Chung et al. 2008; Mimitou and Symington 2011). The MRN complex also has a key role in the

end resection process. Due to its endonucleolitic activity it was originally thought that Mre11 was also in charge of end resection; however, Mre11 has a 3' to 5' endonuclease activity, as opposed to a 5' to 3' processing activity needed to create the 3' overhang (Furuse, Nagase et al. 1998; Trujillo, Yuan et al. 1998). By studying the roles of different helicases during end resection at a DSB created by the HO endonuclease in yeast, different groups have concluded that the MRX complex together with Sae2 work in the early stages of end resection. Recent studies have shown that MRN works in early stages of resection possibly by promoting binding of Exo1 and Sgs1-Dna2 (Neale, Pan et al. 2005; Mimitou and Symington 2008; Zhu, Chung et al. 2008). It has been reported that the MRX complex interacts with Sgs1–Dna2 and that addition of MRX to an *in vitro* assay that contains Sae1-Dna2 increases resection fourfold. (Cejka, Cannavo et al. 2010; Niu, Chung et al. 2010). At the same time, Exo1 activity greatly increases in the presence of MRX-Sae2 Exo1 (Nicolette, Lee et al. 2010). The end resection process seems to be conserved in mammals and yeast. The mammalian Sgs1 homolog, BLM, also works in parallel with the mammalian Exo1 to promote DSB resection (Gravel, Chapman et al. 2008). The mammalian CtIP, the homolog of yeast Sae2 protein, physically and functionally interacts with the MRE11 complex (Sartori, Lukas et al. 2007). In addition both CtIP and MRE11 are required for efficient homologous recombination (Sartori, Lukas et al. 2007). To this date, no homolog of Sae2/CtIP in *Drosophila* has been described.

1.2.4.2. Formation of the presynaptic filament

After the 3' overhang is created, RPA and Rad51 bind to the ssDNA to form the presynaptic filament (see figure2). The first step in the process is binding of RPA; RPA is an essential protein that binds tightly to the single stranded DNA to stabilize it and prevent the formation of secondary structures (Wang and Haber 2004). As a result, RPA has a stimulatory effect on the formation of the presynaptic filament, but its tight binding to the ssDNA also inhibits the binding of key enzymes needed for the formation of the filament (Sung 1997; Wang and Haber 2004). The next step is binding of Rad51 to the ssDNA and displacement of RPA. Rad51 is a highly conserved protein, and it is the main protein that catalyzes homology search and strand exchange (Shinohara, Ogawa et al. 1992; Sung and Robberson 1995; Baumann, Benson et al. 1996). Yeast *Rad51* null mutants are viable; however, they are highly sensitive to DNA damage agents and show defects in recombination during meiosis and mitosis (Shinohara, Ogawa et al. 1992). In contrast to yeast, *Rad51* null mutations in mice are lethal (Tsuzuki, Fujii et al. 1996). In *Drosophila*, the homolog of Rad51 is spn-A; spn-A is 64% identical and about 80% similar to human Rad51. In addition, spn-A is not required for viability, but is required for oogenesis. *spn-A* mutants are sensitive to ionizing radiation, are thought to accumulate un-repaired DSBs, and have defects in chromosomal disjunction and recombination during meiosis (Staeva-Vieira, Yoo et al. 2003; Yoo and McKee 2005). It has also been shown that spn-A mediates strand exchange *in vitro* (Alexiadis and Kadonaga 2002).

There is another group of proteins known as mediators that help in the formation of the presynaptic filament. In order for Rad51 to bind and form the presynaptic filament, the inhibitory effect of RPA needs to be overcome. In yeast, Rad52 is the mediator protein that helps loading of Rad51 onto the ssDNA (Sung 1997; Wang and Haber 2004). Several studies have shown that Brca2 is the functional human homolog of Rad52 and that it functions as a mediator during HR (Chen, Chen et al. 1998; Moynahan, Pierce et al. 2001; Holloman 2011). Additionally, the *Drosophila* Brca2 homolog, dBRCA2, has been also characterized and has been shown to be requier for homologous recombinational repair (Klovstad, Abdu et al. 2008).

In yeast, Rad55 and Rad57 are Rad51 paralogs and are also considered to be mediators of strand exchange. Rad55 and Rad57 form a heterodimer and, like Rad52, Rad55 and Rad57 promote strand exchange when RPA is present (Sung 1997). The phenotype of *Rad55-Rad57* mutant cells is partially overcome and the HR repair defects are suppressed when Rad51 and Rad52 are over-expressed (Hays, Firmenich et al. 1995; Johnson and Symington 1995). Vertebrates have five Rad51 paralogues: RAD51B, RAD51C, RAD51D, XECC2, and XRCC3, all of which have a role in the formation and/or maintenance of the presynaptic filament (Symington 2002; Yonetani, Hochegger et al. 2005).

It has been suggested that there are also Rad51 paralogs in *Drosophila*. Two studies have proposed that spn-B and spn-D are the *Drosophila* homologs of XRCC3

and Rad51C, respectively (Ghabrial, Ray et al. 1998; Abdu, Gonzalez-Reyes et al. 2003). spn-B is 35% identical and 49 % similar to XRCC3; however, spn-D only has 23% identity and 38% similarity to Rad51C (Ghabrial, Ray et al. 1998; Abdu, Gonzalez-Reyes et al. 2003). *spn-B, spn-D* mutations cause defects in activation of the meiotic checkpoint, meiotic recombination, and also affect oogenesis (Ghabrial, Ray et al. 1998; Abdu, Gonzalez-Reyes et al. 2003). Studies suggest that in contrast to XRCC3 and Rad51C, in *Drosophila* both spn-B and spn-D are mostly involved in meiosis and do not function in somatic cells (Abdu, Gonzalez-Reyes et al. 2003). *spn-B and spn-D* mutants are not sensitive to ionizing radiation, suggesting that these genes may have different roles from those of the Rad51-like genes (Abdu, Gonzalez-Reyes et al. 2003). In *Drosophila* there are two more proteins that are part of the spindle class genes (Rad51 like genes): spn-C and spn-E. spn-E encodes an RNA-dependent ATPase that does not seem to have a role in DSB repair (Abdu, Gonzalez-Reyes et al. 2003). As opposed to spn-E, spn-C seems to be required for meiotic and mitotic DSB. *spn*-C mutants are hyper-sensitive to DNA damage and also have defects in oogenesis. As opposed to spn-B and spn-D, spn-C does not seem to have a homolog in the rad51 class genes, but it seems to be the homolog of the human helicase HEL308 (McCaffrey, St Johnston et al. 2006). HEL308 is a helicase conserved amongst eukaryotes and thought to have a function in early stages of homologous recombination.

Another protein with a key role in the formation of the presynaptic filament is

Rad54. Rad54 is part of the Swi2/Snf2 super family of proteins and has dsDNA-dependent ATPase, DNA translocase, DNA supercoilig and chromatin remodeling activities (Heyer, Li et al. 2006; San Filippo, Sung et al. 2008). Rad54 has roles in different steps of the repair pathway. First, it stabilizes Rad51 filaments, thus helping in presynaptic filament formation (Mazin, Alexeev et al. 2003). Second, Rad54 stimulates the strand exchange reaction by its ATPase activity but the exact way in which Rad54 facilitates this process is not completely understood (Mazin, Alexeev et al. 2003). Finally, Rad54 promotes removal of Rad51 from the ssDNA at the end of the process (San Filippo, Sung et al. 2008). Okra is the Drosophila homolog of Rad54. *okra* mutants are hypersensitive to ionization radiation and have defects in oogenesis (Ghabrial, Ray et al. 1998). More importantly, Okra, as its mammalian homolog, is necessary for proper resolution of meiotic and mitotic DSBs (Ghabrial, Ray et al. 1998; Alexiadis and Kadonaga 2002).

1.2.4.3. ATR in the processing of DSBS

ATR is another PIKK activated in response to DNA damage (Bensimon, Aebersold et al. 2011). ATR is activated by the presence of single stranded, incompletely replicated or UV damaged DNA (Kim, Minter-Dykhouse et al. 2006;Bensimon, Aebersold et al. 2011). For all of its functions, ATR requires ATR interacting protein (ATRIP). ATRIP is needed for ATR stability, signaling, regulation, localization and activation of the kinase (Nam and Cortez 2011). During HR, ATR is activated after

end resection when the ssDNA 3' overhang is created and RPA and ATRIP are bound to the single-stranded DNA. (Lee and Paull 2007). *In vivo and in vitro* studies suggest that ATM and ATR DNA specificities differ; ATM is mainly activated by double-stranded DNA breaks (DSBs), whereas ATR responds to a broad spectrum of DNA damage (Marechal and Zou 2013). Additionally, yeast studies have shown that tel1 and mec1 have redundant roles in the DNA damage response. *tel1* and *mec1* double mutants are more sensitive to radiation than *mec1* mutants (regulation of genome stability by Tel1 and Mec1 yeast homologous of the mammalian ATM and ATR genes). As opposed to tefu, mei-41 (ATR *Drosophila* homolog) is essential for G2/M DNA dependent cell cycle checkpoints. Upon introduction of damage at several doses of γ–irradiation, *mei-41* mutants have cell cycle checkpoints defects (Laurencon, Purdy et al. 2003;LaRocque, Jaklevic et al. 2007). Some of the first screens in which *mei-41* mutants were characterized showed that weak alleles have meiotic recombination defects and most strong alleles die as embryos (Sibon, Laurencon et al. 1999). In contrast to ATR, ATM alleles were not found in genetic screens for meiotic mutants but for telomere fusion and genome rearrangements (Queiroz-Machado, Perdigao et al. 2001). This suggests that Mei41 appears to have a unique and essential role in meiosis.

1.2.4.4. Homology search strand invasion

Once formed, the presynaptic filament captures a duplex DNA molecule, begins strand invasion, and then initiates homology search (see figure2). During homology search, one strand is displaced and a displacement loop (D-loop) is formed (Sung and Klein 2006; Ciccia and Elledge 2010). The duplex structure that is generated after strand invasion is resolved by either synthesis-dependent strand annealing (SDSA) or double-strand break repair (DSBR). During SDSA, the invaded strand is extended by DNA synthesis, and because the D-Loop is unwound, this newly-synthesized invading strand re-anneals to the second resected end of the break (see figure 2)(Sung and Klein 2006). SDSA occurs in somatic cells and results only in NCO (Sung and Klein 2006; Mimitou and Symington 2009). In DSBR, the invaded strand is ligated to the other end of the break that has been captured by the D loop (second end capture), then this process forms a two cross strand or an X-shaped intermediate structure known as the double Holliday Junction (dHJ) (see figure3) (Sung and Klein 2006; Ciccia and Elledge 2010). This X-shaped structure is resolved by helicases that cleave across the axes of the intermediate and can result in CO or NCO.

1.2.4.5. Resolution of crossovers and non-crossovers

The human BLM (yeast Sgs1)-TOPO3alpha-RMI helicase complex dissolves dHJ, which results in two duplex molecules that are not recombined (NCO) (see figure 2)

(Wu and Hickson 2003; Cheok, Bachrati et al. 2005). Another protein involved in the resolution of dHJ is the human MUS81-EME1 (yeast Mus81-Mms4), which promotes meiotic recombination by the resolution of dHJ and results in CO. In *MUS81* mutants, COs are eight to 25-fold affected and non-crossovers are unaffected (Boddy, Gaillard et al. 2001; Osman, Dixon et al. 2003). Yen-1 in yeast (GEN1 in humans) is another helicase known to function in the dissolution of the dHJ. It cuts HJs in a symmetrical re-ligatable manner, and seems to give rise to CO and NCO with equal efficiency (Ip, Rass et al. 2008).

Orthologs of these human and yeast helicases have also been found in *Drosophila,* however they are less understood. dmBLM is the *Drosophila* ortholog of BLM, which is encoded by the *mus-309* gene. *dmBLM* mutants have defective DNA repair through SDSA. If dHJ are not correctly resolved homologous chromosomes can fail to properly segregate at meiosis and thus can result in unequal number of chromosomes in daughter cells; this unequal separation is called non-disjunction. Non-disjunction is the major source of aneuploidy, in which some cells can have one chromosome missing from one of its pairs and some cells will have an extra chromosome in addition to its pairs (Lamb, Sherman et al. 2005). *dmBLM* Mutants have increased non-disjunction, chromosomal loss and are infertile; *dmBLM* males produce an excess of XY sperm and nullo sperm, consistent with a high frequency of non-disjunction and/or chromosome loss (Kusano, Johnson-Schlitz et al. 2001).

Mei-9, Mus-312 and Hold'em are another set of *Drosophila* factors known to be involved in meiotic recombination and with a possible role in resolution of dHJ. *mei-9* mutants, are part of a group of mutants refer to as the exchange mutants, they have reduced CO rates but not alter distribution of CO in the genome. Specifically, *mei-9* show a 90%-95% decrease in the levels of meiotic CO uniformly throughout the *Drosophila* genome. However, in *mei-9* mutants, gene conversion is not affected. Taking into consideration these phenotypes and the high levels of post-meiotic segregation events (PMS) observed in *mei-9* females, it has been suggested that Mei-9 is involved in the resolution of meiotic crossover, most likely at later stages (Sekelsky, McKim et al. 1995; Yildiz, Majumder et al. 2002). PMS defects occur when mismatches in the heteroduplex DNA are not repaired during meiosis (Sekelsky, McKim et al. 1995). Since Mei-9 is structurally similar to an endonuclease, it has been suggested that its actual role is during HJ resolution (Yildiz, Kearney et al. 2004). However, direct evidence of a role of Mei-9 in resolution of heteroduplex structures has yet to be obtained. Mus-312 is another *Drosophila* protein known to interact with Mei-9 and is necessary for meiotic crossovers (Yildiz, Majumder et al. 2002). Studies done by Joyce *et al.* also suggest that Hold'em forms a complex with Mei-9 and Mus-312, and that together may work in the resolution of intermediates into meiotic crossovers (Joyce, Tanneti et al. 2009).

1.2.5. Amplification of the DNA damage signal

Mediator of DNA Damage Checkpoint Protein 1 (MDC1) is one of the key molecules that participate in the amplification of the DNA damage response signal. MDC1, as characteristic for many DNA repair and checkpoint factors, has two BRCT repeats in the C-terminus and an FHA domain in its N-terminus (Stucki and Jackson 2004). In addition, the middle part of the protein has 19 consecutive repeats of 40 amino acids that are ATM/ATR consensus target phosphorylation motifs (Stucki and Jackson 2004). When the expression of MDC1 was down-regulated by sRNAi, the accumulation of MRN and BRCA1 into repair foci was affected (Stucki and Jackson 2004). Additionally, deletion of the MDC1/NFBD1 BRCT domains affects focal concentration of MDC1/NFBD1, and ectopic expression of the MDC1/NFBD1 BRCT domains abolished formation and maintenance of large γ-H2AX, 53BP1, MRN foci as well as MDC1/NFBD1 foci. MDC1 interacts specifically with the phosphorylated form of H2A.X through its BRCT repeat and its foci formation is dependent on γ-H2A.X (Stewart, Wang et al. 2003; Lou, Minter-Dykhouse et al. 2006; Soutoglou and Misteli 2008). Binding of the MRN complex and γ-H2A.X seem to be a key limiting factor for the recruitment of MDC1. By using stably immobilized Nbs1, Mre11, and γ-H2A.X to chromatin Soutoglou and Misteli showed that MDC1 was recruited to these regions even in the absence of DSB (Soutoglou and Misteli 2008).

All the available data from MDC1 suggests that a feedback loop mechanism exists to amplify the DNA damage response (DDR). MDC1 binding requires that early recognition events have occurred: binding of MRN, activation of ATM, and phosphorylation of H2A.X. At the same time, binding of MDC1 seems to be needed for formation of larger MRN foci. This indicates that there is an early or initial basal response of recognition factors, then binding of scaffold proteins, followed by an

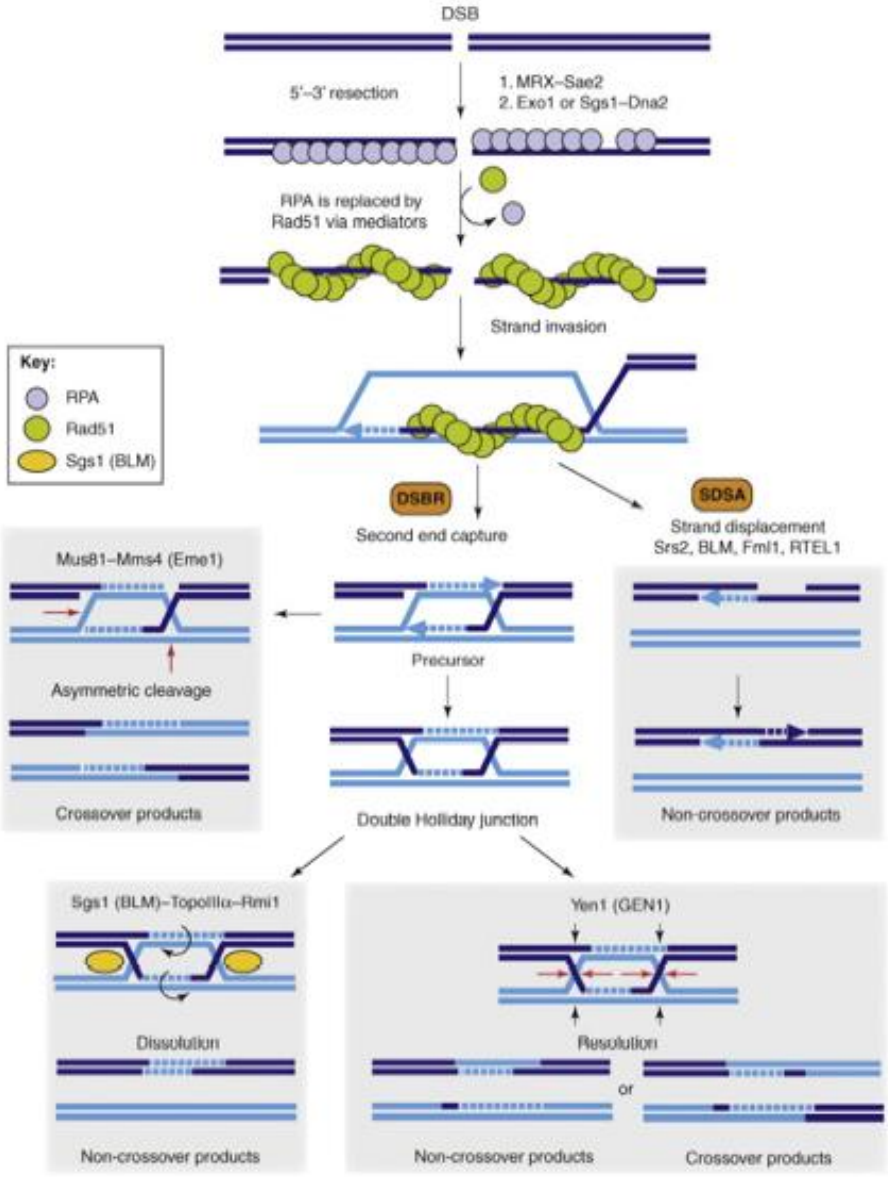

.

Figure 2: Homologous Recombinational (HR) repair and its different outcomes. After sensing of the break the following steps characterize HR: 1. End resection occurs 5' to 3' to create a 3' overhang. 2. Binding of RPA to stabilize the template. 3. Replacement of RPA by Rad51 with the help of mediators to form the presynaptic filament. 4. Strand invasion, homology search and synthesis. There are two different models for HR resolution: first, SDSA in which the newly synthesized invading strand re-anneals to the second resected end of the break. Second, DSBR in which second end capture forms an early intermediate or ligation to the other resected end forms a double Holliday Junction (dHJ). Resolution of the early intermediate by Mus81-Mms4 (Eme1) results in crossover products. dHJ can be resolve by Sgs1 (BLM)-TopoIIα–Rmi and result in crossover products or by Yen-1 (GEN1 in humans) and result in crossover of non-crossovers (Mimitou and Symington 2009)

accumulation of MRN during later phases of DSB repair.

There are no known yeast homologs of MDC1 (Fillingham, Keogh et al. 2006). In addition, mediator proteins like Mdc1, Brca1, and 53BP do not have clear homologs in flies and it is not clear whether a similar feedback loop exists in other eukaryotes. More recent studies suggested that flies might have a protein with similarity to MDC1. Mutator Protein 2 (MU2) seems to have similar structure and functions as the human MDC1 (Dronamraju and Mason 2009). The MU2 protein has in its N-terminal an FHA domain and in its C-terminal BRCT repeats (Dronamraju and Mason 2009). Like MDC1, MU2 seems to interact with components of the MRN complex. Additionally, MU2's BRCT repeats interact with γ–H2Av, and this interaction seems

to affect γ–H2Av foci formation, albeit to a much lesser extent than the human MDC1.

1.3. Nuclear localization of DNA repair sites

Accumulation of repair factors into microscopically discernible structures and the spatial organization of these structures within the nucleus have been described and seem to be of key importance in the prompt and correct repair of DSBs. These structures have been studied in humans, mice, plants and flies and are referred to here as repair foci. The exact organization of repair foci is not completely known, but studies done by Simon Bekker-Jensen *et al*. suggest that foci are composed of specific repair factors, which were classified in two groups (Bekker-Jensen, Lukas et al. 2006). The first group is composed of proteins such as Rad51, RPA, ATR and ATRIP. These proteins form "micro foci," bind to ssDNA, and are involved in HR. The other group of proteins is related to chromatin modifications that have been shown to spread mega-bases away from the break (γ-H2Av, Mre11, and MDC1, ATM) and were found surrounding the "micro foci" (Bekker-Jensen, Lukas et al. 2006). Additionally, members of the NHEJ pathway Ku80 and Ku70 and DNAPK do not accumulate in repair foci as do HR repair factors (Bekker-Jensen, Lukas et al. 2006). This suggests that the foci observed in microscopy studies are a function of the accumulation of several factors. Studies in yeast have also suggested that there is a spatial organization of DSBs within the nucleus in structures known as centres. Upon low doses of irradiation, only a few repair foci were visible (about 2-4 foci).

However, at high doses of irradiation the amount of foci does not increase, suggesting that newly-formed lesions go to pre-existing repair foci (Lisby and Rothstein 2004). These studies were confirmed by the use of a fluorescent tag near the break site showing that two independent breaks can co-localize in foci (Lisby, Mortensen et al. 2003).

Accumulations of repair factors also seem to occupy specific regions within the nucleus. In yeast, persistent or slowly-repaired DSBs migrate from an internal nuclear position to the nuclear periphery (Oza, Jaspersen et al. 2009). At the periphery the persistent DSBs are anchored by Msp3 protein, a Sun domain protein that traverses the inner nuclear membrane (Oza, Jaspersen et al. 2009). Other studies in yeast show that DSBs accumulate in the periphery and co-localize with Nup49 and Nup84 nuclear pore proteins; furthermore, this localization in the nuclear periphery seem to be dependent on mec1 and tel1, since mutation in these genes abolishes nuclear periphery localization of the breaks (Nagai, Dubrana et al. 2008). In mammals, thus far, the only known localized accumulation of repair factors within the nucleus is in Promyelocytic leukemia nuclear bodies (PML NB). PML NBs are dense spherical structures of 0.1–1.0 μm in diameter observed by electron microscopy (Lallemand-Breitenbach and de The 2010). PML NBs are matrix-associated and composed of several proteins involved in a variety of different cellular processes (Lallemand-Breitenbach and de The 2010). The following supports the fact that PML-NB bodies are involved in DNA damage response: 1) Several DNA damage response and DNA repair factors localize to PML-NB (Dellaire, Ching et al.

2006), 2) the numbers of PML-NB increase and also their sub-nuclear distribution changes in response to DNA damage (Dellaire, Ching et al. 2006), 3) upon introduction of DNA damage by ultraviolet radiation, foci of single-stranded DNA co-localizes with PML-NB (Boe, Haave et al. 2006), 4) Recent studies have shown that disruption of PML NB affects HR, mainly during the later steps of the repair pathway (Yeung, Denissova et al. 2012).

Similar to yeast, studies in *Drosophila* conducted by Chiolo *et al.* demonstrate that DSBs (foci) appear in heterochromatic regions at about 10 minutes post-irradiation and that foci move from these heterochromatic domains to non-heterochromatic domains toward the nuclear periphery (Chiolo, Minoda et al. 2011). The movement of foci toward non-heterochromatic regions seems to be dependent on ATR and resection; since the RNAi-mediated depletion of ATR, CtIP/Tosca/Blml retards the movement from the heterochromatic domain to outside the heterochromatic domain suggesting that these foci are exclusively repaired by HR (Chiolo, Minoda et al. 2011).

Although DSB repair mechanisms and factors have been studied for nearly 3 decades, there are still many open questions. For example, the exact composition, organization and order of assembly of repair foci are not yet completely understood. Additionally, very little is known about the spatial organization of repair foci within the nucleus, especially with respect to the association of the nuclear localization of repair foci with a specific stage of repair.

1.4. Meiosis, a specialized form of HR

Meiosis is a process of cellular division common to all sexually reproducing organisms. During meiosis, a diploid cell becomes tetraploid, recombines its DNA, and eventually produces four haploid gametes or spores. Genetic recombination takes place during prophase of meiosis I. Prophase occurs in four stages: leptotene, zygotene, pachytene and diplotene. During leptotene and zygotene, the synaptonemal complex (SC) forms. The SC is a proteinaceous structure that holds homologues together during recombination, which takes place in pachytene (Review in (Zickler and Kleckner 1999). Meiotic recombination is considered a specialized form of HR, during which DSBs are endogenously introduced and then repaired through HR in such a way that at least one CO is generated per chromosome arm. In meiotic recombination the DSB is made by Spo11, a topoisomerase conserved throughout eukaryotes. After cleavage, a Spo11 remains covalently attached to the end of the break and poses a block for the next recombinational steps (Keeney and Kleckner 1995; Keeney, Giroux et al. 1997). As previously mentioned, the nuclease activities of Mre11 together with Sae2 are necessary for processing of meiotic DSBs (Keeney and Kleckner 1995; Moreau, Ferguson et al. 1999). During meiosis Mre11 and Sae2 cut the DNA strand and release an oligonucleotide of about 10 to 40 nucleotides with Spo11 bound to it (Neale, Pan et al. 2005). After the Spo11-bound oligonucleotide is released, the rest of the recombination repair steps proceed.

In *Drosophila*, *mei-W68* encodes the Spo11 homolog (McKim and Hayashi-Hagihara 1998). The *mei-W68* gene is required for all meiotic gene conversion and crossing-over (McKim and Hayashi-Hagihara 1998). Although both Spo11 and mei-W68 are necessary for initiation of recombination in both species, their roles differ to some extent. As opposed to Spo11, mei-W68 is not required for synaptonemal complex formation and does have a mitotic role (McKim and Hayashi-Hagihara 1998).

Mismatch repair proteins are a family of highly conserved polypeptides involved not only in mismatch repair but also in meiotic recombination (Buermeyer, Deschenes et al. 1999). In yeast, mismatch repair proteins MSH4 and MSH5 are expressed only in meiotic cells and are specifically required to maintain wild type levels of meiotic crossing over (Buermeyer, Deschenes et al. 1999; Sekelsky, Brodsky et al. 2000). Yeast also have four more mismatch repair (MMR) proteins that play other roles in different DNA repair pathways: MSH 1-4 and MSH6 (Buermeyer, Deschenes et al. 1999). Another set of MMR proteins have been identified: Pms1 in yeast (MLH1, PMS2 in mammals), and Mlh3 in yeast (PMS1 in mammals) (Buermeyer, Deschenes et al. 1999). PMS2 and MLH1 have roles in both mismatch repair and meiosis. Studies show that *PMS2* knockout mice are male sterile and have abnormalities in chromosome synapsis during prophase of meiosis I (Baker, Bronner et al. 1995). *MLH1* deficient mice are male and female sterile (Baker, Plug et al. 1996;Edelmann, Cohen et al. 1996). Importantly, studies by Baker S, et al showed that MLH1 localized to synapse homologues in a pattern that correlated

with the observed distribution and numbers of crossover in wild type mice germ cells during meiosis (Baker, Plug et al. 1996).

While Orthologs of each of these mismatch repair proteins have been identified in mammals, in *Drosophila* the only gene that has been identified thus far is the *Msh2* ortholog,, encoded by *spellchecker1* (Buermeyer, Deschenes et al. 1999; Flores and Engels 1999; Sekelsky, Brodsky et al. 2000). Flores *et al* reported that *spel1*-null mutants are viable and fertile but have high increased rates of instability in dinucleotide repeats when these repeats are transmitted normally through the germ line or when copied into the site of a double-strand break during gene conversion (Flores and Engels 1999)

1.4.1 Recombination nodules

Meiotic recombination is also associated with a structure called the recombination nodule (RN); RNs have been observed in plants, *Drosophila*, humans, and mice during meiosis and are thought to contain repair factors (Carpenter 1975; Anderson, Offenberg et al. 1997). In 1975, Carpenter reported the existence of RNs as electron-dense structures located between and adjacent to the chromatin of paired homologues during meiosis in *Drosophila* females (Carpenter 1975). Based on her electron microscope studies, Carpenter described the progression of RNs and reported that the average size of recombination nodules increases with advancing developmental age. In addition, Carpenter reported the existence of two different

types of RNs: ellipsoidal and spherical. Ellipsoidal nodules, which were smaller in diameter, were observed first and spherical nodules, which were bigger in diameter, appeared last (Carpenter 1979). It remains unclear if ellipsoidal RNs are precursors of spherical RNs or if they both emerge in separate stages (Carpenter 1979). Early and late RNs have also been described in other organisms (Anderson, Offenberg et al. 1997; Anderson and Stack 2005).

It was suggested by Carpenter and others that RNs may represent recombination sites and late RNs/spherical RNs may correspond to CO (Carpenter 1979, Anderson, Offenberg et al. 1997, Plug, Peters et al. 1998). Carpenter's description of RN correlates with the number and chromosomal location of recombination sites during zygotene-pachytene of meiosis 1 (Carpenter 1975; Carpenter 1979). For example, the average number of late RNs per nucleus (5 RNs) is in agreement with the number of CO sites per nucleus (5 to 6), as established by genetic experiments in flies (Carpenter 1975; Miller, Takeo et al. 2012). In addition, RNs were found in the distal portions of the bivalent arms, associated with SC of euchromatic morphology; none were found associated with the proximal, chromocentral portions of SC (Carpenter 1975). Later studies in plants showed that certain RNs contain Rad51, providing some evidence that RNs may correspond to complexes of proteins involved in recombination (Anderson, Offenberg et al. 1997). RNs in Anderson *et al*. studies were observed on an electron micrograph after immunogold labeling of an antibody against Rad51 (Anderson, Offenberg et al. 1997).

Studies done in mammalian cells using fluorescence immunocytochemistry techniques suggest that other proteins, such as RPA, MLH, and Rad51, may be components of RNs (Plug, Peters et al. 1998). It seems likely that the foci labeled by antibodies against these DNA damage repair factors correspond to RNs because of their striking similarities in the distribution pattern on synapse chromosomes and the similarities in the numbers of late RN and CO found in meiotic chromosomes. However, these electron-dense structures found in EM studies are not a reliable predictor for HR foci, due to the following reasons: 1) in some studies, the number of early RNs exceeded the one of actual Hr foci (Anderson, Offenberg et al. 1997, Anderson and Stack 2005), 2) in the case of flies, the studies were not exhaustive; however, the number of total RNs counted (including early and late) was fewer than the later determined average with □-H2Av (Carpenter 1975), 3) data provided by Lohmiller *et al*. using *Arabidopsis thaliana* and *Solanum lycopersicum* (tomato) as the model organisms showed that Mre11 is associated with SC components, but Mre11 is not a major component of most early RNs (Lohmiller, De Muyt et al. 2008), and 4) Carpenter published that MeiW68 mutants have some late large abnormal foci (Carpenter 2003).

RNs were described nearly 3 decades ago and since then no other studies have addressed the relationship between RNs and HR sites. Although there are some inconsistencies, RNs could be a potential predictor of persisting DSBs. This makes it important to develop more reliable markers with direct links to DNA damage

1.5. Introduction to *Drosophila* female meiosis

Drosophila is a great system for the study of DNA repair events during meiosis. In *Drosophila,* as in other organisms during meiosis, the breaks are made endogenously and can be studied without artifacts; however in Drosophila the progression of breaks can be followed in a temporal order in the same structure due to the organization of the *Drosophila* ovary. *Drosophila* germ cells going through meiotic recombination are contained in cysts that are arranged in temporal order according to developmental stage. As outlined above, flies have all repair factors and ionizing radiation-induced foci (IRF) have been observed in flies (Kusch, Florens et al. 2004). *Drosophila* and human DDR factors, such as components of the MRN complex, γ-H2Av, spn-A/Rad51, Okra/Rad54, are highly conserved both in structure and function. Furthermore, factors such as spn-A/Rad51 could be studied due to the fact that, in contrast to humans, mutants are viable in *Drosophila*, but specifically impaired in HR.

Drosophila females have two ovaries and each ovary is composed of about 16 ovarioles. Each ovariole has a structure called the germarium (see figure 3a, 3b) and a structure called the vitellarium (see figure 3a). The vitellarium is a successive array of egg chambers that develop while they move posteriorly inside the ovariole. The germarium contains several cysts of 16 cells that move from the tip or anterior part of the germarium to the bottom or posterior end or the germarium as it goes through meiosis I. It is believed that each cyst is positioned or organized according

to developmental stage. However, the position of a cyst is only a rough guide to its meiotic stage and thus a cyst's absolute position in the germarium is not necessarily equivalent to a specific stage in meiotic prophase, (Carpenter 1975; McKim, Jang et al. 2002). The germarium is divided into 3 regions: Region 1, 2 and 3 (figure 3b). Region 1 is considered a pre-meiotic stage. Cyst formation starts in region 1, when a stem cell divides asymmetrically into a stem cell and a cystoblast. The cystoblast then divides four times with incomplete cytokinesis. After the four divisions, a cyst with 16 cells interconnected by specialized cleavage furrows or ring canals is produced. The cystoblast divides in such a way that the first two daughter cell have four ring canals, the next two cells have three ring canals, the next four retain two ring canals and the rest of the cells retain one ring canal. The two cells that have four ring canals become the pro-oocytes and the other 14 cells are referred to as nurse cells. In later stages, one of the two pro-oocytes will become the oocyte and the other will take on a nurse cell fate. Region 2 is further divided into region 2a and 2b.

Region 2a starts with the completed 16 cells cysts. It is believed that during region 2a zygotene ends and pachytene begins. Cysts move rapidly through zygotene and thus when germaria were analyzed, few cysts were observed in this meiotic stage (Huynh and St Johnston 2000; Mehrotra and McKim 2006). Most of the 2a cysts are found in pachytene, the region where meiotic recombination takes place. The following findings support the idea that pachytene occurs in region 2a: 1) Pro-oocytes and 3 ring canal nurse cells have their homolog chromosomes aligned

along the SC (Carpenter 1975; Carpenter 1979; Huynh and St Johnston 2000), 2) the presence of RNs has been reported in region 2a and some circumstantial evidence associates RNs with recombination sites (see above)(Carpenter 1975; Carpenter 1979), and 3) The appearance in this region of γ-H2Av (Mehrotra and McKim 2006).

In region 2b the pro-oocytes have a more elongated shape and the cyst expands the whole width of the germarium. Additionally, in region 2b Orb (a cytoplasmic RNA binding protein) accumulates in the oocyte indicating that oocyte specification has occurred (Lantz, Chang et al. 1994). However, it is unknown exactly when and how oocyte specification occurs, studies done by the St. Johnston and Richman groups suggest that oocyte specification starts as early as region 2a and is dependent on factors such as BicD and Egl (Huynh and St Johnston 2000), (Riechmann and Ephrussi 2001). Since the transition between region 2a and 2b is not clearly definable, it is still debated whether HR is completed in 2a (Riechmann and Ephrussi 2001) or in early 2b (Mehrotra and McKim 2006). Therefore, region 2b is not very useful for the staging of meiocytes for HR studies.

By region 3, the oocyte has already been singled out, and it is believed that meiotic DSBs have been repaired, as in this stage no RNs were observed nor γ-H2Av staining seemed to be present in the oocyte. Due to the absence of RNs and γ-H2Av it is believed that at this stage meiotic DSBs have been repaired. (Carpenter 1979; Mehrotra and McKim 2006),. Although DSBs are most likely repaired, pachytene continues; the phase between completion of HR and onset of diplotene is referred

to as late pachytene (lpt) (Ashburner 1989; Mehrotra and McKim 2006). In the case of female meiosis, lpt would include a developmental phase beginning with the singling out of the oocyte in region 2b until the vitellogenic stage 14 of oogenesis (Ashburner 1989; Spradling 1993).

1.5.1. Markers for meiotic progression

Localization and dynamics of C(3)G, a structural component of the SC, have been extensively characterized by the Hawley group and it is thus a useful marker for oocytes, pro-oocytes and definition of cyst staging (Page and Hawley 2001). When the *Drosophila* germarium is stained with anti-C(3)G antibodies, the two cells with four ring canals (pro-oocytes) of each cyst in region 2a begin to show a thread like staining (Page and Hawley 2001). In addition some of the three ring canal cells in region 2a cysts show C(3)G staining to a variable extent (Page and Hawley 2001). In region 2b, according to Page and Hawley studies anti-C(3)G antibody marks the two pro-oocytes and even though both pro-oocytes stain with C(3)G in region 2b only one of the two pro-oocytes is marked with Orb (Page and Hawley 2001). However, it has also been observed that C(3)G staining is more prominent in one of the two pro-oocyte (present study). In addition a study has reported that C(3)G staining is only present in the oocyte in 2b (Riechmann and Ephrussi 2001). These observations may be due to the fact that oocyte selection is a continuous process, as not all of the depicted stages are simultaneously present in one germarium *in vivo* (Riechmann

and Ephrussi 2001). Furthermore, if one considers that the cysts are positioned relative to the developmental stage, then, the observation of C(3)G staining being more prominent in one of the two pro-oocyte or only in one can represent a more advance region 2b. By region 3 only the oocyte shows C(3)G staining, however C(3)G treat like staining starts disintegrating or falls apart until it is lost at about stage 6 of the vitellarium (Page and Hawley 2001).

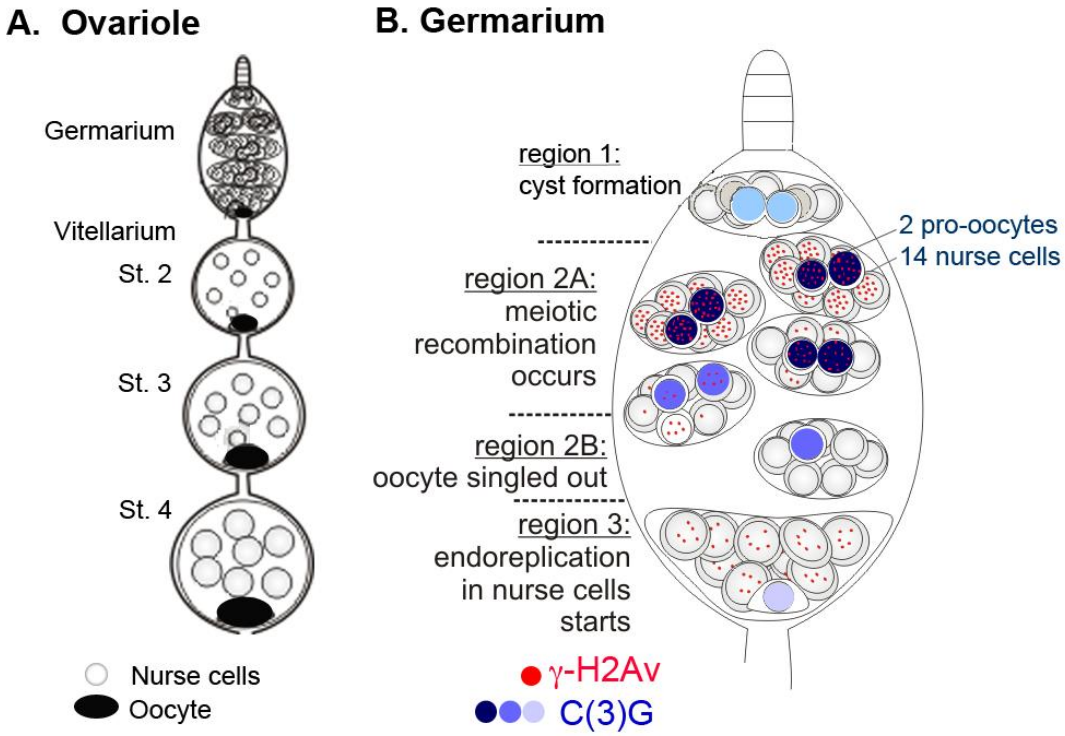

Figure 3: Structure of the Drosophila ovary. (A) Ovariole. Each ovariole is composed of a structure called the germarium and another called the vitellarium. The vitellarium is a successive array of egg chambers that develop while they move posteriorly inside the ovariole. Each egg chamber is composed of the oocyte, 15 nurse cells and follicle cells. (B) The germarium is divided into three regions: Region 1, region 2, and region 3. Region 1 is where cyst formation takes place, a stem cell divides asymmetrically into a cystoblast and a stem cell and then the cystoblast has four round of incomplete division creating a 16 cell cyst in which two cells become the pro-oocytes and the rest of the cells are refer to as nurse cells. Region 2 is divided into 2a and 2b. Region 2a starts with the complete cyst and it is the region where meiotic recombination is believed to take place. Early 2a, or early pachytene, is characterized by the appearance of γ-H2Av (red dots) in pro-oocytes and nurse cells; in addition to the complete formation of the synaptonemal complex (blue), usually marked by the synaptonemal protein, C(3)G, in both pro-oocytes. In late 2a -2b, between early and late pachytene,γ--H2Av numbers start decreasing in the pro-oocytes and are very reduced in the nurse cells. In this region the synaptonemal complex starts disintegrating in one of the pro-oocytes and the oocyte is singled out. By region 3, late pachytene, only the oocyte is marked by C(3)G and □-H2Av has been lost from the oocyte; however, □-H2Av appears in this the nurse cells.

In addition to C(3)G, the dynamics of γ-H2Av have also been characterized and serve to identify stages in oogenesis. γ-H2Av is observed in region 2a, and its appearance in this region is used to mark entry into pachytene. γ-H2Av foci in this early region 2a, also referred to as early pachytene, are detectable in nurse cells and in pro-oocytes (Jang, Sherizen et al. 2003; Mehrotra and McKim 2006). The numbers of γ-H2Av foci in pro-oocytes/oocytes decrease by region late 2a-2b; in addition the

number of γ-H2Av foci in nurse cells is very reduced at this stage. By region 3 (late pachytene) γ-H2Av foci have disappeared from the oocyte (Page and Hawley 2001; Jang, Sherizen et al. 2003), Mehrotra and McKim 2006). However, γ-H2Av is detected in nurse cells of region 3 (Lake, Holsclaw et al. 2013). The observed γ-H2Av in nurse cells in region 3 is not attributable to meiotic induced DSBs but rather to the first endocycle S phase, which occurs only in the nurse cells (Lilly and Spradling 1996) (Hong, Narbonne-Reveau et al. 2007).

2. DNA repair within chromatin

In eukaryotes, the DNA is compacted into and protected by a protein-DNA structure called chromatin. The fundamental repeating unit of chromatin is the nucleosome, a structure that consists of 147 base pairs of DNA wrapped around two copies of each of the four core histones (Margueron and Reinberg 2010). In order for processes such as DSB repair to take place, the cell must locally and transiently open up chromatin to allow access for repair factors. Chromatin can be modified and thus be opened or closed by different mechanisms, such as posttranslational modification of histones, incorporation and/or exchange of histone variants, and ATP-dependent chromatin remodeling (Price and D'Andrea 2013; Smeenk and van Attikum 2013). During the DNA damage response, chromatin needs to be modified most likely at several different steps. First, once the break is made, chromatin modifications need to occur promptly to allow the binding of the DSB recognition

machinery. At later stages of the HR pathway, chromatin must also be modified to allow homology search and strand invasion. Finally, once DNA is repaired, chromatin needs to be resected (Kusch, Florens et al. 2004; Smeenk and van Attikum 2013).

2.1. Histone posttranslational modification

Histones have highly basic N-terminus and C-terminus tails that protrude out of the nucleosome. Histone tails can be posttranslational modified by acetylation, phosphorylation, methylation, ubiquitination, sumoylation, ADP-ribosylation, and others (Bannister and Kouzarides 2011). These modifications can affect chromatin structure primarily via two mechanisms: first, modifications of histone tails that protrude out affect inter-nucleosomal interaction, and as a result affect the chromatin structure. Second, histone tail posttranslational modifications also serve as docking platforms for other proteins, such as ATP-dependent chromatin modifier complexes that can alter the chromatin landscape (Bannister and Kouzarides 2011).

The important roles of phosphorylation of H2Av in DSB repair have already been explained above; however, there are other histone posttranslational modifications that have functions at different stages of DSB. For instance, H3K4me3 marks meiotic recombination initiation sites in *Saccharomyces cerevisiae* (Borde, Robine et al. 2009) and hot spots in mammals (Buard, Barthes et al. 2009; Grey, Barthes et al. 2011). Another important histone modification is dimethylation of histone H4 on lysine 20 (H4K20me2). In yeast, Set9 is the methyltransferase

responsible for this methylation, and in mammals it is set7/8. Mutations in Set9 and H3K20me2 severely reduce cell viability after exposure to genotoxic agents. H4K20me2 is linked to the recruitment of Crb2 and its mammalian homolog, 53BP1, to the DSB (Sanders, Portoso et al. 2004; Botuyan, Lee et al. 2006). Thus, this histone posttranslational modification may function as a scaffold for DDR factors.

After repair has occurred, chromatin has to be restored. Studies done by Chen et al suggested that, in yeast, Histone H3 acetylation on lysine 56 (H3K56ac) is necessary for reassembly of chromatin after DNA repair has occurred (Chen, Carson et al. 2008). Later studies showed that CBP in *Drosophila* and p300 in humans acetylate H3K56; additionally, chaperones Caf1 and CAF1 in *Drosophila* and humans, respectively, are needed for H3K56ac nucleosome incorporation into chromatin. It was shown that H3K56ac-containing nucleosomes are incorporated into chromatin after DNA damage (Das, Lucia et al. 2009). *Drosophila* Tip60 (dTip60) is an example of a chromatin modifier complex involved in chromatin restoration post repair. (Kusch, Florens et al. 2004). *Drosophila* S2 cells where dTip60 was knocked down lose the transient acetylation of H2Av that normally occurs after exposure to γ-irradiation; in addition S2 cells showed persistent accumulation of phosphorylated H2Av following exposure to DNA damaging agents. (Kusch, Florens et al. 2004). Additionally, in humans, cells with mutated Tip60 fail to repair DSB efficiently and lose their apoptotic competence (Ikura, Ogryzko et al. 2000).

Another example of histone posttranslational modification involved in DNA repair is ubiquitination of H2B (uH2B). This histone posttranslational modification

has been shown to be involved in mitotic cell growth and meiosis in (Robzyk, Recht et al. 2000). Rad6 was identified as the major ubiquitin conjugating enzyme that ubiquitinates H2B in yeast (Robzyk, Recht et al. 2000). *Rad6* mutants of *S. cerevisiae* showed higher X-ray sensitivity and abolish meiotic spore formation, in addition to failure to commit to meiotic recombination (Game and Chernikova 2009). These studies demonstrate the role of chromatin-remodeling complexes during the repair of DSBs; in addition, they show that histone modifications can recruit complexes that are able to manipulate chromatin in order to assist in repair

2.2. ATP-dependent chromatin remodeling complexes

All ATP-dependent chromatin-remodeling complexes contain a similar ATPase domain and are part of the SNF2 family, which has four subfamilies: SWI/SNF, ISWI, CHD and INO80 (Eberharter and Becker 2004; Morrison and Shen 2006). Members of the SNF2 family utilize energy from ATP hydrolysis to slide nucleosomes, to remove or exchange H2A-H2B dimers, to disrupt DNA/histone interactions, to evict histones, and to restructure nucleosomes (Eberharter and Becker 2004; Morrison and Shen 2006). All of the subfamilies share a role in transcription activation and/or repression. In addition, each family member seems to have special functions; for instance, the ISWI family has been shown to be important for DNA chromatin reorganization after replication, members of the CHD family have roles in the maintenance of pluripotency in stem cells, and the INO80

and SWI/SNF family have roles in DSB repair (Review in: Wang, Allis et al. 2007; (Clapier and Cairns 2009).

2.2.1. INO80 family of chromatin remodelers

The two main subfamilies of this group of remodelers in yeast are SWR1 and INO80, with Swr1 and Ino80 being the catalytic subunits, respectively (Bao and Shen 2007; Conaway and Conaway 2009). We already talked about one SWR1-like complex in higher eukaryotes: Tip60. dTip60 is the *Drosophila* related SWR1 complex (Kusch, Florens et al. 2004). Humans have two SWR1 like complexes: SRCAP and TRRAP/Tip60 (Kusch, Florens et al. 2004; Cai, Jin et al. 2005). The catalytic subunits of dTip60 are dTip60,an acetyltransferase, and Dom, an ATPase. The catalytic subunit of SRCAP and TRRA/Tip60 are SRCAP and p400, respectively (Watanabe and Peterson 2010).

The catalytic subunit of each complex has a characteristic insertion in the middle of ATPase domain (split ATPase domain). Deletion of this middle insertion abolishes the binding of helicase-related (AAA-ATPase) Rvb1 and Rvb2 proteins, two highly-conserved ATPases that are also part of INO80 and SWR1 complexes. Rvb1 and Rvb2 are essential for viability and for the chromatin remodeling of the INO80 complex. (Bao and Shen 2007; Conaway and Conaway 2009; Watanabe and Peterson 2010). Aside from the ATPase domain, each catalytic subunit within this family also shares a highly-conserved helicase associated SANT domain (HAS). HAS is known to

be the binding site for actin and actin-related protein 4 (Arp4), which are two common components of the yeast INO80 and SWR1 complexes. Actin and Arp4 share an ATP-binding pocket known to bind ATP, but mutations in this domain do not seem to affect the function of the INO80 complex (Bao and Shen 2007; Conaway and Conaway 2009; Watanabe and Peterson 2010).

2.2.1.1. SWR1

As mentioned before, the major known function of SWR1 is incorporation of H2AZ into nucleosomes; it specifically replaces the H2A/H2B dimer for the H2AZ/H2B dimer (Kobor, Venkatasubrahmanyam et al. 2004; Mizuguchi, Shen et al. 2004). Each of the histone H2A variants, H2AX and H2AZ, has been shown to be important in DSB repair. I have already discussed the very important roles of H2AX; however, H2AZ also plays a role in DDR and is highly conserved throughout eukaryotes (reviewed in: (Zlatanova and Thakar 2008). Studies conducted by Marian Kalocsay *et al* 2009 in *S. cerevisiae* showed that H2AZ was found transiently around DSBs and that H2AZ deletion mutants are hypersensitive to DSB-inducing agents. This study also showed that DSB repair foci movement to the periphery seems to be highly dependent on H2AZ sumoylation (Kalocsay, Hiller et al. 2009). Although H2AZ functions have been studied in yeast, not much is understood about its role during DSB repair in higher eukaryotes. H2AZ has also been involved in several cell processes: regulation of transcription, controlling genomic integrity, spreading of

heterochromatin and progression through the cell cycle (reviewed in: (Zlatanova and Thakar 2008).

Besides the above described subunits that are common between INO80 and SWR1, each subfamily has specific subunits. Yeast SWR1 unique subunits are Arp6, Yaf9, Bdf1, Swc2, Swc3, Swc4, Swc5, Swc6, and Swc2. Arp6 interacts with the ATPase domain, but its precise role is not known. Yaf9 is similar to Taf14, and *in vitro* studies indicate that Yaf9 and Swc4 are required for the transfer of H2AZ. Swc2 is the second largest subunit in the complex, and its N-terminus interacts with the histone H2AZ. In addition, Swc2 binds to Swc6 and Arp6, forming a histone chaperone sub-complex that binds to Swr1 and is important for chromatin remodeling activities of the complex (Bao and Shen 2007; Watanabe and Peterson 2010). The functions of Swc3/5 are not known but they do not affect the remodeling activity of the complex. Bdf1 contains a bromodomain, which is capable of recognizing acetylated lysine residues on histone tails, known to be important for H2AZ incorporation. (Raisner, Hartley et al. ; Zhang, Roberts et al. 2005; Altaf, Auger et al. 2010).

2.2.1.2. INO80 complex

INO80 complex has been greatly studied in yeast and it has been shown that it differs from the human and the *Drosophila* INO80 complex (Jin, Cai et al. 2005; Klymenko, Papp et al. 2006; Wu, Shi et al. 2007; Yao, Song et al. 2008). The yeast

INO80 complex subunits are Arp5, Arp8, Ies2, Ies6, NHP10, Taf4, Ies1, and Ies3-5. Arp5 and Arp8 are required for the chromatin remodeling activities of the complex. *Arp5* and *Arp8* mutants have compromised *in vitro* ATP binding, nucleosome mobilization, and ATPase activity (Bao and Shen 2007; Watanabe and Peterson 2010). It is important to note that Arp4 has been shown to bind to all four histones, and Arp8 has been shown to bind to H3 and H4; as such, they may also be helping in the complex-chromatin interactions. A unique yeast INO80 subunit is NHP10, a HMG-1-like protein that can bind to DNA wrapped around histones. Mutations in the NHP10 subunits reduce the ability of the complex to bind DNA; however, the ability of the complex to remodel nucleosomes is not affected (Bao and Shen 2007). Taf4, Ies1, and Ies3-5 are also yeast INO80 unique subunits, although not much is known about their structure and molecular function. However, Ies2 and Ies6 subunits may have important roles in the complex, due to the fact that they are highly conserved in yeast and humans. (See Table 1)

Our laboratory has characterized the *Drosophila* INO80 (dINO80) complex (see Table 1 –data generated by Thomas Kusch-, unpublished data), which had only been partially characterized before (Klymenko, Papp et al. 2006). Our studies showed that arp5, arp8, Ies2 and Ies6 are conserved subunits between yeast, humans and flies, (table 1) (Jin, Cai et al. 2005). Interestingly, when INO80 complex composition was studied via mass spectrometry, several independent tandem-affinity purifications of Ino80 showed substoichiometric amounts of dMre11 and dRad50 peptides (see table 1). In addition the dINO80 complex shares subunits with

the human complex that are not present in yeast; these subunits include YY1, UCHL3, and NFRKB (Jin, Cai et al. 2005; Klymenko, Papp et al. 2006; Wu, Shi et al. 2007; Yao, Song et al. 2008). YY1 and its *Drosophila* homolog, pho (polycomb group protein pleiohomeotic) are DNA-binding proteins with a role in maintaining chromosome integrity. A study conducted by Su Wu *et al*. 2007 showed that mouse embryonic fibroblasts (MEF) deficient in YY1 have chromosomal abnormalities such as aneuploidy, polyploidy, chromatid and chromosome breaks (Wu, Shi et al. 2007). Additionally, RNAi-mediated knockdown of YY1 resulted in increased sensitivity to genotoxic agents (Wu, Shi et al. 2007). UCHL3 is a deubiquitinating enzyme that is part of the proteasome, but not much is known about its role in DNA repair. NFRKB is a DNA-binding protein but very little is known about its function. A recent study by the Conaway group shows that UCHL3 association with INO80 is mediated by an interaction with the N-terminus of NFRKB (Yao, Song et al. 2008).

The INO80 complex has roles in replication, transcription, and DNA repair. For example, it has been shown that during DNA replication in yeast, the INO80 complex contributes to the efficient progression of the replication fork by stabilizing stalled replication forks and reinitiating replication under stress conditions (Papamichos-Chronakis and Peterson 2008; Shimada, Oma et al. 2008). Studies done by Vincent et al suggest that yeast INO80 may also help in efficient replication fork progression in the absence of replication stress (Vincent, Kwong et al. 2008). INO80 in humans as well as in yeast is involved in transcription regulation of some

genes (Jonsson, Jha et al. 2004; Mizuguchi, Shen et al. 2004; Cai, Jin et al. 2007). INO80 has been shown to regulate transcription of up to 20% of the genes in yeast; the expression of this subset of genes can be negatively and positively regulated by INO80 (Jonsson, Jha et al. 2004; Mizuguchi, Shen et al. 2004).

2.2.1.2.1.INO80 complex in DSB repair

Several studies primarily using yeast as the model organism show that INO80 is involved in DSB repair. Mutations in different subunits of the yeast INO80 complex exhibit hypersensitivity to agents such as Methyl methane sulfonate (MMS) and Hydroxyurea (HU) (Shen, Xiao et al. 2003; Morrison, Highland et al. 2004; van Attikum, Fritsch et al. 2004). The exact contribution of INO80 in HR or NHEJ is debatable in part due to the difficulty of obtaining viable null *Ino80* mutants. Null mutants of *Arp5* and *Arp8* have been obtained, and it has been shown that they exhibit decreased efficiency in NHEJ and HR (Morrison, Highland et al. 2004; van Attikum, Fritsch et al. 2004; Tsukuda, Fleming et al. 2005; Tsukuda, Lo et al. 2009). However, studies conducted by Papamichos-Chronakis *et al* reported that when the first 900 bp of the Ino80 protein were deleted, a viable null mutant was obtained; although the extent of the ATPase functionality in the mutant was not addressed, the mutant did not show a significant decrease in HR and NHEJ efficiency (Papamichos-Chronakis, Krebs et al. 2006). In yeast, the recruitment of chromatin remodelers to DSBs has been studied mostly in asynchronous cell populations, making it difficult to distinguish their involvement in either NHEJ or HR. Recent

studies in which a single DSB was induced within yeast cells synchronized in either G1 or G2/M cell cycle phases in conjunction with chromatin Immunoprecipitation (ChIP) assays to follow recruitment of many chromatin regulators showed that INO80 is primarily involved in HR and not in NHEJ (Bennett, Papamichos-Chronakis et al. 2013).

Two studies in mammalian cells suggest that Ino80 is important for DNA repair --INO80 deficient cells are hypersensitive to DNA damage and exhibit DNA repair defects (Wu, Shi et al. 2007). Furthermore the use of an HR reporter assay where DSBs were introduced by the endonuclease I-SceI suggests that INO80 may function in Homologous recombinational repair (Gospodinov, Vaissiere et al. 2011).

Moreover, Immunoprecipitation experiments (ChIP) have shown that INO80 subunits, (Ino80p, Arp8, Arp5, and Arp4), are recruited to a DSB (Downs, Allard et al. 2004; Morrison, Highland et al. 2004; van Attikum, Fritsch et al. 2004). ChIP assays have also shown that Ino80 maximum levels are found in the region 0.2 to 1.6 Kb away from the break, and that these levels are back to non-inducible levels at about 9 to 10 kb away from the break (Morrison, Highland et al. 2004; van Attikum, Fritsch et al. 2004; Tsukuda, Fleming et al. 2005). There are indications that INO80 is recruited to the DSB to open up chromatin by evicting nucleosomes. Histones are lost around the DSB after induction with an HO endonuclease (Tsukuda, Fleming et al. 2005; Chen, Carson et al. 2008), and INO80 mutants are deficient in the loss of histone around the DSB (van Attikum, Fritsch et al. 2004; Tsukuda, Fleming et al.

2005). All together these suggest that INO80 is involved in nucleosome remodeling around the DSB.

But how is INO80 recruited to the DSB? INO80 recruitment has been extensively studied in yeast; however, the available data from different groups is conflicting, and there is only one study in higher eukaryotes addressing INO80 recruitment to the DSB (Kashiwaba, Kitahashi et al. 2010). Three independent studies done in yeast support a model in which the INO80 complex is recruited to a DNA damage site through an interaction with γ-H2AX (Morrison, Highland et al. 2004; van Attikum, Fritsch et al. 2004; van Attikum, Fritsch et al. 2007). Morrison *et al* and Van Attikum *et al* suggest that INO80 is recruited to DSBs via a direct interaction of NHP10 or ARP4 with γ-H2AX (Morrison, Highland et al. 2004; van Attikum, Fritsch et al. 2004; van Attikum, Fritsch et al. 2007)). As mentioned before, Arp4 is also present in SWR-C, NuA4 and Swi/Snf complexes; thus, specific recruitment of INO80 to DSB via Arp4 binding to γ-H2A.X is questionable. In the case of NHP10, it is important to note that mammals do not have a homolog for this subunit; as such, it can be surmised that an alternative mechanism must occur in higher eukaryotes (Conaway and Conaway 2009, (Bennett, Papamichos-Chronakis et al. 2013).

In addition to the discrepancies in the interaction of INO80 subunits with γ-H2AX, several other facts argue against this mechanism: first, Ino80 and γ-H2AX distribution patterns in the genome after DSB induction do not overlap; as

mentioned before, in yeast H2A is phosphorylated up to 50 kb from the break, and is thus not found at 1-2 kb away from the break. In contrast, Ino80 is found in a region 0.2 to 1.6 kb from the break. Besides the fact that they do not overlap**,** it would be very difficult to have a specific recruitment of INO80 to the DSB via γ-H2AX interaction, since phosphorylation of H2AX spreads away from the break. Second, INO80 interaction with H2AX is not damage-specific since it has been shown in yeast that INO80 and H2AX interact before and after damage (Mizuguchi, Shen et al. 2004; van Attikum, Fritsch et al. 2004). Far more importantly Ino80 interacts with all four core histones at equal levels before and after induction of DNA damage by MMS (Morrison, Highland et al. 2004). Third, studies suggest that histone loss around the DSB is not the result of INO80 recruitment by γ-H2AX, due to the fact that histone loss around the DSB occurs normally in a yeast strain where H2A.X cannot be phosphorylated (Tsukuda, Fleming et al. 2005). Importantly, a recent study in yeast using CHIP assays showed that γ-H2AX is not essential for the recruitment of several chromatin remodeler complexes, including INO80, to the DSB (Bennett, Papamichos-Chronakis et al. 2013). Furthermore, studies done using mammalian cell lines show that INO80 is recruited to a laser-induced DNA damage site independently of □-H2AX (Kashiwaba, Kitahashi et al. 2010).

Studies done by other groups suggest that a different mechanism for INO80 recruitment to the DSB may exist. Van Attikum *et al* 2007 showed that yeast INO80 mutants, specifically Arp8 and NHP10 mutants, have impaired binding of MRE11, ku80, Mec1/Tel1 at DSB (van Attikum, Fritsch et al. 2007). These studies suggest that

INO80 recruitment is a very early step, and that the complex may get to the break before the MRN complex and also before the kinases ATR and ATM that are in charge of phosphorylating H2AX.

Several other yeast studies suggest that INO80 may be remodeling chromatin around the DSB during formation of the presynaptic filament, facilitating strand resection, and also helping in later stages during homology search (Morrison, Highland et al. 2004; van Attikum, Fritsch et al. 2004; Tsukuda, Fleming et al. 2005; Tsukuda, Lo et al. 2009). A role of INO80 in end resection is suggested by studies in which Arp8 mutants have a significant reduction in the formation of ssDNA and reduce recruitment of Mec1; interestingly, as mentioned before, γ-H2A.X has been claimed to recruit Ino80 to DSBs (Morrison, Highland et al. 2004; van Attikum, Fritsch et al. 2004; Tsukuda, Fleming et al. 2005; Tsukuda, Lo et al. 2009). Studies conducted by the Nickoloff and Osley group made use of the matting type switching system in yeast to address a possible role of INO80 in homology search. The mating type switching is a good system because the dynamics of HR factors in a single locus after DSB induction can be studied. Mating type is determined by the *MAT* locus which contains either the **a**1 gene (*MAT**a***) or the α1 and α2 genes (*MAT*α). Switching occurs through intrachromosomal gene conversion where an HO endonuclease-induced a double-strand break (DSB) at *MAT.* The break is repaired by recombining with *HML*α or *HMR***a** two conserved regions located at opposite ends of the chromosome. Although the recognition sequence for the HO

endonuclease is within one of the conserved sequences of *MAT*, *HML*, and *HMR,* cleavage by HO only occurs at MAT because of the silenced chromatin at *HMR* and *HML* blocks access of the endonuclease to these loci (Haber 2012). As opposed to other INO80 studies where the homolog template was deleted, Nickoloff and Osley's study was done in the presence of a homolog template enabling the authors to address a possible role of INO80 in homology search. In this study it was shown that *arp8* mutants have decreased kinetics in strand invasion, have a delay in the binding of Rad51 to the donor strand, and have defective gene conversion tracks (Morrison, Highland et al. 2004; van Attikum, Fritsch et al. 2004; Tsukuda, Fleming et al. 2005; Tsukuda, Lo et al. 2009).

Ino80 has also been implicated in DNA damage checkpoint adaptation in yeast. Upon DNA damage, cell cycle arrest is induced and maintained until the damage is repaired. In yeast, cells are able to exit the cell cycle checkpoint arrest without repairing the DSB after an adaptation period of about 15 hours. Papamichos-Chronakis *et al* have shown that Ino80-deficient cells have defects exiting the adaptation checkpoint upon DSBs (Papamichos-Chronakis, Krebs et al. 2006).

Recent studies have suggested that INO80 enhances the general mobility of chromosomal loci. Neumann, Dion *et al* have showed that a tagged locus increases its mobility upon induction of a DSB in an INO80-dependent manner and suggested that the chromatin remodeling activity of INO80 most likely 'frees up' DSBs for further mobilization (Neumann, Dion et al. 2012). This mechanism could be

important because movement of chromosomal loci can contribute to a homology search during repair processes.

In addition to its ability to remodel chromatin by evicting histones, INO80 also has the ability of dimer-exchange, similar to SWR-C. INO80 has been implicated in the dynamics of H2AZ at a DSB. Some of the first studies show that *Ino80* mutants have drastically increased H2AZ levels and decreased levels of H2AX phosphorylation around the DSB (Papamichos-Chronakis, Krebs et al. 2006). In addition, this study showed that double *Ino80 and swr1* mutants eliminate H2AZ accumulation at DSB, but restore γ-H2AX function (Papamichos-Chronakis, Krebs et al. 2006). These studies suggested that Swr1 might exchange γ-H2AX with H2AZ, and Ino80 might exchange H2AZ with H2AX. However, later studies done by Van Attikum *et al* suggested that Swr1 does not incorporate or remove H2AZ near the DSB, but INO80 may be evicting H2AZ and γ-H2AX in this region to reincorporate H2A.X (van Attikum, Fritsch et al. 2007).

More conclusive studies done by the Peterson group in which *in vitro* histone exchange assays were used showed that Ino80 removes H2AZ/H2B dimers from nucleosomes and incorporates free H2A/H2B dimers (Papamichos-Chronakis, Watanabe et al. 2011). It is important to note that exchange assays were not DSB specific (Papamichos-Chronakis, Watanabe et al. 2011). Additionally, this study supported previously published data that suggested that Swr1 incorporates H2AZ into H2A nucleosomes. It must be noted that the work has been conducted in yeast,

which utilizes H2A.X as the canonical histone. Therefore, there could be significant differences in higher eukaryotes, especially in flies where the H2AZ variant is fused with H2AX (as mentioned previously, H2AZ is a bifunctional molecule that has conserved sequences of both H2AX and H2AZ).

All of the findings explained above support the idea that ATP-dependent chromatin remodelers have very important roles during different steps of the DNA damage repair pathway. For example, and as mentioned before, INO80 has been shown to have a role in homology search and during the recognition of DNA damage, where it opens up chromatin to allow the loading of recognition and repair factors. Although INO80 has been extensively studied in yeast, little is understood about the exact mechanism that recruits this remodeler to the break. As outlined above, there are a large number of studies in yeast; however, their data suggest a contradictory model in which INO80 is recruited to DNA damage sites via interaction with phosphorylated H2AX. In addition, there are not many studies addressing the role of this remodeler during the repair of meiotic DSBs in higher eukaryotes

Table1. Subunit compositions of the yeast, human and *Drosophila* INO80 chromatin remodeling complexes

Saccharomyces C	***Human***	***Drosophila***
Ino80p	INO80	dIno80
Rvb1p	RUVB-like 1	Pontin
Rvb2p	RUVB-like 2	Reptin
Actin	β-actin	Act5c
Arp8p	ARP8	dArp8
Arp5p	ARP5	dArp5
Arp4p	BAF53a	dArp4/BAP55
Nhp10p		
Taf14		
Ies1p		
Ies2p	IES2	dIes2
Ies3p		
Ies4p		
Ies5p		
Ies6p	IES6	dIes6
	YY1	Pho
	UCHL3	dUCHL3
	NFRKB	dNFRKB
	MCRS1	dMCRS1
	FLJ20309	CG7832
	CCDC95	CG18004
	Amida	
		Mre11
		Rad50

Subunits of the *Saccharomices Cerevisiae*, left column (data obtained from Shen 2000) and human INO80 complex, middle column (data obtained from Conaway 2008). The Drosophila IN080 complex subunits were obtained by mass spectrometry after purifying recombinant double-tagged dArp5, Ies6, UCHL3, and dIno80. In these independent mass spectrometry analyses, few peptides for dMre11 and dRad50 were obtained (data generated by Thomas Kusch).

I. RATIONALE AND OVERVIEW OF OBJECTIVES

The main objective of this work was to establish *Drosophila* female meiosis as a model to study the dynamics of HR site turnover with emphasis on chromatin modifiers like INO80. *Drosophila* female germ cells undergoing meiotic recombination are an excellent system for studying chromatin modification during DNA repair due to the fact that during meiosis, the breaks are made endogenously, and are thus not artifacts. Additionally, progression of breaks can be followed in a temporal order due to the organization of the *Drosophila* ovary. *Drosophila* germ cells going through meiotic recombination are contained in cysts that are arranged in temporal order according to developmental stage.

This work is divided in three sections. In section I, I set out to develop tools that allow the study of early and late repair events during *Drosophila* female meiosis. Although the *Drosophila* female is a great system, there is currently no way to directly and accurately label DSB repair sites. The only antibodies that had been used are antibodies against γ-H2Av (Jang, Sherizen et al. 2003; Mehrotra and McKim

2006; Lake, Holsclaw et al. 2013). Phosphorylation of H2Av does not mark the appearance or disappearance of DSBs accurately. Phosphorylation of H2Av occurs because of ATM activation, which could be induced by chromatin modifications similar to the ones involved in DDR (Bakkenist and Kastan 2003); γ-H2Av is widely spread into chromatin flanking the damage sites (Shroff, Arbel-Eden et al. 2004), and it is not clear whether clearance of γ-H2Av from chromatin after the induction of DSBs indicates that the breaks were repaired or not (Kusch, Florens et al. 2004; EF, M et al. 2011). It should be noted that γ-H2Av could disappear because of signaling problems regardless of whether or not repair has occurred; additionally, γ-H2Av could persist despite successful repair. As mentioned before, Kusch *et al* efficiently demonstrated that the dTip60 complex has a role in γ-H2Av clearance and that the phenotype observed when dTip60 was knocked down is abnormal persistence of γ-H2Av (Kusch, Florens et al. 2004).

Here, I used an antibody against the major component of the MRN complex, Mre11, as a DSB marker and developed a fixation and a staining method that permits the visualization of early and late repair foci through fluorescent microscopy. Mre11 was chosen for this study due to the fact that it is a key factor involved in early and late phases of the repair process, it is in charge of sensing DSBs, tethering the two broken ends and it is involve in later steps of repair process during end resection (Trujillo, Yuan et al. 1998; Trujillo and Sung 2001; Rupnik, Lowndes et al. 2010). In addition when ChIP assays where performed Mre11 signals were found in very close proximity to the break (Shroff, Arbel-Eden et al. 2004). The other two

components of MRN, dNbs and dRad50 were not considered for the development of antiserum for the following reasons: 1) dNbs main function is the nuclear import of MR (Borde, Lin et al. 2004; Rupnik, Lowndes et al. 2010), 2) dRad50 seem to have a less crucial function in recognition and/or repair of DSBs, studies where dRad50 germ line clones were generated showed that γ-H2Av foci are still made (Mehrotra and McKim 2006). In addition, it has been reported that Mre11 binds to chromatin in very close proximity to a DSB during meiosis in Rad50 deficient yeast (Borde, Lin et al. 2004). Therefore, Mre11 could function independent of Rad50 or Rad50 could dissociate from meiotic DSBs during later stages of DSB repair

In section II, I used these methods to study the dynamics of MRN foci in various *Drosophila* mutants for meiotic regulators. Analysis of mutants shed light on the following events: 1) establishment of meiotic recombination foci, 2) differentiation between crossovers and non-crossovers events, 3) subnuclear localization of DSBs and migration of these DSBs to the nuclear periphery, 4) factors involved in the signaling of DSBs movement to the nuclear periphery, and 5) factors involved in the amplification of the DNA damage response in *Drosophila*.

In section III, I assess the potential role of the dINO80 complex during meiotic HR. To date it is still unclear when dINO80 functions at DSBs and how it is recruited to DNA damage sites in higher eukaryotes. As outlined before, studies in yeast suggest a contradictory model in which INO80 is recruited to DNA damage sites via interaction with phosphorylated H2AX (Morrison, Highland et al. 2004; van Attikum,

Fritsch et al. 2004 Morrison, 2004). To summarize, the following discrepancies suggest that other factors are responsible for the recruitment of Ino80: 1) γ-H2AX and INO80 chromatin distribution do not coincide at DSBs (Shroff, Arbel-Eden et al. 2004), 2) histone loss around the DSB occurs normally in a mutant that cannot be phosphorylated (Tsukuda, Fleming et al. 2005), 3) yeast INO80 and H2AX interact before and after damage (Mizuguchi, Shen et al. 2004; van Attikum, Fritsch et al. 2004), and more importantly, 4) INO80 interacts with all four core histones at equal levels before and after induction of DNA damage by MMS (Morrison, Highland et al. 2004). As shown in table 1, preliminary data from our research group, showed that dMre11 and dRad50 peptides were found in substoichiometric amounts in mass spectrometric analyses of several independent tandem-affinity purifications of INO80 complexes. These findings in addition to the fact that: 1) MRE11 mutated strain showed that histone loss around the DSB is significantly impeded (Tsukuda, Fleming et al. 2005). 2) yeast INO80 mutants, specifically arp8 and NHP10 mutants, have impaired binding of MRE11, ku80, Mec1 at DSB (van Attikum, Fritsch et al. 2007) suggested an interaction of dINO80 with MRN. Since MRN has functions during DSB recognition as well as later processes of HR, I first used a series of experiments to address whether or not dINO80 directly interacts with MRN during meiotic HR in *Drosophila* females. Once dIno80-dMre11 interaction was established I also attempted to analyze the functional role of such interaction.

II. MATERIALS AND METHOS

1. Nuclear extracts and Immunoblotting: S2 nuclear extracts were made from 500-ml cultures at a density of 3 x 10^6 cells/ml. The cells were washed twice with ice cold solutions in 10 mM HEPES (pH 7.4)–1 mM dithiothreitol (DTT)–150 mM NaCl and once in cell lysis buffer (20 mM HEPES, pH 7.4, 0.1% Triton X-100, 1 mM DTT, 0.5 mM phenylmethylsulfonyl fluoride (PMSF), 0.1% (wt/vol) leupeptin, 0.2% (wt/vol) pepstatin A). Lyses occurred in 40 ml of lysis buffer when 20 to 30 strokes of a dounce homogenizer were applied (loose pestle; Wheaton). Cell lysis buffer was used to wash the nuclei twice, followed by centrifugation at 2,000g for 10 min. The nuclei were extracted for 1 hour in extraction buffer (20 mM HEPES, pH 7.4, 10% glycerol, 350 mM NaCl, 0.1% Triton X-100, 1 mM DTT, 0.5 mM PMSF, 0.1% (wt/vol) leupeptin, 0.2% (wt/vol) pepstatin A) at 4°C; the amount of extraction buffer used was equivalent to 5 times the volume of the nuclear pellet. Extracts were cleared from the nuclear debris by centrifugation at 20,800g for 10 min at 4°C. The protein concentration was determined with Bradford assays (Bio-Rad). Bio Rad assays were done by first preparing five dilutions of a protein standard (BSA) known concentrations in addition to dilutions of the sample solution. Then, 800 µl of each standard and sample solution were put into a clean, dry test 1.5 ml microcentrifuge tube and incubated at room temperature for at least 5 minutes with 200 µl of Bio Rad dye reagent. Absorbance was then measured at 595 nm. Protein solutions were assayed in triplicates. A standard curve was created by plotting the

absorbance readings obtained from the standard samples and their known concentrations, and then a best-fit line was drawn through the points. Finally, the concentration of the sample was determined using its absorbance reading and the standard curve

After sample concentration was obtained, nuclear extracts (ne) were adjusted to a protein concentration of 5 mg/ml with extraction buffer. For antibody specificity test the ne from wild-type cells, together with ne samples from stable transgenic FH-mre11 tagged cells and mock cells, were separated by an 8% Sodium dodecyl sulfate polyacrylamide gel electrophoresis (SDS-PAGE). Proteins were electrotransferred from the gel to a nitrocellulose membrane (blot). Blot was immunostained for detection of the protein of interest. Proteins bands were visualized by chemiluminescent methods.

2. Antibodies used in Immunoblotting: Guinea pig anti-dMre11 (1:6,000, generated by Thomas Kusch unpublished results), mouse anti-tubulin (1:2000, Sigma), rabbit anti-Rad50 (a gift of M. Gatti) 1:1,000 (Ciapponi, Cenci et al. 2004), rabbit anti-Nbs (a gift from S. Rong) 1:1000 (Gao, Bi et al. 2009), rabbit anti γ-H2Av (1:1,000, Rockland Immunochemicals cat. #600-401-914), rabbit anti-H2Av was used at 1:500 (Joyce, Pedersen et al. 2011), rabbit and guinea pig anti-Ino80 used at 1:6,000 (generated by Thomas Kusch unpublished results).

3. RNAi experiments: dMre11-encoding DNA was amplified by PCR using *Pfu* DNA polymerase. PCR-generated template was used to make dMre11 dsRNA. dMre11 dsRNA was made by using the RNAMaxx High Yield Transcription Kit (Stratagene Catalog #200339) to yield 300-400µg of dsRNA. 1 x 10^7cells in 10 ml medium were transfected with .5 µg dsRNA. As a control, dsRNA from *E. coli* lacZ was added to the same amount of S2 cells. After three days of incubation with RNAi, cells were harvested and nuclear extracts were used for Immunoblotting.

4. Immunoprecipitation: Protein A-Sepharose Resin (Roche) was used for the co-immunoprecipitations. Resin was equilibrated by washing three times at five minute intervals at 4 °C with ice-cold 1 x Phosphate buffered saline, PBS. For these assays, 4 µl of antibody (anti-dMre11, anti-rad50, anti-Nbs or anti-dIno80) were conjugated with 20 µl of equilibrated Resin (Roche). After overnight incubation, the conjugates were washed three times with Immunoprecipitation buffer (20mM HEPES, pH 7.4, 120-350 mM NaCl, 0.1% Triton X-100, 1mM DTT). In addition a 1:5 dilution of a Complete Cocktail of Protein Inhibitors from Roche was added. Then, samples were incubated with 200 µg of nuclear extract for 2 hours at 4 °C in 500 ul of Immunoprecipitation buffer. Immunoprecipitates were washed three times for 10 minutes at room temperature in IP buffer prior before immunoblotting.

5. Genetic techniques: All fly stocks were maintained in standard culturing media at 25°C. Oregon R strain was use as a wild type control for all experiments.

Alleles analyzed in this study include the following:: *mei-218*^{1} (McKim, Dahmus et al. 1996), *mei9*^{a} (Yildiz, Kearney et al. 2004), *mei-W68*^{Z4572} (Bhagat, Manheim et al. 2004), *mei-41*^{D3} (Sibon, Laurencon et al. 1999), *okr*^{WS} (Schupbach and Wieschaus 1991; Ghabrial, Ray et al. 1998), *spn-A*^{1} (Staeva-Vieira, Yoo et al. 2003), *spn-D*^{150} (Tearle and Nusslein-Volhard 1987; Ghabrial, Ray et al. 1998; Abdu, Gonzalez-Reyes et al. 2003), *spn-B*^{BU} (Ghabrial, Ray et al. 1998),(Ghabrial and Schupbach 1999) , *mus301*^{D1} (Boyd, Golino et al. 1981), *H2Av*^{810}*; His2Av*$^{\Delta CT}$ (Clarkson, Wells et al. 1999; Ghabrial and Schupbach 1999), and *tefu*^{8} *e* (Silva, Tiong et al. 2004) *tefu*^{8} is a temperature-sensitive mutant; it was raised at permissive temperature (18 °C), and once flies emerged they were shifted to restrictive temperature (25 °C for the different studies)**.**

6. For studies on INO80 complex: w^{1118}; *Mi{ET1}Ino80*^{MB09416} (minos insertion in the dIno80 locus), *P{EPgy2}Ino80*^{EY09251} (p-element insertion into the dIno80 locus), and *P{EPgy2}l(3)L1231*^{EY04982} (p-element insertion in the ORF of L1231-RA CG 7832) (Bloomington stock center).

For RNAi experiments the UAS-Gal4 system was used. Gal4 is a driver that directs tissue-specific expression of Gal-4 protein. Gal-4 protein is a transcriptional activator that specifically binds to UAS (upstream activation sequence) to enhance transcription of the gene of interest. The following fly lines were used: *y*^{1} *sc***v*^{1}*; P{y*$^{+t7.7}$*v*$^{+t1.8}$*=TRiP.HMS00586} attP2* (Expresses dsRNA for RNAi of dIno80

(FBgn0086613) under the control of UAS), y1sc**v*^{1}*; P{y*$^{+t7.7}$*v*$^{+t1.8}$*=TRiP.HMS00809} attP2* (Expresses dsRNA for RNAi of arp5 (FBgn0038576) under UAS control), and *y*^{1} *v*^{1}*; P{y*$^{+t7.7}$ *v*$^{+t1.8}$*=TRiP.JF01720}attP2/TM3, Sb*^{1} (Expresses dsRNA for RNAi of Arp8 (FBgn0030877) under UAS control). These three stocks were obtained from TRiP, (a genome-scale shRNA resource for transgenic RNAi in *Drosophila)* and have short dsRNAs hairpin under UAS-Gal4 control. In addition, two fly stocks that express Gal4 in the ovary were used: 1. *w[1118];P{GAL4::VP16nos.UTR}*^{MVD1,}(Rorth 1998). 2. *P{COG-Gal4:VP16}*; *P{Gal4-nos.NGT}40*; *P{nos-Gal4-VP16}* (Bloomington stock 31777), a stock that contained homozygous insertions of three *Gal4* constructs and provides robust germline and maternal *Gal4* expression. For knock down of dIno80, *y*^{1} *sc***v*^{1}*;P{y*$^{+t7.7}$*v*$^{+t1.8}$*=TRiP.HMS00586}attP2* was crossed to *w*^{1118}*;P{GAL4::VP16nos.UTR}*^{MVD1,}. For knock down of Arp5 and Arp8 dsRNAi fly lines were crossed to *P{COG-Gal4:VP16}*; *P{Gal4-nos.NGT}40*; *P{nos-Gal4-VP16}*.

Ino80K566A flies: Transgenic flies were generated by the lab (Thomas Kusch, Cristina Ochoa Cardona) and have a mutation in the ATP binding site of dIno80, were lysine at position 566 was mutated to alanine. K566 is a highly conserved residue among different ATPases-helicases; when this residue is mutated in yeast, a functional complex is formed but the protein ATPase activity is affected. (A chromatin remodeling complex involve in transcription and DNA processing). The flies carry a pCaSpeR4 containing a ubiquitin promoter fused to the mutated *dIno80* ORF that drives a moderate level of expression in all tissues. The transgenic flies

were crossed into the *Mi{ET1}Ino80*^{MB09416} homozygous and heterozygous background.

Rescue flies: Rescue constructs (*pUASP(Ino80*) were generated by the lab (Thomas Kusch, Cristina Ochoa Cardona, Grace Chen), the Ino80 ORF (4917 bp) was cloned in the pUASP transformation vector. For rescue experiments, *w*$^{-}$*; pUASPIno-1, Ino{MiET}/TM6B, Tu Hu*, (generated by recombining *pUASP(Ino80*) with *Ino{MiET}/TM6B*) were crossed with w-; *Mi{ET1}*^{Ino80MB09416}*, nos VP16 gal4/TM3, Tb.*

7. Immunohistochemistry: Females were aged for 2-4 days in vials containing males and yeast paste; then females were dissected in ice cold HEM buffer (25mM HEPES pH 7.0, 10mM EGTA, 4mM $MgSO_4$). For dissection: flies were anesthetized and placed in a dissection well. Usually 6 flies per staining were used. In order to separate the ovaries from the body the heads were cut off, then the bodies were transferred to a well with ice-cold HEM buffer. Once in the buffer, the tip of the posterior abdomen was gently pinched off, a small incision was made to expose the ovaries, and then the ovaries were gently pulled off and separated from the rest of the organs. After separation from the body, the two ovaries were placed in a separate well with fresh ice-cold HEM buffer. After all the flies were dissected, the ovaries were fixed. Ovarioles were fixed for a total time of 15 minutes at room temperature (RT) in HEM buffer containing 2% (wt/vol) paraformaldehyde (fixative solution) as follows: 1) Ovaries were transferred to the fixative solution, then the

ovariole sheath was removed and the ovarioles were teased apart, carefully without separating them completely. 2) Ovarioles plus fixative solution were transferred to a 1.5 ml microcentrifuge tube and fixed for the remaining time while rotating at room temperature (RT). Fixed ovarioles were rinsed quickly three times with PBST (1 x PBS plus 0.1% Triton X- 100) and washed twice for five minutes while rotating in PBST. Blocking was done by incubating with PBST containing 1% Fetal Bovine Serum (FBS) for 20 minutes rotating at RT. After blocking, the ovarioles were incubated overnight with primary antibody in PBST containing 1% FBS while rotating at 4°C. Ovarioles were then rinsed twice with PBST and washed three times for ten minutes with PBST while rotating at RT. Secondary antibodies were incubated in PBST for one hour and then washed. Washes were done as follows: first, two quick rinses and three 10-minute PBST washes were performed while rotating at RT. The DNA was then labeled with 4-6-diamidino-2-phenylindole dihydrochloride (DAPI; stock solution, 10 μg/ml in methanol; final concentration, 1:2,000 in PBST). Finally, the ovaries were rinsed once with 1 x PBS and washed once for 10 minutes with 1 x PBS prior to mounting.

8. Antibodies used in Immunohistochemistry: Guinea pig anti-dMre11 (1:30,000); Rabbit anti-γ-H2Av (1:20,000), rabbit anti-Rad50 (1:2,000), rabbit anti-Nbs (1:1000), mouse anti-C(3)G and guinea pig anti-C(3)G, a gift of S. Hawley (1:2000 (Page and Hawley 2001), mouse anti-orb 6H4 and 4H8 were combined and used at

1:500 each ((Lantz, Chang et al. 1994), rabbit anti-H2Av (1:500), mouse anti-lamin ADL67.10 (1:1000; (Riemer, Stuurman et al. 1995), rabbit and guinea pig anti-Ino80 (1:20,000), HP1 (1:1000;(Shareef, King et al. 2001), and Glycoprotein 210 (gp210) (1:000;AGP78.20 Developmental Studies Hybridoma Ban (Filson, Lewis et al. 1985).

The following secondary antibodies were used: DyLight594-conjugated donkey anti-rabbit IgG (1:6,000; Jackson Labs, cat. #711-515-152), DyLight594-conjugated donkey anti- guinea pig IgG (1:6,000; Jackson Labs, cat. # 706-515-148), DyLight488-conjugated anti-guinea pig IgG (1:12,000; Jackson labs, cat. #706-545-148), DyLight488-conjugated anti-rabbit IgG (1:12,000; Jackson labs, cat. #711-485 -152) and alexa350-conjugated goat anti-mouse IgG (1:8,0000; Molecular Probes, cat. #21049).

The ovaries were mounted in Vectashield mounting medium (Vector Labs) prior to microscopy. A Delta vision II Deconvolution Microscope System (Applied Precision, Issaquah, WA) equipped with an Olympus 1x 71 inverted microscope and a high-resolution CCD camera (CoolSnap-fx; Roper Scientific) was used for the collection of the images. Ovarioles were photographed in 0.5 µm optical sections with an Olympus UPLANAPO 20x oil immersion objective (0.8 NA). Series of 0.2µm optical sections of germaria were taken using an Olympus UPLANAPO 60x oil immersion objective (1.4 NA). In addition, pro-oocytes and oocytes were photographed in 0.1 µm optical sections using a UPLANAPO 100x oil immersion objective (1.35 NA). Further processing of the images was as follows: All images

were deconvolved using Huygens software (Scientific Volume Imaging, Hilversum, The Netherlands). Pictures were processed using ImageJ (NIH) and Photoshop (Adobe version 12,1 x64). Image stacks or projections were generated with ImageJ (NIH) using maximum intensity averages. Unless otherwise noted, all images are projection of a series of optical sections taken through whole-mounted germarium and/or ovarioles (maximum intensity projections). 3D reconstructions of pro-oocytes and/or oocytes were done using ImageJ to create three dimensional movies.

9. Statistical analysis of foci nuclear localization: In order to calculate if HR sites have a specific nuclear localization in early and mid-pachytene pro-oocytes, nuclei were each divided into 3 equal zones and the probability of HR sites being found at certain zones was subsequently calculated. First, the diameter of early and mid-pachytene pro-oocyte nuclei was measured using Delta Vision software. Average diameter of early and mid-pachytene pro-oocytes nuclei was calculated and then, average diameter was used to calculate the average volume of the nuclei. Once average volume was calculated, nuclei were further divided into 3 equivoluminal spheres (zones); the diameter of each zone was also calculated. Localization of each focus was determined by measuring the spot to periphery distance using Delta Vision software and its position in any of the 3 concentric zones was then classified according to each zone's calculated diameter. P-values were

calculated by χ^2 analysis comparing actual values to a hypothetical random distribution of 33% foci in each zone.

10. Irradiation of Oocytes: Drosophila females were yeasted for at least two days with wild type males at room temperature prior to irradiation. Females were X-ray with 12Gy (at a dose rate of 1 Gy/min) at room temperature using an X-ray machine (Faxitron). After irradiation, female ovaries were dissected, fixed and stained at different time points: 15 minutes, 30 minutes 1 hour and 3 hours.

11. Irradiation of S2 cells: S2 cells were irradiated with 15 Gy and 45 Gy at a dose of 150 rads/minute at room temperature using a Faxitron X-ray machine. An average of 2 x 10^8 cells were collected at 0, 12 and 30 minutes post irradiation and immediately processed for nuclear extractions and histone extractions.

12. Histone extraction: *Drosophila* S2 cells were collected and spun down for 1 minute at 800g, after which the supernatant was carefully discarded**.** Nuclei were then extracted by adding nuclear extraction buffer to the pellet and then rotating for 30 minutes at 4°C. The amount of nuclear extraction buffer added was the equivalent of 5 volumes of the pellet volume. The extracts were centrifugation at 14,000g. The supernatant was then discarded and the pellet was

washed 1 time with nuclear extraction buffer. Then, histones were extracted by adding 0.25 N HCL, (using the equivalent of 5 volumes of the nuclear pellet volume of 0.25 N HCL) and incubating at room temperature while rotating for 20 minutes. Histone extracts were cleared by centrifugation at maximal speed (14,000g) for 1 minute. After centrifugation, histones extract (supernatant) was neutralized with 1M Tris pH 8 by adding the equivalent of ½ volumes of the histone extract volume. In some cases, the histone preparations were dialyzed against PBS to reduce the salt concentration.

13. Sensitivity assay: *Mi{ET1}Ino80*^{MB09416}*/TM6C*, *Sb* heterozygote males and females were mated in yeasted vials for 2 days. The progeny of these vials were used as the untreated controls. After 2 days, the parents were transferred to newly yeasted vials. The progeny from these vials were irradiated with 20 Gy using an X-ray machine (Faxitron). Vials were irradiated at either, 24-or 48hours after egg laying. Upon eclosion, the number of homozygous mutant progeny was compared to the heterozygous progeny (N= number of mutants/ heterozygotes). These numbers were then compared to untreated samples to establish the DNA damage sensitivity ratio (N treated/N untreated =X). If X equaled 1, then there was no sensitivity. If x<1, then the mutant embryos exhibited sensitivity to the ionizing radiation

14. Imaginal disc irradiation and staining: Wandering third-instar larvae were collected and irradiated with 20Gy at room temperature using an X-ray machine (Faxitron). Larvae were dissected by cutting the larva about one-third of the way down from the mouth hook and then the anterior portion of the larva was turned inside out. The dissected, inside-out larval tissues were transferred into a tube containing 4% (wt/vol) paraformaldehyde in 1 x PBS and fixed by rotating the tube for 10 minutes at room temperature. After fixation, two quick washes were performed followed by three 5 minutes washes with 1 x PBS. The tissues were incubated with primary antibody overnight 4°C while rotating, and were subsequently rinsed two times and washed three times for 10 minutes with PBST (0.3% Triton X-100/1 x PBS) follow by one hour incubation with secondary antibody in PBST. After incubation with secondary antibody, tissues were rinsed two times and washed three times for 10 minutes with PBST (0.3% Triton X-100/1 x PBS). Imaginal disc were separated from the rest of larvae tissue and mounted with Vectashield for immunohistochemical studies.

15. Ovary lysates: Ovaries of well-fed females were dissected in ice-cold PBS, washed twice with ice-cold PBS and homogenized in lysis buffer (50mM Tris-HCL pH6.8, 100mM Dithiothreitol (DTT), 2% Sodium dodecyl sulfate (SDS), 5mM PMSF, 10% glycerol). Homogenized ovaries were heated at 95°C for 5 minutes, and extracts were cleared up by centrifuging the samples twice at 13,000 rpm for 5 min each.

16. Developmental westerns: Embryos were obtained by letting the flies lay eggs on apple juice agar plates smeared with freshly prepared yeast paste. The embryos were collected and dechorionated by adding 50% bleach directly onto the apple juice plate. The surface of the plate was then gently scraped with a fine brush to loosen the embryos. After two minutes, the bleach-embryos slurry was poured off into a plastic sieve, and the embryos were washed with cold tap water several times until the eggs started aggregating. The following embryonic stages were dechorionated to obtain lysates: Blastoderm (0 to 3 hours), gastrulation-germ band extension (3 to 7 hours), germ band retraction (7 to 12 hours), and specification-differentiation (12-24 hrs). After dechorionation, embryos were homogenized using sodium dodecyl sulfate (SDS) sample buffer (sample buffer (2X): 100 MTris-HCl (pH 6.8), 4% SDS, 0.2% bromophenol blue, 20% glycerol, 200 mM β-mercaptoethanol), were heated at 95°C and spun down at maximal speed (14,000 rpm for 5 min) to clear up lysates. The other developmental stages taken into consideration in this study, including larvae, pupae, ovaries and heads, were also extracted with SDS sample buffer, heated at 95°C, and spun down twice at maximal speed (14,000 rpm for 5 min) to clear up lysates. Aliquots of lysates were run in an 8% SDS-PAGE gel and immunoblot with anti-dIno80 and anti-tubulin antibodies.

IV RESULTS

1. Development of a marker to label and follow DSBs during homologous recombination in the *Drosophila* female meiosis

,

Substantial circumstantial evidence provided by Carpenter using electron microscopy (EM) and *Drosophila* females as the model organism suggest that RNs may represent recombination sites (Carpenter 1975; Carpenter 1979). In addition, studies in precondition and exchange mutants suggested that spherical or large RNs correspond to cross over sites and ellipsoidal or small RNs correspond to gene conversion sites (Carpenter 1979). As mentioned before, other EM studies in plants support the idea that RNs may represent recombination sites (Anderson, Offenberg et al. 1997). But other EM studies also in plants showed that the recognition factor Mre11 is not a major component of early RNs (Lohmiller, De Muyt et al. 2008). Furthermore, different studies have also shown discrepancies in the number of early RNs and HR foci (Anderson, Offenberg et al. 1997, Anderson and Stack 2005); the lack of antibody staining in EM studies makes this difficult to assess. Thus, it is still unknown whether RNs do, in fact, represent HR sites. Importantly, the study of early and late RNs could be very useful to elucidate the mechanism of crossover and gene conversion formation and resolution.

Since the EM studies were published, only two other publications have attempted to describe the progression of meiotic recombination sites during

Drosophila female meiosis using immunocytochemical methods and γ-H2Av as a DSB marker (Jang, Sherizen et al. 2003; Mehrotra and McKim 2006). However, as mentioned before, phosphorylation of H2Av does not mark the appearance or disappearance of DSBs accurately due to the following reasons: 1) phosphorylation of H2Av occurs as a consequence of ATM/ATR activation and possibly chromatin modification (Bakkenist and Kastan 2003), 2) γ-H2Av does not specifically mark DSBs because it is widely spread into chromatin flanking the damage sites (Shroff, Arbel-Eden et al. 2004), and 3) it is not clear whether the clearance of γ-H2Av from chromatin after the induction of DSBs indicates that the breaks were repaired; dTip60 studies using *Drosophila* S2 cells with knocked down dTip60 show accumulation of γ-H2Av, however repair of the DSB could be unaffected (Kusch, Florens et al. 2004). Interestingly, studies done in *Drosophila* germ cells suggest that γ-H2Av may be exchanged with H2Av independent of DSB repair, it was proposed that the removal of γ-H2Av from DSB sites could depend on cessation of ATM and ATR activity (Joyce, Pedersen et al. 2011). Additionally, when *Drosophila* ovaries are stained with γ-H2Av antibodies, endoreplication sites are also marked in region 3 nurse cells (present study and (Lake, Holsclaw et al. 2013). Thus, γ-H2Av does not necessarily only mark meiotic DSBs, but can label non-meiotic DSBs, which makes analyses in repair mutants with persisting DSBs unreliable.

Importantly, Carpenter's observations of the differences in size and cyst position in early and late RNs hint at a means of distinguishing between crossovers (CO) and non-crossovers (NCO); however, to date there has been no differentiation

between CO and NCO by size reported when using γ-H2Av. Due to these discrepancies and the lack of a system to visualize and distinguish early from late repair foci, I set out to establish a system to detect DSB repair sites with a direct marker, Mre11, in order to follow their progression and to possibly differentiate between crossovers and non-crossovers with the help of genetic experiments involving precondition and exchange mutants, mutants with reduce crossover rates.

1.1. dMre11 as a marker to label early and late repair sites

1.1.1. Generation and specificity of anti-dMre11 antiserum: To be able to study early and late events in DSB repair, the Kusch lab developed a polyclonal antiserum directed against a his6-tagged protein fragment that corresponds to amino acids 121-600 of dMre11. The next step in this study was to characterize the anti-dMre11 antiserum, test its specificity, and determine if it marks DSBs during pachytene of *Drosophila* female meiosis I. To confirm that the antiserum was raised against dMre11 (CG16928), the anti-dMre11 antiserum obtained from immunized animals as well as the serum obtained from animals prior to immunization (pre-immunization bleed) were conjugated with agarose A beads and incubated with nuclear extracts from *Drosophila* S2 cells. The immunoprecipitated (Iped) material was loaded into a sodium dodecyl sulfate polyacrylamide gel electrophoresis (SDS-PAGE), and proteins were detected by Coomassie Brilliant Blue staining. Bands that were not present in the

pre-immunization bleeds but in immunization bleed, were excised and analyzed by mass spectrometry. The bands were 68kDa and 150 kDa. The analyses showed that the 68 kDa band corresponded to dMre11 (with 57 peptide hits), and the larger band corresponds to dRad50 (with 173 total peptides). I did not observe a band close to the NBS1 molecular weight (92 KDa), probably due to the use of 350 mM salt in the Immunoprecipitation buffer, as at this salt concentration NBS1 could dissociate from the $Mre11_2Rad50_2$ core complex.

When nuclear extracts of *Drosophila* S2 cells were loaded into an SDS-PAGE and blotted with pre-immune bleed and the immune bleed of anti-dMre11 antibody, it was observed that the immune bleed serum recognizes a band of the predicted molecular mass not observed when the pre-immune bleed serum was used (figure 4a). Additionally, when affinity purified material obtained from nuclear extracts of cells transfected with FH -dMre11 expression vector were loaded into an SDS-PAGE gel and blotted with anti-dMre11 antiserum, the antiserum recognized a band of the expected size not present when nuclear extracts from mock transfected cells were used (figure 4a). To further prove the specificity of the antiserum, dMre11 was knocked down in *Drosophila* S2 cells. RNAi of dMre11 specifically knocks down a protein of the right size that is labeled by anti-dMre11 anti-serum in control samples (figure 4b). I also tested the ability of the antiserum to Ip the other two components of the MRN complex. Figure 4c shows that anti-dMre11 antiserum efficiently pulls down dRad50 and dNbs (figure 4c).

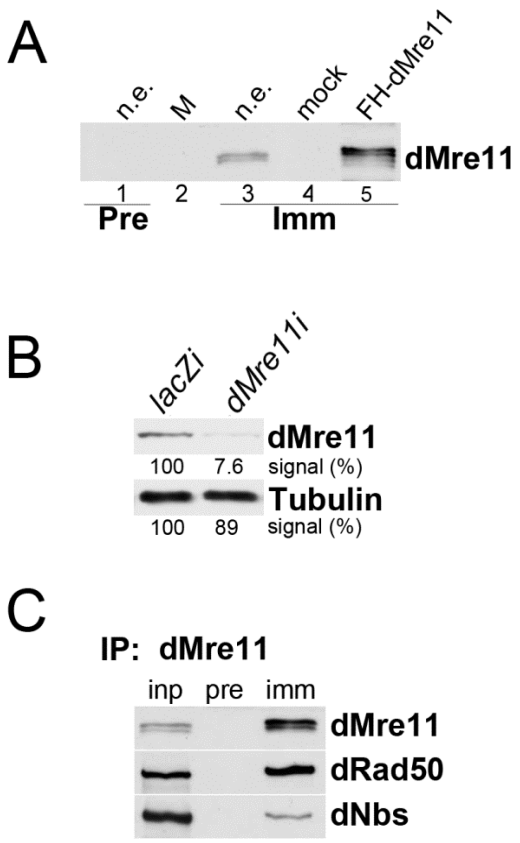

Figure 4: Characterization of anti-dMre11 antiserum (A) Immunoblot of 5 µg of nuclear extracts (n.e) from wild-type cells or 5 µl of affinity-purifications from cells transfected with FH (mock) or FH-dMre11 expression vector; (M) pre-stained marker. The membrane was probed with anti-dMre11 pre-immune bleed antiserum (lane 1) or anti-dMre11 immune bleed antiserum (lanes 3-5). (B) Western blot analysis of nuclear extracts from RNAi-treated *Drosophila* S2 cells. Control cells were treated with dsRNAi for *E. coli lacZ (lacZ*). Tubulin served as loading control. Values below each lane represent the relative intensity of each band in comparison with the representative *lacZ* lane as quantified by Image J. (C) Western analysis of components of the MRN complex that co-immunoprecipitated with dMre11 from *Drosophila* S2 nuclear extracts. Immunoprecipitations were done using ani-dMre11 pre-immune bleed antiserum (pre) and anti-dMre11 immune-bleed antiserum (imm). Membranes were probed with anti dMre11 antiserum, dRad50, and dNbs antibodies. (inp) input lane.

1.1.2. Anti-dMre11 antiserum labels distinct foci when a novel ovary immunostaining protocol is used. In order to study DSBs during *Drosophila* female meiotic recombination, my next goal was to test the ability of anti-dMre11 antiserum to detect repair sites in *Drosophila* oocytes. During *Drosophila* meiotic recombination γ-H2Av foci are readily detectable, but detection of repair foci with anti-dNbs and anti-dMre11 antibodies has not been reported. Detection of repair sites with anti-dRad50 antibodies was attempted, but they diffusely stained --no distinct repair foci was observed (Dronamraju and Mason 2009). Thus, I next attempted to determine if repair sites can be detected with our dMre11 antibody. I stained *Drosophila* ovarioles with anti-dMre11 antiserum and anti-C(3)G antibodies and I was able to observe that anti-dMre11 antiserum stains pro-oocytes and oocytes as marked by C(3)G (figure 5a); however, no DSB repair foci were observed when established dissection and staining protocols were used (figure 5a). Several different protocols and combinations of protocols were tested. Some examples of the different dissection and fixation buffers used in these protocols were: 1) protocol based on a buffer named "buffer A" and 2) a PBS-based dissection buffer protocol (see review for buffer and condition details: (McKim, Joyce et al. 2009). There are three possible explanations as to why Mre11 foci were not observed: 1) MRN is not in foci, which would be very different from mammalian repair foci that are readily visualized using antibodies against Mre11 (Mirzoeva and Petrini 2001), 2) the foci are too small to be visualized using immunocytochemistry methods, and 3) fixation conditions are suboptimal,

The fact that Carpenter used a PBS-based buffer for dissection and was able to visualize some RNs in his/her electron microscope studies suggests that some nucleoprotein structure stably associates with DSBs in *Drosophila*. Thus, I decided to systematically test fixation conditions. I assayed dissection buffers with different components and different concentrations of these components. I focused on HEPES and PIPES, buffers known to preserve mitotically active spindle, kinetochore and microtubules (Przewloka, Zhang et al. 2007). I also tested different mild salts at low concentrations due to the fact that hypotonic solutions with low concentrations of cations have proven to be optimal for the study of DNA binding proteins, such as MRE11, Nbs1, 53BPA, to repair foci (Nakamura, Rao et al. 2010). In addition, hypotonic solutions with low cation concentrations are optimal for the study of factors that spread to chromatin around the DSB, such as MDC1 and phosphorylation of H2AX (Nakamura, Rao et al. 2010). During buffer optimization, I used different concentrations of $MgS0_4$ that help in the maintenance of the DNA structure during dissection and fixation protocols. I also used EGTA, a chelating agent that, like EDTA, binds to metal ions and makes them unavailable in solution. After several tests I was able to develop a fixation and dissection buffer (HEM buffer) composed of: 25mM HEPES, 10mM EGTA and 4 mM $MgSO_4$ that allows the visualization of dMre11 foci during meiotic recombination in *Drosophila* pro-oocytes (figure 5b).

Chromatin within the nuclei of the *Drosophila* ovary seems to be very sensitive to fixation conditions; due to the fact that to be able to observe histones through

Immunohistochemistry a rapid ovary fixation is required (Ashburner 1989). Since the ultimate goal of this work is to study chromatin remodeler complexes during DNA repair, I implemented a quick fixation protocol in which the tissue is fixed while dissecting (see material and methods). The quick fixation protocol together with the HEM dissection buffer gave me the best overall staining results. To test if the foci observed were due to precipitation or lack of specificity, I stained wild type (WT) *Drosophila* ovaries with dMre11 pre-immune bleed serum. The staining showed no detectable staining with the pre-immune bleed antiserum, suggesting that the observations were not due to background effects (figure 5c).

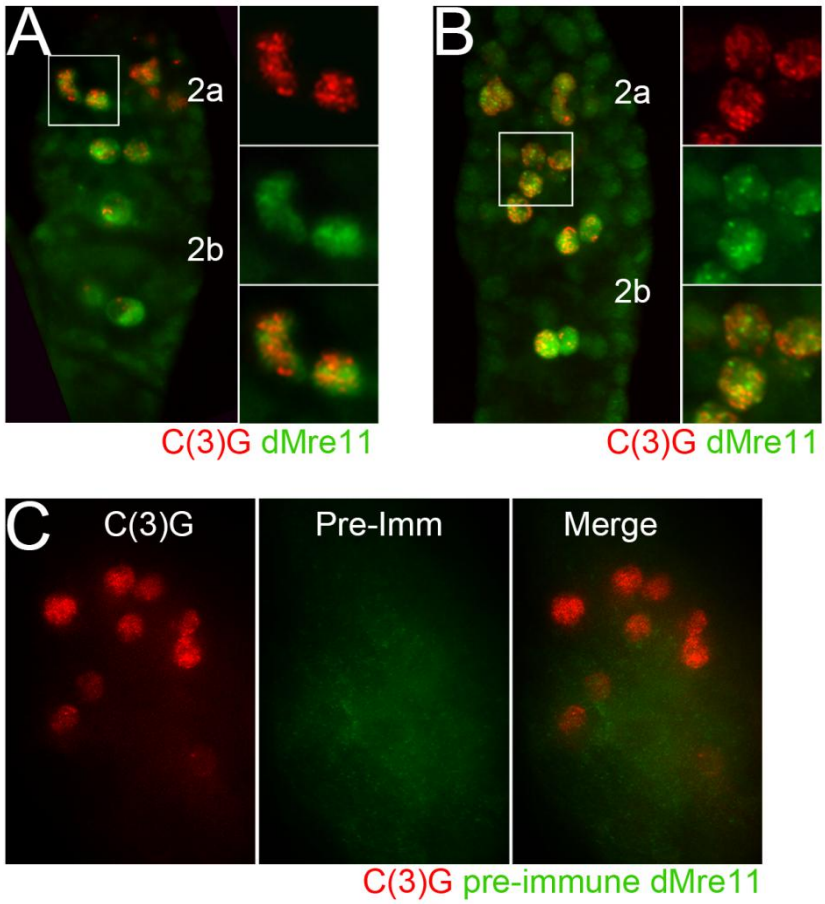

Figure 5: Anti-dMre11 antiserum labels distinct foci when a novel ovary immunostaining protocol is used. (A, B) Maximum intensity projection (see material and methods) of wild type germarium stained with antibodies to C(3)G (red) and anti-dMre11 antiserum (green). (A) Ovaries were dissected and fixed using PBS. Right hand side shows magnification of the pro-oocyte nuclei marked with the white box**.** (B) Ovaries were dissected and fixed using HEM buffer (see material and methods). Right hand side shows magnification of the pro-oocyte nuclei marked with the white box. (C) Maximum intensity projection of a whole mount wild type germarium stained with anti-C(3)G antibody (red) and anti-dMre11 pre-immune bleed antiserum (green).

1.1.3. Anti-dMre11 antiserum marks distinct nuclear foci in region 2a and labels the nuclei of pro-oocytes and oocyte in subsequent developmental stages.

In order to determine the stages at which anti-dMre11 antibody stains distinct foci, I used wild type germaria stained with antibodies against Orb, a RNA binding protein that is first detectable in region 2a, in the cytoplasm of the 16 cell cyst. Orb is then localized to the cytoplasm of the future oocyte once region 2b is reached. Orb is subsequently maintained in the cytoplasm of the oocyte through later stages of oogenesis (Lantz, Chang et al. 1994). The staining showed that anti-dMre11 antiserum marks foci in region 2a, where Orb signal is observed in the cytoplasm of the 16-cell cyst (figure 6 a, b). When region 2b is reached and Orb signal is confined to the oocyte cytoplasm, dMre11 foci are no longer observed, but dMre11 is still present in the nucleoplasma of the pro-oocytes

(figure 6b). dMre11 signal is maintained in the nucleoplasma of oocytes in the vitellarium, during the subsequent stages of oogenesis (figure 6a, 6b).

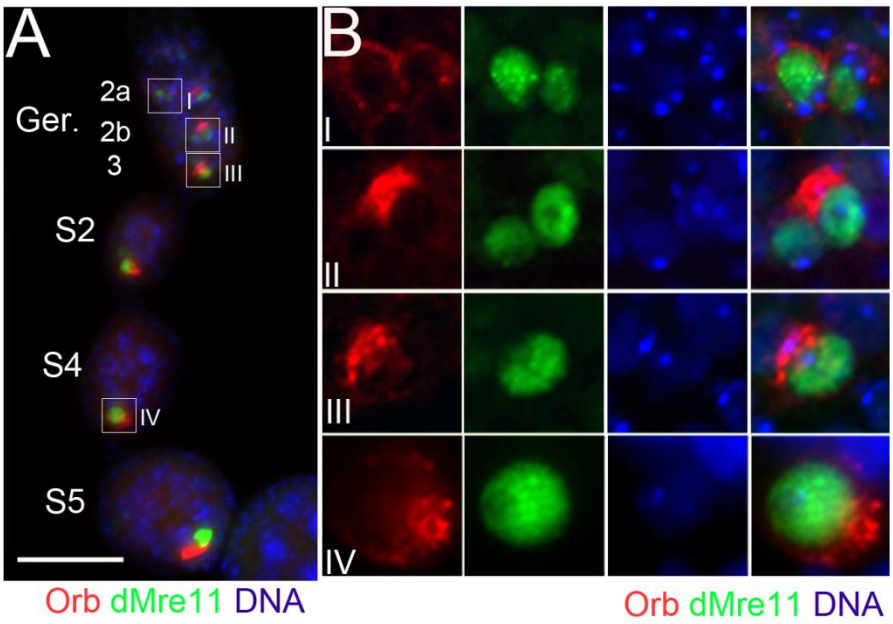

Figure 6: Anti-dMre11 antiserum marks distinct nuclear foci in region 2a and labels the nuclei of pro-oocytes and oocyte in subsequent developmental stages. (A, B) Maximum intensity projection of whole mount wild type ovariole stained with antibodies against Orb (red), and dMre11 (green). Orb is first detected in the cytoplasm of region 2a pro-oocytes and later accumulates in the cytoplasm of the oocyte. DNA was labeled with DAPI (blue). (A) Ovariole overview shows a germarium (Ger) and egg chambers at different developmental stages in the vitellarium (S2 to S5). Scale bar, 40µm. (B) Magnified projections of pro-oocytes and oocyte nuclei marked by white boxes in (A).

I next set out to determine if antibodies against dRad50 and dNbs in conjunction with the new fixation protocol would co-localize with dMre11 in foci in pro-oocyte nuclei from meiocytes in region 2a. *Drosophila* ovaries were immunostained with anti-dMre11 antiserum and co-immunostained with antibodies to anti-dRad50 or anti-dNbs. The results showed that dRad50 and dNbs antibodies stain in foci in region 2a; additionally, dRad50 foci co-localize with dMre11 foci and dNbs foci co-localize with dMre11 (figure 7a, c). In the subsequent stages of oogenesis (region 2b and onwards) there are no detectable MRN foci (7b, 7d). For a more accurate naming of the different meiotic stages that take place in the germarium, region 2a, where MRN foci are observed, will be referred to as early pachytene. Also, later stages, where no more MRN foci are observed are refer to as late pachytene (see figure 7a and 7b), in accordance with the widely accepted nomenclature (Mehrotra and McKim 2006)

The appearance of MRN foci in early pachytene is in accordance with the belief that DNA double strand breaks are induced during this stage. Furthermore, the detection of MRN foci in early pachytene and their absence in later developmental stages seemed to be reminiscent of the already described γ-H2Av foci distribution in the pro-oocytes (Mehrotra and McKim 2006). I next set out to study the behavior of dMre11 foci in wild type *Drosophila* female meiosis and compare it to γ-H2Av dynamics in the germarium. It is not clear yet whether MRN foci could represent HR sites; as such, I also attempted to study a possible relation between RNs and MRN foci. .

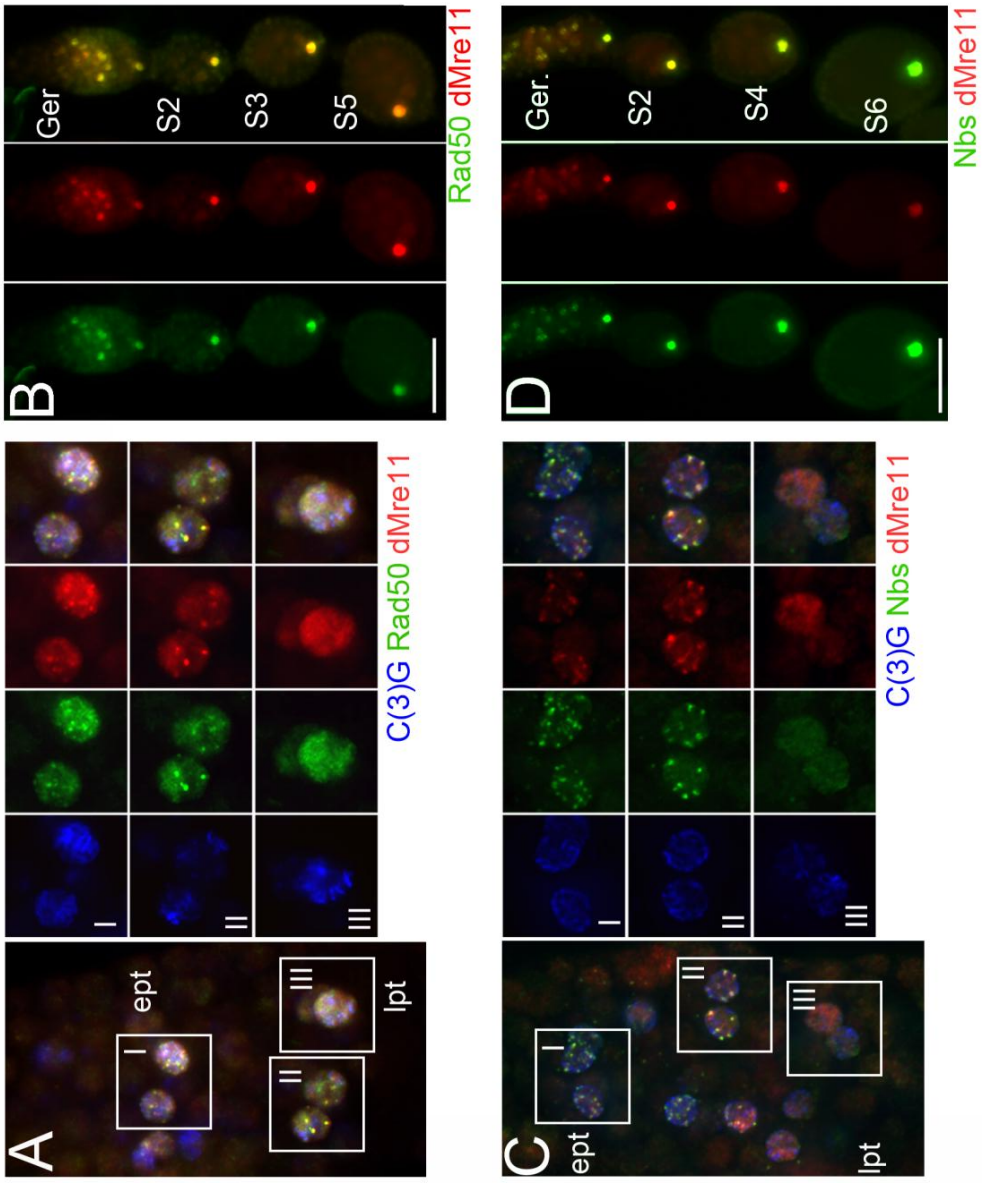
A
ept
lpt
I
II
III
C(3)G Rad50 dMre11
B
Ger
S2
S3
S5
Rad50 dMre11
C
ept
lpt
C(3)G Nbs dMre11
D
Ger.
S2
S4
S6
Nbs dMre11

Figure 7: MRN complex forms foci in pro-oocytes in early pachytene. (A) Left shows projection of wild type germarium stained with antibodies to C(3)G (blue), dRad50 (green), and anti-dMre11 antiserum. ept (early pachytene), lpt (late pachytene). Right shows magnified projections of pro- oocytes and oocytes from the germarium overview on the left marked with white boxes. (B) Projections of wild type ovariole stained with antibodies against dRad50 (green) and anti-dMre11 antiserum (red)**.** The picture shows a germarium (Ger) and vitellarium from stage2 to stage 6 (S2-S6). (C) Left shows projection of wild type germarium stained with antibodies to C(3)G (blue) dNbs (green), and anti-dMre11 antiserum (red). Right shows magnified projections of pro-oocytes and oocytes marked with white boxes in (C). (D) Projection of a whole mount ovariole stained with antibodies against dNbs (green) and anti-dMre11 antiserum (red) as shown in (B). Scale bars, 40μm

1.1.4. Anti-dMre11 antiserum marks homologous recombination sites in pro-oocytes.

In order to test if the dMre11 foci observed during early pachytene are repair sites, I immunostained wild type *Drosophila* ovaries with anti-dMre11 antiserum and antibodies against γ-H2Av (figure 8). The results in figure 8a show a germaria overview in which dMre11 stains in foci in region 2a pro-oocytes and γ-H2Av stains in foci in region 2a in both pro-oocytes and nurse cells. No γ-H2Av and dMre11 foci were observed in region 2b pro-oocytes. However, γ-H2Av foci are present in the nurse cells in region 3 (figure 8a). Moreover, I could occasionally observe some dMre11 foci in the three ring canal nurse cells. Magnification of pro-oocytes in figure 8b, as well as overview in figure 8a show that dMre11 foci co-localize with γ-H2Av foci in region 2a of the germarium. Co-localization of dMre11

foci with the other components of the MRN complex and with γ-H2Av in addition to the results obtained after staining with anti-dMre11 pre-immune bleed (figure 5a) suggest that dMre11 foci is not nonspecific background staining and that the observed foci represent DSB repair sites (from now on referred to as to HR sites).

1.2. dMre11 foci dynamics during *Drosophila* meiotic recombination

So far I had established a reliable tool to detect repair sites during *Drosophila* female meiosis; however, a more detailed analysis of the dynamics of the HR foci during meiotic recombination was needed. Appearance of dMre11 foci is similar to early and late RN described by Carpenter, which were only found in pro-oocytes in early pachytene; thus it is possible that the dMre11 antibody labeled RNs. In order to establish a relation between RNs and the foci labeled by dMre11, I first attempted to determine the number of dMre11 foci per pro-oocyte relative to cyst position in the germaria. I used wild type germaria and took advantage of the fact that dMre11 foci are distinct and could be easily counted when ovaries are stained with anti-dMre11 antibody (figure 8c). The position of a cyst within the germaria is only a rough guide to its meiotic stage and is not necessarily equivalent to a specific stage in meiotic prophase (Carpenter 1975; McKim, Jang et al. 2002). As such, in this analysis all of the cysts of the germaria from region 2a, early pachytene, to region 3, late pachytene, were taken into consideration (figure 8c). The first cyst that was taken into consideration was the first cyst in pachytene as previously characterized

by C(3)G staining plus appearance of γ-H2av in the nurse cells and pro-oocytes. In this analysis, the first cyst with the above characteristics has an average of 11.5 dMre11 foci per pro-oocyte (+/-2.7 n=30 pro-oocytes). It should be noted that in rare occasions (3 germaria out of 16 analyzed), pairs of pro-oocytes with an average of 2.6 (+/-1.9 n=5) dMre11 foci and with C(3)G signals similar to what has being described for a cyst in late zygote were observed (Tanneti, Landy et al. 2011). These late zygotene cysts were not taken into consideration for further analysis of HR foci during pachytene. As shown in figure 8c, the dynamics of dMre11 foci are similar to what has been published for γ-His2Av foci, in that they both increase in number in region 2a before decreasing by region 2b and disappearing by region 3. dMre11 foci numbers increase from cyst number 1 to 4 (a region corresponding to 2a). The higher number of dMre11 foci observed was in cyst number 3, were I counted an average of 15 dMre11 foci per pro-oocyte (+/-2.6 n=26 pro-oocytes). dMre11 foci numbers displayed a steep decline between cyst 4 and 6 (a region most likely corresponding to late 2a early 2b), with numbers decreasing through cyst 7 (a region most likely corresponding to late 2b) and are completely gone by cyst 8 (region 3).

Due to the fact that the transition between region 2a and 2b is not clearly definable, as it is still debated whether HR is completed in 2a (Riechmann and Ephrussi 2001) or in early 2b (Mehrotra and McKim 2006), I subdivided pachytene into early pachytene (ept), mid pachytene (mpt) and late pachytene (lpt), for a more accurate analysis of the different events that take place during pachytene. Staging

was based on the dynamics and number of dMre11 foci in each cell relative to cyst position, as shown in figure 8c, and characteristic behavior of C(3)g and γ-H2Av signals during the stages analyzed (figure 8a, 8b). Early pachytene (ept), from cyst 1 to cyst 4, has the higher number of dMre11 foci and is characterized by full C(3)G in both pro-oocytes, and as previously mentioned, by γ-H2Av appearance in the pro-oocytes and nurse cells. Pro-oocytes in early pachytene have an average of 13.5 (+/- 3, n=100) dMre11 foci per pro-oocyte.

Second, an intermediate stage between early and late pachytene, mid-pachytene, characterized by a steep decline in the number of dMre11 foci from about cyst number 4 to cyst number 6 (figure 8a, 8b, 8c), γ-H2Av and C(3)G serve as another marker for mid-pachytene. In mid-pachytene, nurse cells have fewer γ-H2Av foci in the three ring canal cells, and they seem to be absent in the other nurse cells of the cyst. Also, C(3)G is less compact than early pachytene (figure 8b, mpt). After analyzing Drosophila wild type germaria I see an average of 5.1 foci per pro-oocyte (+/- 1.5 n=26 pro-oocytes).

In late pachytene C(3)G is less compact than mid- pachytene; there are no more dMre11 foci or γ-H2Av foci in the pro-oocytes and/or oocytes. In addition, a drop in dMre11 and/or C(3)G levels is observed in the losing oocyte γ-H2av had disappeared from all nurse cells in the cyst; however, once oocyte specification has occurred and region 3 is reached, γ-H2Av is observed again in nurse cells. It is important to keep in mind that, as previously mentioned, pachytene continues to about stage 14. Here,

I refer to advanced pachytene as occurring from region 3 to stage 14 (figure 8a, 8b, 8c).

Although the number of HR foci is higher than the number of RNs, RNs and HR foci seem to have the same dynamics in the germaria, they both increase in number to then decrease. In addition, Carpenter reported differences in size between early and late RNs. In here, I attempted to measure dMre11 size in ept and mpt using immunocytochemistry and a Delta vision II Deconvolution Microscope software.

An increase in the diameter of dMre11 repair foci was also observed in mid-pachytene when compared to the diameter of dMre11 foci in early pachytene (8d). Early pachytene foci have an average size of 0.165 µm (+/- 0.0324 n=20 pro-oocytes). Late foci have an average size of 0.335 µm (+/-0.05 n=22 pro-oocytes) (Figure 8d). My results correlate with the electron microscope studies described by Carpenter where the average sizes of RNs have a tendency to increase with developmental age. However, it is important to note that, as observed in figure 8 and 7, not all ept foci are small and not all lpt foci are larger (Carpenter 1979). Additionally, the number of HR foci observed in mpt correlates with the average of 5.4 spherical RNs per nuclei observed by Carpenter, (Carpenter 1975). Base on the observed similarities of early RN and late RN with HR sites, it is possible that the dMre11 signal corresponds to some RNs, especially the late RNs where the average number are very similar to the average number of late large HR foci in mpt.

Next, I did a thorough analysis of the appearance, disappearance and co-localization of dMre11 foci and γ-H2Av foci as the cysts proceed through meiotic recombination in ept and mpt (figure 8e). Pro-oocytes at the start of early pachytene have several small dMre11 foci in the pro-oocytes, most of which co-localized with γ-H2Av, however, few dMre11 positive foci had no γ-H2Av (figure 8b, 8e). More advanced cysts in early pachytene are characterized by a complete co-localization of all of the dMre11 foci with γ-H2Av (figure 8b and figure 8e). In the analyses of region mpt, I observed that γ-H2Av staining decreases in mid pachytene; however to a much lesser extent compared to dMre11 staining. In early cysts of mid pachytene I counted an average of 7 +/-3 γ-H2Av and 5.1 +/- 1.5 dMre11 and γ–H2Av (figure 8e)

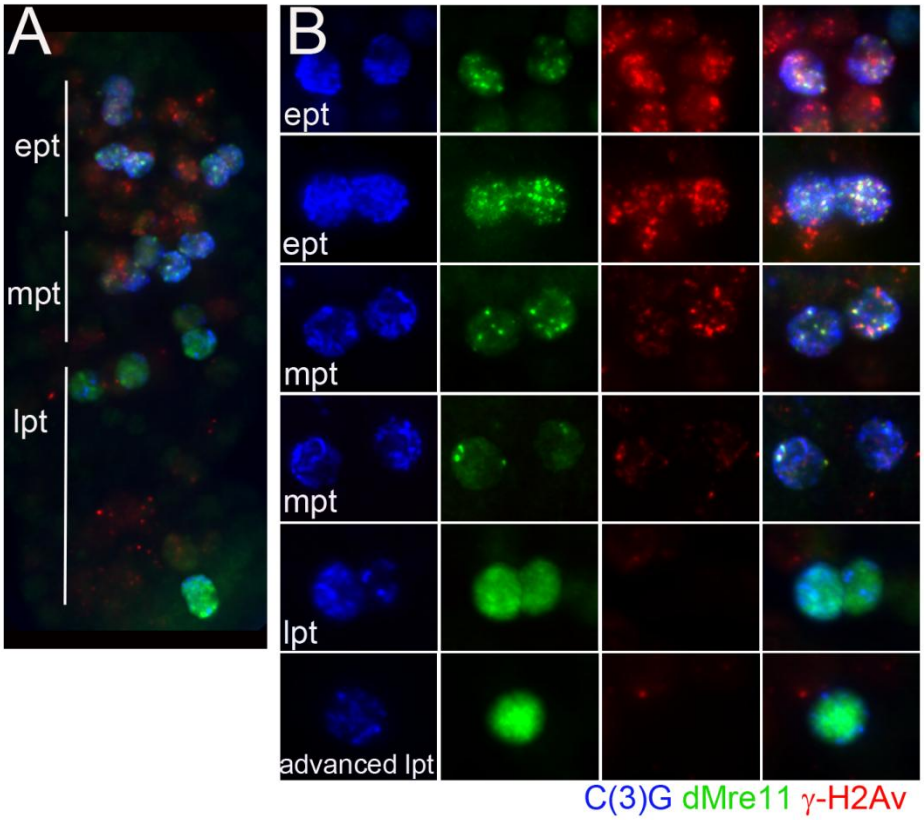
A
ept
mpt
lpt
B
ept
ept
mpt
mpt
lpt
advanced lpt
C(3)G dMre11 γ-H2Av

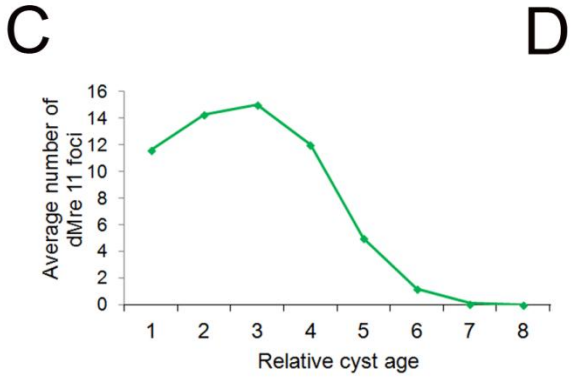
C
Average number of dMre 11 foci
Relative cyst age

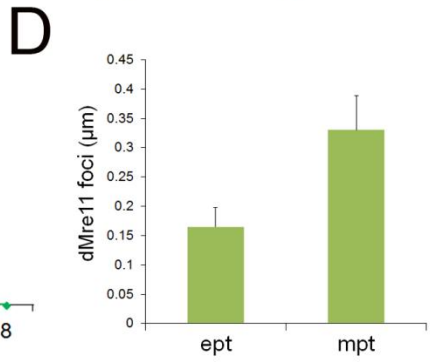
D
dMre11 foci (μm)
ept
mpt

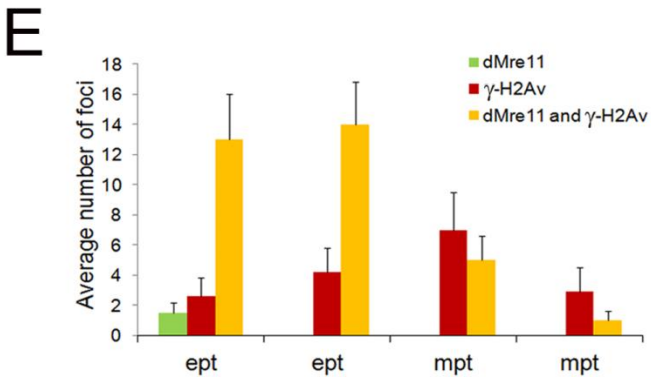
E
Average number of foci
dMre11
γ-H2Av
dMre11 and γ-H2Av
ept
ept
mpt
mpt

Figure 8: **Most of ept-mpt dMre11 foci co-localize with γ–H2Av foci and show distinct changes in number and size during progression from early to mid pachytene.** (A-B) Wild type germarium stained with antibodies to γ-H2Av (red), dMre11 (green) and C(3)G (blue). (A) Projection of a whole mount wild type germarium showing early pachytene (ept), mid-pachytene (mpt) and late pachytene (lpt). (B) Magnified projections of pro-oocytes and oocytes from whole mount germarium. Each row shows a representative pair of pro-oocytes for each developmental region within the germaria. (C) Plot showing the average number of dMre11 foci as a function of relative cyst age in wild-type germarium. The first cyst analyzed was the first cyst in pachytene characterized by treat like C(3)G staining and γ-H2Av signals in the nurse cells and pro-oocytes. Last cyst analyzed (cyst number 8) was a region 3 cyst. (D) Bar graphs show average size of dMre11 foci in ept and mpt in µm. ept foci have an average size of 0.165 +/- 0.0324 µm (n=20). mpt foci have an average size of 0.335 +/-0.05 µm (n=22). Foci were measured using the Deltavision microscopy software**.** All error bars show the standard deviation. (E) Graph shows counts of dMre11 and γ-H2Av foci in ept to mpt of wild type *Drosophila* females. Green bar graphs show average number of dMre11 foci, red bars graphs show average number of γ-H2Av foci and yellow bar graphs show average number of foci with dMre11 and γ-H2Av co-localization. 10 germaria were analyzed in total

Based on the above observations, the following landmarks are used to distinguish between early pachytene, mid-pachytene and late pachytene in this study.

1. Early pachytene: Has an average of 4 consecutive cysts where pro-oocytes show a compact thread-like C(3)G staining and an average of 13.5 HR sites. γ-H2Av signals

are evident in the pro-oocytes and all nurse cells. Overall, ept HR foci are smaller when compared to mpt HR foci.

2. Mid-pachytene: Although both pro-oocytes still have C(3)G, signals are less compact than ept. Nurse cells have less γ-H2Av foci in the three ring canal cells, and the foci seem to be absent in the other nurse cells of the cyst. There is a drastic decrease in the number of dMre11 foci (average of 5.1). Overall, mpt HR foci are larger when compared to ept HR foci.

3. Late pachytene: Characterized by a less compact C(3)G than mid-pachytene. There are no detectable HR foci in pro-oocytes and/or oocytes. γ-H2Av has disappeared from all nurse cells in the cyst. In addition, a drop of dMre11 and/or C(3)G is observed in the losing oocyte. When region 3 is reached, γ-H2Av signal is observed in the nurse cells

1.3. HR sites occupy different nuclear sub-regions in ept and in mpt pro-oocytes.

Previous reports using yeast as the model system have tried to address nuclear localization of unrepaired DSBs. In these studies persistent or slowly repaired DSBs migrate from an internal nuclear position to the nuclear periphery (Nagai, Dubrana et al. 2008; Oza, Jaspersen et al. 2009). While analyzing the behavior of HR sites in several wild type *Drosophila* females, it became evident that besides increasing in size, HR sites in mpt seem to primarily accumulate towards the periphery of the

nuclei while HR foci in ept pro-oocytes seem to be distributed towards the inner zones of the nucleus. To be able to determine if HR sites in *Drosophila* meiotic recombination have different localization patterns in the nucleus at different stages of the DNA damage response pathway, I first focused in the nuclear localization of MRN foci and stained wild type *Drosophila* ovaries with antibodies against dNbs, dMre11 and C(3)G. In order to have a clear view of the localization of foci, I also compared maximum intensity projections of all optical sections through pro-oocyte nuclei of whole mounted germarium (stacks) and single optical sections of the middle of the pro-oocyte nuclei (medial) in ept and mpt pro-oocytes. Comparison of both medial and stack deconvoluted images showed that most HR sites in ept pro-oocytes seem to be located towards the center of the nuclei, in contrast to HR sites in mpt pro-oocytes, where most if not all foci are located at the nuclear periphery (figure 9a). To test if HR foci are in the nuclear periphery in mpt, I stained wild type ovarioles with antibodies against lamin, dMre11 and γ–H2Av. Lamins are important structural proteins of the nuclear membrane (Burke and Stewart 2013). The staining showed that in ept, dMre11 and γ-H2Av foci seem to have a tendency of being located towards the center of the nuclei, away from lamin, while those HR sites in ept pro-oocytes seem to be primarily located at the nuclear periphery and co-localize with lamin (Figure 9a').

Although in general HR foci in mpt are larger than HR foci in ept, I find that in some cases within the same mpt pro-oocyte there are peripheral HR sites with different sizes and mark differences in the intensities of dMre11 and γ-H2Av after

immunostaining procedures. There are big HR foci in the periphery that stain brightly for dMre11 and for γ–H2Av and smaller HR foci that stain bright for dMre11 but fainter for γ-H2Av (figure 9a'). Since this is observed in a later region, one could assume that the small HR foci are "older" or were introduced first, and the larger foci are "newer" or were introduced last. Large foci could be initiating repair and accumulating repair factors, and thus appear larger. Small foci at the periphery could be repaired or be ending the repair process and disassembly of factors is taking place. In the case of small foci the break could be repaired but it is possible that dMre11 is still detected because it has not been completely disassembled. As previously explained, some of the latest studies of the McKim group suggest that there is a constant exchange of γ-H2Av during repair in the germ line (Joyce, Pedersen et al. 2011). In these small periphery foci γ-H2Av is fainter than dMre11, probably due to re-phosphorylation being impaired either because the heterochromatin in the periphery impedes it or ATR/ATM (the kinases that phosphorylate H2Av) are not readily available at this stage or active. Interestingly, I have also observed pro-oocytes in earlier 2a stages with small foci in the center of the cell that stain brightly for γ-H2Av and fainter for dMre11. It is possible that in these sites, DSBs are repaired and there is still a constant re-phosphorylation of H2Av; alternatively, at this early stage disassembly of MRN foci may occur at a faster rate than chromatin clearance. All together the staining results suggest that DSBs are introduced and repaired asynchronously.

After the different stainings were analyzed it also became noticeable that not only HR foci in mpt seem to be located towards the nuclear periphery, but also entire stretches of chromosomes that were flanking the DSBs. In order to test this, I stained ovaries with anti-C(3)G and anti-lamin antibodies. The immunocytochemistry assay showed that long stretches of C(3)G would co-localize with lamin (figure 9b); when medial sections where analyzed, it seemed as if most of the C(3)G in the cell had been dragged to the nuclear periphery and formed a hollow sphere.

To do a statistical analysis of the localization of HR sites within the nucleus, pro-oocyte's nuclei were divided into 3 concentric zones of equal surface area with region I being the outermost layer (figure 9c). Then the position of each repair focus was scored relative to the 3 different nuclear zones. If there is no difference in the distribution of foci within the nuclei of pro-oocytes in ept and those in mpt, then there should be an equal distribution of foci through the nuclei in both stages (33% HR foci in each concentric zone = random distribution). Deviation from the random distribution of 33% in each one of the 3 concentric zones was tested for statistical significance. Our statistical analysis indicates that in ept, the observed distribution is statistically significant: HR sites in early-pachytene are not distributed randomly in the nucleoplasma and as shown in figure 9c, they tend to be found in the two inner most zones: Zone II has 37% of the total foci, Zone III (inner most) has 42% of the total foci, and Zone I (outermost) has 21% of the total foci (figure 9c).

The next step was to determine the statistical significance of the observed nuclear distribution of HR sites in mpt. In order to accurately analyze the position of HR foci related to cyst stage, the pro-oocytes found in mpt were grouped into two categories: 1) pro-oocytes with 7 to 4 HR sites and 2) pro-oocytes with 4 to 1 HR sites. Pro-oocytes were classified in these two groups due to the fact that there seemed to be a high correlation between number of late HR sites and their position relative to the periphery. The older the mpt cyst is, the smaller the number of HR sites left to be repaired and the greater percentage of these HR sites in the periphery. These dynamics suggest a migration to the periphery and that most likely the DSBs are getting repaired while migrating; however it poses a problem to study localization of DSBs within the nuclei; thus, in order to get a more accurate reading I divided mpt pro-oocytes into two groups. In this statistical analysis it would be expected that group 1, which has pro-oocytes with a higher number of foci, would have the lower percent of HR sites in periphery due to the fact that a great majority of HR sites are still in migration to the periphery to be repaired. Likewise group 2, which has pro-oocytes with fewer foci, would be expected to have a higher percent of DSBs in the periphery because the great majority of HR sites were repaired.

After the two groups of mpt pro-oocytes were scored for HR localization within any of the 3 concentric zones, the deviation from the distribution obtained in ept was tested. Statistical analysis agrees with previous observations and shows that there is a significant localization of HR foci towards the nuclear periphery in mpt pro-

oocytes nuclei, group 1 has 60% of HR sites in the outermost zone and group 2 has 83% of foci in the outermost zone (figure 9d).

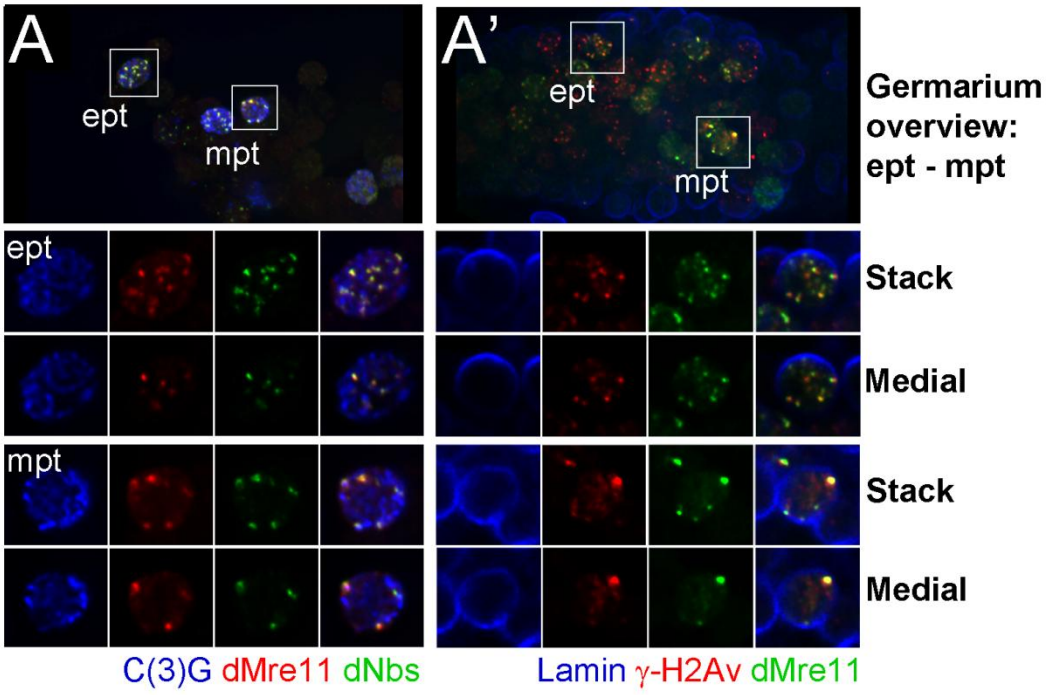

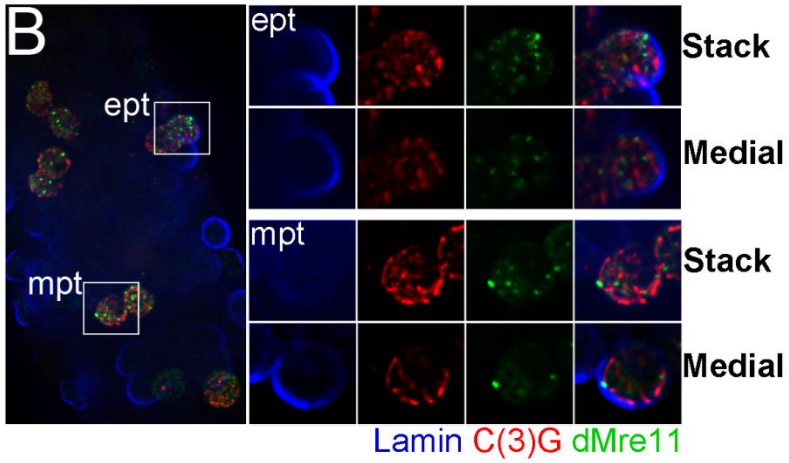

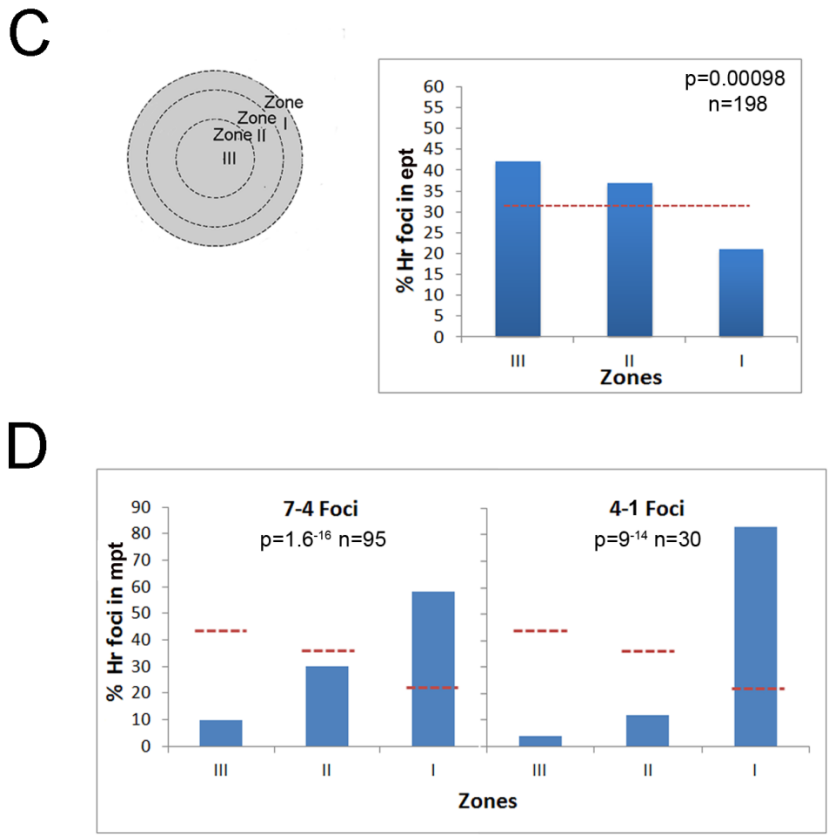

Figure 9: In early pachytene DSBs are localized towards the center of the nuclei and in mid-pachytene most DSBs accumulate at the nuclear periphery. (A) Top panels show overviews of the highlighted early pachytene and mid-pachytene pro-oocytes from a wild type germarium. Germarium in panel A was stained with antibodies against C(3)G (blue), dMre11 (red), and dNbs (green). Germarium in panel A' was stained with antibodies to lamin (blue), γ-H2Av (red), and dMre11 (green). Bottom panel shows maximum intensity projection of all optical sections through whole mounted pro-oocytes (stacked) and single plane sections through the middle of the nuclei (medial) of a magnified ept pro-oocyte and mpt pro-oocyte marked by the white boxes in the top overview. (B) Left show overview of the highlighted early pachytene and mid-pachytene pro-

oocytes from a wild type germarium. Germarium was stained with antibodies to lamin (blue), C(3)G (red), dMre11 (green). Right shows magnifications of stacked (maximum intensity projection of pro-oocytes) and medial (single plane) ept and mpt pro-oocytes. (C-D) Statistical analysis of DSB localization within the pro-oocyte's nuclei. (C) Ept and mpt pro-oocyte nuclei were divided into 3 zones with equal surface area as shown in diagram on right. Localization of each focus was determined and then its position was classified into any of the 3 concentric zones according to each zone's calculated diameter. Distribution of HR foci in the three zones is plotted as a percent of the total number of foci counted (n=198). Red dash line at 33% represents an idealized random distribution. P values were calculated by χ^2 analysis comparing actual values to the hypothetical random distribution. (D) Pro-oocytes in mpt were divided into two populations: pro-oocytes with 7 to 4 foci and pro-oocytes with 4-1 foci. Distribution of HR foci in the three zones was calculated and plotted as in (C). Red dash lines represent an expected distribution for each one of the 3 zones, as if mpt pro-oocytes would maintain the same distribution as early 2a oocytes (expected distribution in late 2a: zone I: 21%, zone II: 37% and Zone III 42% of the total foci).

As shown above, in ept a lower percent of HR foci is observed in the nuclear periphery and a higher one in the two more inner zones. Due to the tendency of HR sites in ept to be in the inner zones, HR foci may be forming mostly towards the center of the nuclei away from highly condensed heterochromatic areas that may interfere with and make difficult the establishment and processing of DSBs. As published for yeast, the center of the nucleus is a heterochromatin-poor region, and the periphery is a heterochromatin-rich region (Gartenberg, Neumann et al. 2004;

Taddei, Van Houwe et al. 2009). In addition, studies done in Drosophila pro-oocytes, oocytes and nurse cells suggested that DSBs do not form in heterochromatic areas (Mehrotra and McKim 2006). However, studies conducted in Drosophila S2 cells, where DSBs were introduced by IR, showed that DSBs were observed within heterochromatin, but moved outside of the heterochromatin prior to their repair (Chiolo, Minoda et al. 2011). In order to see if early HR sites can be found in heterochromatic areas in *Drosophila* oocytes, I stained *Drosophila* ovaries with antibodies against Heterochromatin protein 1 (HP) and co-immunostained with anti-dMre11 antiserum (figure 10a). In early pachytene all HR foci are found outside of the heterochromatin domain. I also stained *Drosophila* ovaries with antibodies against dMre11 and H3K9me2, a histone post-translational modification that marks heterochromatic areas (Figure 10b). dMre11 and H3K9me2 signals as well as HP1 and dMre11 signals show that HR foci are found outside of heterochromatic areas. Additionally, figure 10b shows that in mpt, peripheral foci did not lie in heterochromatic areas.

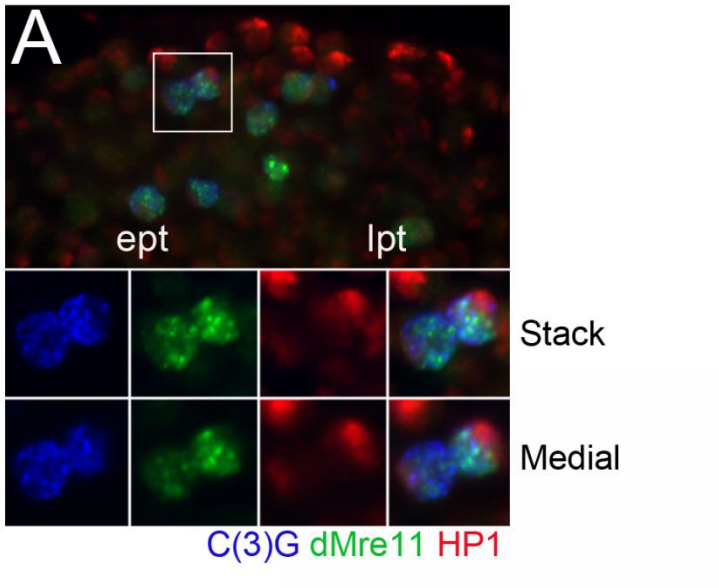
A
ept
lpt
Stack
Medial
C(3)G dMre11 HP1

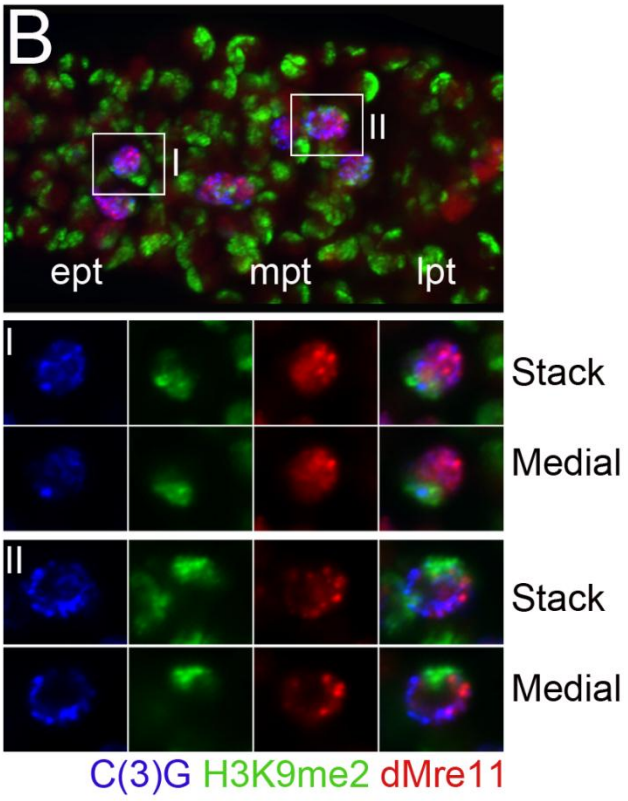
B
I
II
ept
mpt
lpt
I
Stack
Medial
II
Stack
Medial
C(3)G H3K9me2 dMre11

Figure 10: HR foci are found ouside or at the boundary of heterochromatin domain. (A) Top panel shows overview of region ept-lpt of a wild type germarium stained with antibodies to C(3)G, anti-dMre11 antiserum (green), and Heterochromatin protein 1, Hp1, (red). Botton panel shows magnified stacked and single plane sections (medial) of ept pro-oocytes obtained from the overview as highlighted with the white box. (B) Top panel shows overview of region ept-lpt of a wild type germarium stained with antibodies to C(3)G, anti-dMre11 antiserum (red), and H3K9me2 (green). Botton panel shows magnified stacked and single plane sections (medial) of late ept pro-oocytes obtained from the overview as highlighted with the white boxes.

Studies done by Nagai *et al* in yeast suggest that an unrepaired DNA damage sites could co-localize transiently with nuclear pore complex components (Nagai, Dubrana et al. 2008). In this study, DSBs seem to relocate to nuclear pores by a sumo-dependent pathway that in turns requires ATM and ATR (Nagai, Dubrana et al. 2008). To date no co-localization of DSBs with nuclear pore complexes components has been published for *Drosophila*. Thus, I tested if HR foci in *Drosophila* females would co-localize with components of the pore complex. I stained *Drosophila* germaria with antibodies to anti-dMre11 and antibodies to nucleoporin glycoprotein 210, gp210, a transmembrane protein that is involved in structural organization of the pore complex (Greber, Senior et al. 1990) (figure 11). The results showed that in mid-pachytene, HR foci are close to nuclear pores but co-localization of gp210 and dMre11 was not observed (figure 11). It is possible that in *Drosophila* the nuclear

pore complex is not involved in the repair of late HR foci at the periphery. However, there is not enough evidence to discard a possible role of this complex in DNA repair, for example, there is still possibility that HR sites are transiently at nuclear pore complexes where some stages of repair take place or to be shuttle to a close compartment where repair will taking place. In yeast an elegant model suggest that DSBS can be dragged to the nuclear periphery, where some proteins serve as a preliminary docking site and then damage sites are transferred to another nuclear membrane protein complex for repair (Gartenberg 2009; Oza, Jaspersen et al. 2009; Polo and Jackson 2011).

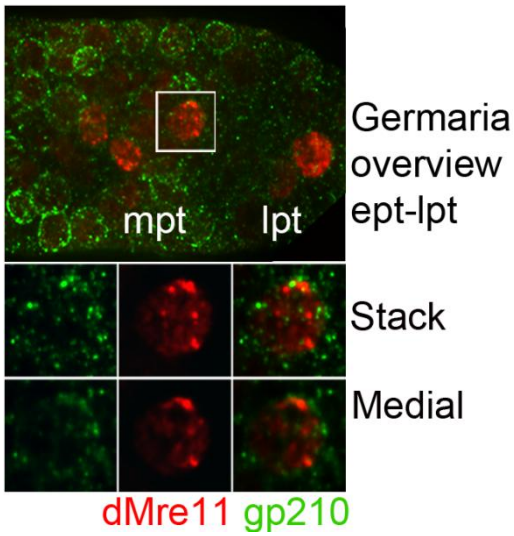

Figure 11: HR foci are found in close proximity to the nuclear pore complex. Top panel shows overview of wild type germarium stained with antibodies to nuclear pore glycoprotein-210 (gp210) (green) and anti-dMre11 antiserum (red). Middle panel shows magnified and stacked mpt pro-oocytes obtained from the corresponding top overview as highlighted with the white box. Bottom panel shows single plane section (medial) of the mpt oocytes marked by the white box in the top.

Mismatch repair proteins, as previously mentioned, are a family of polypeptides involved in post-replication mismatch repair and DNA repair pathways. Interestingly, some of these mismatch repair proteins are meiosis specific; for example, yeast MSH4 and5 are two mismatch repair proteins necessary to maintain wild type levels of meiotic crossing over and are expressed only in meiotic cells (Sekelsky, Brodsky et al. 2000). Orthologs of mismatch repair proteins specifically involved in meiosis have also been identified in mammals. However, in *Drosophila* the only gene that has been identified is *spellchecker,* Msh2 ortholog (Flores and Engels 1999; Sekelsky, Brodsky et al. 2000). If late HR foci move from the center of the nuclei to the periphery, it is possible that HR sites are directed to periphery for the specific repair of certain intermediates. Taking advantage of the fact that our lab had produced and characterize the antibodies to *Drosophila* Msh2 (manuscript in submission) I attempt to determine if Msh2 is at or close to the nuclear periphery and if it co-localizes with HR sites. I stained *Drosophila* ovaries with antibodies to

lamin, Msh2 and dMre11 (figure 12). I observed that Msh2 protein was enriched in the nuclear membrane and co-localized with lamin. Msh2 was also in close proximity to some mpt peripheral HR foci. This data supports the idea that CO may be directed to the periphery for repair, where meiosis specific proteins are enriched

Thus far, a specific antiserum against dMre11 was developed in addition to a staining and fixation method that allows for the visualization of foci. The following support the fact that the observed foci are HR sites: 1) dMre11 foci co-localize with dRad50 and also with dNbs foci, 2) dMre11 foci co-localize with γ-H2Av foci, 3) dMre11 foci appear in the pro-oocytes in region 2a, where HR takes place, and disappear by region 3, where HR is thought to be completed, and 4) dMre11 foci behavior is very similar to what had been published about RNs by Carpenter -- that the average size of HR foci increases with developmental age, and the smallest HR sites were observed first and bigger HR sites were observed last (Carpenter 1979). Although the behavior of dMre11 signals during meiotic recombination highly suggests that it marks HR foci and possibly some RNs, these findings have yet to be confirmed.

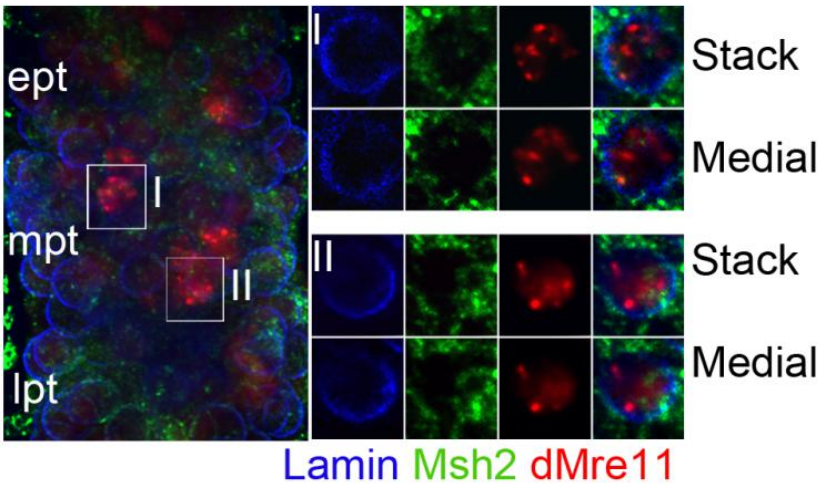

Figure 12: Peripheral mpt HR foci are in close proximity to the *Drosophila* DNA mismatch repair protein spellchecker 1, Msh2, which localizes to the nuclear periphery. (A) Maximum intensity projection of Z-series taken through whole mount wild type germarium stained with antibodies to lamin (blue), Msh2 (green), and dMre11 (red). Right, shows maximum intensity projection of Z-series taken through mpt pro-oocytes as mark with the white boxes

More importantly, this is the first study in *Drosophila* female meiosis to describe a specific nuclear localization of HR sites. HR sites in ept are located towards the center of the nuclei, in contrast to mpt, where most if not all foci are located at the nuclear periphery. An average of 5 late foci are in the periphery when meiocytes are in mpt; this number is close to the genetically determined CO numbers (McKim, Jang et al. 2002). Additionally, this number corresponds to the reported late RNs, which were suggested to be COs by Carpenter based on similar statistical analyses

(Carpenter 1979; Carpenter 1982). Thus, it is possible that the late big peripheral HR sites observed here correspond to CO.

The data obtained when studying nuclear localization also suggests that DSBs form in ept towards the inner zones of the nuclei and move to the nuclear periphery in mpt, possibly for repair. But the possible factors or signals involve in these processes are still unknown in *Drosophila.* Since an average of 5 HR sites are found at the periphery it is possible that only COs go to the periphery; however, there is still the possibility that all DSBs can go to the periphery if a repair pathway or a developmental signal is disrupted. The study of *Drosophila* females with deficiencies in DNA damage response and repair factors as well as meiotic regulators of the NCO/CO decision will aid in the understanding of the nuclear localization of HR sites and the way COs and NCOs are differentiated and repaired.

2. HR foci turnover during homologous recombination in *Drosophila* female meiotic mutants

In this part of the study, I set out to analyze different *Drosophila* females with deficiencies in factors involved in the recognition and repair of DSBs during meiotic recombination in order to address some of the questions that arose after the wild type analysis described above. First, I began this part of the study by analyzing *Drosophila* females deficient in the endonuclease responsible for meiotic DSB formation and factors involved in the recognition of DSBs. Second, in order to test if

late periphery HR sites correspond to CO, I analyzed *Drosophila* females with defective crossover rates. Next, in order to elucidate some of the factors responsible for the localization of HR sites to the nuclear periphery, I analyzed *ATR* and *ATM Drosophila* mutants. Studies in yeast have reported that ATM and ATR are involved in the movement of late repair foci to the nuclear periphery (Nagai, Dubrana et al. 2008). *ATR* and *ATM Drosophila* mutants have been reported to have defects in DSB repair; however, to date there are no studies in *Drosophila* addressing the role of these PIKK in nuclear localization of DSBs. In order to determine if all HR sites have the ability to go to the periphery, I analyzed *Drosophila* female mutants with deficient or delayed DSB repair. Mutants such as *spindle-A* (*spn-A*) and *okra* (*okr*) are defective in DSB repair and have being shown to have persistent DSBs. Lastly, I studied some other *Drosophila* mutants that may be important for the observed accumulation of recognition and repair factors to the DSB.

2.1. HR focus formation is dependent on the cutting endonuclease, Mei-W68, and proper accumulation of recognition factors into the pro-oocyte's nuclei.

2.1.1. *mei-W68* mutant females have very reduced number of dMre11 foci. Based on the data provided here, it is highly possible that dMre11 signals in ept and mpt pro-oocytes represent HR sites and probably some RN. However, in the wild type description above, there were instances in early

pachytene where few dMre11 foci were observed lacking γ-H2Av. To test whether MRN signals correspond to sites where a break was introduced and recognition factors assembled, I studied HR foci formation in the absence of DNA damage.

In flies, the endonuclease mei-W68 is the *Drosophila* homolog of spo11, the enzyme that catalyzes break formation (McKim and Hayashi-Hagihara 1998). It has been shown that DSBs do not form in *mei-W68* mutants, as *mei-W68* mutants do not have gene conversion and COs rate is very reduced (McKim, Green-Marroquin et al. 1998). To investigate this I used the fly line *mei-W68*^{Z4572}, one of the strongest *mei-W68* alleles that eliminate recombination (Bhagat, Manheim et al. 2004).

When *mei-W68* mutants were stained with anti-dMre11 and anti-γ-H2Av antibodies, I did not observe ept or mpt HR sites (figure 13 a-b). The data obtained suggest that repair factors do not accumulate in the absence of breaks. As such, it is possible that in early stages of ept the dMre11 antibody is labeling breaks where recognition factors have probably been loaded, but signaling to chromatin has not yet occurred and thus H2Av has not been phosphorylated. The dynamics observed in later stages of ept and early stages of mpt, where full co-localization of dMre11 and γ-H2Av was observed supports this idea. However, there is the possibility that few repair factors accumulate at chromatin-friendly environments in the absence of a break; as such, the foci could be very small and not detectable via fluorescent microscopy. This is similar to what has been observed in yeast, in which Mre11 was transiently localized at hot spots in Spo11 mutants (Borde, Lin et al. 2004).

Furthermore, these results provided more evidence that MRN foci indeed correspond to HR sites and that the dMre11 antibody is specific.

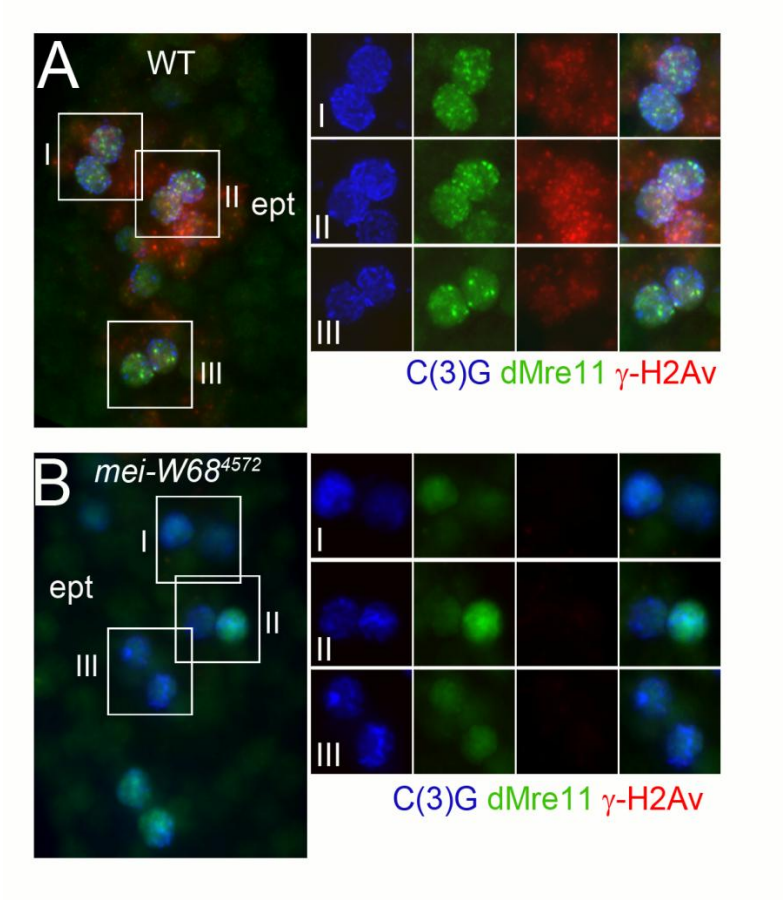

Figure 13: ***Mei-W68*** **mutant females lack HR foci.** (A-B) Maximum intensity projections of whole mount (A) wild-type, (B) *mei-W68*^{4572} germaria stained with antibodies to C(3)G (blue), dMre11 (green) and γ-H2Av (red). Left shows germaria overview of early pachytene to mid-pachytene and right shows magnified projections of only pro-oocytes and oocytes from germaria on the left as highlighted by the white boxes.

2.1.2. *Nbs^{2K}* mutants have deficient accumulation of dMre11 in ept-mpt pro-oocytes nuclei and deficient formation of HR foci. In *Drosophila,* null mutations in genes encoding MRN complex components are lethal. Thus, in order to further characterize the requirements of dMre11 in the formation of HR foci, I used *Drosophila* hypomorphic *Nbs* mutants. As mentioned before, Nbs1 (Xrs2 in yeast) has a conserved function in eukaryotes; it localizes the MRN complex to the nucleus (Borde, Lin et al. 2004; Ciapponi, Cenci et al. 2006; Gao, Bi et al. 2009; Rupnik, Lowndes et al. 2010). In *Nbs* mutants, the break is formed; but since loading of dMre11 and dRad50 into the nuclei should be affected, dMre11 foci formation would also be impaired. I studied the *nbs^{2K}* allele, which is predicted to encode an N-terminally truncated Nbs protein; previous studies using *Nbs^{2k}* showed that dMre11 and dRad50 (MR) are excluded from chromatin (Gao, Bi et al. 2009).

I stained *nbs^{2k}* mutants with antibodies to C(3)G, dMre11 and γ-H2Av, and as expected for *Nbs* mutants, I observed that in ept dMre11 seems to be excluded from the nuclei. In ept pro-oocytes dMre11 levels were very reduced in the pro-oocytes nuclei and there was not dMre11 foci. However, there seem to be a slight accumulation of dMre11 in mpt to lpt pro-oocytes and oocytes (figure 14a b). After the oocyte exits the germaria it has higher level of dMre11 when compare to region 3 (figure 14 b). Surprisingly, γ-H2Av was observed in some ept-mpt pro-oocytes, but there was a delay in its appearance as well as a reduction in the number of γ-H2Av foci (figure 14a b). This could be due to dNbs being partially functional and/or enough dMre11 is diffusing into the nucleus and some DSBs are recognized, but

there is not enough dMre11 in the nuclei to form a focus that can be readily observed via fluorescence immunocytochemistry techniques. The fact that some dMre11 is detected in stage 2 *nbs*^{2k} oocytes, support that there is some import of dMre11 into the nuclei of pro-oocytes, which probably accumulates more over time allowing the observation of dMre11 in this later pachytene stages.

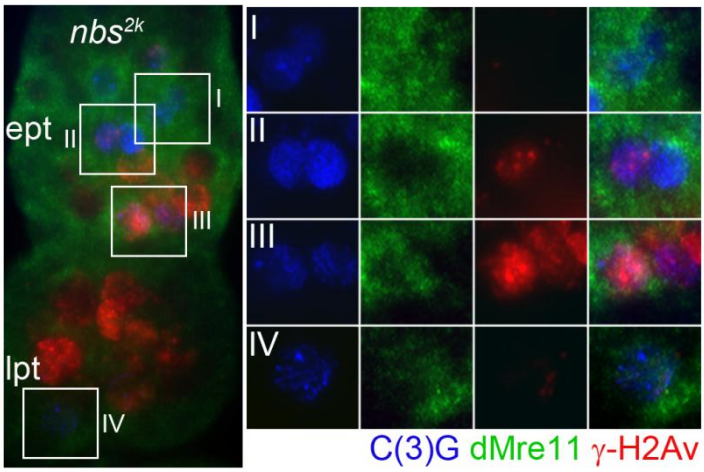

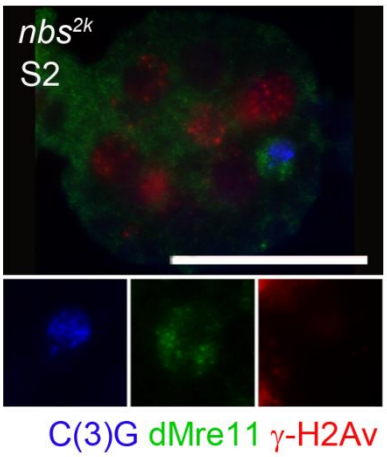

Figure 14: *Nbs^{2K}* mutants have deficient accumulation of dMre11 in ept-mpt pro-oocytes nuclei and deficient formation of HR foci. (A-B) Shows maximum intensity projections of whole mount *Nbs^{2K}* germarium (A) and stage 2 egg chamber (B). Ovarioles were stained with antibodies to C(3)G (blue), dMre11 (green) and γ-H2Av (red). Scale bar, 20μm. (A) Left shows germarium overview of early pachytene to late-pachytene and right shows magnified projections of only pro-oocytes and oocytes from germarium on the left as highlighted by the white boxes. (B) Top shows overview of a stage 2 egg-chamber and bottom shows magnification of a stage 2 oocyte.

2.2. *Drosophila* meiotic mutants with reduced crossover rates have defects in formation, localization and or repair of late large peripheral HR foci.

2.2.1. *mei-218^{1}* mutants have very reduced number of late big peripheral mpt HR foci.

Carpenter described early and late RNs, and proposed that the late RNs represent CO; as such, are the late big and peripheral HR foci observed in mpt the same as late RNs previously described? The observed behavior and characteristics of the late HR foci highly suggests that this is the case. The average number of late HR foci observed in mpt correlates to the number of crossovers per nuclei that was established after genetic analyses of crossover events in *Drosophila melanogaster* (McKim, Jang et al. 2002). The number of late HR foci observed it is in accordance with the average number of late spherical RNs reported

by Carpenter (Carpenter 1975). In addition, the increase in size of HR foci in mpt is also reminiscent of what had been described for spherical RN, which are bigger in diameter and appear later than the earlier ellipsoidal RNs.

Although there is a lot of circumstantial evidence supporting the idea that HR sites are indeed COs, in here I set out to confirm that late HR sites do indeed represent COs. If late HR sites are indeed COs, then in classical mutants in which COs are missing, it would be expected that late peripheral HR sites would also be missing.

Drosophila mutants defective in crossing over have been classified into two groups by genetic studies: precondition mutants and exchange mutants. The exact nature of each mutation in terms of how endogenous molecular functions are altered is still unclear. Precondition mutants are thought to be involved in the establishment of crossovers, they have defects in the non-random distribution of crossovers (Liu, Jang et al. 2000; Bhagat, Manheim et al. 2004). Exchange genes, on the other hand, do not affect the distribution of crossovers and are thought to function in the later steps of repair, in the actual resolution of intermediates. In both exchange and precondition mutants, NCO rates seem to be unaffected (Liu, Jang et al. 2000; Bhagat, Manheim et al. 2004). In here I used the precondition mutant *mei-218. mei-218* mutants have a reduction in crossovers by more than 90% of the wild type, but formation of non-crossovers events and initiation of recombination is unaffected (Liu, Jang et al. 2000; Bhagat, Manheim et al. 2004). In addition, Carpenter 1979 reported a reduction of late, large RNs to 16% of the wilds type and a slight reduction of early RNs in *mei-218* mutant flies (Carpenter 1979; Carpenter 1982)

When *mei-218*^{1} mutants were stained with anti-dMre11, anti-C(3)G and anti-γ-H2Av antibodies I observed a reduction in the number of big dMre11 foci that are found in the periphery in mpt (figure 15). In *mei-218*^{1} germaria, HR foci in ept pro-oocytes seem to be slightly reduced in number; more importantly HR foci were small and located towards the center of the nuclei. mpt pro-oocytes had very reduced numbers of HR foci, and the few foci that were observed were small and rarely found in the nuclear periphery (figure 15a-b). Figure 15A' shows single planes of ept and mpt pro-oocytes showing that most HR repair sites are in the middle of the pro-oocyte nuclei in ept meiocytes and mostly absent by mpt. There was an average of 1.3 foci +/- 0.8 (n=26) small non-peripheral foci in mid-pachytene (15b). My results, together with previous studies on *mei-218*, suggest that the big late HR foci found at the periphery of the mpt nuclei are crossover sites and are also likely to correspond to late RNs.

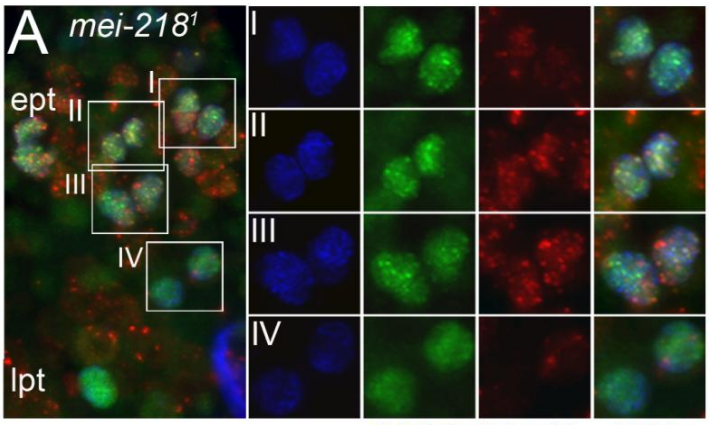
A
mei-218¹
ept
lpt
I
II
III
IV
C(3)G dMre11 γ-H2Av

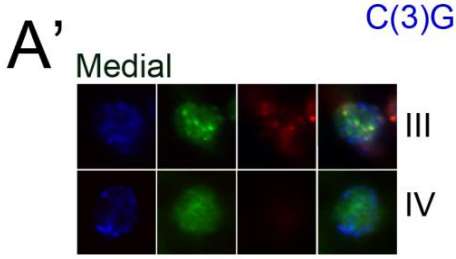
A'
Medial
III
IV

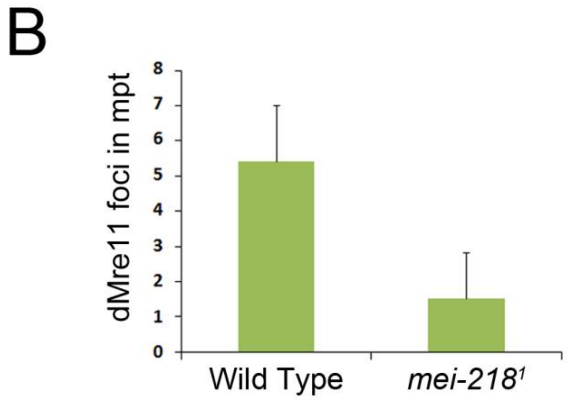
B
dMre11 foci in mpt
0
1
2
3
4
5
6
7
8
Wild Type
mei-218¹

Figure 15: Large peripheral foci are missing in mid-pachytene meiocytes from *mei-218*^{1} mutants females. (A) Left panel shows maximum intensity projection of *mei-218*^{1} germarium. *mei-218*^{1} germaria were stained with antibodies to C(3)G (blue), dMre11 (green), and γ-H2Av (red). Right shows magnification of stacked region ept-mpt pro-oocytes from the *mei-218*^{1} germarium on left as shown by the white boxes. (A') Shows single plane sections of magnified pro-oocyte's nuclei from region ept (III) and mpt (IV) of figure A. (B) Counts of dMre11 foci observed in mid pachytene pro-oocytes of wild type (wt) and *mei-218*^{1} females. Bar graph represents average number of dMre11 foci per pro-oocyte. Error bars represent standard deviation. Wt n= 18, *mei-218* n=20.

2.2.2. *mei-9a* mutants have a transient delay in the repair of large peripheral HR foci.

Next, I studied the exchange mutant *mei-9*. Just as in *mei-218* mutants, *mei-9* mutants also have defective crossover rates (Sekelsky, McKim et al. 1995). However, as opposed to *mei-218*, it has been reported that *mei-9* mutants do not have a reduced number of late RNs (Carpenter 1979; Carpenter 1982). *mei-9* encodes an endonuclease homologous to XPF/Rad1 which may have a role in the resolution reaction that generates crossovers (Sekelsky, McKim et al. 1995). I stained *mei-9*^{a} mutants with C(3)G, dMre11 and γ-H2Av antibodies and observed that large foci form and go to the periphery in mpt. In addition, these foci seem to persist at the periphery to later stages of oogenesis (figure 16a and a'). The observed persistence of foci is in accordance with the published role of mei-9 in the actual resolution of crossovers. Most likely, COs and NCOs were made and COs were

moved to the periphery as in wild type; however, once at the periphery some COs failed to be resolved. It is also important to note that not all COs persist; this suggesting that some COs are getting repaired, but the repair process is not at 100% efficiency.

2.2.3. *mei-41^{D3}* mutants have impaired formation and nuclear localization of late HR foci. Another factor that has been reported to be important for normal occurrence of crossovers is *Drosophila* homolog of ataxia telangiectasia–related kinase (ATR), mei-41 (Carpenter 1979; Liu, Jang et al. 2000; McKim, Jang et al. 2000; Sonam Mehrotra, R. Scott Hawley et al. 2008). Females carrying strong *mei-41* alleles are sterile, and thus crossover rates had only been assayed in weak alleles. In carriers of weak alleles, DSB formation was reported to be normal and crossover rates reduced (McKim, Jang et al. 2000; Sonam Mehrotra, R. Scott Hawley et al. 2008). Mei-41 has important roles in the cellular response to DNA damage, and is involved in DSB repair and checkpoint activation (Carpenter 1979; Sibon, Laurencon et al. 1999; McKim, Jang et al. 2000; Goodarzi, Block et al. 2003; Laurencon, Purdy et al. 2003)

In order to test if *mei-41* females have a reduced number of late HR foci, I stained ovaries from *mei-41* mutant flies with anti-dMre11, anti-γ-H2Av and anti-C(3)G antibodies (figure 17). Most of the current studies that assess number of CO events

use genetic techniques, for which the progeny need to be analyzed. In here I intended to analyze appearance of COs in *Drosophila* females during the early stages of oogenesis using Immunohistochemistry techniques, and thus I used *mei-41*^{D3} homozygous females. *mei-41*^{D3} is one of the strongest alleles that has been described as a null base on female sterility and absence of protein (Sibon, Laurencon et al. 1999). After staining of *mei-41*^{D3} females, I observed that HR foci in *mei-41*^{D3} pro-oocytes did not seem to increase in size from early to mid-pachytene (Figure 17a). More importantly, in *mei-41*^{D3} pro-oocytes HR foci failed to localize to the nuclear periphery in mpt and persist to latter stages of oogenesis, where they are also found towards the center of the nuclei as opposed to the nuclear periphery (Figure 17a b). Thus, Mei-41 may also be essential for the proper localization of HR foci to the nuclear periphery; in addition, Mei-41 may have a role in the accumulation of repair factors to the DSB not only in mid-pachytene but also throughout early pachytene. Interestingly, in yeast it has been shown that slowly repaired foci move to the nuclear periphery, and that this movement is dependent on both Mec-1, the yeast ATR homolog, and Tel-1, the ATM homolog (Nagai, Dubrana et al. 2008). This further supports that Mei-41 in flies is most likely involved in the localization of CO to the nuclear periphery.

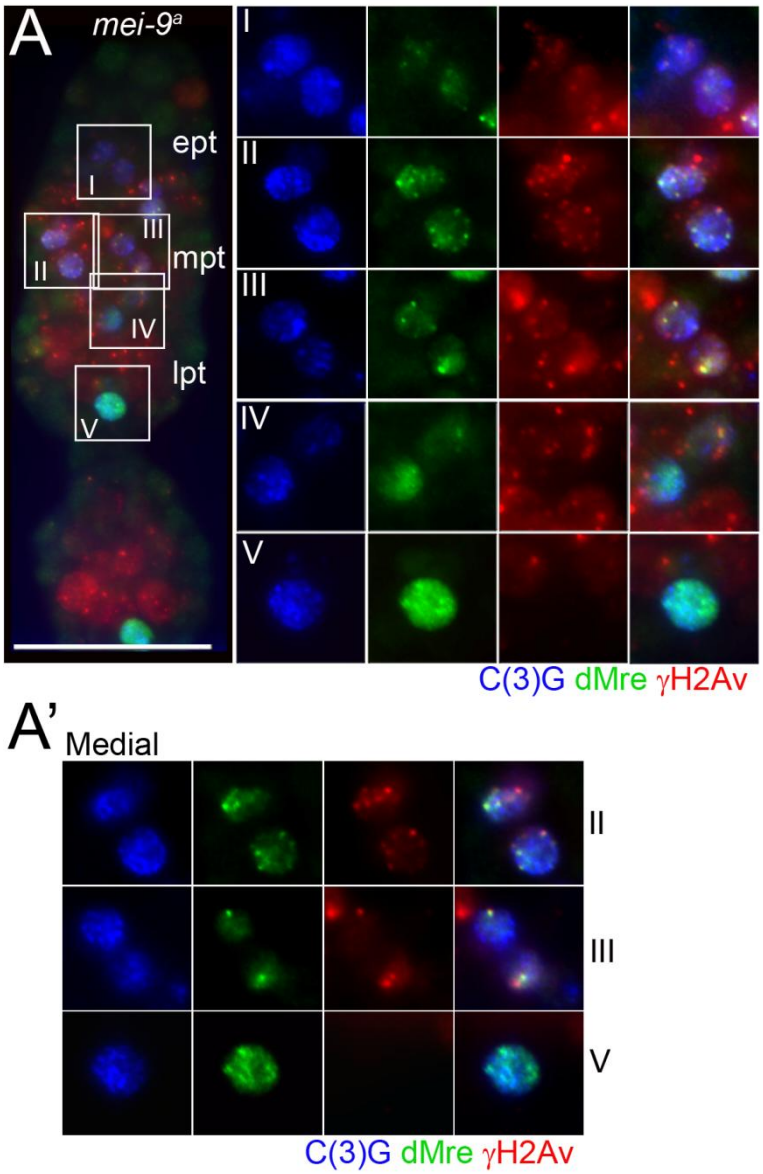

Figure 16: *mei-9*^{a} mutants have a transient delay in the repair of large peripheral HR foci. (A) Left panel shows maximum intensity projection of an entire *mei-9*^{a} germarium. *mei-9*^{a} germaria were stained with antibodies to C(3)G (blue), dMre11 (green), and γ-H2Av (red). Right shows magnification of stacked region ept, mpt and lpt pro-oocytes from the *mei-9*^{a} germarium on left as shown by the white boxes. Scale bar, 20µm (A') Single plane sections of magnified pro-oocyte or oocyte nuclei from region mpt (II), mpt (III) and advanced lpt (V) of figure A.

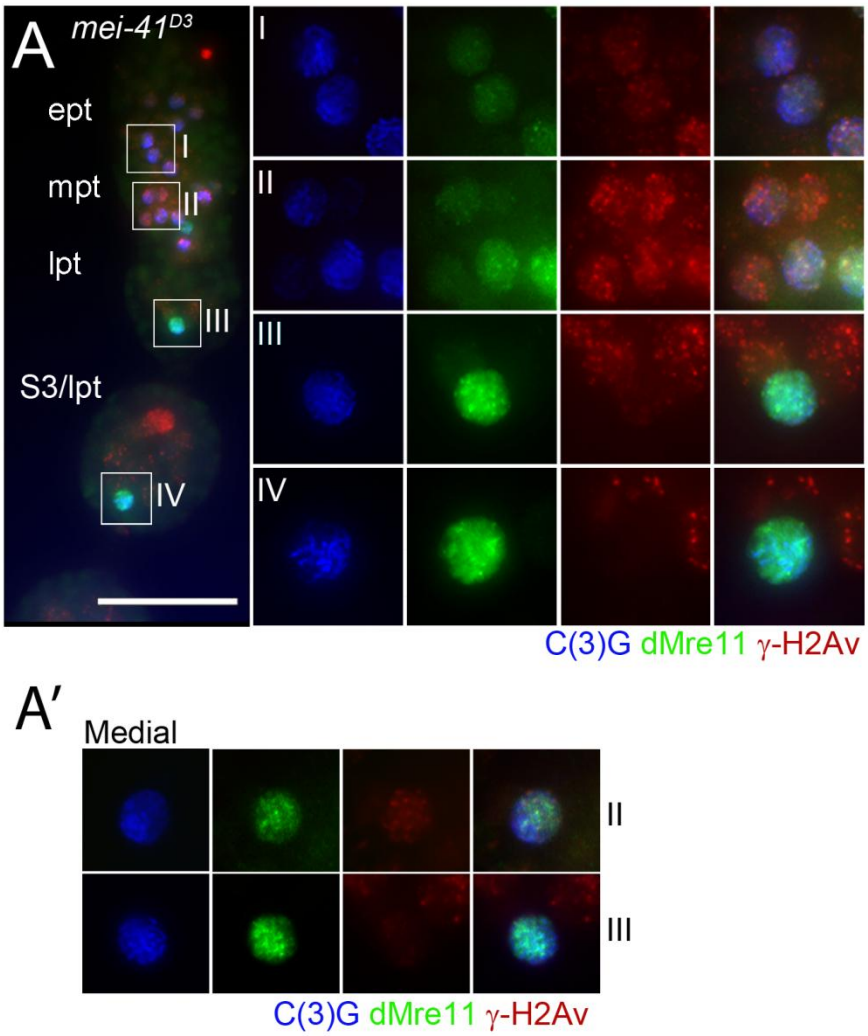

Figure 17: HR foci in *mei-41^{D3}* mutant females are small, persist to latter stages of oogenesis, and fail to localize to the nuclear periphery. (A). Left panel shows maximum intensity projection of a *mei-41^{D3}* ovariole stained with antibodies to C(3)G (blue), dMre11 (green) and γ-H2Av (red). Right shows magnified projections of pro-oocytes and oocytes from the germarium on the left as marked with the white boxes. Scale bar, 20µm. (A') Median plane of nuclei from magnified pro-oocytes or oocytes mark with the white boxes in the overview shown in A.

2.3. Role of tefu protein kinase in the nuclear localization of late HR foci.

Like ATR, Ataxia telangiectasia–mutated (ATM) is a member of the phosphatidyl inositol 3-kinase-like family of serine/threonine protein kinases (PIKKs), which are conserved regulators of cellular responses to double strand breaks (DSBs) and, as mentioned previously, it has been implicated in the movement of slow repair foci to the periphery in yeast (Nagai, Dubrana et al. 2008). In mammals, ATM is the primary kinase for checkpoint and regulation of DSB damage response. Since ATR and ATM are protein kinases involved in the regulation and signaling of the DNA damage response, it is possible that both are also involved in the regulation and/or signaling of movement to periphery of late HR foci. As such, I next studied ATM mutants to determine their involvement in the regulation and/or signaling of the movement of late HR foci to periphery

The *Drosophila* homolog of ATM is Tefu, named base on its role in preventing spontaneous telomere fusions. *tefu* mutants die as pupae, and the few escapers observed are sterile and die at a young age. Developing larval discs exhibit substantially increased chromosomal and telomere fusions and a high level of spontaneous apoptosis (Song, Mirey et al. 2004). Recent studies used a temperature sensitive allele of *tefu, tefu*^{8}, in order to bypass the lethality associated with homozygous *tefu* mutants. This study showed that ATM in flies is also involved in DSB repair and that it phosphorylates H2Av (Joyce, Pedersen et al. 2011). In addition, this study together with studies done by the Keeney group suggest that the number of DSBs is controlled by ATM; it was proposed that ATM negatively

regulates Spo11 to prevent the formation of additional breaks (Joyce, Pedersen et al. 2011; Lange, Pan et al. 2011).

In here I also take advantage of the temperature sensitive allele *tefu*^{8}. *tefu*^{8} mutants were shifted from the permissive temperature (18 degrees) to the restrictive temperature (25 degrees), as established in studies where this allele was characterized (Silva, Tiong et al. 2004). I then stained ovaries at different time points after switching to the restrictive temperature. I observed defects as early as 6 hours; at this time point I observed an increase of γ-H2Av in the nurse cells in ept to mpt. In addition I observed persistence of few very large HR foci to late pachytene in oocytes (Figure 18a).

A more severe phenotype was observed after 2 days at the restrictive temperature, where I observed massive accumulation of γ-H2Av in ept to mpt pro-oocytes and nurse cells. At this stage, γ-H2Av accumulated to such an extent that a single repair focus could not be identified in pro-oocytes (figure 18b). γ-H2Av staining was continuous and seems to paint long stretches of chromosomes. Surprisingly, in this mutant dMre11 foci did not accumulate as heavily in the pro-oocytes as γ-H2Av. ATM's phenotype seems to be dependent of cyst staging; in early stages of ept, I observed pro-oocytes with distinct dMre11 foci that co-localized with γ-H2Av foci. Towards the end of ept and the beginning of mpt there is a very heavy phosphorylation of H2Av and distinct foci could not be observed; although dMre11 staining was not thread like as γ-H2Av, distinct dMre11 foci could not be observed either. Furthermore, in mpt γ-H2Av seem to concentrate more in

the nuclear periphery (figure 18b'). Towards later stages of mid-pachytene I observed abnormal HR foci; they are larger than HR foci observed in wild type pro-oocytes and they persist to late pachytene.

These observations suggest that ATM and ATR in *Drosophila* play important roles in the phosphorylation of H2Av, and each of these kinases seem to have different roles in the localization of HR foci to the periphery. In addition, ATM and ATR functions seem to also be tightly regulated according to the developmental stage of the cyst.

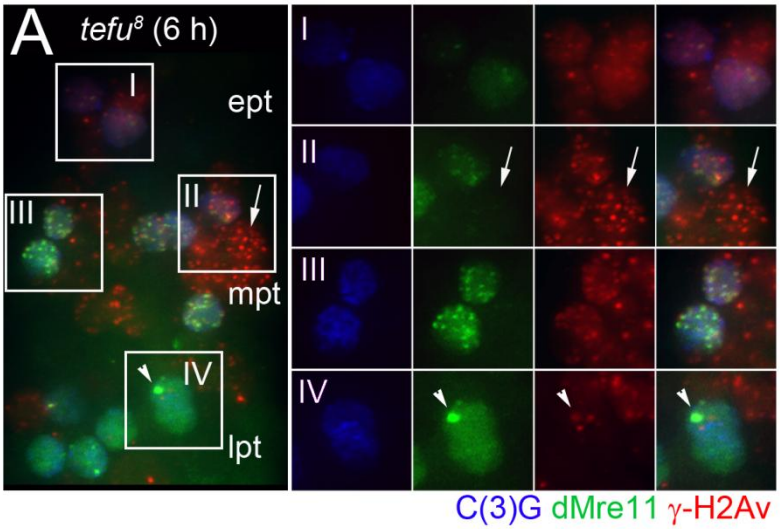
A
tefu8 (6 h)
I
ept
II
III
mpt
IV
lpt
I
II
III
IV
C(3)G dMre11 γ-H2Av

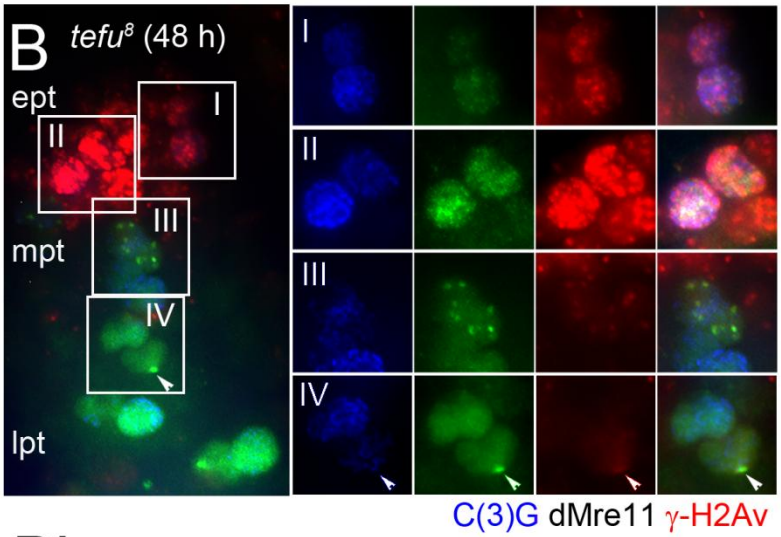
B
tefu8 (48 h)
ept
I
II
III
mpt
IV
lpt
I
II
III
IV
C(3)G dMre11 γ-H2Av

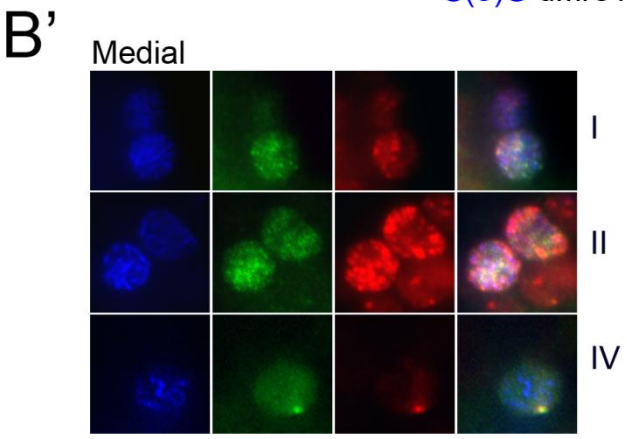
B'
Medial
I
II
IV

Figure 18: *tefu*^{8} mutants have increased levels of γ–H2Av only in early to mid pachytene and persistence of peripheral HR foci. (A-B) Maximum intensity projection of whole mount *tefu*^{8} *Drosophila* germarium stained with antibodies to C(3)G (blue), dMre11 (green) and γ–H2Av (red). *tefu*^{8} mutants were shifted to the restrictive temperature for 6 hours (6 h) or for 2 days (48 h) prior to dissection. (A) Shows defects in *tefu*^{8} germaria after 6 hours at the restrictive temperature. Arrows show strong γ-H2Av in the nurse cells. Arrow heads show large persisting dMre11 foci in the nuclear periphery. Right side shows magnification of the cells as marked by the white boxes. (B) *tefu*^{8} germarium after two days at the restrictive temperature. Left shows germarium overview; arrow shows large persisting HR foci in the nuclear periphery. Right shows maximum intensity projection of Z-series taken through the entire nucleus of *tefu*^{8} pro-oocytes showing a moderate γ-h2av response in early pachytene versus a heavy γ-H2av response in mid pachytene. (B') Shows magnifications of single

2.4. Large peripheral foci can be observed in mpt and lpt mei-W68 oocytes after DSBs are introduced by X-rays:

mei-W68 mutants fail to form DSBs, and therefore have very reduced crossovers rates. Studies by Bhagat *et al* using *mei-W68* mutants showed that crossovers can be re-established upon DSB induction by X-rays (Bhagat, Manheim et al. 2004). Since *mei-W68* mutants do not form any foci and irradiation may introduce some late HR foci, irradiation of *mei-W68* could be a good tool for studying the appearance and or disappearance of late HR foci. For example, a time course study of HR foci formation after irradiation of *mei-W68* mutants would give a better idea

of when HR foci initiate movement to the periphery. As suggested by data that I've previously shown (figure 8 and figure 9), late peripheral HR foci are dragged to the periphery after ept and during mpt; one would then expect to see small HR foci in early pachytene, and late big peripheral HR sites in mid-pachytene or from mid-pachytene on, depending on the damage caused by the irradiation and the ability of the females to repair in a timely manner.

mei-W68 mutants were X-ray irradiated at 12 Gy using a Faxitron machine and were subsequently immunostained (figure 19). Ovaries were stained at two different time points: early time point, 15 minutes (figure 19a) and a later time point, 3 hours (figure 19b). Surprisingly, after irradiation in the early time points, dMre11 and γ-H2Av signals were fuzzy and there were very few and small foci in ept pro-oocytes of both wt and *mei-W68* mutants. In the early time point, HR foci were readily distinguishable from mid to late pachytene in both wild type and *mei-W68* (figure 19a)

When analyzing mid-late pachytene HR sites in wild type and *mei-W68* irradiated pro-oocytes by comparing early time points to later time points (for analysis only pro-oocytes in the same position were taken into consideration), I observed that in 3 hours HR foci appear more concentrated in the periphery, especially in the wild type germaria (figure 19 a-b). HR sites in mpt-lpt pro-oocytes or oocytes of *mei-W68* germaria seem to have a greater tendency to localize towards the nuclear periphery as early as 15 minutes. Our observation of HR foci as early as 15 minutes agrees with previous findings, where X-rayed *mei-W68* females re-establish CO rates and

with the idea that late HR sites may correspond to COs. In addition, the fact that that I observed HR foci getting lesser and accumulating in the periphery of irradiated pro-oocytes in mid-pachytene at 3 hours post irradiation furthers agrees with a model in which late HR foci represent COs and move from the center of the nuclei to the nuclear periphery for repair.

2.5. All HR sites, COs and NCOs, have the possibility to relocate to the nuclear periphery when repair is abolished or delay

2.5.1. HR foci persist to region 3 and accumulate in the nuclear periphery of oocytes from females with deficient DSB repair. As mentioned, there are two types of HR foci -- early and late. Early HR sites are small and form in the center of the nuclei, and most of them are repaired there. The large HR foci persist and then move to the nuclear periphery. Considering that COs are repaired more slowly (Allers and Lichten 2001), it is therefore possible that a developmentally controlled signal occurring at advanced ept or the beginning of mpt causes their peripheral movement. As such, the timing of repair could be sufficient; if not repaired by a certain developmental stage, the unrepaired or slow HR site is moved to the periphery.

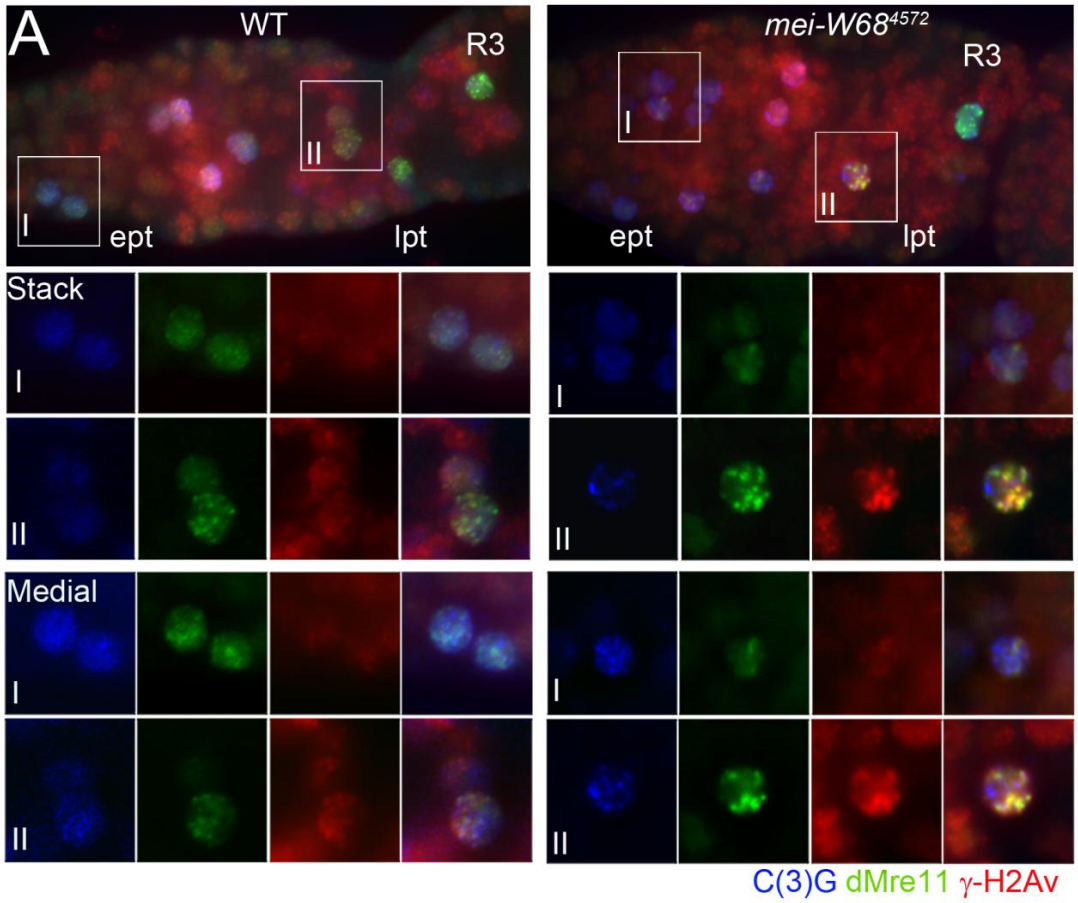
A
WT
R3
I
II
ept
lpt
mei-W68^4572
R3
I
II
ept
lpt
Stack
I
II
Medial
I
II
C(3)G dMre11 γ-H2Av

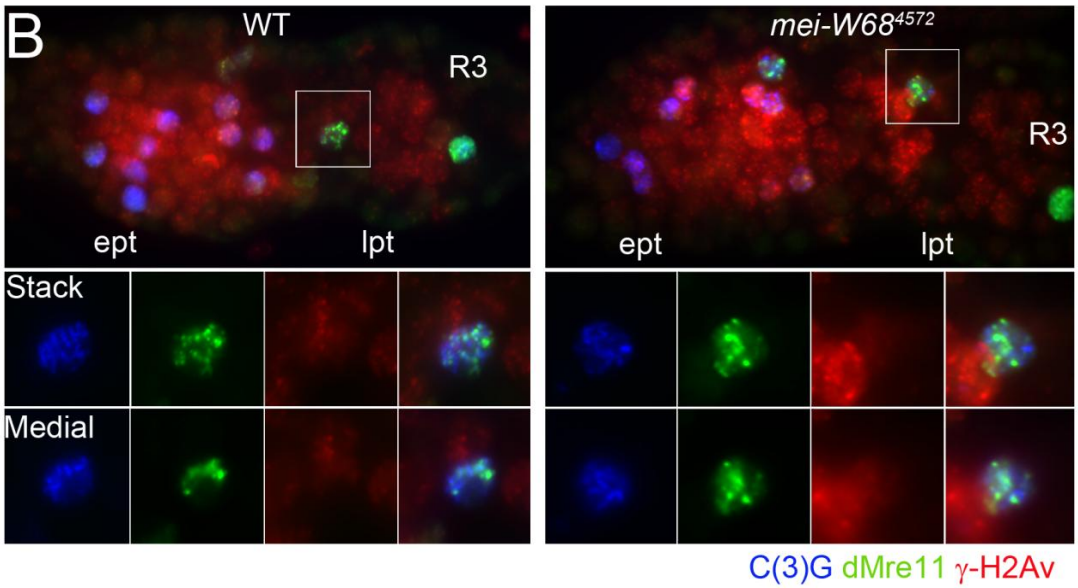
B
WT
R3
ept
lpt
mei-W68^4572
R3
ept
lpt
Stack
Medial
C(3)G dMre11 γ-H2Av

Figure 19: Large peripheral foci can be observed in mpt and lpt of *mei-W68* oocytes after DSBs are introduced by X-rays. (A-B) Top shows maximum intensity projection of an entire wild type (WT) and *mei-W68*^{4472} germarium after 15 minutes (A) and 3 hours (B) of irradiation with 12Gy using an X-ray Faxitron machine. Germaria were stained with antibodies to C(3)G (blue), dMre11 (green), and γ-H2Av (red). (A) Middle shows magnified stack of ept (I) and mpt (II) pro-oocytes/oocytes nuclei as marked by the white boxes in the top overviews. (A) Bottom shows magnified single plane section of ept (I) and mpt (II) pro-oocytes/oocytes in the top overviews. (B) Bottom shows stacks and medial sections of nuclei mark with the white boxes as on the top overview.

In order to test if all slow or unrepaired DSBs are able to go to the periphery or only the preselected COs can do so, I next set out to study *Drosophila* mutants with delayed or abolished DNA repair. I studied the behavior of HR foci in *spn-A* (Rad51 homolog) and *okr* (Rad54 homolog) mutant females. *Spn-A* and *okr* are genes essential for recombinational repair. In *Drosophila*, null *spn-A* mutants are viable, but oogenesis is disrupted (Staeva-Vieira, Yoo et al. 2003; Yoo and McKee 2005). Studies of *Drosophila* female meiosis have shown that *spn-A* and *okr* mutants have persistent accumulation of γ-H2Av foci. Phosphorylation of H2Av was observed to persist through later stages of oogenesis (Jang, Sherizen et al. 2003; Klovstad, Abdu et al. 2005). Consistent with these studies, when *spn-A* ovaries were stained with anti-dMre11, anti-C(3)G and anti-γ-H2Av antibodies, I observed an accumulation of dMre11 foci that persisted to region 3 (advance pachytene) oocytes (figure20). In

spn-A mutants, there was an average of 20 foci +/- 4 (n:20) in region 3. A comparison of maximum intensity projections through region 3 pro-oocyte nuclei (stacks) and single plane sections of region 3 pro-oocytes nuclei suggest that most of the persistent foci localized to the nuclear periphery in *spn-A* (figure 19 a-a'). Additionally, the staining suggests that in *spn-A* females HR foci seem to localize to the nuclear periphery starting in mpt (figure 20 a-a'). In order to confirm the peripheral localization of persisting HR foci, I stained *spn-A* germaria with antibodies to lamin, C(3)G and dMre11 (figure 20 b). As expected, the majority of the foci in region 3 oocytes were found in close proximity to lamin.

When *okr* mutants were stained and images were analyzed, the comparisons of stacks and single plane section of HR foci in *okr* mutants also showed that HR foci persisted up to region 3 and seem to be mostly located in the nuclear periphery (figure 21). The results obtained from both *spn-A* and *okr* mutants provide evidence that all DSBs have the ability to re-localize to the periphery if they persist until later stages. Therefore, it is most likely not the quality of the DSB but the timing that is key for movement to the periphery. If breaks are not repaired by certain time, they are dragged to the periphery for repair

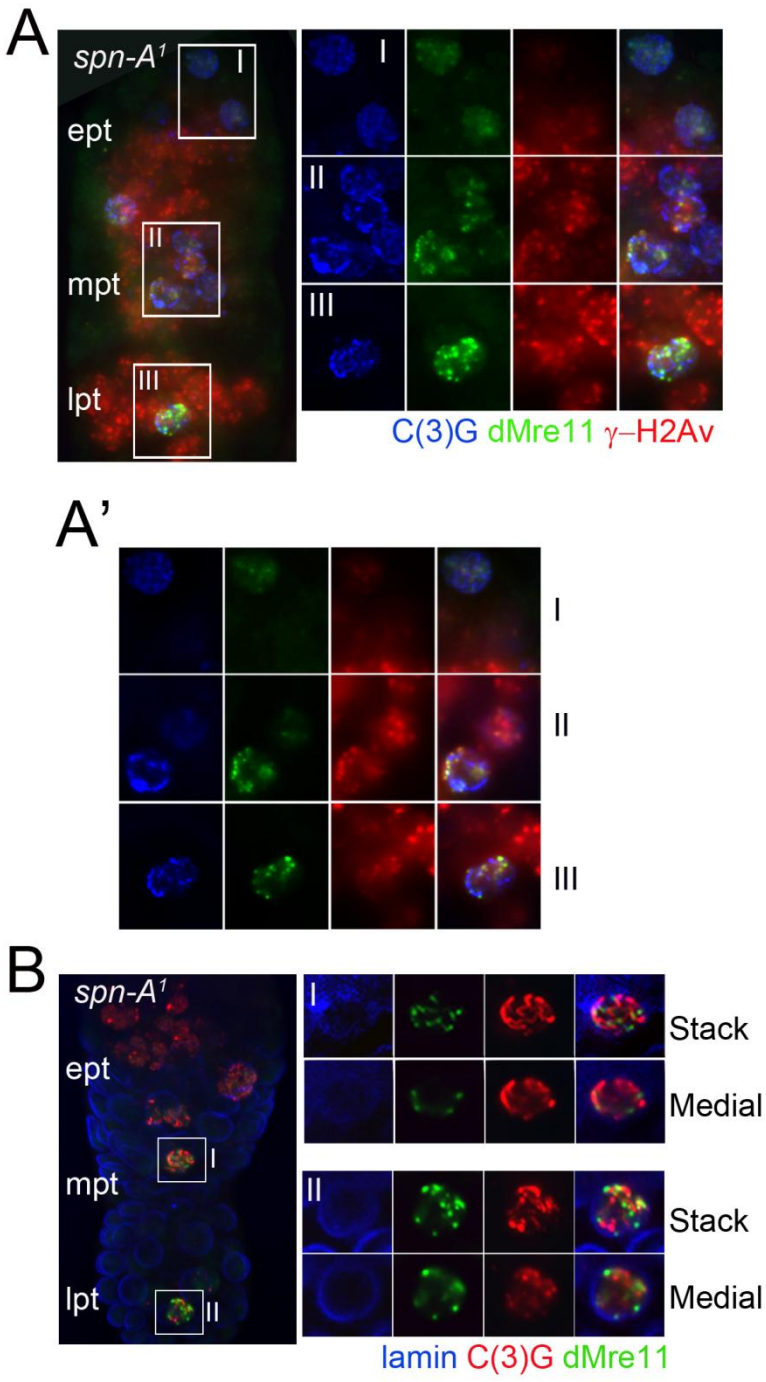
A
spn-A¹
ept
mpt
lpt
I
II
III
C(3)G dMre11 γ–H2Av
A'
B
spn-A¹
Stack
Medial
lamin C(3)G dMre11

Figure 20: *spn-A* mutants have persistent HR foci most of which accumulate in the nuclear periphery (A-B) Maximum intensity projections of a whole mount ovariole from *spn-A*^{1} females stained with antibodies to C(3)G (blue), dMre11 (green), and γ-H2Av (red). (A) Left shows overview of *spn-A*^{1} germarium. Right shows magnified projections of ept, mpt and lpt pro-oocytes and oocytes nuclei taken from overview on the left as shown by the boxes. (A') single plane sections of ept, mpt and lpt nuclei as marked by the white boxes in A. (B) Left shows overview of *spn-A*^{1} germarium stained with antibodies against lamin (blue), C(3)G (red) and dMre11 (green). Right shows magnified projections of mpt and lpt pro-oocytes and oocytes nuclei from germaria on left (stack). Right shows single plane section of ept and mpt nuclei as denoted by the white boxes.

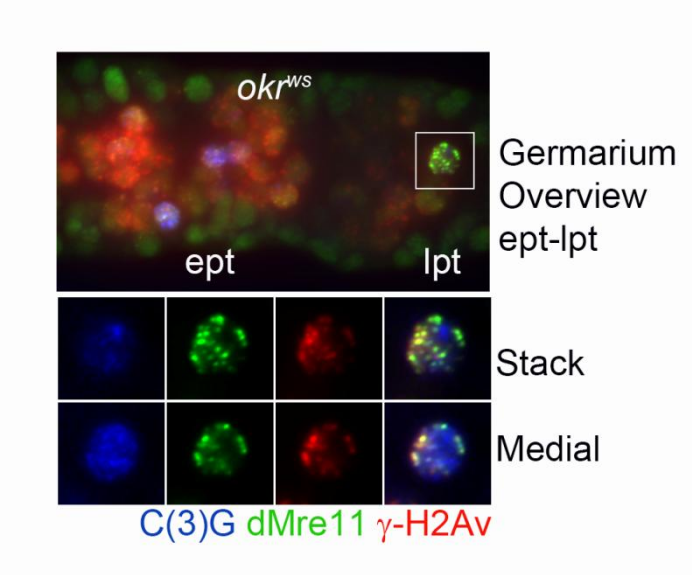

Figure 21: *okr*^{ws} mutants have persistent HR foci and they accumulate in the nuclear periphery. Top shows maximum intensity projections of a whole mount germarium from *okr*^{ws} females stained with antibodies to C(3)G (blue), dMre11 (green) and γ-H2Av (red). Bottom shows maximum intensity projection (stack) of the late pachytene oocyte nuclei (R3) and single plane (medial) of the same late pachytene nuclei.

2.5.2. dMre11 foci persist to later stages of oogenesis and γ-H2Av signaling is reduced from advanced pachytene on. *spn-A* ovarioles were stained to see if HR foci will persist to later stages of oogenesis. When ovarioles were stained, I observed that dMre11 foci persisted up to at least stage 4 in the vitellarium (figure22). In addition, HR foci seemed to localize primarily at the nuclear periphery in these later stages. Surprisingly, I saw a reduction of γ-H2Av staining in the oocyte of advanced pachytene, when the oocyte entered the vitellarium (S2-S4), however, dMre11 foci were still present in these oocytes (figure 22). It is possible that in these later stages of oogenesis phosphorylation of H2Av is defective due to compaction and inaccessibility to H2Av.

To ensure that the lack of phosphorylation of H2Av in later stages was not due to the absence of H2Av, I stained wild type *Drosophila* females with H2Av antibodies (figure 23). The results showed that H2Av is present in the nuclei of pro-oocytes, oocytes, nurse cells and follicle cells of the *Drosophila* germaria (figure 23). Although the H2Av signal is to maintain in the follicle cell through later stages of oogenesis, the H2Av signal in the oocyte differs: The signal is strong in S2 and S3 oocytes, starts decreasing in S4-S5 oocytes, and is completely gone by S6 oocytes (figure 23). As such, it is highly likely that reduction of γ-H2Av is not due to a lack of H2Av.

In order to further study the appearance of dMre11 in relationship to γ-H2Av in later stages of oogenesis and see if oocytes in these later stages retain the ability to phosphorylate H2Av, irradiated wild type *Drosophila* females were analyzed. After

dissection, ovaries were fixed and stained at different time points. The earliest time point at which ovaries could be fixed and stained was 15 minutes post-irradiation (figure 24). Ovaries were also fixed and stained at 30 and 60 minutes after irradiation (figure 24). Oocytes from stage 2 were analyzed and compare to region 3 oocytes, which seem to maintain higher levels of γ-H2Av. I observed dMre11 foci as early as 15 minutes post irradiation in both region 3 and stage 2 oocytes. However stage 2 oocytes had very reduced levels of γ-H2Av foci when compared to region 3 oocytes at 15 minutes post-irradiation (figure 24). γ-H2Av foci were visible at 30 minutes in both region 3 and stage 2 oocytes. However, by 60 minutes region 3 γ-H2Av signals seem to be decreasing, and stage 2 γ-H2Av signal seem to be still increasing. Thus, during later stages of oogenesis the ability to signal to chromatin seemed to be delayed or slower. As suggested from the H2Av staining, this is likely not due to the disappearance of the histone variant, but could be due to the cell getting ready for the compaction of its genome into the karyosome. Alternative, it is possible that ATM and ATR kinases are not readily available in S2 oocytes.

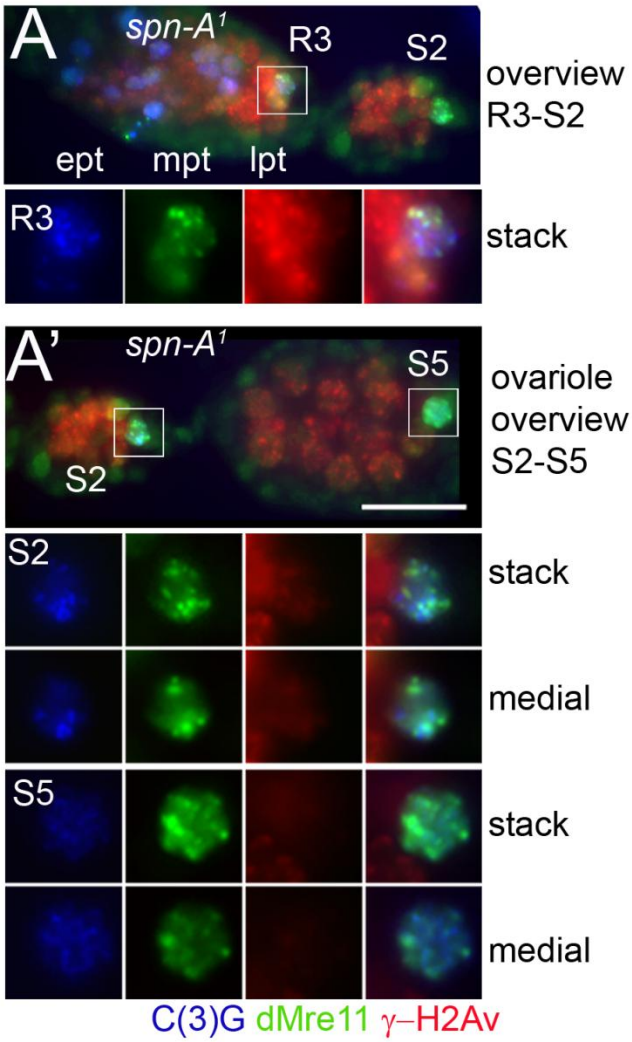

Figure 22: In *spn-A*^{1} females, dMre11 foci persist in oocytes to later stages of oogenesis, but reduced levels of H2Av phosphorylation are observed in the oocyte. **(**A-A') Top shows maximum intensity projections of a whole mount germaria showing region 3 to stage 2 (A) and ovariole showing S2 to S5 (A') from *spn-A*^{1} females stained with antibodies to C(3)G (blue), dMre11 (green), and γ-H2Av (red). (A) Bottom shows maximum intensity projection of the entire region 3 oocyte's nuclei (stack). (A'). Bottom shows magnified stage 2 and stage 5 *spn-A*^{1} oocytes nuclei taken from overview on top as shown by the boxes. Stack represents maximum intensity projection of the entire oocyte nuclei; medial represents single plane section through the middle of the nuclei. Scale bar, 20 μm.

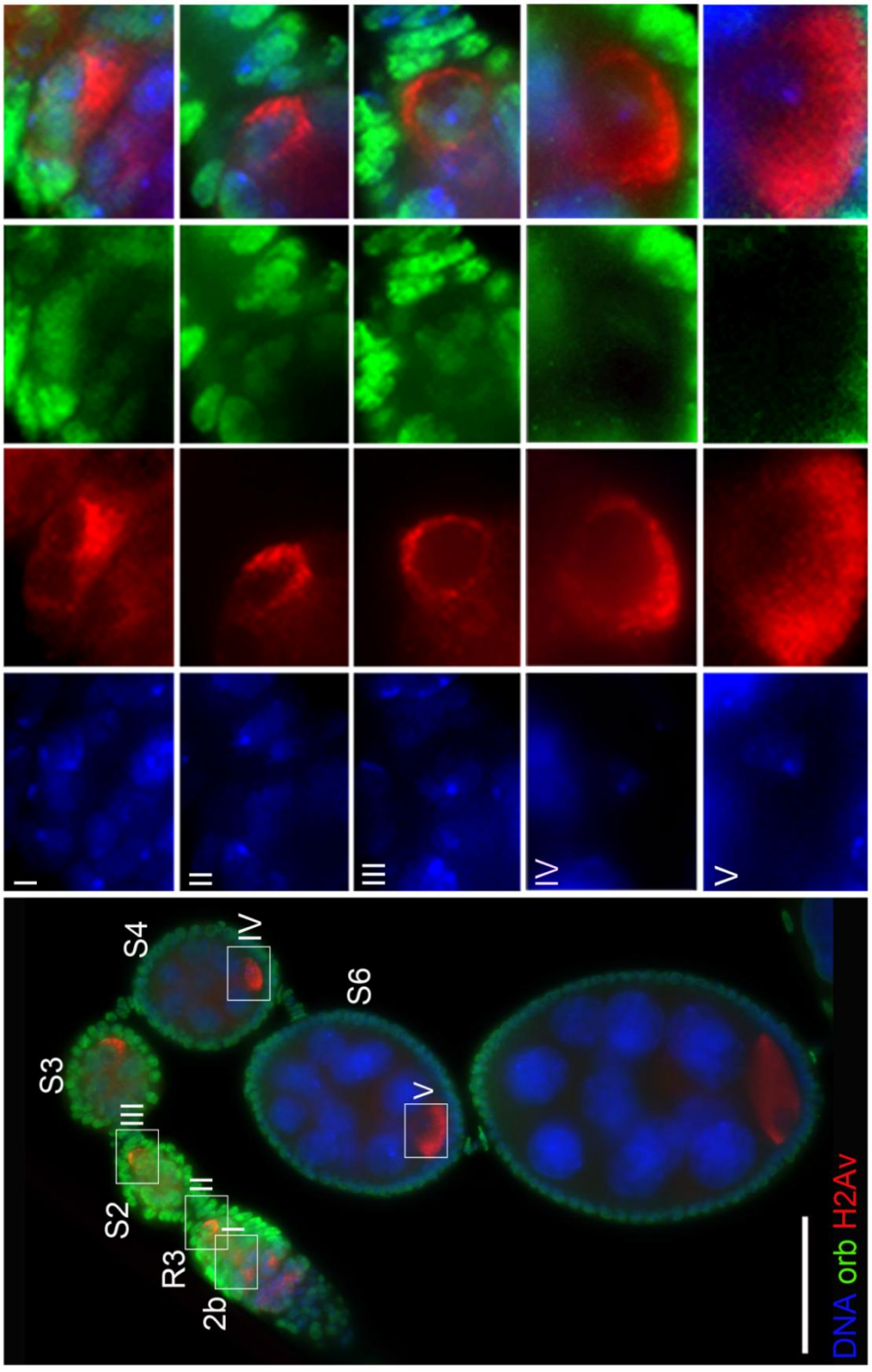
I
II
III
IV
V
S3
S4
S6
S2
R3
2b
DNA orb H2Av

Figure 23 Histone variant H2Av is detectable up to S4 oocytes. Left shows projection of wild type *Drosophila* ovariole stained with antibodies to Orb (red) and H2Av (green). DNA was labeled with DAPI (blue). Scale bar, 40µm. Right shows magnified projection of oocytes and pro-oocyte nuclei from ovariole overview in figure on the left.

2.6. *Spindle B, C, D* genes and phosphorylation of H2Av play important roles in the amplification of the DNA damage response.

2.6.1. Mutations in the spindle genes, *spn-B, spn-C, spn-D*, have defects in the accumulation of dMre11 to repair foci.

In section 2.4 I introduced the *spn-A* gene and showed that this gene product is necessary for the timely repair of meiotic DSBs. In *Drosophila* there are at least three more genes related to *spn-A*; they are spindle genes *spn-B, spn-C* and *spn-D*. Previous studies have shown that spindle class genes *spn-A, spn-B* and *spn-D* have similar phenotypes when stained with γ-H2Av antibodies. It was observed that the *spn-A, spn-B* and *spn-D* mutants have persistent γ-H2Av foci up to later stages of oogenesis (Mehrotra and McKim 2006). Based on this result, it was believed that in *Drosophila* these genes have very similar functions in the DNA damage repair pathway. However, recent studies in mice cell lines with mutants for spindle gene homologs do not show identical phenotypes, suggesting that their functions may differ; similar results were obtained in loss-of-function studies done in *Arabidopsis* (Bleuyard, Gallego et al. 2005; Yonetani, Hochegger et al. 2005).

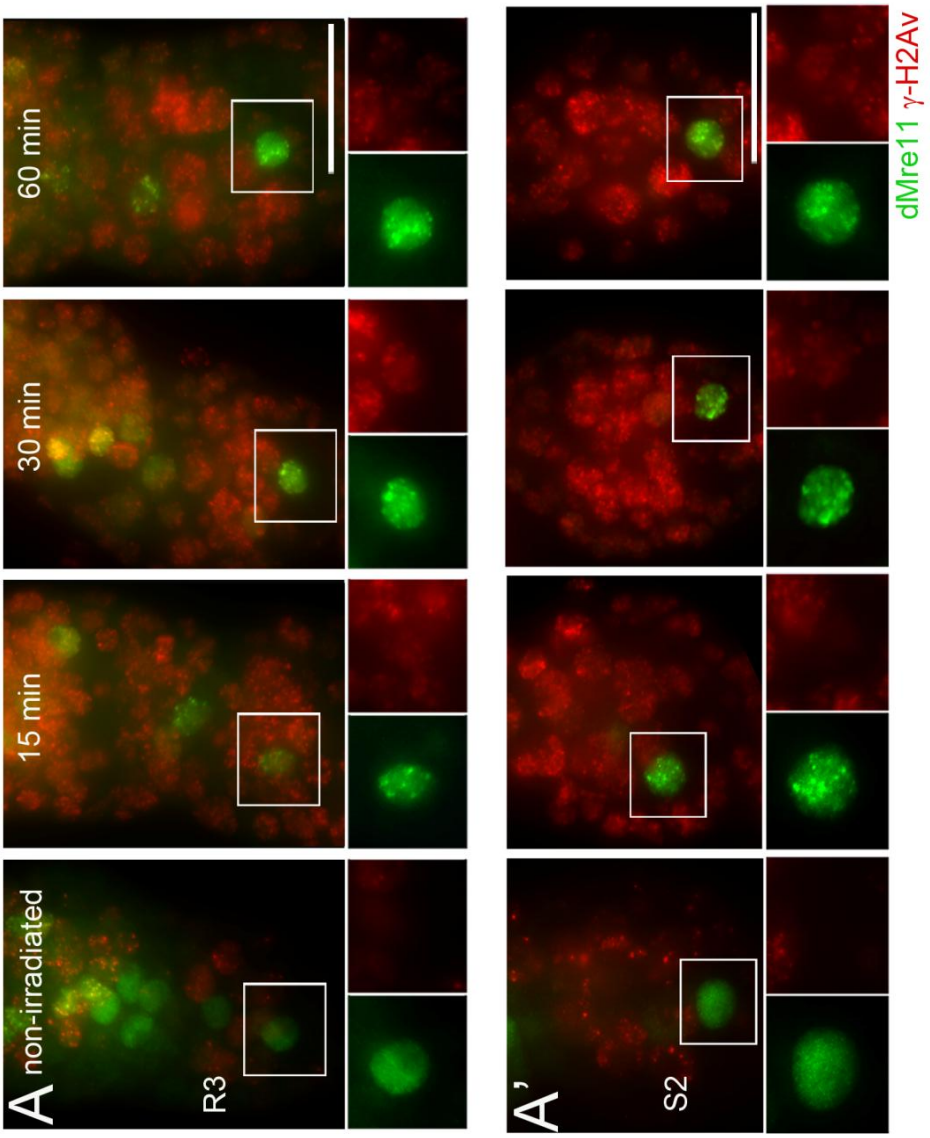
A non-irradiated
15 min
30 min
60 min
R3
A'
S2
dMre11 γ-H2Av

Figure 24: Late pachytene oocytes have attenuated phosphorylation of H2Av after irradiation-induced DSBs. Wild type *Drosophila* region 3 (A) and stage 2 (A') oocytes stained with anti-dMre11 (green) and γ-H2Av (red) antibodies. Oocytes were fixed and stained at different time points after irradiation with 12 Gy using a faxitron x-ray machine**.** The time points chosen were 15, 30 and 60 minutes. Bottom panels of A and A' show magnification of whole mount oocytes nuclei. Scale bar, 20μm.

In order to see if these genes had similar phenotypes to *spn-A* and *okr* in regards to HR behavior and nuclear localization, I stained ovaries from *spn-B, spn-C* and *spn-D* female mutants with anti-dMre11, anti-γ-H2Av and anti-C(3)G antibodies (figure 25). Surprisingly, none of the 3 mutants had dMre11 foci throughout ept-lpt, but γ-H2Av foci were present and persisted up to region 3 (figure 25). Thus, *spn-B*, *spn-C* and *spn-D* genes must function differently from *spn-A*. Since I observed γ-H2Av foci and it persists to region 3, it is possible that *spn-B*, *spn-C* and *spn-D* have roles in the accumulation of dMre11 to foci in addition to a defect in repair.

2.6.1. Accumulation of dMre11 into repair foci is deficient in mutants unable to phosphorylated H2Av and deficient in end resection.

As previously explained, it is believed that in the mammalian DNA Damage Amplification Response there is a basal loading of dMre11 to the break, followed by phosphorylation of H2Av and binding of MDC1. Upon binding of MDC1

there is a further accumulation of dMre11, γ-H2Av and other repair factors. In organisms where this system was elucidated, when γ-H2A.X is mutated there is no binding of MDC1 and thus no formation of observable MRN foci (Soutoglou and Misteli 2008). In order to see if, in *Drosophila,* the HR factors observed at the HR site can be a matter of accumulation and if there is an amplification of the DNA damage response similar to mammals, I use *Drosophila* females that cannot phosphorylate H2Av. If flies have a similar mechanism for amplification of DNA damage response as mammals do, then H2Av mutants should have impaired growth of dMre11 foci and thus it may not be observable when using Immunohistochemistry fluoresce techniques

Homozygous null H2Av mutants are lethal; as such, we obtained a fly line with the null $H2Av^{810}$ allele coupled to a transgene that expresses H2Av lacking the last 14 amino acids ($His2Av^{\Delta CT}$) so it cannot be phosphorylated, but viability is rescued. When I stained germaria from $H2Av^{810}$; $His2Av^{\Delta CT}$ mutant females, I could not see dMre11 foci or dRad50 foci (Figure 26). Thus, it is possible that as in mammals, phosphorylation of H2Av is essential for the accumulation of repair factors to DNA damage sites in *Drosophila*.

Furthermore, end resection generates 3' ssDNA tails that are essential for the assembly of DNA damage repair protein complexes and probably accumulation of recognition factors to the left and right of the break (Raynard, Niu et al. 2008). In here I took advantages of the availability of a resection mutant in *Drosophila*, mre^{585}, to see if defects in end resection will affect the accumulation of factors at DSB sites.

mre^{58S} is a hypomorphic mutation. Mutation was made in an vital residue for the nuclease activity of Mre11 in both yeast and humans (Paull, Rogakou et al. 2000; Usui, Ogawa et al. 2001; Gao, Bi et al. 2009). When *mre*^{58S} were stained I observe very defective HR foci formation, in early stages of ept only very small and very few dMre11 foci were observed (figure 27). The accumulation of dMre11 into the nuclei of ept-mpt pro-oocytes seem to be affected, interestingly accumulation into the oocyte seems to increase as the oocyte develops and moves into the vitellarium (figure 27). The defects in HR foci could indicate that resection is necessary for the amplification of the DNA damage response; however, it should be noted that in this case loading of dMre11 into the pro-oocytes nuclei is also affected and hence this could also be the reason of the observed phenotype.

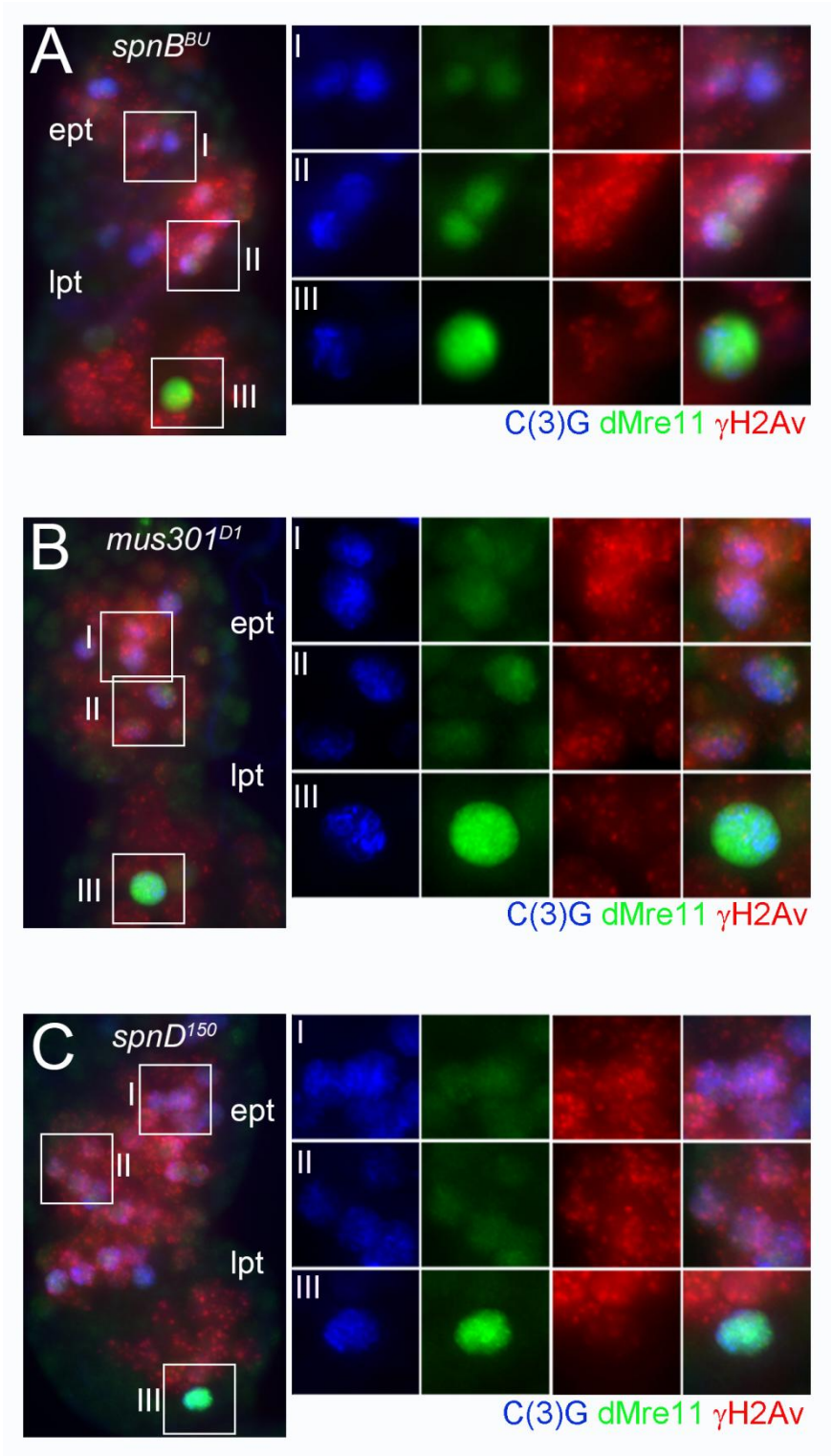
A
spnB^BU
ept
lpt
I
II
III
C(3)G dMre11 γH2Av
B
mus301^D1
ept
lpt
I
II
III
C(3)G dMre11 γH2Av
C
spnD^150
ept
lpt
I
II
III
C(3)G dMre11 γH2Av

Figure 25: spindle B, C and D mutants have impaired accumulation of dMre11 in repair foci. (A-C) Maximum intensity projection of Z-series taken through whole mount *spnB*^{BU} (A), *mus301*^{D1} (*spn-C*) (B), and *SpnD*^{150} (D) germaria stained with antibodies to C(3)G (blue), dMre11 (green), and γ-H2Av (red). Right shows maximum intensity projection of Z-series taken through pro-oocyte nuclei as marked with the white boxes.

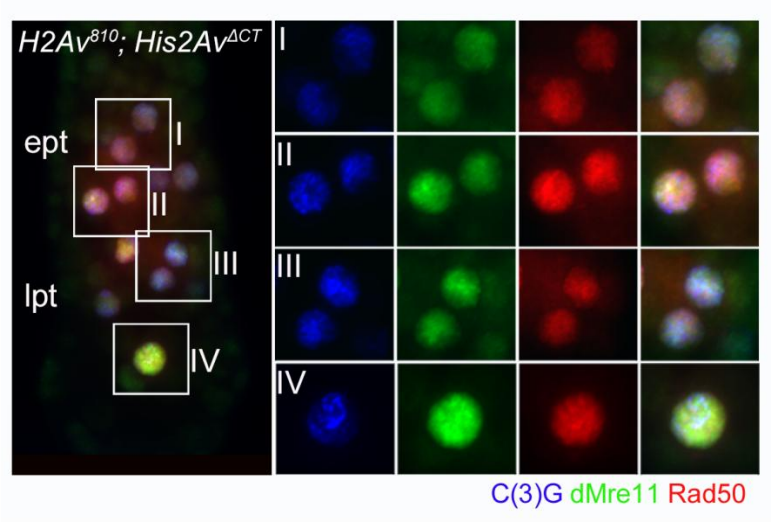

Figure 26: H2Av phosphorylation is required for the proper formation of MRN foci. (A) Maximum intensity projection of *H2Av*^{810}; *H2Av*$^{\Delta CT}$ germarium stained with antibodies to C(3)G (blue), dRad50 (red), and dMre11 (green). Right shows magnification of pro-oocytes and oocyte nuclei.

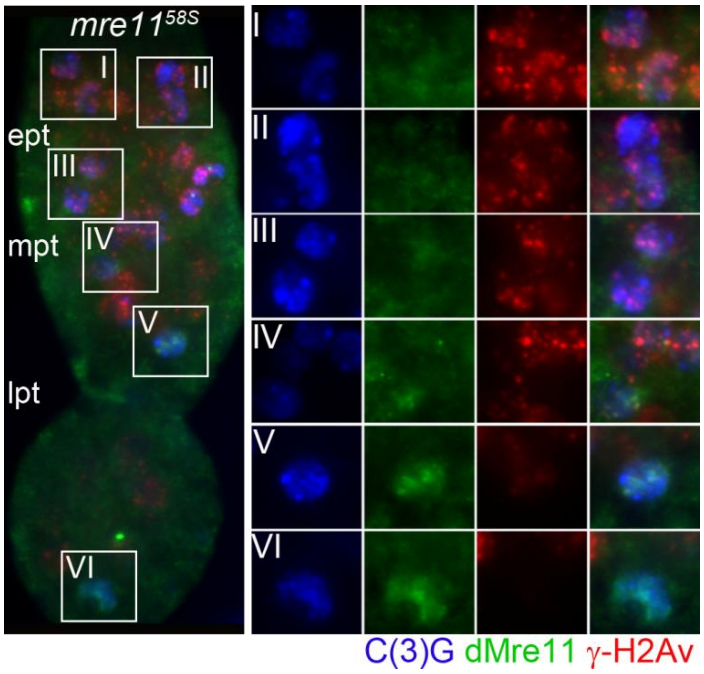

Figure 27: *mre11*^{58S} mutants have impaired formation of HR foci (A) Maximum intensity projection of *mre11*^{58S} germarium stained with antibodies to C(3)G (blue), dMre11 (green), γ–H2Av (red), and. Right shows magnification of pro-oocytes and oocyte nuclei.

3. The chromatin modifier INO80 and its role in meiotic recombination

In this section I focus on the role of INO80 during the early stages of meiotic DSB repair. Currently, most of the information available in regards to INO80 and its role in DNA repair have been obtained by using yeast as the model organism. One of the roles attributed to INO80 seems to be the modification of chromatin around the DSB, possibly to allow binding of recognition and/or repair factors (van Attikum, Fritsch et al. 2004; Tsukuda, Fleming et al. 2005). Studies in yeast show that INO80

subunits are recruited to a DSB in a DNA damage-dependent manner, and INO80 mutants are deficient in the loss of histone around the DSB (Downs, Allard et al. 2004; Downs, Allard et al. 2004; Morrison, Highland et al. 2004; van Attikum, Fritsch et al. 2004). However, the exact way INO80 is recruited to DSBs and its role at DNA damage sites is not completely understood. One of the most studied models of INO80 recruitment to the damage site suggests that INO80 directly interacts with γ-H2AX, and that it is recruited to the DSB via an interaction with γ-H2A.X (Morrison et al. 2004 and Attikum et al. 2004). As explained above, several discrepancies in this model suggest that γ-H2AX may not be the main factor that recruits INO80 to the DSB; as such, it is still currently unclear how INO80 is recruited to DNA damage sites.

Here I used *Drosophila* to study the role of INO80 during the early stages of DSB repair. The composition of the yeast INO80 complex greatly differs from the composition of the human INO80 complex, and thus the yeast INO80 complex may not be a suitable study model. The *Drosophila* INO80, on the other hand, is a closer homolog to the human INO80 complex (see table 1). Besides the similarities in composition of both *Drosophila* and Human INO80 complexes, there is also a high conservation structurally and functionally in DSB recognition complexes, repair factors and the mechanism used in the DNA Damage Response pathway (van den Bosch, Bree et al. 2003; Gorski, Romeijn et al. 2004; Oikemus, Queiroz-Machado et al. 2006; Williams, Lees-Miller et al. 2010).

To study dINO80 complex and its interaction partners, the Kusch Lab purified various recombinant dINO80 complex subunits. S2 cells were stably transfected with expression constructs of Arp5, Ies6, and Ino80 subunits. Constructs were double tagged with flag-HA either in the N terminus or C terminus. As a control, cells expressing an empty vector were prepared in parallel. The dIno80HAFlag, dArp5HAFlag, dIes6HAFlag associated proteins were isolated from nuclear extracts by sequential affinity purification. Samples were analyzed via mass spectrometry. Interestingly, in the three different mass spectrometer outputs (dIno80HAFlag, dArp5HAFlag and dIes6HAFlag) dMre11 and dRad50 peptides were observed (See table 1).

These data suggest a possible interaction of dINO80 and the MRN complex. Interestingly, MRN might be a potentially conserved candidate to recruit INO80: 1) CHIP assays of H2B and MNase analyses of an *mre11* mutated strain showed that histone loss around the DSB was significantly impeded (Tsukuda, Fleming et al. 2005). 2) yeast *ino80* mutants, specifically *arp8* and *nhp10* mutants, have impaired binding of Mre11, Ku80, Mec1 at DSB (van Attikum, Fritsch et al. 2007). Although the result suggested a role of INO80 and MRN in the recognition of DSBs, the author did not provide any other experimental evidence that would support this conclusion. Here, I first confirmed an interaction between *Drosophila* Ino80 (dIno80) and *Drosophila* Mre11 (dMre11) and then I set out to investigate the nature and possible roles of the dIno80 and dMre11 interaction

3.1. dIno80 and dMre11 interact and the interaction increases upon DSB induction

3.1.1. dIno80 directly interacts with components of the MRN complex.

As mention above, the spectrometry data obtained suggests a possible interaction between dINO80 complex and dMRN complex. I next set out to study the nature of this apparent interaction. In order to do this, I first tested the specificity of dIno80 antibodies, previously generated by the Kusch lab. RNAi assays of dIno80 knocks down a band of the right size that is labeled by dIno80 antibody in control samples (figure 28a). Next, to test for a direct interaction between dINO80 and the dMRN complex co-Immunoprecipitation (co-Ip) assays were done. Anti-dIno80 antibodies were used to precipitate dMre11, dRad50 and dNbs proteins present in nuclear extracts of *Drosophila* S2 cells. Western blot analyses of the Immunoprecipitates showed that dIno80 pulled down the three components of the dMRN complex --dMre11, dRad50 and dNbs (figure 28b). In addition, I did the reciprocal co-IPs with the 2 core components of the MRN complex and assayed their ability to pull down dIno80. As shown in the western blots in figure 28c, dMre11 antibody is able to IP the other two components of the MRN complex and dIno80 (28c). However, dRad50 had poor IP efficiency; it did pull down some dMre11 and dIno80, but did not pull down dNbs. It is possible that the polyclonal dRad50 antibody was raised against the domain interacting with dNbs.

These results, together with the mass spectrometry results, strongly suggest that dINO80 directly interacts with the components of the MRN complex. However, it is important to note that the interaction was assayed in somatic cells that had not been damaged, and that S2 cells were not synchronized prior to this study; most of unsynchronized *Drosophila* S2 cells are in S phase (Kusch, Florens et al. 2004). Studies in several organisms may explain the reason why dIno80 and dMre11 interact in non-damaged cells: 1) dMre11 co-localizes at replication sites with repair and replication proteins, and it prevents fork associated damage at both normal replication and replication under stress conditions (Costanzo, Robertson et al. 2001; Borde and Cobb 2009). 2) INO80 has been found at replication sites, enriched at stalled replication forks where it is important for resumption of replication (Shimada, Oma et al. 2008). 3). INO80 is also involved in the regulation of DNA damage tolerance during replication through modulation of PCNA, proliferation cell nuclear antigen, and RAd51-mediated processing of recombination intermediates at impeded replication forks (Falbo, Alabert et al. 2009). Therefore, the data supports the idea that dIno80 and dMre11 could interact during S-phase. This is also of particular interest since DNA damage repair during S-phase is exclusively repaired by HR (Saleh-Gohari and Helleday 2004).

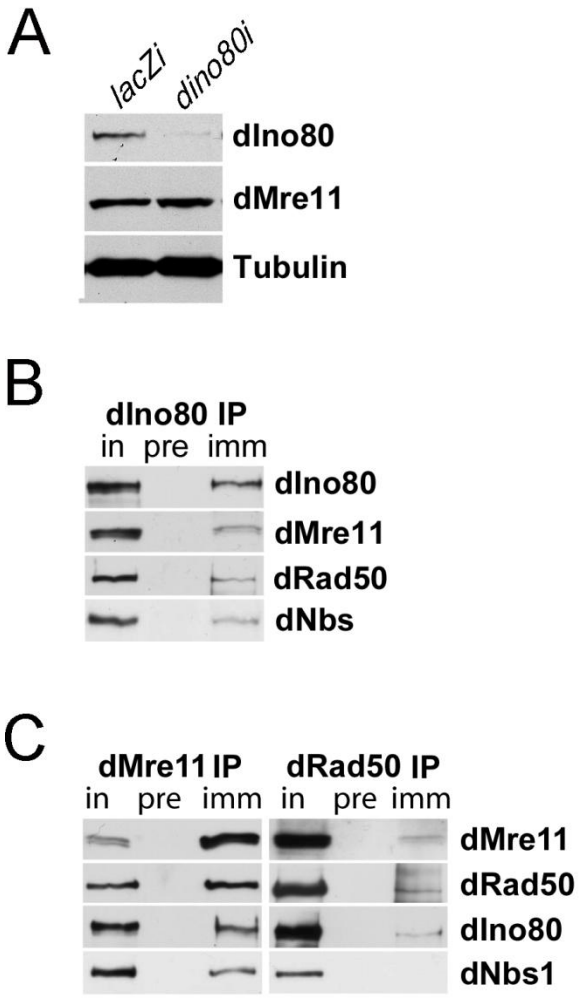

Figure 28: dIno80 interacts with the MRN complex in *Drosophila* S2 cells. (A) Western blot analysis of nuclear extracts from Ino80 RNAi-treated *Drosophila* S2 cells. Control cells were treated with dsRNAi for *E. coli lacZ (lacZ*). Tubulin served as loading control. (B) Western analysis of components of the MRN complex co-immunoprecipitated with dIno80 antibodies. Immunoprecipitations were done using pre-immune bleed antibodies (pre) and immune bleed antibodies (imm). Input lane (in) shows 10% of the IP material. (C) Immunoblot of co-immunoprecipitations done using dMre11 and dRad50 antibodies as indicated in IP lane. Western blots were probed for dMre11, dRad50, dIno80 and dNbs antibodies.

3.1.2. dIno80 and dMre11 interaction is stimulated by DNA damage. Next, I attempt to determine whether dMre11 and dIno80 interact during the repair of DSBS. If dIno80 and dMre11 interaction is important for recognition and/or repair of DSBs, then it would be expected that the interaction will be stimulated upon introduction of more DSBs. To examine if dIno80-dMre11 interaction is affected by DNA damage, I irradiated *Drosophila* S2 cells using an X-ray Faxitron machine and then assayed the effects of the damage on the dMre11-dIno80 interaction by doing co-IPs. *Drosophila* S2 cells were irradiated with 15 Gy and 45 Gy at a dose of 150 rads/minute at room temperature; immediately after irradiation, nuclear extracts and histone extracts from irradiated and non-irradiated S2 cells were obtained. Histone extracts were used to check for DNA damage response; irradiated (15Gy) and non-irradiated extracts were run in a SDS PAGE and membranes were blotted using γ-H2Av antibodies and H2Av antibodies as a loading control. As expected, in the irradiated sample lane there was γ-H2Av signal, whereas in the non-irradiated sample lane no signal was observed (figure 29a). This suggests that 15 Gy are enough to elicit a DNA damage response.

Nuclear extracts of both non-irradiated and irradiated samples were analyzed. I calculated the total protein amounts of each sample to normalize for changes in overall protein levels. In addition, to corroborate protein quantification, nuclear extracts of irradiated and non-irradiated were loaded into an SDS-PAGE and the membrane was blotted with anti-dIno80, anti-dMre11 and anti-tubulin antibodies. After nuclear extracts were normalized samples were then incubated with dMre11

antibodies to see if higher amounts of dIno80 will be pulled down in irradiated samples. The pull-down material was loaded into an SDS-PAGE gel and the membrane was blotted with dIno80 antibodies (figure 29b). Membranes were also probed with dMre11 antibodies to see if the same amount of protein was immunoprecipitated (figure 29b). It is important to note that I loaded amounts and chose exposures in which the interaction between dMre11 and dIno80 was only observed in non-irradiated samples after very long exposures. The purpose was to avoid any saturation effects that could affect quantification of band intensities.

Intensities of the bands observed in the western blots were measured by image J (NIH) software. All the intensity values were calculated relative to the efficiency of the IP. Quantification showed that there was a 6-fold increase in interaction when cells were exposed to 15 Gy; interestingly, the increase of interaction when irradiated with 45 Gy was about 4-fold more than the control (figure 28c). Importantly, input and IPed Mre11 samples showed no stimulation of Mre11 production during the experimental time, so the increased interaction was not due to an increase of Mre11 amounts. Thus it is highly possibly that the dIno80-dMre11 interaction is damage-dependent and is important for the repair of induced DSBs in somatic cells.

3.2. *P{EPgy2}Ino80*^{EY09251} and *Mi{ET1}Ino80*^{MB09416}, two transposon insertion in the dIno80 locus, have somatic DNA repair and cell cycle checkpoint defects

In order to determine the significance of the dIno80-dMre11 interaction, I obtained two fly lines with transposable element insertions in the dIno80 locus (figure 29). The first fly line, *Mi{ET1}Ino80*^{MB09416} *(dIno80*^{Mi}*)*, was caused by integration of a *Minos* transposable element. This transposon is a member of the *Tc1/mariner* family of transposable elements that leads to stable insertion into germ-line chromosomes of various insects (Metaxakis, Oehler et al. 2005). This transposable element catalyzes precise integration and excision without involvement of flaking DNA (Metaxakis, Oehler et al. 2005). The second fly line has a transposon that is part of the P element class of mobile elements, *P{EPgy2}Ino80*^{EY09251} *(dIno80*^{P}*)*.

The *Minos* transposable element inserted 11 base pairs downstream of the 3' end of exon number 8. The P-element inserted in an intron of the dIno80 locus at 380 nucleotides away from the 3'end of exon 11 (figure 30). If the transposable elements were not spliced out properly, two truncated Ino80s would be produced; due to *Minos* insertion the first 1245 amino acids could be made, producing a truncated protein of 145kDa, and a truncated protein of about 169 kDa could theoretically be made in the case of *dIno80*^{P}. The ATPase domain of dIno80 is located in the N-terminal from aa 555 to aa 700, and the helicase domain is located from aa 1158 to aa 1277. Transposon insertion could be affecting the helicase domain of dIno80, thus possibly impairing its nucleosome remodeling function.

The dIno80 locus is very complex with several other open reading frames within the locus (figure 30); as such, it is unclear whether the transposon insertions affect dIno80 or not. To further characterize these fly stocks several confirmatory experiments were necessary. In the following I first addressed whether the transposable element insertions showed any defects characteristic of *Drosophila* DNA repair defective mutants, such as: 1) sensitivity to X-ray-induced DSBs, 2) defects in the cell cycle checkpoint, 3) dorso-ventral egg shell phenotypes and 4) defects in the repair of meiotic DSBs. Second, I attempted to determine whether the transposon insertions affected dIno80.

3.2.1. *Ino80^{Mi}* transposon insertion flies are sensitive to X ray-induced DSBs

Since Ino80 is required for the DNA damage response in all eukaryotes, I next set out to determine if *dIno80^{Mi}* flies are sensitive to DNA damage. DSBs were introduced by irradiating the progeny of heterozygous *dIno80^{Mi}* with 20 Gy, using an X-ray Faxitron machine. Progeny were irradiated at 24-48 hours after egg laying (AEL). Upon eclosion, survival ratio was established by comparing the survival of the irradiated progeny to that of their un-irradiated siblings (see material and methods). At 20 Gy wild type *Drosophila* did not exhibit sensitivity, however *dIno80^{Mi}* showed some sensitivity (figure 31). The sensitivity of *dIno80^{Mi}* flies to induce DNA damage suggests a role of the protein in somatic DSB repair.

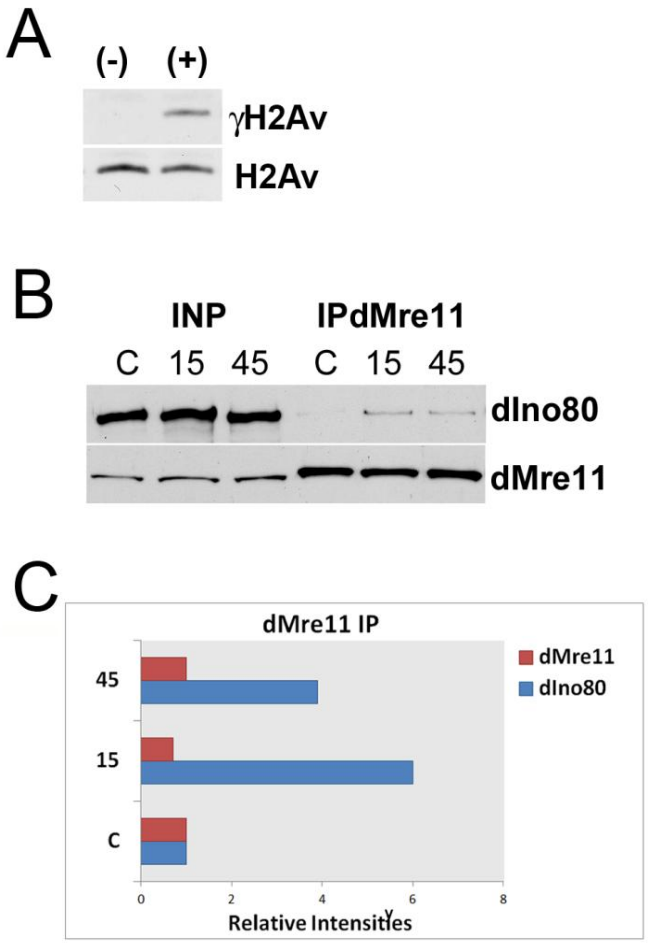
A
(-)
(+)
γH2Av
H2Av
B
INP
IPdMre11
C
15
45
C
15
45
dIno80
dMre11
C
dMre11 IP
45
15
C
dMre11
dIno80
0
2
4
6
8
Relative Intensities

Figure 29: dIno80-dMre11 interaction is stimulated by DNA damage. (A) Immunoblot of histone extracts prepared from *Drosophila* S2 cells irradiated (+) at 15Gy using a Faxitron x-ray machine and non-irradiated (-). Membranes were probed with γ-H2Av. Membrane was also probed with H2Av antibodies for loading control. (B) Immunoblot of Immunoprecipitations (Ips) done using dMre11 antibody and nuclear extract from non-irradiated and irradiated *Drosophila* S2 cells. S2 cells were irradiated at 15 Gy (15) and at 45 Gy (45). Protein levels were normalized prior to immunoprecipitations. Immunoprecipitates were loaded into and SDS gel and then membranes were probed with dIno80 antibodies, showing a higher IP efficiency in irradiated samples when compared to non-irradiated samples. Membranes were also probed with dMre11 antibodies showing that the same amount of protein was immunoprecipitated in both samples. INP, input. (C) Relative intensity of the bands in western blot (B), showing dIno80-dMre11 interaction in irradiated and non-irradiated cells. Intensities were calculated relative to the intensities of dMre11 Immunoprecipitation efficiency. ImageJ (NIH) software was used to calculate the intensities.

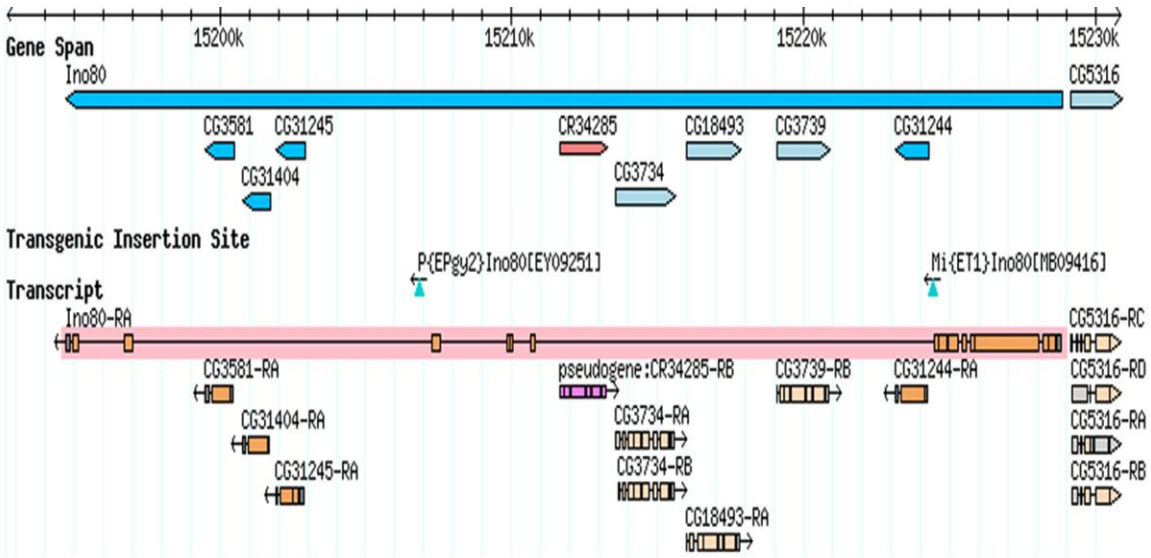

Figure 30: Two transposable elements within the dNO80 locus. Top shows gene sequence location (3R:15194717..15228875.). Middle shows seven different genes coding sequences within the dIno80 locus (Blue) and a pseudogene. (red). Bottom (pink) shows dIno80 transcript, its intron (line) and exons, (orange boxes). Figure also shows two transposable element insertions into the dIno80 locus: 1. dIno80 transposable element, w[1118];MI^{ET1}Ino80, CG5316 is close to the Ino80 TSS . The insertion of w[1118];MI^{ET1}Ino80i is located 11 nucleotides downstream of the 3 ’ end of exon 8.. 2. P element P^{EPgy2}Ino80^{EY09251} is located 380 nucleotides downstream from the 3’end of exon 11. (figure adjusted from G browser).

3.2.2. *Ino80*^{Mi} flies have normal activation of the G2-M cell cycle checkpoint but their exit for the checkpoint is delayed. Some *Drosophila* DSB repair deficient mutants have altered cell cycle checkpoints (Bi, Gong et al. 2005). To gain a better understanding of the role of dIno80 during DSB repair and its possible involvement in cell cycle checkpoints, I used a well-established assay in the wing disc of *Drosophila* third instar larvae which monitors how the checkpoints respond to irradiation. In wild type wing discs, γ-irradiation induces the G2-M checkpoint. Proper function of the G2-M checkpoint can be assayed by a steep decline in the number of mitotic cells within one hour of damage induction (Bi, Gong et al. 2005). In addition it has been shown that wing disc cells exit the checkpoint after 4 hours and normal patterns are reached at 6 hours (Neufeld, de la Cruz et al. 1998). Mitotic cells can be visualized by immunofluorence using the Anti-*phospho*-Histone H3 (*Ser10*) antibody. I irradiated homozygous *dIno80*^{Mi} third instar larvae and then assayed for the presence of mitotic cells in the wing disc after 1 and 6 hours of irradiation. This assay showed that wing disc cells of *dIno80*^{Mi} homozygous flies enter the checkpoint properly; however the cells stay longer in mitotic arrest (figure 32). This could be due to a failure to exit mitotic checkpoint, although it could also be due to a failure to properly repair DNA.

3.2.3. *dIno80*^{Mi} flies exhibit Dorso-ventral patterning defects. *Drosophila* DNA repair mutants such as *Spn-A*, *Spn-B*, and *Okr* are characterized by sensitivity to

DNA damage, reduced fertility, defects in ventralization of eggshell and also dorsalized eggs with defects in the dorsal appendages (Morris and Lehmann 1999; Staeva-Vieira, Yoo et al. 2003). *dIno80*^{Mi} homozygous females are sensitive to ionization radiation and have defects in the G2-M cell cycle checkpoint. If dIno80 protein is affected by the transposon insertion and dIno80 function in DSB repair is conserved as in yeast, flies and mammals, one would expect to observed fertility problems and some of the dorsal and ventral egg shell phenotypes. Thus, I next set out to test if the transposon insertion flies showed defects in the eggshell and if they were infertile.

dIno80^{Mi} Heterozygous virgin females where mated with *dIno80*^{Mi} heterozygous virgin males. Homozygous *dIno80*^{Mi} females emerging from this cross were viable but 100% sterile, and males were viable and non-sterile. When the same cross was made for *dIno80*^{P}, homozygous progeny were viable and non-sterile. As mentioned above, besides fertility problems some *Drosophila* DNA repair mutants are characterized by defects in ventralization of eggshell and dorsalized eggs. It has also been shown that these mutants have reduced levels of the Gurken protein, which controls dorso-ventral patterning of the eggs and anterior polarity of the embryo (Ghabrial, Ray et al. 1998). Thus, it is speculated that reduction of Gurken is due to activation of meiotic check point response and that the low levels of the protein results in a dorso-ventral patterning defects. In order to check for eggshell defects in *dIno80*^{Mi}, I used *dIno80*^{Mi} and *dIno80*^{P} homozygous or heterozygous virgin females and mated them with wild type males. The eggs laid were observed, counted and

classified based on their morphology. Dorso-ventral patterning defects were classified in three classes: Class I, eggs with both dorso-ventral appendages almost fused at the base; Class II, eggs with one fused dorso-ventral appendage; Class III, eggs with no appendages. Besides, the dorso-ventral patterning defects observed, homozygous females laid collapsed eggs

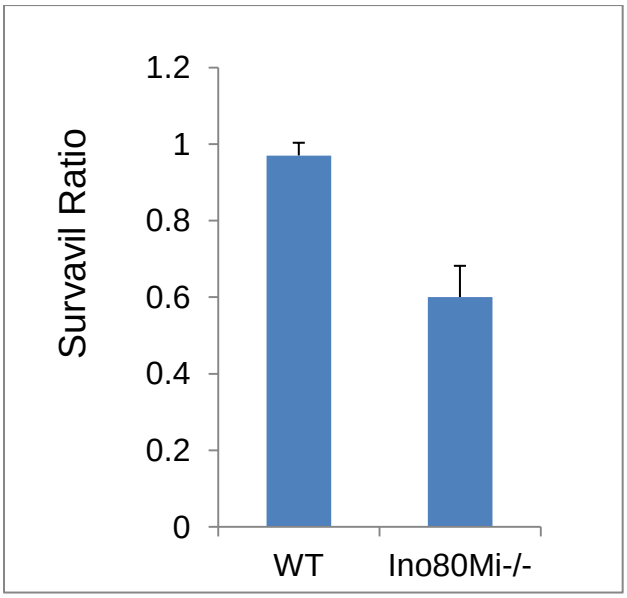

Figure 31: *dIno80* mutants are sensitive to ionizing radiation. Bar graphs show survival ratio of *Mi{ET1}Ino80*^{MB09416} *(dIno80*$^{Mi-/-}$*)Drosophila* larvae after γ-irradiation. Larvae were irradiated with 20 Gy at 48 -72 hours after egg laying (AEL). Survival ratio was calculated by comparing the survival of irradiated progeny to the survival of un-irradiated siblings Error bar represent standard deviation of 4 independent experiments.

I found that *dIno80*^{Mi} heterozygous embryos had mild eggshell phenotypes; 10% of the eggs laid were defective. 90 % of eggs laid were wild type, 9% were Class II and 1% was class III. (figure 33a). However, *dIno80*^{Mi} homozygous embryos had very strong eggshell phenotypes, with 100% of the eggs laid being defective. 97% of eggs laid were Class I, 1.6% were Class II and less than 1% were Class III (figure 33b). Not wild type looking embryos were observed. *dIno80*^{P} homozygous had milder phenotype: 90% of the eggs were wild type, 7% were Class I and 3.9 % were Class II (figure 33c). To my surprise, eggshell phenotypes in *dIno80*^{Mi}were more detrimental than eggshell phenotypes of DNA repair mutants such as *Spn-A or Okra.* (Ghabrial, Ray et al. 1998; Staeva-Vieira, Yoo et al. 2003).

3.3 Expression of dIno80 in *Drosophila*

I next checked the expression profile of dIno80 in different developmental stages and different tissues to see whether there might be a particular developmental stage or tissue where dIno80 is needed most. Total cell lysates from different developmental stages of wild type *Drosophila* were loaded into an SDS-PAGE and immunoblotted using anti-dIno80 antibodies (figure 34). I found that dIno80 was highly expressed during the embryonic stages (3-7, 7-12, 12-24) and down regulated in the larva stages L1 to L3(figure 34). Surprisingly, when ovaries and head lysates were compared, ovary lysates had much higher amounts of dIno80 protein (figure 34).

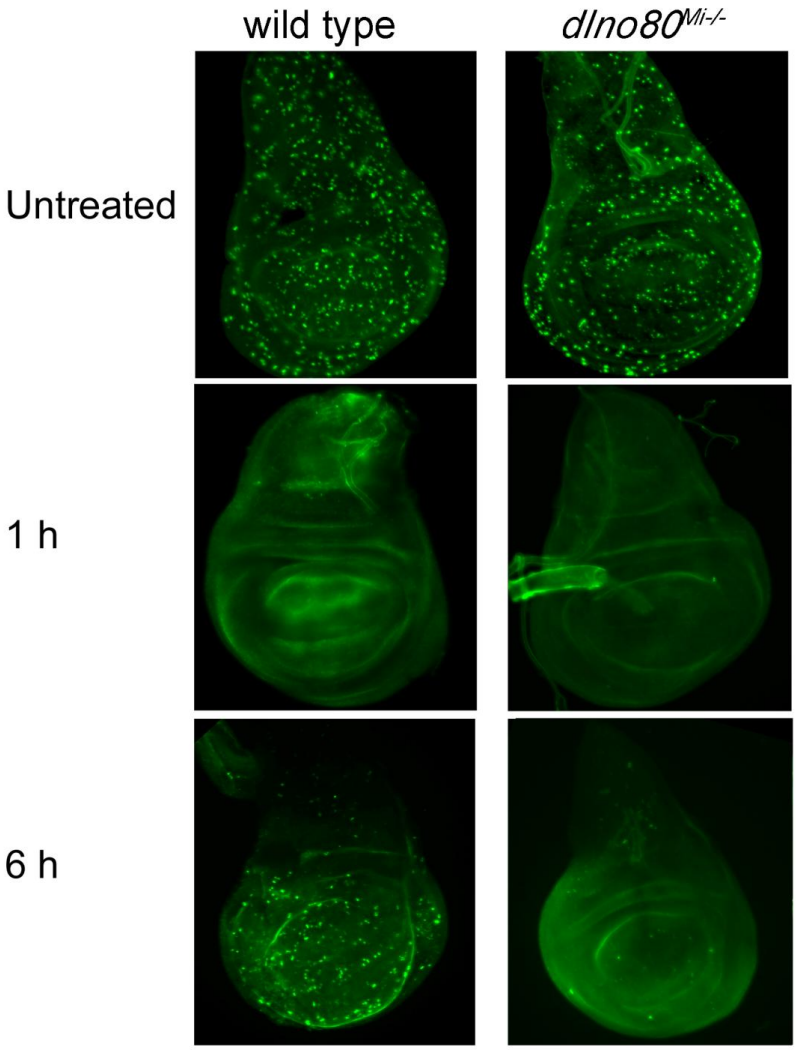

Figure 32: *dIno80* mutants enter the G2-M cell cycle checkpoint normally but the exit from this cell cycle checkpoint is delayed. Figure shows wild type and *Mi{ET1}Ino80*^{MB09416} homozygous mutant (*dIno80*$^{Mi-/-}$) wing discs at 1 hour and 6 hours post γ-irradiation.. Third instar larvae were irradiated with 20 Gy using an X ray Faxitron machine. After irradiation, wing discs were dissected out of the third instar larvae and stained with an antibody against the meiotic marker, phospho-histone H3 (*Ser10*).

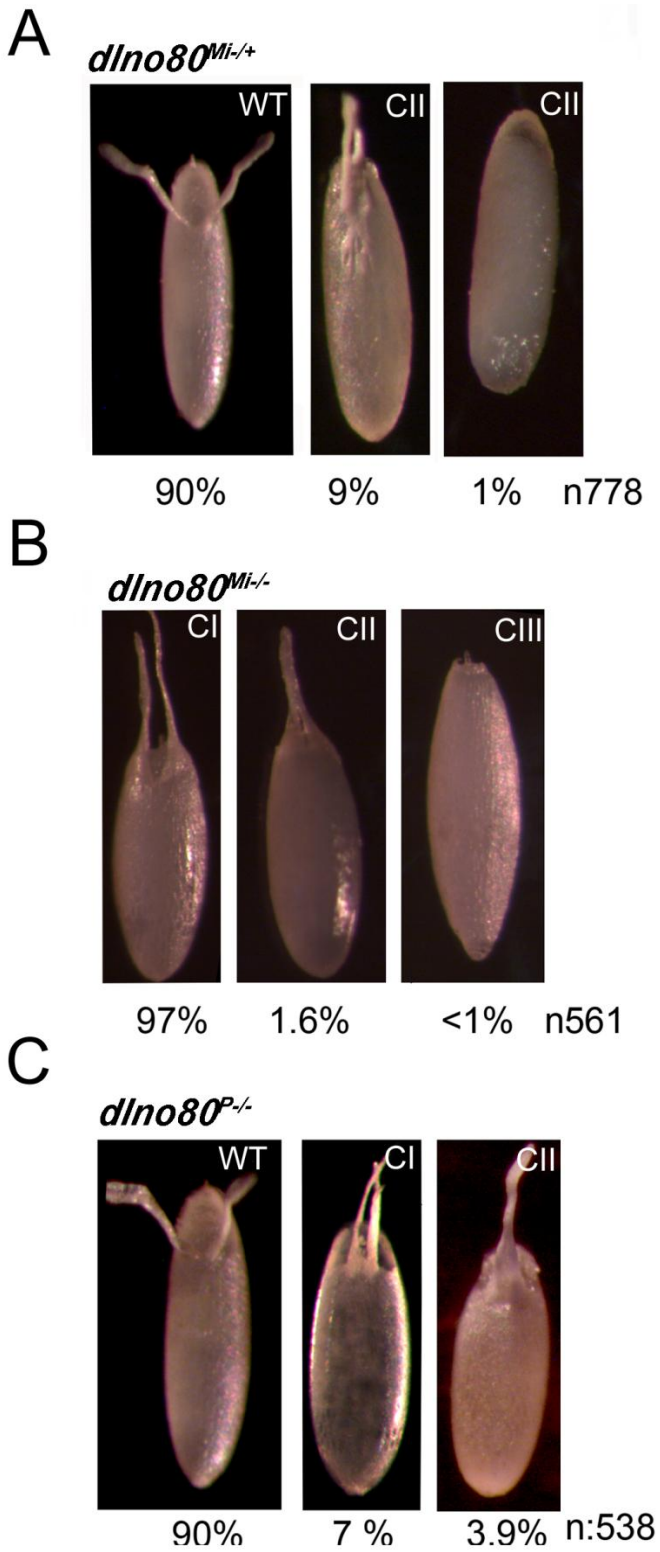
A
dlno80Mi-/+
WT
CII
CII
90%
9%
1%
n778
B
dlno80Mi-/-
CI
CII
CIII
97%
1.6%
<1%
n561
C
dlno80P-/-
WT
CI
CII
90%
7 %
3.9%
n:538

Figure 33: *dIno80* mutant exhibit Dorso-ventral patterning defects. *Drosophila* embryos laid by (A) *Mi{ET1}Ino80*^{MB09416} heterozygous females, (*dIno80*$^{Mi-/+}$), (B) *Mi{ET1}Ino80*^{MB09416} homozygous females, (*dIno80*$^{Mi-/-}$), (C) *P{EPgy2}Ino80*^{EY09251} homozygous females (*dIno80*^{P}$^{-/-}$). Defects were classified in 3 classes (CI, CII, and CIII). CI: Both dorsal appendices were very close to each other, CII: Dorsal ventral appendices were fused, CIII: No appendices.

Since *dIno80*^{Mi} homozygous females are viable but 100% sterile, I wanted to further compare the levels of dIno80 in heads versus ovaries in *dIno80*^{Mi} flies (Figure 35a). When western blots of *Drosophila* heads and ovaries extracts from *dIno80*^{Mi} and wild type flies were blotted with anti-dIno80 antibodies, I observed that there was a much greater amount of dIno80 protein in ovaries when compared to heads, as it had been observed in figure 34. Intensities of the bands observed in the western blots in figure 35a were measured by image J (NIH) software. After band quantification, it was determined that ovaries have about 75% more dIno80 protein than heads (figure 35a). dIno80 protein was very reduced in the ovaries and heads of *dIno80*^{Mi}. However, a very faint band of dIno80's molecular weight was observed in the lane where lysates from homozygous *dIno80*^{Mi} ovary was loaded. In addition, a smaller molecular weight band was observed. The band had a molecular weight very similar to the predicted size of the truncated *dIno80*^{Mi} protein. These results suggest that low amounts of full length dIno80p had been produced. *dIno80*^{Mi}

homozygous embryos have only 4% of the full length protein, an amount that seemed to be sufficient for viability, but may be too low to support fertility.

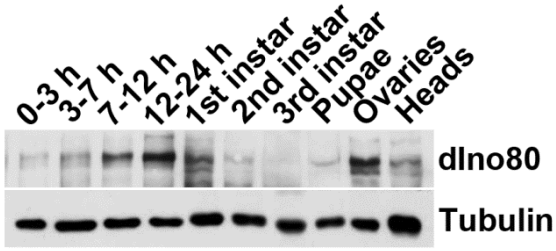

Figure 34: dIno80 protein levels during development. Lysates from Oregon R animals were electrophoresed on an SDS-8% polyacrylamide gel and analyzed by Western blotting. Embryonic lysates: 0-3 (blastoderm), 0-7 (gastrulation), 7-13 (germ band retraction), and 13-24 (differentiation). Larval stages: first, second, and third instars. Adult females extracts from ovaries and heads. Antibodies against tubulin served as loading controls.

These results correlate to the expression data published by modENCODE, where males have lower expression levels of dIno80 compared to females (figure 35b). In addition, when specific tissues of both males and females such as testis and ovaries were compared by modENCODE, it was shown that the testis had very low expression levels of dIno80 when compared to the high expression in ovaries (figure 35c). These differential expression profiles of dIno80 suggest a role of the protein in

female specific tissues such as the ovary. As opposed to females, *Drosophila* males do not recombine. As such, it is possible that dIno80 is so highly expressed in female ovaries because it plays important roles in recombination.

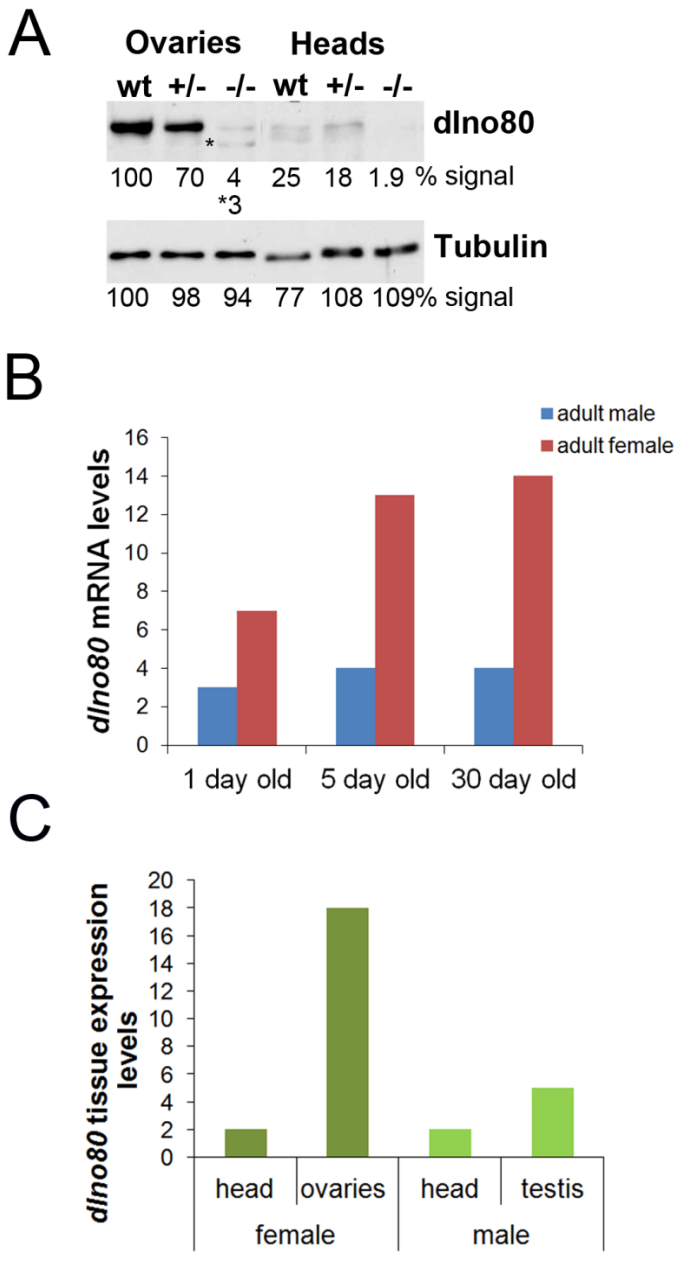

Figure 35: dIno80 is highly expressed in the ovaries of *Drosophila* females (A) Western blots of ovary and head extracts from Oregon R (WT), *Mi{ET1}Ino80*^{MB09416} heterozygous (+/-) and *Mi{ET1}Ino80*^{MB09416} homozygous (-/-) flies. Blots were probed with anti-dIno80 and anti-tubulin antibodies. Tubulin was used as a loading control. Values below each lane represent the relative intensity of each band in comparison with the respective wild type lane as quantified by ImageJ (NIH) software and normalized for tubulin. (* marks the incompletely translated mRNA from homozygous *dIno80* mutant). (B) Bar graph showing the expression levels of *dIno80* in males and females as shown in FlyBase, data collected and analyzed by modENCODE Temporal Expression Data. (C) Bar graph showing the expression levels of *dIno80* in males and females as shown in FlyBase, data collected and analyzed by modENCODE Tissue Expression Data.

3.4. dIno80 functions in *Drosophila* meiotic recombination.

3.4.1. dIno80 co-localizes with dMre11 in pro-oocytes. As shown above, wild type females have very high levels of dIno80 protein in the ovaries when compared to other tissues. In addition, *dIno80*^{Mi} homozygous females are sterile, but males are not. Since males do not recombine, it is possible that dIno80 may function during meiotic recombination. In order to study a possible role of dIno80 during meiotic DSBs, I first stained wild type and *dIno80*^{Mi} homozygous germaria with anti-dIno80 and anti-C(3)G antibodies to determine dIno80 presence in the germaria.

Results show that *dIno80*^{Mi} homozygous females have reduced levels of dIno80 protein throughout ept, mpt and lpt (figure 36). However, dIno80 is present in high levels in all the cell of the wild type germaria. This staining confirms the finding that *dIno80*^{Mi} flies have highly reduced levels of dIno80.

Since, it was shown that dIno80 and dMre11 interact in S2 cells and both proteins are expressed in *Drosophila* germ cells; it is possible that dIno80 localizes to DSBs and interacts with dMre11 in *Drosophila* germ cells. As such, I next tested if dIno80 interacts with dMre11 in the *Drosophila* ovary. In order to do this, ovary extracts were used to pull down dIno80 with anti-dMre11 antibodies. Results show that as in S2 cells, dMre11 and dIno80 also interact in the ovaries (figure 37). Since the *Drosophila* ovary is composed of germ cells as well as somatic cells, next I examined the localization of dIno80 during meiotic prophase in the *Drosophila* germaria to see if dIno80 and dMre11 interact in pro-oocytes. This was done by staining wild type *Drosophila* ovaries with anti-dIno80 and anti-dMre11 antibodies. As shown in figure 36-37, in wild type *Drosophila* ovaries dIno80 is expressed in the nuclei of most of the cells in the germarium. When co-localization of dIno80 and dMre11 was analyzed, I observed that some of the dMre11 foci co-localize with dIno80 in ept-mpt pro-oocytes (figure 37b, b').

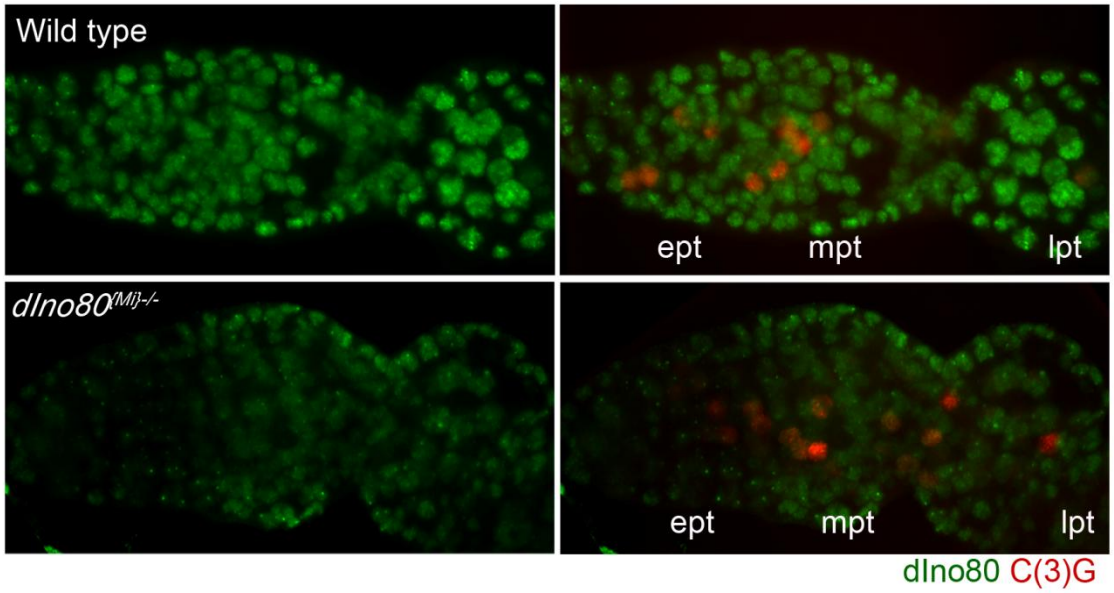

Figure 36: *Mi{ET1}Ino80*^{MB09416} mutants have reduced levels of dIno80 protein. Maximum intensity projections of whole mount wild type germarium and *Mi{ET1}Ino80*^{MB09416} (*dIno80*$^{Mi-/-}$) germarium stained with antibodies to dIno80 (green) and C(3)G (red).

3.4.2. *dIno80*^{P} and *dIno80*^{Mi} flies have defective formation of HR foci.

Based on these findings, it is possible that dIno80 has roles in the repair of meiotic DSBs. To establish if the lack of dIno80 protein will affect meiotic DSB repair, I first immunostained *Drosophila* female ovaries of *dIno80*^{Mi} and *dIno80*^{P} homozygous flies with anti-dMre11, anti γ-H2Av and anti C(3)G antibodies. After staining, I did not see morphological problems in any of the *dIno80* germaria; additionally, C(3)G staining in both homozygous mutants showed that formation of the synaptonemal complex was not affected. However, both *dIno80*^{Mi} and *dIno80*^{P} mutants have problems in the accumulation of dMre11 and γ-H2Av into a repair focus in ept pro-oocytes

(figure 38a-c). *dIno80*^{Mi} homozygous mutants apparently have a more severe defect than *Ino80*^{P} mutants (figure 38 a-c). In addition, when transheterozygote animals *Ino80*^{Mi}/ *Ino80*^{P} were studied, very similar phenotypes to the single mutants were observed. This observation suggests that both transposon insertions are affecting dIno80 locus. Later in the chapter, I describe additional genetic experiments that were needed to further understand the effects of the two transposon insertions into the dIno80 locus.

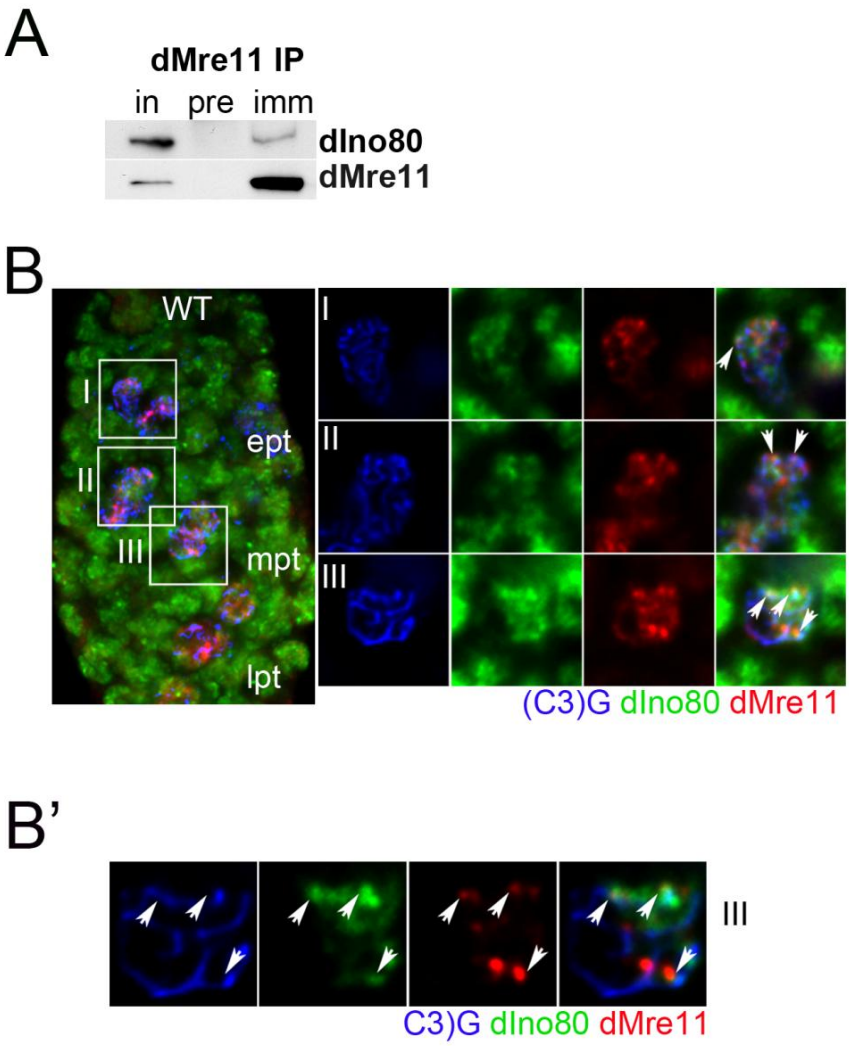

Figure 37: **dIno80 interacts with dMre11 during oogenesis** (A) Immunoblot of nuclear extracts from ovaries after immunoprecipitations with dMre11 antibodies. Immunoblots were probed for dIno80 and dMre11. Immunoprecipitations were done using pre-immune bleed antibodies (pre) and immune bleed antibodies (imm). Input lane (in) showed 10% of the IP material. (B) dIno80 co-localizes with dMre11 in *Drosophila* oocytes. Maximum intensity projection of whole mount wild type germarium stained with antibodies against dIno80 (green), dMre11 (red) and C(3)G (blue). (B') Shows single plane magnification of oocyte nuclei (III) from germarium blow ups in (B). Channels have been adjusted to better visualize Ino/Mre11 foci.

I next studied if the p-element insertion *P{EPgy2}* in the ORF of *l(3)L1231-RA CG 7832*, another subunit of the INO80 complex as confirmed by mass spectrometry (see table 1), also had a reduced number of DSBs. The gene *lethal (3) L1231* is referred to in Fly Base by the symbol *Dmel\l(3)L1231*. The p-element inserted in lethal sits in intron 13, 4216 bp downstream of the first exon and 2000bp upstream of the second exon. When *Dmel\l(3)L1231* flies where immunostained with antibodies against C(3)G, dMre11 and γ-H2Av, I observed similar phenotypes to those of $Ino80^{Mi}$ homozygous flies. HR foci were very reduced, and occasionally pro-oocytes in region 2a were found with no HR foci (figure 39). Table 3 shows that *Dmel\l(3)L1231* mutants have an average of 5 foci (+/- 2 n=325). Similarly, $Ino80^{Mi}$ homozygous mutants have an average of 4 dMre11 foci per pro-oocyte +/-2.2 (n=34)

and *Ino80*^{P} do indeed have a less severe phenotype with an average of 6 foci per pro-oocyte +/- 2.5 (n=38) (table3)

As observed in part 2 of the results, figure 24, wild type region 3 oocytes have the ability to respond to irradiation induce DSBs and HR foci is observed as quickly as 15 minutes post irradiation. Since *dIno80*^{Mi} have defective HR foci formation, I next determine if *dIno80*^{Mi} flies have also defects in the formation of HR foci upon irradiation. Ovaries of wild type and homozygous *dIno80*^{Mi} flies were irradiated with 12 Gy and stained 30 minutes and 3 hours post-irradiation. Ovaries from homozygous *dIno80*^{Mi} flies showed very delayed HR foci formation; after 30 minutes, no foci were observed in region 3 oocytes and after 3 hours very few foci were observed (figure 40). In contrast, wild type region 3 oocytes showed foci at 30 minutes and 3 hours after irradiation.

Since the dINO80 complex has roles in transcription, replication and DSB repair, a reduction of dMre11 foci could be attributed to a defect in the transcription of dMre11. To be able to rule out a role of dINO80 in dMre11 and H2Av transcription, I analyzed the dMre11, dRad50 and H2Av levels in the ovaries of *dIno80*^{Mi} homozygous mutants. Immunoblot of the ovary extracts showed that dMre11, dRad50 and H2Av levels were not reduced, but were instead seemed to be slightly up-regulated (Figure 41). As such, dMre11 foci reduction in these mutants cannot be attributed to a defect in transcription. The defect in foci formation in ept *dIno80*^{Mi} pro-oocytes and *Dmel\l(3)L1231* pro-oocytes, the delay formation of HR

foci in irradiated oocytes, in addition to the interaction studies of dIno80 and dMre11, support a possible role of dIno80 in the recognition of DSBs and/or the accumulation of factors to the DSB.

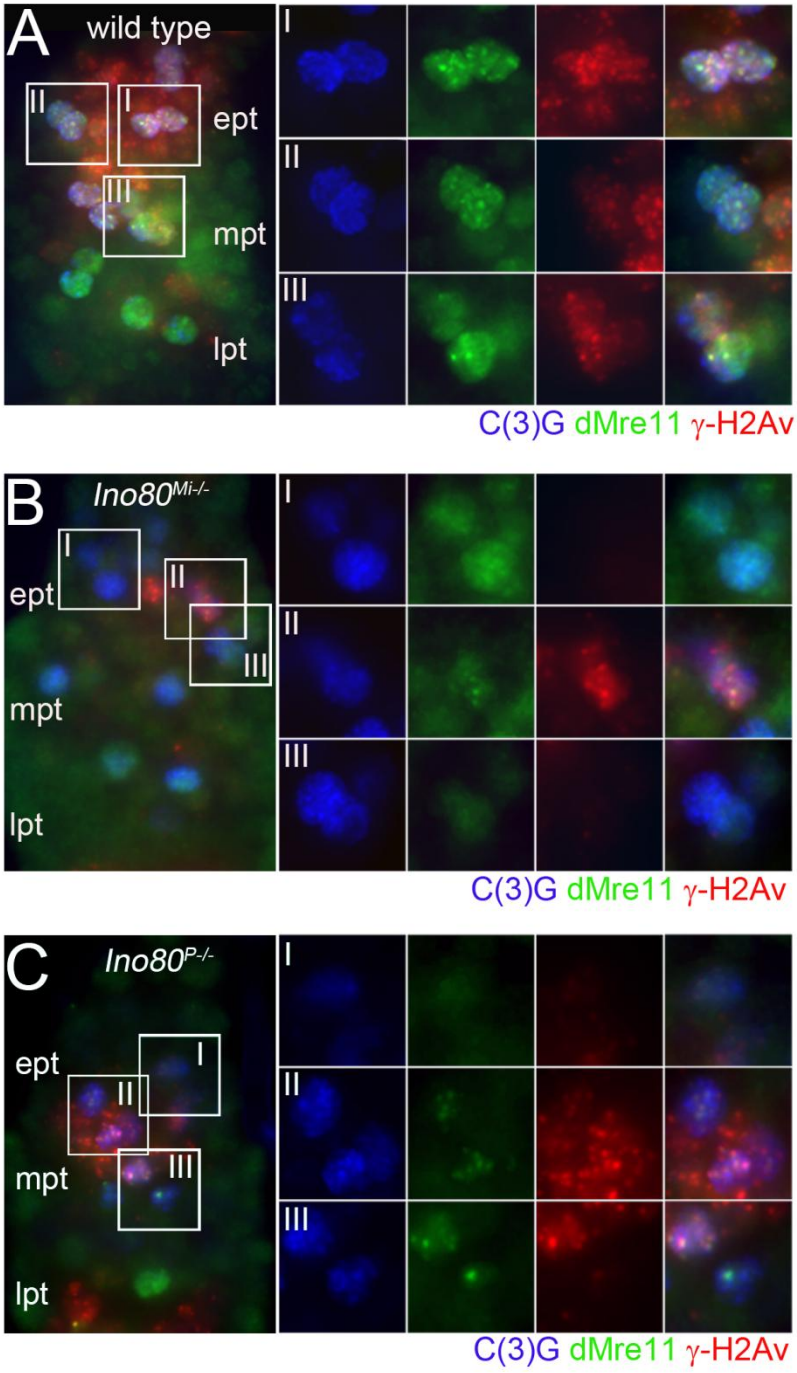

Figure 38: *dIno80* mutants have reduced number of dMre11 foci. (A-C) Maximum intensity projections of whole mount wild type germarium (A), *Mi{ET1}Ino80*^{MB09416} *(dIno80*$^{Mi-/-}$*)* (B), and *P{EPgy2}Ino80*^{EY09251} *(dIno80*$^{P-/-}$*)* (C) immunostained with anti-C(3)G antibody (blue), anti-dMre11 antiserum (green) and γ-H2Av-specific (red) antibodies. (A-C) Left shows germaria overviews. Right shows magnifications of pro-oocytes nuclei from ept-mpt regions as marked with the white boxes.

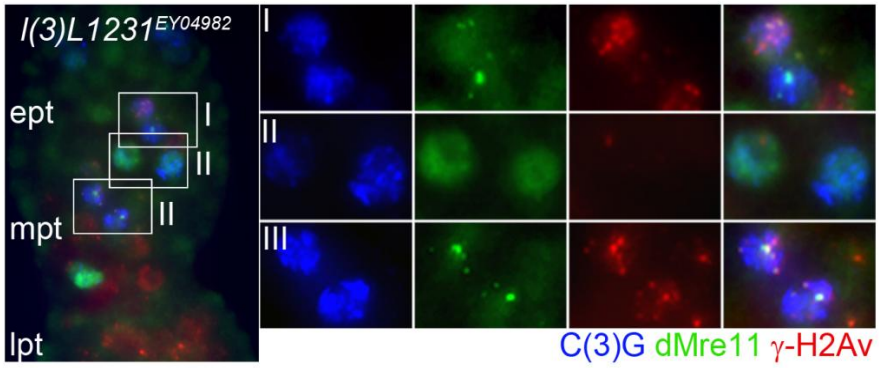

Figure 39*: {EPgy2}l(3)L1231*^{EY04982} mutants have reduced number of dMre1foci. Left shows a maximum intensity projection of whole mount *{EPgy2}l(3)L1231*^{EY04982} germarium immunostained with anti-C(3)G (blue) antibody, anti-dMre11 antiserum (green) and γ-H2Av (red) antibodies. Right shows magnifications of pro-oocytes from region ept as marked with the boxes.

Table 2. Frequency of dMre11 foci in mutant subunits of the INO80 complex

	Average foci in Early pachytene	Standard Deviation	Total numbers of Pro-Oocytes counted
Wild type	13.5	+/- 3	100
W^{1118}; $\underline{Mi\{ET1\}Ino80^{MB09416}}$ $Mi\{ET1\}Ino80^{MB09416}$	4	+/- 2.2	34
$\underline{P\{EPgy2\}Ino80^{EY09251}}$ $P\{EPgy2\}Ino80^{EY09251}$	6	+/-2.5	38
$\underline{P\{EPgy2\}l(3)L1231^{EY04982}}$ $P\{EPgy2\}l(3)L1231^{EY04982}$	5	+/- 2	25

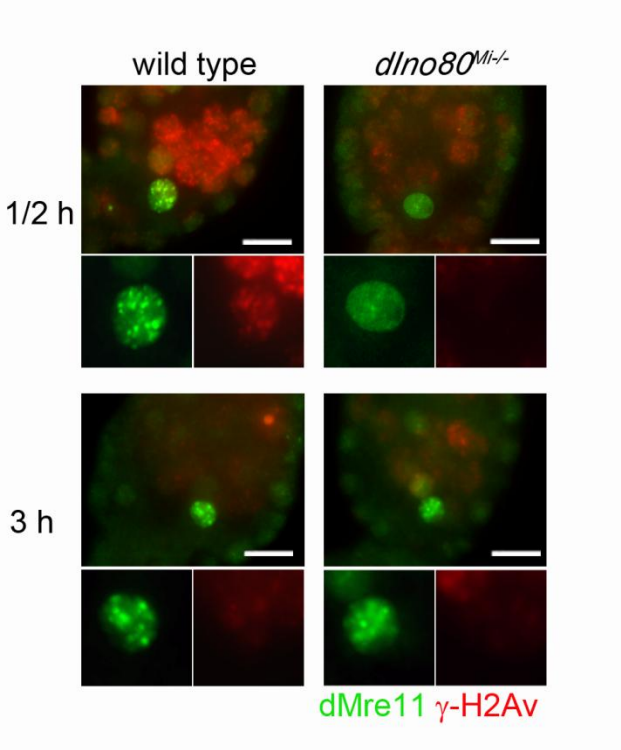

Figure 40: *Mi{ET1}Ino80*^{MB09416} homozygous mutant have impaired DNA damage response: Magnification of region 3 oocytes from maximum intensity projection of whole mounted -irradiated wild type and *Mi{ET1}Ino80*^{MB09416} homozygous (*dIno80*$^{Mi-/-}$) germaria. Flies were irradiated with 12 Gy using X-ray machine (Faxitron) and fixed after ½ hour and 3 hours post irradiation. Germaria were stained using anti-dMre11 antibody (green) and anti-γH2Av antibody (red). Scale bar, 5 μm

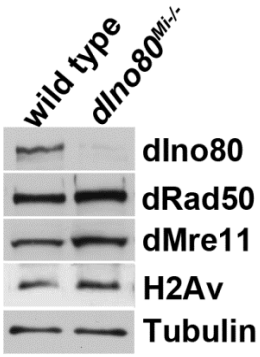

Figure 41: DNA repair recognition factors are not down-regulated in *Mi{ET1}Ino80*^{MB09416} homozygous mutants. Immunoblots of Oregon R animals (wild type) and *Mi{ET1}Ino80*^{MB09416} (*dIno80* $^{Mi-/-}$) homozygous mutant ovary extracts. Tubulin was used as a loading control and the membranes were probed with anti-dIno80, anti-dRad50, anti-dMre11, and anti-H2Av antibody as indicated to the right.

3.5. Phenotypes observed in *Ino80^{Mi}* are due to mutations in dIno80.

Thus far I had shown that not only a p-element insertion in a subunit of the dINO80 complex has defects in HR foci formation, but also 2 different transposon insertions in introns of the *dIno80* locus. Although the presented data suggest that both transposon insertions in the dIno80 locus are the cause of the observed phenotypes, further analysis of these mutants needs to be done. As shown in figure 30, the *dIno80* locus is very complicated, with seven other genes embedded in it. Therefore, it is necessary to demonstrate that the phenotypes are caused by the transposable element insertions, and is indeed due to issues with *dIno80* expression. Next, I set out to determinate through different genetic analyses if the phenotypes observe in both transposon insertion lines are due to a disruption of dIno80.

1) It is possible that *dIno80^{Mi}* and *dIno80^{P}* carry secondary mutations somewhere else in the genome. To exclude this possibility, it was necessary to remove the transposable elements and examine the resulting animals for meiotic HR defects and DV defects. During the excision of transposable elements, an imprecise excision could be generated and could affect the exon-intron boundaries of the *dIno80* locus. This experiment, however, would only be of limited value since deletions could affect other transcription units as well.

2) Due to the nature of the dIno80 locus with 7 other genes embedded on it, a rescue experiment using an ectopically-expressed Ino80 transgene will be key to show that

the *minos* transposable element insertion affected *dIno80*, causing all the observed phenotypes

3) Other means of reducing Ino80 levels in the germline, such as RNAi. The dosage-dependent role of Ino80 in HR has been suggested by the high levels in ovaries and the sterility despite the presence of low levels of full-length protein in the mutants.

First, in order to prove that the phenotypes observed are due to insertion in the *dIno80* locus and not to an insertion in any of the other seven genes or to some genetic background I excised *the* $Ino80^{P}$ *p*-element and the *minos* transposable element in $Ino80^{Mi}$. To excise the p-element in $Ino80^{P}$, homozygous mutant flies were crossed with flies carrying the transposase. I then scored for and recovered homozygous animals lacking the marker for the p-element. Precise excisions were detected by the restoration of the egg lying phenotype --offspring had no DV phenotypes, and all animals developed to adulthood and were fertile. Few imprecise excisions were recovered; flies were sterile and exhibited stronger defects by a worsening of the $Ino80^{P}$ phenotype (data no shown).

In the case of $dIno80^{Mi}$, homozygous mutant flies were crossed with flies carrying the helper chromosome PhsILMiT, which encodes a transposase under the control of an hsp70 promoter on a balancer chromosome. Most excision events of the *minos* transposon are precise, and the original pre-insertion sequence is restored (Metaxakis, Oehler et al. 2005). Excisions were scored by loss of the *minos* element

marked by a GFP-expression cassette. I recovered several excision lines where the GFP marker was lost and fertility was restored to 100% of WT levels in homozygous animals. Excision of the p-element or transposable element tells us most likely there is no other mutations somewhere else in the genome associated with the phenotype; however, it does not show that the transposable elements are not affecting any of the other 7 genes within the *dIno80* locus.

Rescue was done using the Gal-4/UAS system. The system uses two transgenes: A driver, Gal-4, and a UAS responsive expression vector (UAS). The driver directs tissue-specific expression of Gal-4 protein, the transcriptional activator that binds to UAS, an upstream activated sequence, next to the gene of interest. In here, I used *nanos-Gal4* (*w[1118]; P{w[+mC]=GAL4::VP16 nos.UTR}CG6325[MVD1]}*) as the driver; it contains the promoter and the 3'UTR of the *nos* gene which is expressed in the germarium and all stages of egg chambers (Rorth 1998). Since the original Gal4/UAS system does not work in the germline during oogenesis (Brand and Perrimon 1993), here I used a modified UAS vector, pUASP, which has been proven to be optimal for expression in the germ line (Rorth 1998).

The rescue construct, *pUASP(Ino80),* was generated by cloning Ino80 ORF into *pUASP* transformation vector. Once the rescue construct was obtained, it was injected into *Drosophila* embryos to generate transgenic flies. Transgenic flies carrying the rescue construct were mated with flies with the driver, *nos-Gal4*, to obtain progeny with the genotype *pUASP(Ino80)Ino80^{-}/nosgal4Mi{ET1}Ino80^{-}*; these

offspring were then used to assay for rescue (check material and methods). Rescue was assayed by restoration of DV phenotypes, fertility and HR foci formation.

In order to assess restoration of *dIno80* phenotypes, I first compared the dIno80 protein levels in wild type, *Ino80^{Mi}* homozygous, and *pUASP(Ino80)Ino80^{-} /nosgal4Mi{ET1}Ino80^{-} (dIno80^{Mi} (nosG4>UASpdIno80)$^{-}$)* by Immunohistochemistry. As figure 42 shows, dIno80 protein levels seem to be higher in *dIno80^{Mi} (nosG4>UASpdIno80)$^{-}$* when compared to *Ino80^{Mi}* homozygous mutants. In order to properly assess rescue of dIno80 protein levels, I analyzed dIno80 protein levels in wild type, *Ino80^{Mi}* homozygous, *Ino80^{Mi}* heterozygous, *pUASP(Ino80)Ino80^{-}/ nosgal4Mi{ET1}Ino80^{-}* and *pUASP(Ino80)Ino80^{-}/nosgal4Mi{ET1}Ino80^{-}* (*dIno80^{Mi} (nosG4>UASpdIno80)$^{-}$*) *Drosophila* ovary extracts by western blotting (figure 43a) As figure 43a shows, dIno80 protein levels are rescued to wild type levels in *dIno80^{Mi} (nosG4>UASpdIno80)$^{-}$* flies. In addition, *dIno80^{Mi} (nosG4>UASpdIno80)$^{-}$* flies also had restored DV phenotype, fertility and the ability of the pro-oocyte and oocyte to generate HR foci (figure 43 b). Wild type flies had an average of 13.5 foci +/- 3, and rescue flies had 10 +/-2 (n=30) (figure 43c). These results show that the *Mi{ET1}Ino80* transposable element is affecting *dIno80* expression, and is most likely not affecting the other 7 genes. Therefore, the observed phenotypes are due to disruption of the dIno80 protein.

3.6. Knockdown of dIno80, arp5 and arp8, three subunits of the INO80 complex, affects the formation of HR foci.

Ino80^{Mi} are sterile but viable most likely due to the amount of protein left in the mutant; as quantified in figure 34, there is about 4% protein left in the mutant. This 4% of the protein is sufficient to confer viability, but not enough to either form foci or support fertility. These requirements of Ino80 suggest that there is a dosage-dependent role of the dIno80 protein in *Drosophila.*

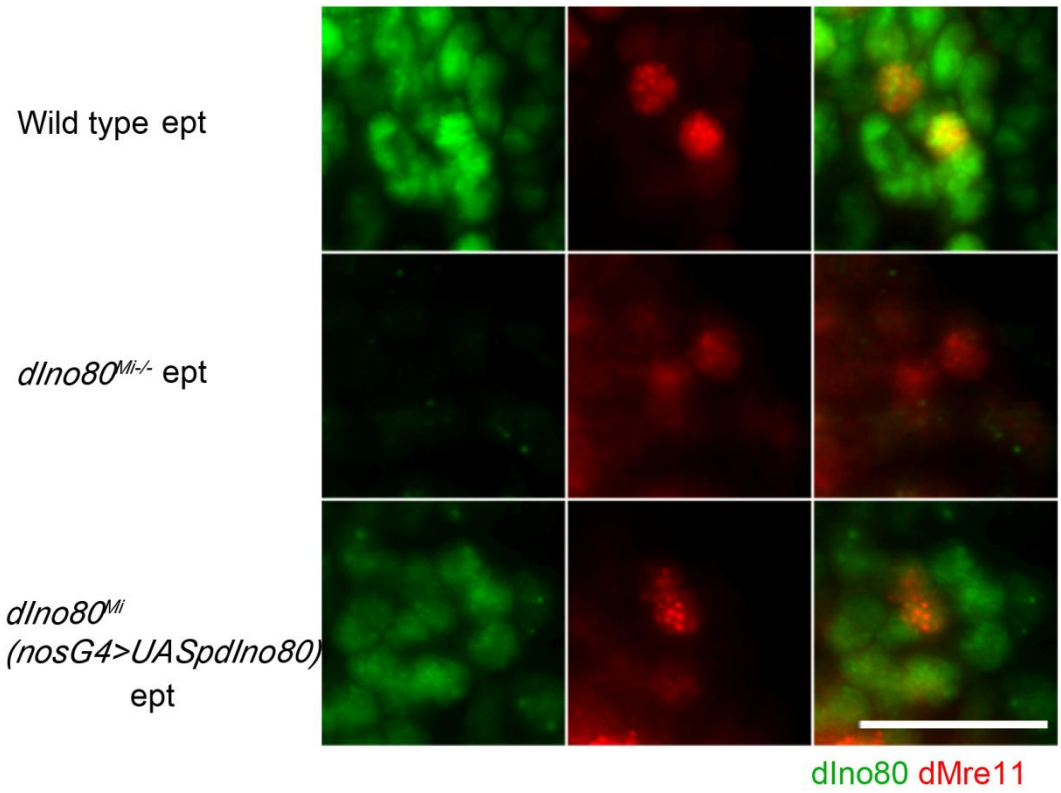

Figure 42: DNA repair recognition factors are not down-regulated in *Mi{ET1}Ino80*^{MB09416} homozygous mutants. Immunoblots of Oregon R animals (wild type) and *Mi{ET1}Ino80*^{MB09416} (*dIno80* $^{Mi-/-}$) homozygous mutant ovary extracts. **Tubulin** was used as a loading control and the membranes were probed with anti-dIno80, anti-dRad50, anti-dMre11, and anti-H2Av antibody as indicated to the right.

In order to determine requirements of dIno80 protein during meiotic recombination, I next set out to test if dIno80 protein can be further reduced using RNAi. Knockdown of dIno80 by RNAi would: 1) Provide further confirmation for a role of Ino80 in HR, 2) test if the mutant phenotype can be enhance and further reduced the number of foci, and 3) provide another piece of evidence that in *dIno80*^{Mi} flies the transposon insertion affected *dIno80* expression. I knocked down dIno80 in *Drosophila* germ cells by the used of two transgenic fly lines; one line, (*y*^{1} *sc***v*^{1}*;P{y*$^{+t7.7}$*v*$^{+t1.8}$*=TRiP.HMS00586}attP2*), expresses short dsRNA hairpin for dIno80 RNAi under UAS-Gal control. RNAi in *Drosophila* using short hairpins have being shown to be optimal for knockdown in the soma and germ cells, as opposed to long hairpins that are ineffective for gene silencing in the female germline (Ni, Zhou et al. 2011). The second transgenic fly line was *p{nos-Gal4-VP16} (w[1118]; P{w[+mC]=GAL4::VP16 nos.UTR}G6325[MVD1]})* construct as the Gal-4 driver. After crossing both fly lines I analyzed ovaries obtained from offspring females (*dIno80i*). First, I stained ovaries with anti-dMre11 and anti-dIno80 antibodies to see if dIno80 protein was successfully reduced (figure 44). When I compare wild type dIno80 expression with dIno80 expression after knock down, I observed a reduction of dIno80 protein levels with this system; in the germline from the tip of the germarium to the mature egg (figure 44)

I stained *dIno80i* ovaries with anti-γ-H2Av, anti-C(3)G and anti-dMre11 antibodies to assess the effect of the knock down in foci formation (figure 45). Staining of *dIno80i* flies showed reduction in the number of HR foci and reduce fertility. *dIno80i*

flies had an average of 7.5 foci +/- 3.5 (n43) (figure 45a,c). In order to check if protein levels could be reduced more than what was observed, I did RNAi in the background of *Ino80^{Mi}* homozygous flies. *Ino80^{Mi}* flies were recombined with *y^{1} sc*v^{1};P{y$^{+t7.7}$v$^{+t1.8}$=TRiP.HMS00586}attP2* (express short dsRNA hairpin for dIno80 RNAi under UAS-Gal control). Additionally, *Ino80^{Mi}* flies were recombined with *p{nos-Gal4-VP16} (w[1118]; P{w[+mC]=GAL4::VP16 nos.UTR}G6325[MVD1]})* (Gal-4 driver). Finally, both recombinants were mated and female progeny homozygous for *Ino80^{Mi}* and expressing *the* Gal-4 driver in addition to the short dsRNA hairpin for dIno80 RNAi under UAS-Gal control (*dIno80i, dIno80^{Mi}*) were analyzed. After immunostaining of *dIno80i, dIno80^{Mi}* ovaries, I did observe a reduction in the number of HR foci when compared to the *dIno80i* HR foci number; however, numbers of HR sites remained pretty similar to the *Ino80^{Mi}* homozygous mutant (figure 45b and c). These results suggest that we do reach a complete knockdown of the protein; it is probable that dIno80 protein levels can't be reduced to 100% due to lethality associated with null Ino80 mutants, as published in other organism (van Attikum, Fritsch et al. 2004; Tsukuda, Fleming et al. 2005; Tsukuda, Lo et al. 2009). As such, I may not be able to reduce the number of foci more than 4 +/- 2.2 foci in the *Drosophila* germ line

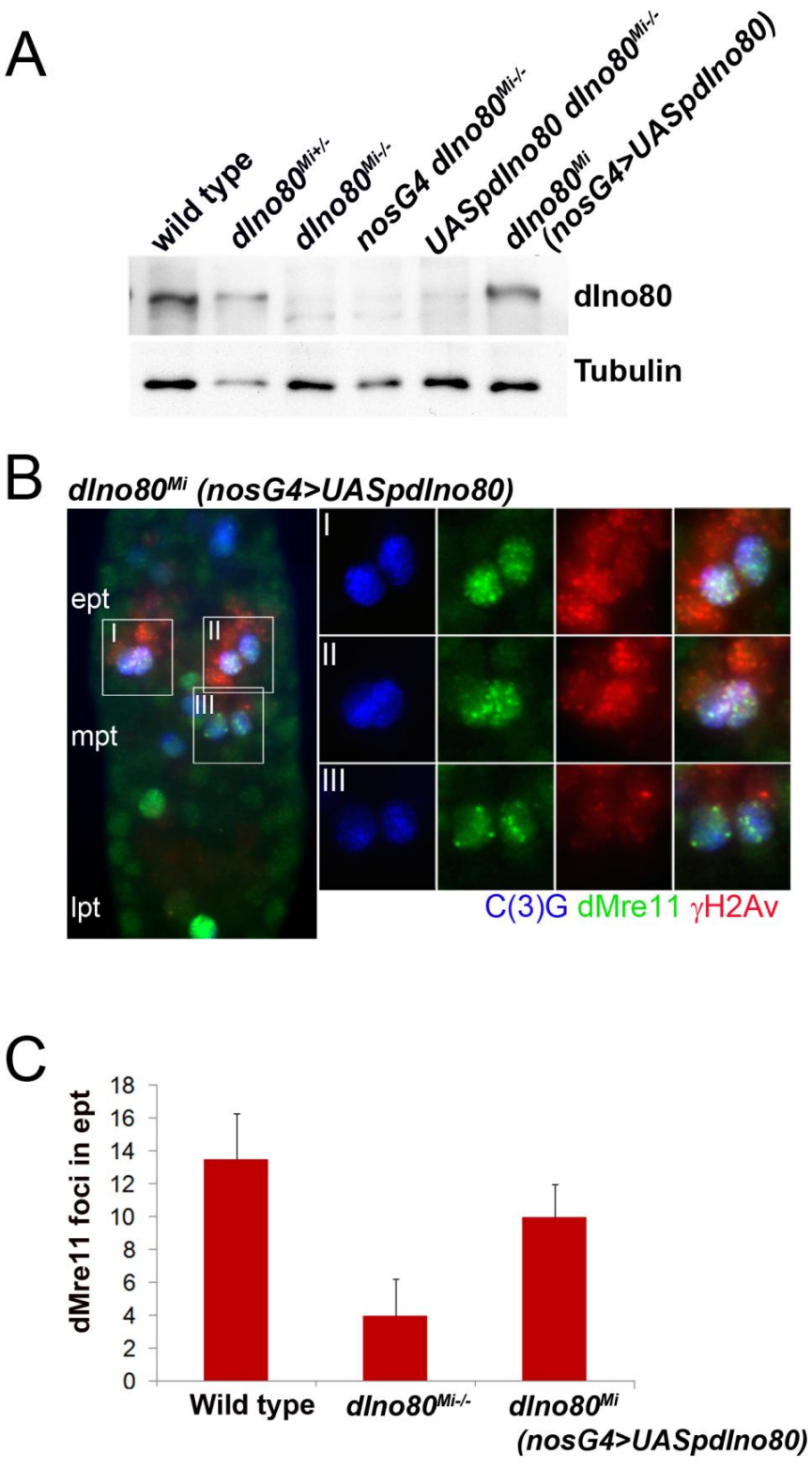
A
wild type
dIno80Mi+/-
dIno80Mi-/-
nosG4 dIno80Mi-/-
UASpdIno80 dIno80Mi-/-
dIno80Mi (nosG4>UASpdIno80)
dIno80
Tubulin
B
dIno80Mi (nosG4>UASpdIno80)
ept
mpt
lpt
I
II
III
C(3)G dMre11 γH2Av
C
dMre11 foci in ept
0
2
4
6
8
10
12
14
16
18
Wild type
dIno80Mi-/-
dIno80Mi (nosG4>UASpdIno80)

Figure 43: *dIno80^{Mi} (nosG4>UASpdIno80)* can rescue the defects of *dIno80$^{M-/-}$* (A) Western blot analyses of *Drosophila* ovary extracts from wild type, *dIno80$^{Mi+/-}$, dIno80$^{Mi-/-}$, nosG4 dIno80$^{Mi-/-}$, UASpdIno80 dIno80$^{Mi-/-}$,* and *dIno80^{Mi} (nosG4>UASpdIno80)* flies. Blots were probed with anti-dIno80 antibodies and anti-tubulin antibodies. (B). Maximum intensity projection of whole mount germarium from *dIno80^{Mi} (nosG4>UASpdIno80)* females**.** Picture shows the entire germarium (left) and magnification of pro-oocytes nuclei (right). Ovaries were stained with anti-C(3)G (blue), anti-dMre11 (green), and anti γ-H2Av (red) antibodies**.** (C) Average number of dMre11 foci present in ept pro-oocytes of Wild type (n=100), *dIno80$^{Mi-/-}$ (n=34) and dIno80^{Mi} (nosG4>UASpdIno80) (n=30) Drosophila* females**.** Error bar graphs represent standard deviation.

Since knock down of dIno80 was successful in the germline, and there are two fly lines available that express dsRNA for RNAi of Arp5 and Arp8, two subunits of the INO80 complex, I next studied if knockdown of these two subunits will have similar phenotypes to dIno80 knockdown. The following fly lines were used: *y[1]sc[*]v[1];P{y[+t7.7]v[+t1.8]=TRiP.HMS00809}attP2* expresses dsRNA for RNAi of Arp5, and *y[1] v[1]; P{y[+t7.7] v[+t1.8]=TRiP.JF01720}attP2/TM3, Sb[1]* expresses dsRNA for RNAi of Arp8. Each of these dsRNA fly lines were crossed to *P{COG-Gal4:VP16}*; *P{Gal4-nos.NGT}40*; *P{nos-Gal4-VP16}*. Immunostaining of ovaries from the progeny of the above crosses also showed defects in the formation of HR foci

(figure 46), further supporting the previous results and a role of the dINO80 complex in formation of HR foci.

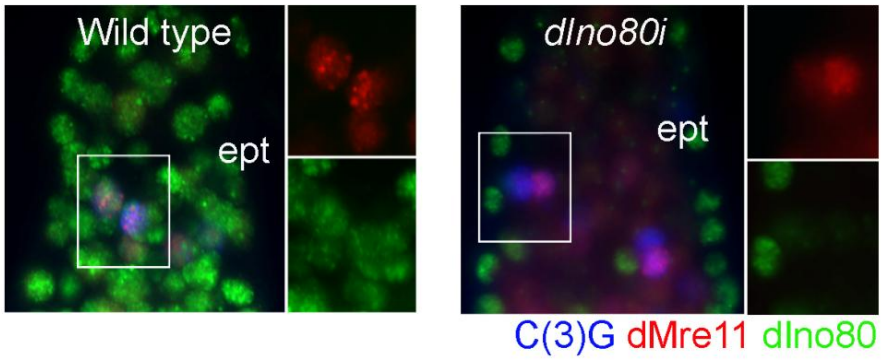

Figure 44: RNAi of dIno80 in the *Drosophila* germaria can reduce dIno80 protein levels. Picture shows Z-stack of early pachytene of a whole mount wild type germaria and dIno80i (Ino80 P{TRiP.HMS00586}attP2 /*nos*-Gal4-VP16). Both germaria were stained with antibodies against dIno80 (green) and dMre11 (red). Left side shows overview of early pachytene and right side shows magnifications of pro-oocyte nuclei marked by the white boxes.

3.7. The ATPase domain of dIno80 plays an important role in the recognition of DSBs and HR foci formation

So far I have shown that dIno80-dMre11 interact in the *Drosophila* ovary and that both proteins are expressed in meiocytes; furthermore, dMre11 foci colocalize with dIno80 in this cells. In addition, *dIno80*^{Mi} mutants have highly reduced numbers of HR foci in early pachytene, and are defective in the response to induce DSBs. Considering these findings and the role of dMre11 in the recognition of DSBs and its direct interaction with Ino80, it is possible that

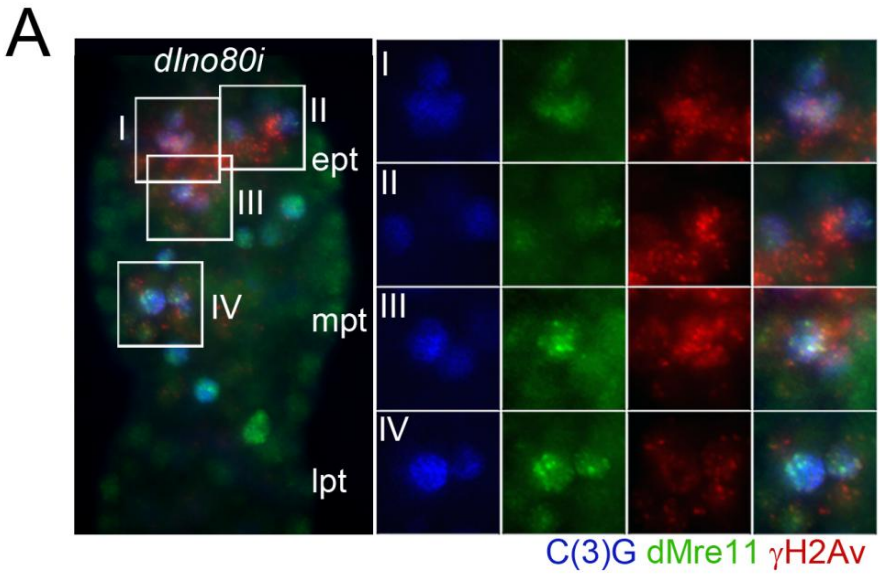
A
dIno80i
I
II
ept
III
IV
mpt
lpt
I
II
III
IV
C(3)G dMre11 γH2Av

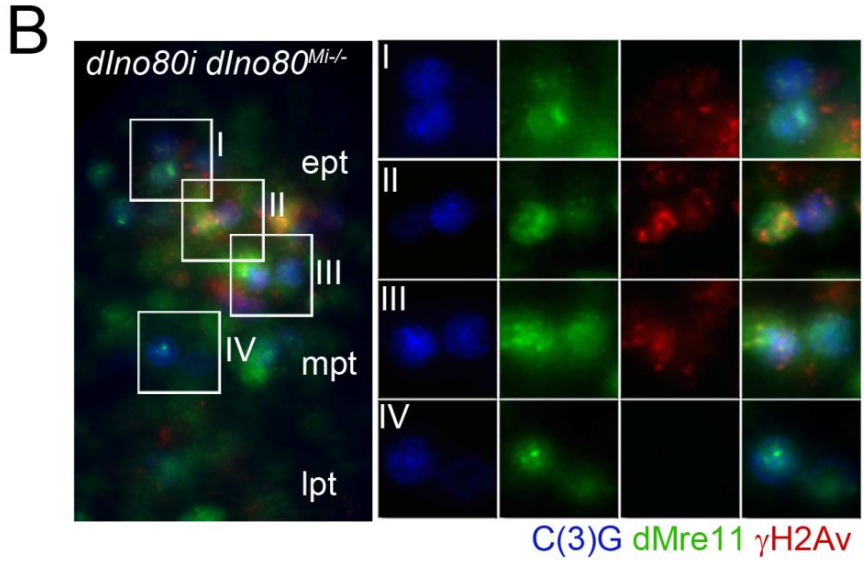
B
dIno80i dIno80Mi-/-
I
ept
II
III
IV
mpt
lpt
I
II
III
IV
C(3)G dMre11 γH2Av

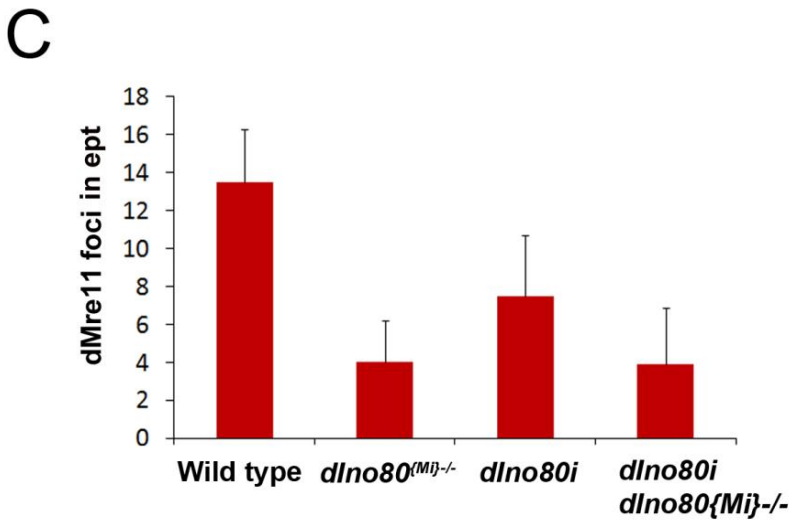
C
dMre11 foci in ept
18
16
14
12
10
8
6
4
2
0
Wild type
dIno80{Mi}-/-
dIno80i
dIno80i
dIno80{Mi}-/-

Figure 45: Pro-oocytes from *dIno80i* females have reduced number of dMre11 foci. (A-B) Picture shows Z-stack of whole mount *dIno80i* germarium (A) and *dIno80i dIno80*$^{Mi-/-}$ germarium (B) stained with antibodies against C(3)G (blue), dMre11 (green) and γ-H2Av (red). Left side shows overviews of the germaria. Right side shows magnifications of the pro-oocyte nuclei marked with the white boxes. (C) Counts of dMre11 foci present in pro-oocytes in early pachytene of wild type, *dIno80*$^{Mi-/-}$*, dIno80i (n=42)*, and *dIno80i dIno80*$^{Mi-/-}$ *(n=40)* flies. Error bars show standard deviation.

dMre11 interacts with dIno80 and through this interaction dIno80 is recruit the break. But at the break does dIno80 has a similar function to that of its yeast homolog? In yeast it has been reported that INO80 is involve in chromatin remodeling around the DSB (van Attikum, Fritsch et al. 2004; Tsukuda, Fleming et al. 2005). In order to study the role of dIno80 ATP-dependent remodeler activity during DNA the repair of meiotic DSBs, a transgenic fly carrying a mutation in the ATPase domain was generated. K566 is a conserved amino acid residue in the ATP binding region of Ino80 protein; when this residue is mutated in yeast *Ino80*, a functional complex is formed but the protein ATPase activity is affected (Shen, Mizuguchi et al. 2000). Homozygous transgenic K566A flies could not be recovered. However, heterozygous K556A were recovered and were crossed with *dno80*^{Mi} flies for studies. Progeny of the cross were 100% infertile. In order to analyze these flies, I first checked if there was enough dIno80 expressed in K566A. Immunoblot of *Drosophila* ovary extracts from wild type*, Ino80*^{Mi} homozygous, *Ino80*^{Mi} heterozygous, *K566A;*

Ino80$^{Mi-/+}$, and *K566A; Ino80*$^{Mi-/-}$ were blotted with anti-dIno80 antibodies and tubulin for loading control (figure 47a). Results showed that dIno80 is highly expressed in the K566A (figure 47a), probably due to the fact that the transgene has a promoter that drives a moderate level of expression in all tissues. I measured the intensities of dIno80 bands in each lane in western blot (figure 47a) and calculated the intensity of K556A relative to the intensity of wild band by using image J. Results showed that the band in *K566A; Ino80*$^{Mi-/-}$ is 4-fold over-expressed in comparison to WT, suggesting that 1/5 or 20 % could be functional dINO80 complex.

In order to test if recognition of DSBs and/or formation of HR foci was defective in *K566A* flies, I immunostained *Ino80*^{Mi} heterozygous, *K566A; Ino80*$^{Mi-/+}$, and *K566A; Ino80*$^{Mi-/-}$ flies with anti-dMre11, anti-C(3)G and anti-γ-H2Av antibodies. *Ino80*^{Mi} heterozygous were immunostained to compare the formation of HR with *K566A; Ino80*$^{Mi-/+.}$ *Ino80*^{Mi} heterozygous flies had a slight defect in the formation of HR as observed in figure 47b; *Ino80*^{Mi} heterozygous flies have an average of 11.5 dMre11

foci per pro-oocyte in ept (+/- 2 n=30). When *K566A; Ino80*$^{Mi-/+}$ were immunostained, I observed that HR foci were highly reduced (figure 47 c). *K566A; Ino80*$^{Mi-/+}$ flies had an average of 5.3 +/- 2.2 foci (n=34) (figure 47 c, e). I also immunostained *K566A; Ino80*$^{Mi-/-}$ flies to see if the number of HR could be further reduced (figure 47 d). Although HR sites were highly reduced, the numbers were quite similar to *K566A; Ino80*$^{Mi-/+.}$ *K566A; Ino80*$^{Mi-/-}$ had an average of 3.9 +/- 1.9 foci (n=28) (figure 47 d, e). All together, these defects in HR foci in K566A flies strongly

suggest that the ATPase domain of dINO80 plays an important role in establishment HR foci.

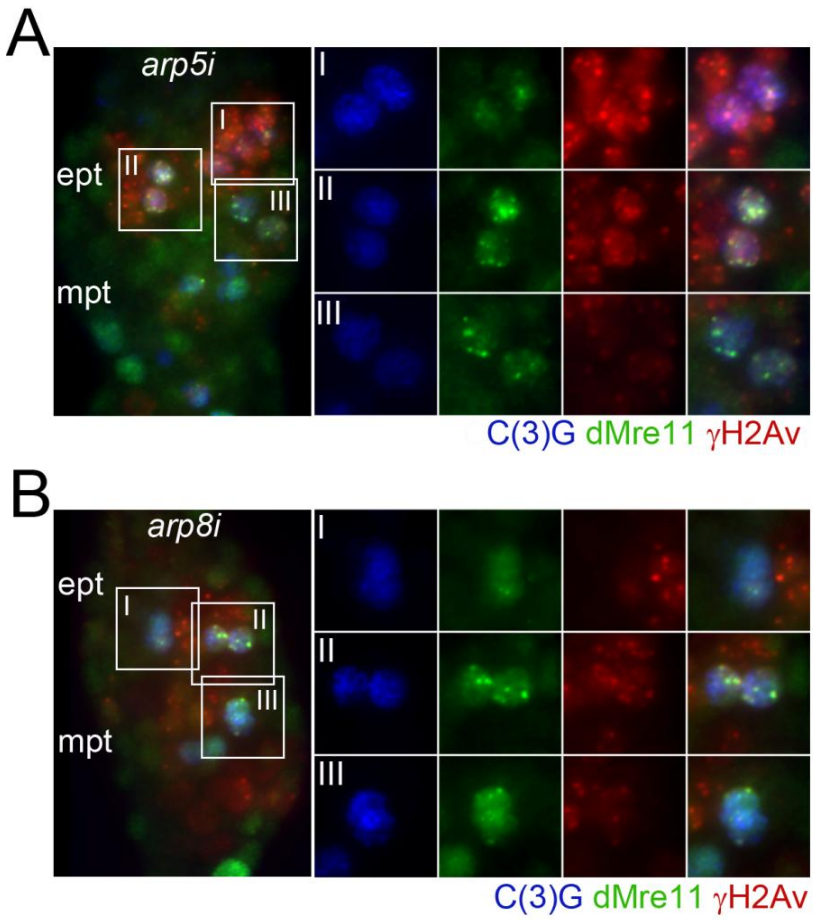

Figure 46: RNAi of Arp5 and arp8, two subunits of the dINO80 complex, have reduced HR foci. (A-B) *Arp5i* germarium (A) and *Arp8i* germarium (B) were immunostained with anti-C(3)G antibody (blue), anti-dMre11 antiserum (green) and anti-γ-H2Av (red) antibody. (A-B) Left side shows overviews of the germaria. Right side shows magnifications of pro-oocyte nuclei from region early pachytene-mid-pachytene as marked with the boxes.

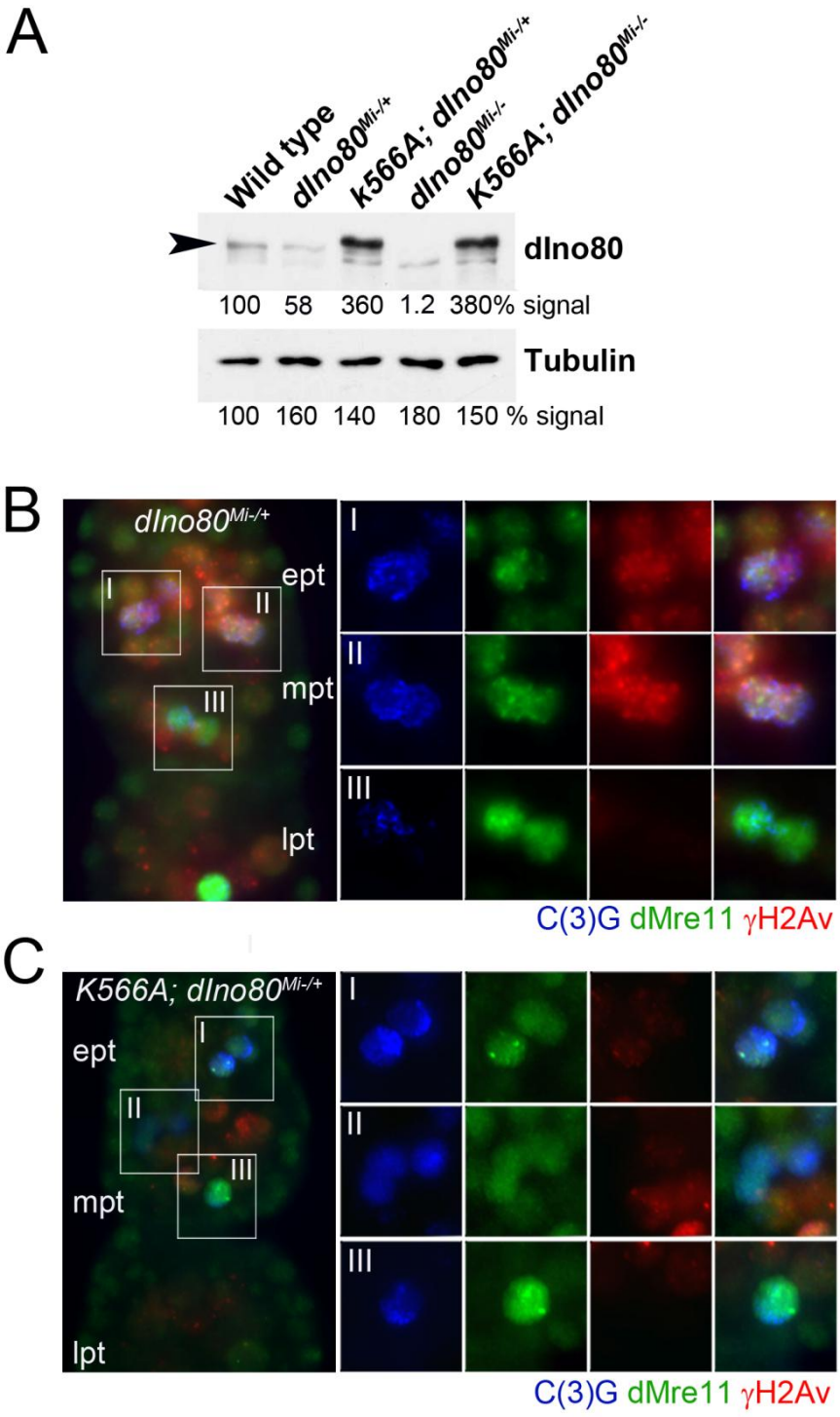
A
Wild type
dIno80Mi-/+
k566A; dIno80Mi-/+
dIno80Mi-/-
K566A; dIno80Mi-/-
dIno80
100 58 360 1.2 380% signal
Tubulin
100 160 140 180 150 % signal
B
dIno80Mi-/+
ept
mpt
lpt
I
II
III
C(3)G dMre11 γH2Av
C
K566A; dIno80Mi-/+
ept
mpt
lpt
I
II
III
C(3)G dMre11 γH2Av

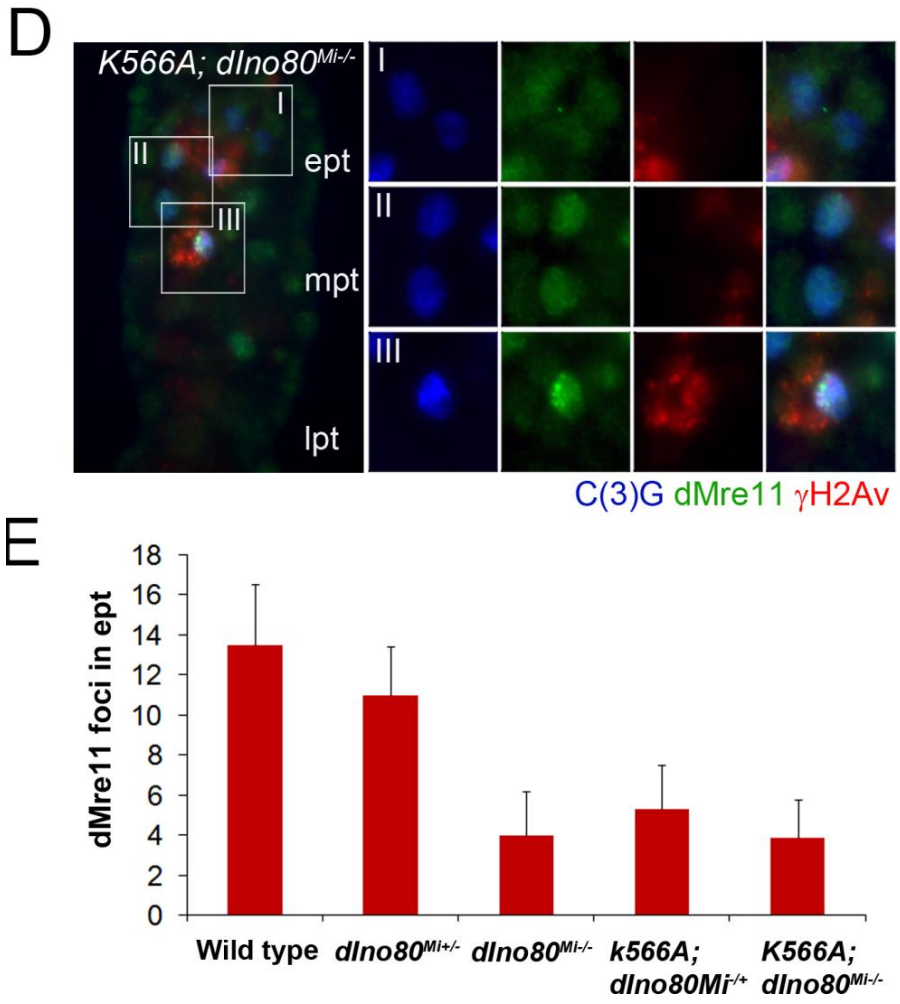

Figure 47: The ATP-dependent chromatin remodeling activity of dIno80 is important for accumulation of dMre11 to repair foci. (A) Western blot analyses of *Drosophila* ovary extracts from wild type, *dIno80*$^{Mi+/-}$, and *dIno80*$^{Mi+/-}$, flies. In addition, blots also contain ovary extracts from transgenic flies with a point mutation in the ATP-binding site (K566 to K566A). Transgene is ubiquitously expressing K566. K656 was recombined with *dIno80*^{Mi} either homozygous (*K566A; dIno80*$^{Mi-/-}$), or heterozygous flies (*K566A; dIno80*$^{Mi+/-}$). Blots were probed with anti-dIno80 antibodies and anti-tubulin antibodies. Values below each lane represent the relative intensity of each band in comparison with the respective wild type lane as quantified by Image J (NIH) software. For proper

quantification of the bands a low exposure blot was used. (B-D) Figure shows maximum intensity projections of whole mount germaria from *dIno80*$^{Mi+/-}$ females (B), *K566A; dIno80*$^{Mi+/-}$ females (C) and *K566A; dIno80*$^{Mi-/-}$ females (D)**.** Pictures show the entire germarium (left) and magnification of pro-oocytes nuclei (right). Ovaries were stained with antibodies to C(3)G (blue), dMre11 (green), γ-H2Av (red)**.** (E) Average of dMre11 foci in ept pro-oocyte of wild type, *dIno80*$^{Mi+/-}$, *dIno80*$^{Mi-/-}$, *K566A; dIno80*$^{Mi+/-}$ (n=34), and *K566A; dIno80*$^{Mi-/-}$ (n=28), *Drosophila* females. Error bar represents standard deviation.

V DISCUSSION

1. Discussion of results part 1 and 2

Anti-dMre11 antiserum labels DSB sites. My studies in the wild type *Drosophila* female during meiotic recombination using a novel fixation and staining method allowed for the visualization of MRN foci. MRN foci behave similarly to what has been published for γ-H2Av foci; they increase in number, subsequently decrease in number and disappear by region 3 (figure 7, 8, 9) (Mehrotra and McKim 2006). Both appear in the same meiotic stage (ept, or region 2a) in an average of 4 consecutive cysts (figure 8). Moreover, the average number of dMre11 foci (13.5 foci per ept oocyte) observed in this study is very similar to the average of γ-H2Av foci already published (Mehrotra and McKim 2006). Even though distribution of MRN and γ-H2Av foci in the pro-oocytes is very similar, their distribution in the nurse cells differs. As opposed to MRN foci, γ-H2Av foci were observed in the pro-oocytes and

all nurse cells of 2a cyst. Interestingly, C(3)G signals are similar to dMre11 signals; C(3)G is observed in pro-oocytes and sometimes in the 3 ring canal cells, but not in the all of nurse cells of a 2a cyst (Page and Hawley 2001). Furthermore nurse cells pro-oocytes and oocytes handled X-ray induced DSBs differently: γ-H2Av signal is robust in mpt-lpt pro-oocytes, oocytes and nurse cells but dMre11 foci are observed only in pro-oocytes and oocytes (figure 19 and 24). The differential loading of dMre11 and C(3)G, in addition to the fact that nurse cells and pro-oocytes and/or oocytes seem to handle X-ray induced DSBs differently (figure 19 and 24), suggest the possibility that DSBs in pro-oocytes behave differently from nurse cells and may be repaired through a different pathway that does not require synapsis of homologs and/or accumulation of recognition factors. This agrees with reports by Carpenter where was claimed that winning pro-oocyte, losing pro-oocyte and cells with three ring canals enter meiosis, but nurse cells do not (Carpenter 1994). Alternative, since nurse cells perform nutritive roles for the oocyte and my data suggest that an observable dMre11 focus depends on the proper accumulation of repair factors at the break (see below for discussion). it is plausible to imagine that there is a gradient like accumulation of repair factors (between the interconnected cells) into the oocytes, pro-oocytes and then into the three ring canal cells that allows the visualization of repair foci in these cells but not in the other twelve obligate nurse cells.

Even thought this differential staining is observed in the nurse cells, the following data strongly suggest that dMre11 signals are indeed labeling HR sites: 1)

the absence of dMre11 foci in *meiw-68* mutants, which are unable to introduce DSBs, and in *Nbs* mutants, which have impaired loading of dMre11 and dRad50 to the pro-oocytes nuclei (figure 13 and 14), 2) *spn-A* and *okr* mutants, which are unable to repair DSBs, show a persistent accumulation of dMre11 foci to later stages of pachytene (figures 20, 21, 22), 3) dMre11, rad50 and Nbs1 signals behave very similar to each other and co-localize (Figure 7) and 4) γ-H2Av and dMre11 co-localize during ept and mpt (figure 8).

*HR sites are introduced and repair asynchronously***.** When the sizes of ept and lpt HR sites were studied, I observed that overall HR sites were smaller in ept and larger in mpt (figure 8d), which correlate with the electron microscope studies described by Carpenter (Carpenter 1979). However, as could be observed in other wild type figures (figure 8 and figure 7), not all ept foci are small and not all lpt foci are large. In addition, even within the same ept or mpt pro-oocytes there are visible differences in the size of foci (figure 9). This is probably due to an asynchronous introduction and repair or DSBs. Asynchronous appearance and repair of DSB during *Drosophila* female meiotic recombination was suggested by Carpenter and McKim groups, when RN and γ-H2Av dynamics were studied (Carpenter 1979; Mehrotra and McKim 2006). Studies in *Drosophila* females deficient in DNA repair have reported that on average about 20 γ-H2Av foci accumulate per pro-oocyte, suggesting that a maximum of 20 foci are formed per pro-oocyte (Staeva-Vieira, Yoo et al. 2003; Mehrotra and McKim 2006). The fact that the maximum number of dMre11 foci

observed in this study was 15 further supports that DSBs are introduced and repaired asynchronously.

*Phosphorylation of H2Av does not accurately mark the appearance or disappearance of DSBs***.** I observed that by the end of mpt the majority of dMre11 foci have disappeared, suggesting that the majority of the breaks could have been repaired and the dMre11 focus has been disassembled. However, there are still a considerable number of γ-H2Av foci left, suggesting that chromatin may have not been completely cleared (figure 8e). This observation would suggest that in germ cells, γ-H2Av functions as a signal in response to damaged DNA, but it does not mark the immediate appearance or disappearance of breaks. This is supported by other studies in germ cells where it was proposed that γ-H2AV is exchanged with H2AV independent of DSB repair and the removal of γ-H2Av was suggested to be depended on ATM or ATR activity (EF, M et al. 2011). Interestingly, my results show that in mpt, ATR and ATM still fairly available and active (figure 17-18). Additionally, in somatic cells γ-H2Av is widely spread into chromatin flanking the damage sites (Shroff, Arbel-Eden et al. 2004), and therefore is not specifically marking the DNA damage site. Furthermore, it is unclear whether or not in somatic cells clearance of γ-H2Av from chromatin after the induction of DSBs indicates that the breaks were repaired (Kusch, Florens et al. 2004).

Interestingly, in this study it was observed that dMre11 foci persist to later stages of oogenesis, but γ-H2Av signaling is reduced when compared to dMre11

signal (figure 22-24). This was noticed when oocytes from stage 2 and stage 4 *spn-A* females, as well as oocytes from γ-irradiated wild type females were studied. Staining with anti-H2Av antibody shows that the histone variant is present in these stages; as such, it is possible that in these later stages of oogenesis, signal to chromatin is attenuated or reduced possibly because the oocyte prepares for compaction of its chromosomes and forms the karyosome. Additionally, according to my data obtained for *mei-41* and *tefu* mutants (figure 17-18), it is possible that these kinases are not fully functional during stage2 and stage4 oocytes

Large peripheral HR foci found in mpt could represent late RNs. As mentioned before, RNs are structures observed in EM studies and do not directly correlate with the HR foci observed in immunocytochemistry studies. However, studies in plants have shown that repair factors such as Rad51 are part of some RNs (Anderson, Offenberg et al. 1997). In addition, fluorescence immunocytochemistry studies suggest that other proteins, such as RPA, MLH, and Rad51, may be components of RNs (Plug, Peters et al. 1998) because of their striking similarities in the distribution pattern on synapse chromosomes and the similarities in the numbers of late RN and COs found in meiotic chromosomes. My studies in the behavior of HR foci during *Drosophila* female meiosis also suggest that it is highly possible that dMre11 signals represent some of the RNs. dMre11 foci behavior is very similar to what has been published for *Drosophila* RNs. The average size of HR foci increases with developmental age. The smallest HR sites were observed first and bigger HR sites were observed last (figure 8). Early HR sites are greater in quantity as opposed to

later HR sites, which are fewer in number (figure 8). The number of late RN is the same as the number of large peripheral HR foci found in mpt; as such, it is highly possible that dMre11 signals represent some RNs, especially the late large HR sites observed in mpt.

*Late peripheral HR foci may represent COs***.** I find that an average of 5 HR foci are peripheral at a time when mpt is reached (Figure 8 and 9). These 5 HR foci are reminiscent of the average number of crossovers per nuclei that was established after genetic analyses of crossover events in *Drosophila melanogaster* (McKim, Jang et al. 2002). It is believe that there is an average of 5 crossover events per nuclei, at least an average of one crossover event per chromosome arm, since there are only 5 chromosome arms in *Drosophila* X, 2L, 2R, 3L, 3R and chromosome number four does not recombine (McKim, Jang et al. 2002). Together these results and previously published data describing late RN suggest that the average 5 peripheral HR foci in mpt represent crossover events (Carpenter 1979). More importantly, these 5 HR foci behave abnormally in both exchange and precondition mutants (Fig. 15, Fig. 16), supporting the idea that these indeed correspond to COs.

COs are most mobilized to the nuclear periphery (figure 9). In yeast, late or unrepaired DSBs also accumulate at the nuclear envelope (Oza, Jaspersen et al. 2009). In this context, it must be mentioned that in this study re-localization was dependant of Rad51. It is therefore tempting to speculate that this signal for the peripheral mobilization might be specific for HR. Interestingly, it has been suggested

that in yeast COs are repaired after NCOs (Allers and Lichten 2001). This would suggest that slow repair of future COs serves the purpose of their developmentally-timed repair in the nuclear periphery.

In mpt there is a higher percentage of foci located in the periphery, but overall the number of foci is diminished when compared to early pachytene; this could be due to either of the following: 1) there are HR sites that were initiated in the periphery, but they are delayed in repair or "late" since the periphery is considered a heterochromatic-silencing region that impedes processes such as repair and replication, or 2) breaks form in the center of the cell and actively migrate to the periphery, presumably for repair. I favor the latter mechanism, due to the fact that the statistical analysis shows that in ept there is not an equal distribution of HR foci throughout the nuclei: 21% of the HR foci are in the outermost zone, and 79% are in the two more inner zones. 21% of the average 13.5 HR foci found in ept is 2.8 HR foci --this is a very small number of HR foci when compared to the late mpt HR foci that were actually counted. As such, if breaks were formed at the periphery and just slow but do not migrate, the number of actual mpt late breaks should be a lot fewer than the 5 counted. When wild type ovaries were stained with antibodies to Hp1 and H3K9me2, peripheral HR foci were observed mostly outside of heterochromatic areas (figure 10b), then it is unlikely that HR foci initiates at periphery and are maintained in these regions longer because repair is impeded. Moreover, in mice, mismatch repair (MMR) proteins assemble with some repair foci during pachytene, which have been suggested to

correspond to COs (Baker, Plug et al. 1996). I find that in *Drosophila* MMR protein, Msh2, is enrich at the periphery (figure12). Thus, it is possible that CO are directed to the periphery for repair and possibly to separate early NCOs from late COs

*dATR and dATM function in the regulation and nuclear localization of HR foci***.** Considering the data obtained after immunostaining of *mei-41* and *tefu*^{8} mutants, the following functions may be attributed to these kinases 1) Mei-41 functions during early-mid pachytene where it phosphorylates H2Av and also seems to promote the accumulation of dMre11 to DSBs (figure 17). My results show that tefu is most likely inactivated as early as 6 hours after shifting the temperature-sensitive *tefu*^{8} mutant to the restrictive temperature. Thus, after being at the restrictive temperature for 2 days, the phosphorylation observed in early pachytene and mid pachytene must be due to the kinase activity of mei-41 (figure 17- 18). In addition, Eric F. Joyce *et al* showed that when *mei-41*^{D3} and *tefu*^{8} double mutants where shifted to the restricted temperature there was a loss of γ-h2Av (Joyce, Pedersen et al. 2011).

2) In mid-pachytene Mei-41 is need for the proper accumulation of HR foci to the periphery. As shown in figure 17, late HR foci in *mei-41*^{D3} fail to go the periphery in mid-pachytene, whereas in *tefu*^{8} mutants, accumulation of repair factors and peripheral localization seem to be enhanced in mid pachytene and persist to late

pachytene (figure 18). Therefore, mei-41 could be in charge of movement of HR foci to periphery and its functions may be restricted to some extent by tefu.

3) Joyce *et al* had suggested that the massive accumulation of γ-H2Av it is due to the presence of more breaks; it was further suggested that tefu is involved in negatively regulating DSB formation (Joyce, Pedersen et al. 2011). However due to the observation in early 2a where single foci marked by dMre11 and γ-H2Av were observed, it is also possible that ATM restricts phosphorylation of H2Av. If ATM were involved in negatively regulating the formation of DSBs, one would expect to see a similar increment of dMre11 and γ-H2Av foci in early stages of ept as the one observed in mpt.

Any persisting DSB can be mobilized to the nuclear periphery; however, localization to the periphery is developmentally controlled and occurs from mid-pachytene on. Analysis of DNA repair deficient mutants shows that all breaks have the possibility to go to the periphery if late repair or unrepaired (figure 20, 21, 22). This suggests that movement to the periphery is not exclusively for CO; regardless, all breaks if delayed or not repaired by a certain meiotic stage, in this case mpt, can move to the periphery. This is based on the fact that in wild type, pro-oocyte movement of HR sites to the periphery is observed in mpt and movement to the periphery is determined by dATR signaling which seems to be stage dependent and controlled by ATM. It is possible that developmental time or meiotic stage plays a key role in the decision of HR foci movement to periphery, and thus it is tempting to speculate that

if a break is slow to repair or had not been repaired by mpt, it is exposed to dATR signaling and directed to the nuclear periphery. Furthermore newly introduce DSBs can form MRN foci that are mobilized to the periphery from mid-pachytene on (figure 19)

The data obtained here when *mei-218* mutants were analyzed, as well as studies by the Selkesky and McKim groups suggests another level of regulation to differentiate CO and NCO and to determine movement to periphery. Studies by Kohl *et al* suggested that mei-218 is involved in ensuring that COs are resolved as COs; *mei-218* encodes a protein that prevents the Bloom Syndrome Helicase (BLM) from premature repair of DSBs as NCOs (Kohl, Jones et al. 2012). BLM helicase generates NCO by unwinding recombination intermediates (Chu and Hickson 2009). Therefore, the Mei-218 protein must persist at meiotic DSBs pre-selected for CO resolution to protect from a premature resolution as NCOs. *mei-218* was named a precondition gene because in mutants, the frequency and distribution of crossovers along chromosome arms is altered (Liu, Jang et al. 2000; Bhagat, Manheim et al. 2004). However, studies in crossover-deficient mutants suggest that *mei-218* is most likely not a gene in charge of only establishing the crossover, but a gene in charge of also maintaining an intermediate that will be resolved as a crossover (Bhagat, Manheim et al. 2004). The view of precondition has been challenged because *Drosophila* females with mutations in genes involved in the actual repair of DSBs, such as *okr* and *spindle* genes, show that they also have altered frequency and distribution of crossovers along chromosome arms (Bhagat, Manheim et al. 2004).

In addition, intragenic recombination experiments using *mei-218* mutants suggest that *mei-218* has a function in the in the molecular transition of the recombination intermediate late in the repair pathway (Bhagat, Manheim et al. 2004). In this context, my observations as well as Carpenter's observation where a low number of early RNs was observed in *mei-218* mutants could be attributed to HR foci being repaired prematurely in the nucleoplasma on *mei-218* mutants (figure 15), which is fully consistent with both the Selkesky and McKim groups' studies (Bhagat, Manheim et al. 2004; Kohl, Jones et al. 2012). As such, all together this data suggests a model in which *mei-218* is involved in the establishment of COs and in the maintenance of CO by preventing their premature repair as NCO. My studies also suggest that mei-9 is involved in later stages in the actual resolution of the intermediate, but it is not clear as to why they also have an apparent reduction in ept HR foci number (figure 16).

Based on the observations explained above, I propose a model for the regulation of CO movement to the nuclear periphery: CO sites are pre-established and maintained as CO by preventing their repair as NCO. *mei-218* is involved in the establishment and maintenance of DSBs as CO; it persists at DSBs and protects the DSB by preventing their repair by BLM as NCOs. Movement to the periphery is not the exclusively for CO; it does not matter if it is a CO or NCO, but what does seem to matter is the timing. If the DSB is not repaired by a specific time, it is moved to the periphery. As published for yeast, CO in flies could also be resolved more slowly than NCO (and in the meantime be protected by *mei-218*), and thus persist until mpt

where they are exposed to Mei-41. Then, NCOs are repaired earlier and towards the center of the nuclei and COs are preferentially resolve later at the periphery. COs may move to the periphery for repair where cross over specific factors such as Msh2 accumulate; --concentrating COs at the periphery with COs specific factors could facilitated repair and ensure repair as COs. Furthermore by moving COs to the periphery away from the bulk of the genome could prevent repair using incorrect homologous sequences.

Formation of a microscopically discernible HR focus depends on proper accumulation of recognition factors. Data obtained after staining of Nbs^{2k} mutants, where dMre11 signal was defective, suggest that the proper availability and accumulation of recognition factors in the nuclei is important for the formation of an observable HR focus. These results, together with: 1) the fact that dMre11 is mostly loaded into pro-oocytes, 2) the observed increments in dMre11 foci size as the cyst develops, 2) the phenotypes observed after staining of *Spindle A, B* and *C* oocytes (figure 25), and 4) the phenotypes observed after staining of oocytes from females deficient in the phosphorylation of H2Av (figure 26) suggest that during repair of meiotic DSBs, there is a system than ensures the constant loading and accumulation of more recognition and repair factors to the damage sites.

Since γ-H2Av is observed in *Spindle A, B* and *C* mutants and MRN foci are defective, is possible that these genes function early in the repair pathway, after an initial recognition of breaks to ensure the accumulation of more recognition factors. This is in accordance with the early functions attributed to the yeast homologs of spn-B and spn-C. Spn-B and Spn-D are the *Drosophila* homologs of XRCC3 and Rad51C, respectively; it has been suggested that XRCC3 has early and late functions during HR due to the fact that XRCC3 mutants have reduced and altered HR product (Brenneman, Wagener et al. 2002). *Rad51c* knockout mice also have marked reduction in Holliday Junction activity (Kuznetsov, Pellegrini et al. 2007). As previously mentioned, Spn-C does not have a homolog within the Rad51 family -- it is the homolog of human helicase HEL308, a conserved helicase that has a function in early stages of homologous recombination (McCaffrey, St Johnston et al. 2006)}.

Additionally, the lack of an observable MRN focus in γ-H2Av mutants is in agreement with its published role in the establishment of mammalian repair foci (figure 26) (Goldberg, Stucki et al. 2003; Stewart, Wang et al. 2003; Xu and Stern 2003). In mammalian the amplification of the DNA damage response is orchestrated by the MDC1 protein; MDC1 plays the role of a scaffold protein required for formation of a repair focus, where the protein itself is needed for the formation of MRN foci, but its binding to the break is also dependent on dMre11 and phosphorylation of H2Av (Goldberg, Stucki et al. 2003; Stewart, Wang et al. 2003; Xu and Stern 2003). Thus, spindle genes and phosphorylation of H2Av could be part of

a mechanism homologous to the amplification of the DNA damage response in mammals.

.

2. Discussion of results part 3

Drosophila Ino80 protein has roles in DSB repair. Immunoprecipitations and mass spectrometry results showed that dIno80 and dMre11 directly interact in somatic cells in a damage-dependent fashion (table 1, figure 28-29). In addition, *Drosophila dIno80*^{Mi} mutants are sensitive to X-rays and have defects in exiting the G2-M cell cycle checkpoint (figure 31-32). My studies in the *Drosophila* ovary provide evidence that dIno80 and dMre11 also interact in germ cells (figure 37). Co-IPs done using ovary extracts showed that dMre11 and dIno80 interact in this tissue; it should be noted that ovary extract has germ cells and somatic cells. Moreover, immunostaining assays of *Drosophila* ovarioles show that both proteins are highly expressed in meiocytes and that they do co-localize in some HR foci. However, not all dIno80 do co-localize with dMre11, it is possible that dIno80 is transiently localized at HR foci. Further supporting a role of dIno80 during meiotic DSB repair are the high levels of dIno80 in the ovaries when compared to heads (figure 35), in addition to the expression data published by modENCODE, where males have lower expression levels of dIno80 compare to females (figure 35). *Ino80*^{Mi} females are infertile and males are fertile; importantly, *Drosophila* males do not recombine. As

such, it is possible that dIno80 is so highly expressed in female ovaries because it plays important roles in meiotic recombination.

As described in my results, *Ino80*^{Mi} embryos laid by homozygous females have dorso-ventral patterning defects (figure 33). Dorso-ventral patterning defects seem to be characteristic of *Drosophila* DNA repair deficient females (Ghabrial and Schupbach 1999). Surprisingly, *Ino80*^{Mi} embryo patterning defects were stronger than those of *spn-A* embryos (Staeva-Vieira, Yoo et al. 2003). As mentioned before, low level of Gurken causes dorso-ventral defects in the polarity of the embryos (Ghabrial and Schupbach 1999). Presumably in mutants such as *spn-A,* the failure to repair DSBs activates the DNA damage checkpoint, which lowers Gurken levels. It has been shown that in *spn-A* and *mei-W68* double mutants, the dorso-ventral phenotypes of *spn-A* are suppressed; this is thought to be due to the fact that the check point is not activated because there are no DSBs in the double mutants (Staeva-Vieira, Yoo et al. 2003). Since the phenotypes were so penetrant in *Ino80*^{Mi} homozygous mutants (figure 33), I used *dIno80*^{Mi} and *mei-W68* double mutants to determine if the dorso-ventral phenotypes could be suppressed. After analyzing eggs laid by the double mutants, I observed that the eggshell phenotypes of *dIno80*^{Mi} flies were not suppressed. This could be due to the following reasons:

1) It is possible that egg shell defects and/or lack of rescue may be due to defects of *dIno80*^{Mi} mutants in later checkpoints, e.g. meiosis II, which up to this point have never been studied, since all repair mutants already seem to affect meiosis I.

2) In addition, the signaling pathways linking Gurken, a gene product that affects egg polarity, to cell cycle progression are not completely clear (Abdu, Brodsky et al. 2002). One proposed mechanism is that activation of cell cycle checkpoint kinases could function in two pathways: one that regulates cell cycle progression through Dwee1, and another that regulates embryo polarity through Gurken (Abdu, Brodsky et al. 2002). Thus, there is not enough evidence to determine whether the defects are solely due to Gurken regulation or regulation of other egg polarity genes, -- especially in the case of dIno80 mutants, where the INO80 complex has been shown to function in transcription, replication and DNA repair.

3) dIno80 could have egg polarity defects independent of meiotic DSB repair. This is supported by studies done by V. Barbosa where a maternal screen for genes affecting oocyte polarity was done (Barbosa, Kimm et al. 2007) Interestingly *trin*, a gene described in the Barbosa study, have egg polarity defects and *mei-W68* and *mei-41* mutants do not suppress them. Furthermore *trin* mutants do not delay meiotic restriction, and show defects in the karyosome in spite of normal Gurken (as mention before Gurken protein controls dorso-ventral patterning of the eggs and anterior polarity of the embryo) levels. Interestingly, similarly to dIno80 mutants, *trin* mutant germ-line clones produce collapsed eggs. Thus, considering that the

levels of Gurken in dIno80 mutants is not known, It is possible that dIno80 mutants have similar roles in the development of the *Drosophila* egg shell

dIno80 complex functions during early stages of the DNA repair pathway. In agreement with a role of dIno80 during early stages of DNA repair, damage studies in S2 cells suggest that dIno80 and dMre11 interaction increases in early stages of the DNA repair response (figure 29). S2 cells were irradiated with 45Gy and 15 Gy at 150 rads/minute; since all samples were irradiated at the same dose of 150rads/minute, it consequently takes more time to receive 45 Gy than 15 Gy. The fact that the 15 Gy sample showed a 6-fold increase in interaction whereas 45 Gy only increased a 4fold suggests that the interaction between dMre11 and dIno80 takes place during early steps of repair rather than later steps. Furthermore, the fact that γ-H2Av is not normally observed in ept pro-oocytes of dIno80 mutants supports an early role probably in the recognition of DSBs. As suggested by the results in part 2 of this study, formation of an MRN focus requires basal loading of MRN and phosphorylation of H2Av, as well as a later accumulation of more recognition and repair factors. In addition, as previously shown dMre11 resection mutants had affected dMre11 foci, but γ-H2Av foci seem to be unaffected, suggesting that resection is needed for accumulation of dMre11, but most likely the initial recognition of the break was done normally. Since γ-H2Av foci as well as

dMre11 foci are reduced in *Ino80*^{Mi} mutants in ept, it is likely that recognition of the break is affected.

The dINO80 complex is required for the proper formation of an observable HR focus during meiotic recombination. *dIno80*^{Mi}, *dIno80*^{P}, and *dIno80i* have defective HR foci formation; the number of HR foci in these dIno80 deficient flies is highly reduced in ept pro-oocytes (table 3 and figures 38-39, 45- 47). In addition, *dIno80*^{Mi} region 3 oocytes fail to properly respond to induced DSBs, the timely formation of HR foci is delayed (figure 40). Moreover, other subunits of the INO80 complex also have highly reduced numbers of HR foci (figure 39, 46). As shown in figure 39, *Dmel\l(3)L1231* phenotypes are very similar to *Ino80*^{Mi} phenotypes. One possible explanation for having such similar phenotypes is that this subunit is needed for dIno80 targeting to the DSB, or that the complex stability is compromised when the subunit is missing. Although the molecular function of lethal *(3) L1231* is not completely known, it is known that it has a DNA binding domain. Knockdown by RNAi of other two dIno80 subunits, arp5 and arp8 also have reduced numbers of HR foci in ept pro-oocytes.

More importantly, the very reduce numbers of HR foci in K566A flies strongly suggest that the ATPase domain in dIno80 plays an important role in the recruitment of recognition, and possibly, repair factors to the break (fig 47). Based on INO80's function in sliding or removing nucleosomes and the available yeast data, one can

speculate that INO80 is brought to the DSB where it helps clear up chromatin, thus allowing for the proper loading and accumulation of recognition factors to the DSB (van Attikum, Fritsch et al. 2004; Tsukuda, Fleming et al. 2005; Bao and Shen 2007; Watanabe and Peterson 2010)**.** These results are also consistent with the fact that Arp5 and Arp8 are required for the chromatin remodeling activities of the yeast INO80 complex (Bao and Shen 2007; Watanabe and Peterson 2010).

As previously mentioned, there is an average of 4 foci left in *dIno80^{Mi}*. It is possible that the few foci observed in *dIno80^{Mi}* mutants could be foci formed in a more permissive chromatin environment, which would eliminate the need for INO80 to clear up chromatin around the DSB. Yeast studies have shown that recognition factors transiently accumulate to future repair sites in the absence of spo11 (Borde, Lin et al. 2004). Results shown in figure 35a, where some full-length protein and some truncated protein were observed, suggest that there could be low amounts of full length dIno80 protein produced. Production of full length protein could be due to either rare events of proper splicing or a residual maternally-loaded dIno80. As such, the availability of some full-length protein might explain the observed foci and more importantly the viability of the dIno80 females, -considering that Ino80 is essential in some other organisms (Bao and Shen 2007; Conaway and Conaway 2009; Watanabe and Peterson 2010). Nevertheless, the amounts of Ino80 are very low and therefore may not support fertility. Furthermore, the results suggest that *Ino80^{Mi}* homozygous generates a dIno80 with some remaining function -- this is

consistent with irradiation assays, where there is a slow response but foci eventually form (figure 45).

The *role of Ino80 during Drosophila female meiosis is dosage-dependent.* The results obtained after the *K566A* and *dIno80i* flies were analyzed suggest that there is a dosage-dependent role of Ino80 during *Drosophila* female meiosis. This could explain such a strong penetrance of the egg shell phenotype, viability of $dIno80^{Mi}$, and high requirements in the ovary. As mentioned above, $dIno80^{Mi}$ mutants have some remaining HR foci (4 +/- 2.2) (table 3); knockdown of dIno80 was done in an attempt to further reduce the amount of protein, and by extension the number of HR foci. Knockdown was performed due to the fact that most genetic analysis will be affected by the nature of the Ino80 locus, which contains seven other open reading frames. When *dIno80i* flies were analyzed, I counted an average of 7.3 +/- 3.2 in *dIno80i and* 3.9 +/- 3.0 in *dIno80i,* $dIno80^{Mi}$ (figure 45) suggesting that 4 foci is the minimum that can be observed when dIno80 is affected. It should be noted that the amount of protein left in *dIno80i* could not be efficiently determined by western blotting due to the fact that the RNAi was done using a specific germ cell driver and ovary extracts will have germ cell plus follicle cells, where the protein levels were not knocked down.

Results of K566 also provide evidence that the number of HR foci could not be reduced more than the observed average 4 foci. *K566A* $Ino80^{Mi-/+}$ has an average of

5.3 (+/-2.2) and *K566A Ino80*$^{Mi-/-}$ has an average of 3.9 (+/-2.2). Comparison of *K566A Ino80*$^{Mi-/+}$ and *Ino80*$^{Mi-/+}$ foci numbers suggest that K566A is affecting HR foci formation. Furthermore, the western blot in figure 47 showed that in *K566A Ino80*$^{Mi-/+}$ and *K566A Ino80*$^{Mi-/-}$, dIno80 protein levels were about 4-fold over expressed in comparison to wild type, suggesting that 1/5 or 20 % could be indicative of functional dINO80 complexes. Although there is the possibility that this transgene, affecting the ATP binding region of Ino80 protein, is disrupting complexes or creating mutant complexes, results in yeast suggest that a functional complex is formed. When K566A residue is mutated in yeast, a functional complex is formed but the protein ATPase activity is affected (Shen, Mizuguchi et al. 2000). The high dosage in the ovary indicates that Ino80 is highly required in this environment. *K566A Ino80*$^{Mi-/+}$, *K566A Ino80*$^{Mi-/-}$ are 100% sterile, and the number of HR foci could not be reduced. Based on these results and the roles of dIno80 in transcription replication and DNA repair in yeast and mammals, it is possible that a reduction in protein levels below a 5% threshold would result in death.

Overall, my data provides evidence that the *Drosophila* dIno80 protein has roles in the repair of meiotic DSBs during recognition and establishment of HR foci. Although there is not yet enough evidence to rule out a function of dIno80 upstream of dMre11 in the DNA damage repair pathway, my data suggest that dMre11 could be in charge of recruiting dIno80 to the break thru a direct interaction. Based on my results and some yeast data, where analyses of an *mre11* mutated strain showed that histone loss around the DSB was significantly impeded (Tsukuda, Fleming et al.

2005) and yeast *ino80* mutants have impaired binding of Mre11, Ku80, Mec1 at DSB (van Attikum, Fritsch et al. 2007), I speculate that dMre11 recruits Ino80 to the DSBs and dIno80 clears chromatin at the break, allowing for the binding of recognition and repair factors.

VI. FUTURE STUDIES

As shown in this study, the use of *Drosophila* female meiosis as a model in conjunction with a novel fixation/staining protocol and markers such as dMre11 provide a powerful system to further study and understand mechanisms associated with meiotic DSB repair. The data that show that HR foci localize to the nuclear periphery at a specific meiotic stage and that *spn-B, C,* and *D* genes have different roles from *spn-A* are great examples of the usefulness of this model and methods.

Movement to the periphery provides an elegant way to resolve DSBs by confining them in a specific nuclear environment separate from the rest of the genome. Several studies in yeast have attempted to elucidate the mechanism by which DSBs are anchored and repaired at the nuclear periphery. Persistent DSBs in yeast are anchored at the periphery by Msp3 protein, a SUN domain protein that traverses the inner nuclear membrane (Gartenberg 2009; Oza, Jaspersen et al. 2009). Here I show that late-repair DSBs move to the periphery and co-localize with lamin, but whether or not they are actually anchored at the periphery (as in yeast) as well as the mechanism and factors involved in this process are still unknown. The

following may aid in the understanding of HR site movement to the periphery during recombination using *Drosophila* female meiosis:

1. As mentioned above, SUN domain proteins are important for anchoring of DSBs to the periphery. SUN domains as well as KASH domains are the main components of LINC complexes --macromolecular assemblies that transverse the membrane of the nuclear envelope (Razafsky and Hodzic 2009). Both SUN and KASH are highly conserved in eukaryotes (Razafsky and Hodzic 2009). Two KASH proteins are known in *Drosophila*: Msp-300 and Klarsicht. Msp-300 and Klarsicht are expressed during oogenesis and localize to the nuclear envelope of the germ line nuclei (Technau and Roth 2008). There are also two known orthologs of the SUN protein in *Drosophila*: Klaroid and sperm-associated antigen 4 (Spag4, previously named Giacomo) (Kracklauer, Wiora et al. 2010). Thus far, there has only been one study in Spag4 that shows that this SUN domain protein is required for centriole and nuclear attachment during spermatogenesis (Kracklauer, Wiora et al. 2010). Klaroid has been more extensively studied, and it has been shown that it plays an important role in the development of the *Drosophila* eye. Although *Drosophila* Msp-300 has been suggested to be dispensable for ovary development, the roles of the *Drosophila* SUN and KASH proteins in meiotic recombination and possibly in the proper resolution of CO in the nuclear periphery has never been addressed. As such, analysis of the localization of late HR sites using the protocol and antibodies use in this study in *Sun* and *Kash Drosophila* mutants could shed some light in the anchoring mechanism of late repair DSBs.

2. My studies show that dMre11 foci represent HR sites and that late peripheral HR sites found in mpt may correspond to CO. As such, these late HR sites should contain factors such as Rad51 and Brca2. Studies by Eric Staeva-Vieira *et al* have described an antibody against Spn-A; although it was used in western blotting in these particular studies, it is possible that with the new fixation protocol it may stain in distinct foci (Staeva-Vieira, Yoo et al. 2003). This will provide a great means to determine the stage and the importance of homology search during the *Drosophila* meiotic recombination. Furthermore, this antibody could aid in defining the composition of early versus late HR sites.

One important factor that could provide direct evidence of late peripheral HR corresponding to CO is Mlh1. Mlh1 is part of the MMS group of proteins. As previously mentioned, MMS proteins are divided in MutS: Msh1 through Msh6, and four MutL homologues, Mlh1 through Mlh3 and Pms1. Mlh1 seems to be conserved in eukaryotes and is a marker for crossover sites in mice, and antibodies against it stain in a pattern that correlated with the observed distribution and numbers of crossovers in wild type mouse germ cells during meiosis (Baker, Plug et al. 1996; Anderson, Reeves et al. 1999). Mlh1 has also been shown to localize to crossovers in plants (Franklin, Higgins et al. 2006). Interestingly, Mlh1 has been implicated at a later stage -- in the finalization of CO recombinational interactions during pachytene (Franklin, Higgins et al. 2006; Hunter 2007). *Drosophila* also has an Mlh1 homolog, Dmel\Mlh1 (CG11482); in accordance with a conserved role in eukaryotes during

meiotic recombination, Mlh1 is highly expressed in the *Drosophila* ovary (data published in Fly Base by modENCODE). The availability of commercial antibodies for MLH1 offers the possibility of identifying CO through Immunohistochemistry studies in the *Drosophila* ovary.

The data obtained from *spindle-B, C, D* mutants and mutants with defective H2Av phosphorylation suggest an elegant model for the accumulation of recognition and repair factors to the break. As proposed above, it is possible that the accumulation of these factors around the break involves mechanisms that are similar to the amplification of the DNA damage response in mammals. MDC1 is the scaffold protein that orchestrates the amplification of the DNA damage response in mammals. Studies by Dronamraju and Mason have described a possible homolog of MDC1 in *Drosophila*. In one such study, it was found that Mutator Protein 2 (MU2) has similar structure and functions as the human MDC1 (Dronamraju and Mason 2009). Like MDC1, MU2 seems to interact with components of the MRN complex. Additionally, MU2's BRCT repeats interact with γ-H2Av, and this interaction seems to affect γ-H2Av foci formation. However, the study did not assay the presence and/or absence of MRN foci or other repair proteins in MU2 mutants. As such, the following could aid in the understanding of a model for accumulation of repair factors to the break in *Drosophila*:

1. Immunostaining of MU2 mutants with MRN antibodies. If MU2 is indeed involved in the accumulation of recognition factors and formation of observable foci, one would expect not to see MRN foci after immunostaining of MU2 mutants.

2. Interaction studies of MU2 and spindle genes as well as MRN complex proteins with spindle genes. In this case, interaction can be studied using the yeast two-hybrid assay -- in this assay, the proteins of interest are fused separately to a DNA-binding domain and to the transcriptional activation domains of the Gal4p transcription factor. If the proteins do interact, a functional Gal4p is formed and activates expression of reporter genes (Miller and Stagljar 2004). Interaction studies of *Drosophila* DNA repair proteins using the yeast two-hybrid assays have been successful (Radford, Goley et al. 2005; Joyce, Tanneti et al. 2009) The two-hybrid experiments in these studies have been performed as described by James *et al* (James, Halladay et al. 1996). Furthermore, molecular characterization of *spnB* and spn-D has been published (Ghabrial, Ray et al. 1998; Abdu, Gonzalez-Reyes et al. 2003).

Future studies part3

My work highlights the importance of a chromatin remodeling complex during DNA damage repair. I showed that the chromatin remodeling complex, INO80, is of paramount importance for the recognition of DSBs and the proper accumulation of

repair factors to the break. Furthermore, this work sets up the basics for the development of a mechanism of INO80 recruitment in higher eukaryotes to the break. According to my studies the DNA damage recognition complex could have the role of recruiting dINO80 to the break, where the complex opens up chromatin and allows the binding of repair factors. The following studies could aid in the further understanding of dINO80 during such early stages of repair and also in downstream events such as the activation of the meiotic cell cycle checkpoint.

The role of dINO80 in the formation of meiotic DSBs

My studies show that dIno80 is important for the recognition of DSBs and the proper accumulation of repair factors to the break. Moreover, interaction studies as well as the fact that dMre11-dIno80 interaction increases upon damage, suggest that dIno80 is recruited to the break by the recognition complex. However, there is not enough evidence to completely rule out a function of dIno80 upstream of recognition. There are at least three factors with known functions in the process of DSB formation in *Drosophila* oocytes. Two of these proteins had been extensively studied and have a role in the initiation of meiotic DSB: MEI-W68 and MEI-P22 (McKim, Green-Marroquin et al. 1998; McKim and Hayashi-Hagihara 1998; Liu, Jang et al. 2002; Bhagat, Manheim et al. 2004; Mehrotra and McKim 2006). A more recent study has shown that Trade Embargo (Trem), a C2H2 zinc finger protein, promotes the formation of DSBs possibly by regulating Mei-P22 localization foci on

meiotic chromosomes (Lake, Nielsen et al. 2011). None of these 3 proteins were found in the dIno80 mass spectrometry data, but this could easily be explained by the unique role of these proteins during meiotic recombination. The following may aid in the understanding of dIno80 in the recognition of DSBs

1. Work by Liu *et al* and Mehrotra *et al* showed localization of MEI-P22 to early pachytene with an anti-HA antibody when a fly line containing an HA epitope-tagged transgene of MEI-P22 *(P{hsp83:mei-P22^{3XHA}}9)* was used (due to the inability to create MEI-P22 antibodies) (Liu, Jang et al. 2002; Mehrotra and McKim 2006) By creating *dIno80^{Mi}; (P{hsp83:mei-P22^{3XHA}}9)* flies, one could attempt to determine if wild type distribution of MEI-P22 is altered in *dIno80* mutants. Trem localization during oogenesis had been previously shown (Lake, Nielsen et al. 2011), thus the defects in Trem localization in *dIno80^{Mi}* mutants may also be determined.

2. Interaction of dIno80 with any or all these three proteins can be studied by using a yeast two-hybrid assay, as explained above.

3. Expression patterns of genes required for initiation of meiotic recombination as well as genes required for embryo polarity and cell cycle checkpoint activation can be studied in wild type and *dIno80^{Mi}* females. One way this could be done is by RNA-seq (RNA Sequencing), also called "Whole Transcriptome Shotgun Sequencing", a technique that can be used to quantify the changing expression levels of each transcript genome-wide. Since dINO80 is involved in transcription of some genes, this assay could aid in understanding if dINO80 is affecting the expression of genes require for initiation of meiotic recombination. Thus, RNA-seq together with the

studies mention above could help determining the role of dIno80 in the initiation of meiotic recombination and activation of the meiotic cell cycle checkpoints.

The role of dIno80 in remodeling chromatin around the DSB

My studies in *Drosophila* female meiosis showed that dIno80 is involved in the recognition of most meiotic DSBs. The ATPase domain in dIno80 seems to play an important role in the recruitment of recognition factors, possibly due to its function in sliding or removing nucleosomes –which will help clear up chromatin and allow the proper loading of recognition factors to the DSB. Biochemical assays could aid in demonstrating the role of Ino80 in chromatin remodeling around the break and further understanding the mechanism of Ino80 recruitment to the break. One could attempt to determine if dIno80 is localized at DSBs in *Drosophila* cell lines and if knockdown of dMre11 affects the biding of dIno80 and vice versa. It will be important to demonstrate if chromatin remodeling at the DSB is affected in dIno80 or dMre11 deficient cells. Binding of dIno80 to a DSB in wild type and dIno80 deficient cells can be determined by chromatin Immunoprecipitation (ChIP) assays. ChIP is used to investigate the interaction between proteins and DNA at specific genomic regions. As such, ChIP assays can be used to determine if lost of histones around the break is affected in dIno80 and dMre11 deficient cells. The nucleosome consists of ~147 bp of DNA wrapped around a protein octamer of histones H2A, H2B, H3 and H4. To determine if nucleosome stability is defective at the DSB, ChIP

can be done in cells expressing Flag–H2B or Flag–H3 as previously done by Tsukuda et al (Tsukuda, Fleming et al. 2005).

Due to the different cell populations in the *Drosophila* ovary and the difficulty of introducing a DSB of known location, a *Drosophila* cellular assay for homologous recombinational repair could be developed. In order to generate a cell line that can serve our purpose, an HR reporter could be generated in *Drosophila* cell lines as done for human cells and yeast where a single break can be introduced. The I-SceI site-specific DSB system has being incorporated in *Drosophila* (Rong and Golic 2003) (Wei and Rong 2007). Studies by Rong *et al* show that sites cut by I-SceI can be repaired by several of mechanisms, which include SSA, GC, and imprecise NHEJ (Rong and Golic 2003). As previously mentioned, mammalian Ino80 has been shown to be important for DNA repair, localizes at a DSB and has roles in HR. Thus, if cell lines expressing a suitable functional reported assay cannot be generated in *Drosophila* cells, one could use mammalian reporter assays. Some studies in mouse cells described the use of a reporter-based functional assay in which the Neo gene can only be expressed upon repair of DSBs produced by the endonuclease I-SceI. Another very elegant assay publish by Gospodinov *et al* using human cell lines U20S with a construct expressing the AsiSI restrictase-estrogen receptor fusion (AsiSI-ER) may be suitable to determine chromatin remodeling in Ino80 mutants. (Gospodinov, Vaissiere et al. 2011).

Role of dIno80 in the meiotic checkpoint

It will be important to understand the reason why dIno80 deficient females lay eggs with such penetrant dorso-ventral patterning defects and why this phenotype was not suppress in the *dIno80; mei-W68* double mutant. Was suppression not observed because dIno80 does not have a role in the actual repair of meiotic DSBs, or are these defects caused by other than the activation of the meiotic checkpoint? It is believed that the persistence of DSBs activates the *Drosophila* checkpoint protein 2 (dChk2) (Ghabrial and Schupbach 1999; Abdu, Brodsky et al. 2002). This activation causes modification of Vasa (Vas), a factor required for translation of *Gurken* (Ghabrial and Schupbach 1999). As previously mentioned, Gurken is required during oogenesis to establish the DV axis of the future embryo and low levels of Gurken causes egg shell phenotypes (Ghabrial and Schupbach 1999). Since dINO80 could potentially affect any of these factors, it would be important to determine the level of these proteins in $dIno80^{MI}$ mutants. Levels of these proteins can be assayed by western blotting or Immunohistochemistry –since there are available antibodies against dCHk2, Vasa and Gurken (Abdu, Brodsky et al. 2002). For example, if dIno80 mutants have normal levels of Gurken, this would be an indication that dIno80 affects egg polarity by other than the activation of the meiotic cell cycle checkpoint

Considering the roles of dIno80 in recognition, and the fact that events and factors involved in cell cycle progression are not completely understood, it is possible that *mei-W68* could not suppress the eggshell phenotypes as efficiently as a mutant with a more direct involvement in the cell cycle checkpoint. Studies by Abdu

et al show that in *dChk2; spn-B* double mutants, the dorso-ventral egg shell phenotypes of *spn-B* are suppressed (Abdu, Brodsky et al. 2002). Furthermore, it was suggested that dChk2 is the main transducer protein in the meiotic checkpoint (Abdu, Brodsky et al. 2002). Since *dChK2* is a gene involve directly in the cell cycle checkpoint, *dIno80*^{Mi}; *dChk2* double mutants may shed some light in dIno80 function in the activation of the meiotic cell cycle checkpoint.

VI. REFERENCES

Abdu, U., M. Brodsky, et al. (2002). "Activation of a meiotic checkpoint during Drosophila oogenesis regulates the translation of Gurken through Chk2/Mnk." Current biology : CB **12**(19): 1645-1651.

Abdu, U., A. Gonzalez-Reyes, et al. (2003). "The Drosophila spn-D gene encodes a RAD51C-like protein that is required exclusively during meiosis." Genetics **165**(1): 197-204.

Acilan, C., D. M. Potter, et al. (2007). "DNA repair pathways involved in anaphase bridge formation." Genes Chromosomes Cancer **46**(6): 522-531.

Alexiadis, V. and J. T. Kadonaga (2002). "Strand pairing by Rad54 and Rad51 is enhanced by chromatin." Genes Dev **16**(21): 2767-2771.

Allers, T. and M. Lichten (2001). "Differential timing and control of noncrossover and crossover recombination during meiosis." Cell **106**(1): 47-57.

Altaf, M., A. Auger, et al. (2010). "NuA4-dependent acetylation of nucleosomal histones H4 and H2A directly stimulates incorporation of H2A.Z by the SWR1 complex." J Biol Chem **285**(21): 15966-15977.

Anderson, L. K., H. H. Offenberg, et al. (1997). "RecA-like proteins are components of early meiotic nodules in lily." Proc Natl Acad Sci U S A **94**(13): 6868-6873.

Anderson, L. K., A. Reeves, et al. (1999). "Distribution of crossing over on mouse synaptonemal complexes using immunofluorescent localization of MLH1 protein." Genetics **151**(4): 1569-1579.

Anderson, L. K. and S. M. Stack (2005). "Recombination nodules in plants." Cytogenet Genome Res **109**(1-3): 198-204.

Arnaudeau, C., C. Lundin, et al. (2001). "DNA double-strand breaks associated with replication forks are predominantly repaired by homologous recombination

involving an exchange mechanism in mammalian cells." J Mol Biol **307**(5): 1235-1245.
Ashburner, M. (1989). Drosophila: A laboratory manual, Cold Spring Harbor Laboratory.
Baker, S. M., C. E. Bronner, et al. (1995). "Male mice defective in the DNA mismatch repair gene PMS2 exhibit abnormal chromosome synapsis in meiosis." Cell **82**(2): 309-319.
Baker, S. M., A. W. Plug, et al. (1996). "Involvement of mouse Mlh1 in DNA mismatch repair and meiotic crossing over." Nat Genet **13**(3): 336-342.
Bakkenist, C. J. and M. B. Kastan (2003). "DNA damage activates ATM through intermolecular autophosphorylation and dimer dissociation." Nature **421**(6922): 499-506.
Bannister, A. J. and T. Kouzarides (2011). "Regulation of chromatin by histone modifications." Cell Research **21**(3): 381-395.
Bao, Y. and X. Shen (2007). "INO80 subfamily of chromatin remodeling complexes." Mutat Res **618**(1-2): 18-29.
Barbosa, V., N. Kimm, et al. (2007). "A maternal screen for genes regulating Drosophila oocyte polarity uncovers new steps in meiotic progression." Genetics. **176**(4): 1967-1977. Epub 2007 May 1916.
Bassing, C. H., K. F. Chua, et al. (2002). "Increased ionizing radiation sensitivity and genomic instability in the absence of histone H2AX." Proc Natl Acad Sci U S A **99**(12): 8173-8178.
Baumann, P., F. E. Benson, et al. (1996). "Human Rad51 protein promotes ATP-dependent homologous pairing and strand transfer reactions in vitro." Cell **87**(4): 757-766.
Bekker-Jensen, S., C. Lukas, et al. (2006). "Spatial organization of the mammalian genome surveillance machinery in response to DNA strand breaks." Journal of Cell Biology **173**(2): 195-206.
Bender, C. F., M. L. Sikes, et al. (2002). "Cancer predisposition and hematopoietic failure in Rad50(S/S) mice." Genes Dev **16**(17): 2237-2251.
Bennett, G., M. Papamichos-Chronakis, et al. (2013). "DNA repair choice defines a common pathway for recruitment of chromatin regulators." Nat Commun **4**: 2084.
Bensimon, A., R. Aebersold, et al. (2011). "Beyond ATM: the protein kinase landscape of the DNA damage response." FEBS Lett **585**(11): 1625-1639.
Berkovich, E., R. J. Monnat, Jr., et al. (2007). "Roles of ATM and NBS1 in chromatin structure modulation and DNA double-strand break repair." Nat Cell Biol **9**(6): 683-690.
Bhagat, R., E. A. Manheim, et al. (2004). "Studies on crossover-specific mutants and the distribution of crossing over in Drosophila females." Cytogenet Genome Res. **107**(3-4): 160-171.
Bi, X., M. Gong, et al. (2005). "Drosophila ATM and Mre11 are essential for the G2/M checkpoint induced by low-dose irradiation." Genetics **171**(2): 845-847.
Bleuyard, J.-Y., M. E. Gallego, et al. (2005). "Differing requirements for the Arabidopsis Rad51 paralogs in meiosis and DNA repair." The Plant journal : for cell and molecular biology **41**(4): 533-545.

Boddy, M. N., P. H. Gaillard, et al. (2001). "Mus81-Eme1 are essential components of a Holliday junction resolvase." Cell **107**(4): 537-548.

Boe, S. O., M. Haave, et al. (2006). "Promyelocytic leukemia nuclear bodies are predetermined processing sites for damaged DNA." Journal of Cell Science **119**(16): 3284-3295.

Borde, V. and J. Cobb (2009). "Double functions for the Mre11 complex during DNA double-strand break repair and replication." Int J Biochem Cell Biol **41**(6): 1249-1253.

Borde, V., W. Lin, et al. (2004). "Association of Mre11p with double-strand break sites during yeast meiosis." Mol Cell **13**(3): 389-401.

Borde, V., N. Robine, et al. (2009). "Histone H3 lysine 4 trimethylation marks meiotic recombination initiation sites." EMBO J **28**(2): 99-111.

Botuyan, M. V., J. Lee, et al. (2006). "Structural basis for the methylation state-specific recognition of histone H4-K20 by 53BP1 and Crb2 in DNA repair." Cell **127**(7): 1361-1373.

Boyd, J. B., M. D. Golino, et al. (1981). "Third-chromosome mutagen-sensitive mutants of Drosophila melanogaster." Genetics. **97**(3-4): 607-623.

Brand, A. H. and N. Perrimon (1993). "Targeted gene expression as a means of altering cell fates and generating dominant phenotypes." Development (Cambridge, England) **118**(2): 401-415.

Brenneman, M. A., B. M. Wagener, et al. (2002). "XRCC3 controls the fidelity of homologous recombination: roles for XRCC3 in late stages of recombination." Mol Cell **10**(2): 387-395.

Buard, J., P. Barthes, et al. (2009). "Distinct histone modifications define initiation and repair of meiotic recombination in the mouse." EMBO J **28**(17): 2616-2624.

Buermeyer, A. B., S. M. Deschenes, et al. (1999). "Mammalian DNA mismatch repair." Annu Rev Genet **33**: 533-564.

Burke, B. and C. L. Stewart (2013). "The nuclear lamins: flexibility in function." Nat Rev Mol Cell Biol **14**(1): 13-24.

Burma, S., B. P. Chen, et al. (2001). "ATM phosphorylates histone H2AX in response to DNA double-strand breaks." J Biol Chem **276**(45): 42462-42467.

Cai, Y., J. Jin, et al. (2005). "The mammalian YL1 protein is a shared subunit of the TRRAP/TIP60 histone acetyltransferase and SRCAP complexes." J Biol Chem. **280**(14): 13665-13670. Epub 12005 Jan 13611.

Cai, Y., J. Jin, et al. (2007). "YY1 functions with INO80 to activate transcription." Nature structural & molecular biology **14**(9): 872-874.

Carpenter, A. T. (1975). "Electron microscopy of meiosis in Drosophila melanogaster females: II. The recombination nodule--a recombination-associated structure at pachytene?" Proc Natl Acad Sci U S A **72**(8): 3186-3189.

Carpenter, A. T. (1979). "Recombination nodules and synaptonemal complex in recombination-defective females of Drosophila melanogaster." Chromosoma **75**(3): 259-292.

Carpenter, A. T. (1979). "Synaptonemal complex and recombination nodules in wild-type Drosophila melanogaster females." Genetics **92**(2): 511-541.

Carpenter, A. T. (1982). "Mismatch repair, gene conversion, and crossing-over in two recombination-defective mutants of Drosophila melanogaster." Proc Natl Acad Sci U S A **79**(19): 5961-5965.

Carpenter, A. T. (1994). "Egalitarian and the choice of cell fates in Drosophila melanogaster oogenesis." Ciba Found Symp. **182**: 223-246; discussion 246-254.

Carpenter, A. T. (2003). "Normal synaptonemal complex and abnormal recombination nodules in two alleles of the Drosophila meiotic mutant mei-W68." Genetics. **163**(4): 1337-1356.

Carson, C. T., R. A. Schwartz, et al. (2003). "The Mre11 complex is required for ATM activation and the G2/M checkpoint." Embo J **22**(24): 6610-6620.

Cejka, P., E. Cannavo, et al. (2010). "DNA end resection by Dna2-Sgs1-RPA and its stimulation by Top3-Rmi1 and Mre11-Rad50-Xrs2." Nature **467**(7311): 112-U149.

Celeste, A., O. Fernandez-Capetillo, et al. (2003). "Histone H2AX phosphorylation is dispensable for the initial recognition of DNA breaks." Nat Cell Biol **5**(7): 675-679.

Celeste, A., S. Petersen, et al. (2002). "Genomic instability in mice lacking histone H2AX." Science **296**(5569): 922-927.

Chen, C. C., J. J. Carson, et al. (2008). "Acetylated lysine 56 on histone H3 drives chromatin assembly after repair and signals for the completion of repair." Cell **134**(2): 231-243.

Chen, C. C., J. J. Carson, et al. (2008). "Acetylated lysine 56 on histone H3 drives chromatin assembly after repair and signals for the completion of repair." Cell **134**(2): 231-243.

Chen, J. M., D. N. Cooper, et al. (2007). "Gene conversion: mechanisms, evolution and human disease." Nature Reviews Genetics **8**(10): 762-775.

.

Cheok, C. F., C. Z. Bachrati, et al. (2005). "Roles of the Bloom's syndrome helicase in the maintenance of genome stability." Biochem Soc Trans **33**(Pt 6): 1456-1459.

Chiolo, I., A. Minoda, et al. (2011). "Double-strand breaks in heterochromatin move outside of a dynamic HP1a domain to complete recombinational repair." Cell **144**(5): 732-744.

Chu, W. K. and I. D. Hickson (2009). "RecQ helicases: multifunctional genome caretakers." Nature reviews Cancer **9**(9): 644-654.

Ciapponi, L., G. Cenci, et al. (2004). "The Drosophila Mre11/Rad50 complex is required to prevent both telomeric fusion and chromosome breakage." Current biology : CB **14**(15): 1360-1366.

Ciapponi, L., G. Cenci, et al. (2006). "The Drosophila Nbs protein functions in multiple pathways for the maintenance of genome stability." Genetics **173**(3): 1447-1454.

Ciccia, A. and S. J. Elledge (2010). "The DNA damage response: making it safe to play with knives." Mol Cell **40**(2): 179-204.

Clapier, C. R. and B. R. Cairns (2009). "The Biology of Chromatin Remodeling Complexes." Annual Review of Biochemistry **78**: 273-304.

Clarkson, M. J., J. R. Wells, et al. (1999). "Regions of variant histone His2AvD required for Drosophila development." Nature **399**(6737): 694-697.

Conaway, R. C. and J. W. Conaway (2009). "The INO80 chromatin remodeling complex in transcription, replication and repair." Trends in Biochemical Sciences **34**(2): 71-77.

Costanzo, V., K. Robertson, et al. (2001). "Mre11 protein complex prevents double-strand break accumulation during chromosomal DNA replication." Mol Cell **8**(1): 137-147.

Da Ines, O., F. Degroote, et al. (2013). "Effects of XRCC2 and RAD51B mutations on somatic and meiotic recombination in Arabidopsis thaliana." Plant Journal **74**(6): 959-970.

Das, C., M. S. Lucia, et al. (2009). "CBP/p300-mediated acetylation of histone H3 on lysine 56." Nature **459**(7243): 113-U123.

de Jager, M., J. van Noort, et al. (2001). "Human Rad50/Mre11 is a flexible complex that can tether DNA ends." Mol Cell **8**(5): 1129-1135.

Dellaire, G., R. W. Ching, et al. (2006). "Promyelocytic leukemia nuclear bodies behave as DNA damage sensors whose response to DNA double-strand breaks is regulated by NBS1 and the kinases ATM, Chk2, and ATR." Journal of Cell Biology **175**(1): 55-66.

Downs, J. A., S. Allard, et al. (2004). "Binding of chromatin-modifying activities to phosphorylated histone H2A at DNA damage sites." Molecular Cell **16**(6): 979-990.

Downs, J. A., N. F. Lowndes, et al. (2000). "A role for Saccharomyces cerevisiae histone H2A in DNA repair." Nature **408**(6815): 1001-1004.

Dronamraju, R. and J. M. Mason (2009). "Recognition of double strand breaks by a mutator protein (MU2) in Drosophila melanogaster." PLoS Genet **5**(5): e1000473.

Eberharter, A. and P. B. Becker (2004). "ATP-dependent nucleosome remodelling: factors and functions." Journal of Cell Science **117**(17): 3707-3711.

Edelmann, W., P. E. Cohen, et al. (1996). "Meiotic pachytene arrest in MLH1-deficient mice." Cell **85**(7): 1125-1134.

EF, J., P. M, et al. (2011). "Drosophila ATM and ATR have distinct activities in the regulation of meiotic DNA." J Cell Biol **195**(3): 359-367.

Errico, A. and V. Costanzo (2010). "Differences in the DNA replication of unicellular eukaryotes and metazoans: known unknowns." EMBO Rep **11**(4): 270-278.

Falbo, K. B., C. Alabert, et al. (2009). "Involvement of a chromatin remodeling complex in damage tolerance during DNA replication." Nat Struct Mol Biol **16**(11): 1167-1172.

Fillingham, J., M. C. Keogh, et al. (2006). "GammaH2AX and its role in DNA double-strand break repair." Biochem Cell Biol **84**(4): 568-577.

Filson, A. J., A. Lewis, et al. (1985). "Monoclonal antibodies prepared against the major Drosophila nuclear Matrix-pore complex-lamina glycoprotein bind specifically to the nuclear envelope in situ." J Biol Chem. **260**(5): 3164-3172.

Flores, C. and W. Engels (1999). "Microsatellite instability in Drosophila spellchecker1 (MutS homolog) mutants." Proceedings of the National Academy of Sciences of the United States of America **96**(6): 2964-2969.

Franklin, F. C. H., J. D. Higgins, et al. (2006). "Control of meiotic recombination in Arabidopsis: role of the MutL and MutS homologues." Biochemical Society transactions **34**(Pt 4): 542-544.

Froelich-Ammon, S. J. and N. Osheroff (1995). "Topoisomerase poisons: harnessing the dark side of enzyme mechanism." J Biol Chem **270**(37): 21429-21432.

Furuse, M., Y. Nagase, et al. (1998). "Distinct roles of two separable in vitro activities of yeast Mre11 in mitotic and meiotic recombination." Embo Journal **17**(21): 6412-6425.

Game, J. C. and S. B. Chernikova (2009). "The role of RAD6 in recombinational repair, checkpoints and meiosis via histone modification." DNA Repair (Amst) **8**(4): 470-482.

Gao, G., X. Bi, et al. (2009). "Mre11-Rad50-Nbs complex is required to cap telomeres during Drosophila embryogenesis." Proceedings of the National Academy of Sciences of the United States of America **106**(26): 10728-10733.

Gartenberg, M. R. (2009). "Life on the edge: telomeres and persistent DNA breaks converge at the nuclear periphery." Genes & development **23**(9): 1027-1031.

Gartenberg, M. R., F. R. Neumann, et al. (2004). "Sir-mediated repression can occur independently of chromosomal and subnuclear contexts." Cell **119**(7): 955-967.

Ghabrial, A., R. P. Ray, et al. (1998). "okra and spindle-B encode components of the RAD52 DNA repair pathway and affect meiosis and patterning in Drosophila oogenesis." Genes Dev **12**(17): 2711-2723.

Ghabrial, A. and T. Schupbach (1999). "Activation of a meiotic checkpoint regulates translation of Gurken during Drosophila oogenesis." Nat Cell Biol. **1**(6): 354-357.

Girard, P. M., E. Riballo, et al. (2002). "Nbs1 promotes ATM dependent phosphorylation events including those required for G1/S arrest." Oncogene **21**(27): 4191-4199.

Goldberg, M., M. Stucki, et al. (2003). "MDC1 is required for the intra-S-phase DNA damage checkpoint." Nature **421**(6926): 952-956.

Goodarzi, A. A., W. D. Block, et al. (2003). "The role of ATM and ATR in DNA damage-induced cell cycle control." Prog Cell Cycle Res **5**: 393-411.

Gorski, M. M., R. J. Romeijn, et al. (2004). "Disruption of Drosophila Rad50 causes pupal lethality, the accumulation of DNA double-strand breaks and the induction of apoptosis in third instar larvae." DNA Repair (Amst) **3**(6): 603-615.

Gospodinov, A., T. Vaissiere, et al. (2011). "Mammalian Ino80 mediates double-strand break repair through its role in DNA end strand resection." Molecular and cellular biology **31**(23): 4735-4745.

Gravel, S., J. R. Chapman, et al. (2008). "DNA helicases Sgs1 and BLM promote DNA double-strand break resection." Genes Dev **22**(20): 2767-2772.

Greber, U. F., A. Senior, et al. (1990). "A major glycoprotein of the nuclear pore complex is a membrane-spanning polypeptide with a large lumenal domain and a small cytoplasmic tail." The EMBO journal **9**(5): 1495-1502.

Grey, C., P. Barthes, et al. (2011). "Mouse PRDM9 DNA-binding specificity determines sites of histone H3 lysine 4 trimethylation for initiation of meiotic recombination." PLoS Biol **9**(10): e1001176.

Haber, J. E. (2012). "Mating-type genes and MAT switching in Saccharomyces cerevisiae." Genetics. **191**(1): 33-64. doi: 10.1534/genetics.1111.134577.

Harvey, A. C., S. P. Jackson, et al. (2005). "Saccharomyces cerevisiae histone H2A Ser122 facilitates DNA repair." Genetics **170**(2): 543-553.

Hays, S. L., A. A. Firmenich, et al. (1995). "Complex formation in yeast double-strand break repair: participation of Rad51, Rad52, Rad55, and Rad57 proteins." Proc Natl Acad Sci U S A **92**(15): 6925-6929.

Hefferin, M. L. and A. E. Tomkinson (2005). "Mechanism of DNA double-strand break repair by non-homologous end joining." DNA Repair (Amst) **4**(6): 639-648.

Henikoff, S. and K. Ahmad (2005). "Assembly of variant histones into chromatin." Annual Review of Cell and Developmental Biology **21**: 133-153.

Heyer, W. D., X. Li, et al. (2006). "Rad54: the Swiss Army knife of homologous recombination?" Nucleic Acids Res **34**(15): 4115-4125.

Hiom, K. (2010). "Coping with DNA double strand breaks." DNA Repair (Amst) **9**(12): 1256-1263.

Holloman, W. K. (2011). "Unraveling the mechanism of BRCA2 in homologous recombination." Nature Structural & Molecular Biology **18**(7): 748-754.

Hong, A., K. Narbonne-Reveau, et al. (2007). "The cyclin-dependent kinase inhibitor Dacapo promotes replication licensing during Drosophila endocycles." Embo J. **26**(8): 2071-2082. Epub 2007 Mar 2022.

Hunter, N. (2007). Meiotic recombination

Molecular Genetics of Recombination. A. Aguilera and R. Rothstein, Springer Berlin / Heidelberg. **17:** 381-442.

Huynh, J. R. and D. St Johnston (2000). "The role of BicD, Egl, Orb and the microtubules in the restriction of meiosis to the Drosophila oocyte." Development **127**(13): 2785-2794.

Ikura, T., V. V. Ogryzko, et al. (2000). "Involvement of the TIP60 histone acetylase complex in DNA repair and apoptosis." Cell **102**(4): 463-473.

Ip, S. C., U. Rass, et al. (2008). "Identification of Holliday junction resolvases from humans and yeast." Nature **456**(7220): 357-361.

Jackson, S. P. and J. Bartek (2009). "The DNA-damage response in human biology and disease." Nature **461**(7267): 1071-1078.

James, P., J. Halladay, et al. (1996). "Genomic libraries and a host strain designed for highly efficient two-hybrid selection in yeast." Genetics **144**(4): 1425-1436.

Jang, J. K., D. E. Sherizen, et al. (2003). "Relationship of DNA double-strand breaks to synapsis in Drosophila." Journal of Cell Science **116**(Pt 15): 3069-3077.

Jin, J., Y. Cai, et al. (2005). "In and out: histone variant exchange in chromatin." Trends Biochem Sci **30**(12): 680-687.

Jin, J., Y. Cai, et al. (2005). "A mammalian chromatin remodeling complex with similarities to the yeast INO80 complex." J Biol Chem **280**(50): 41207-41212.

Johnson, R. D. and L. S. Symington (1995). "Functional differences and interactions among the putative RecA homologs Rad51, Rad55, and Rad57." Mol Cell Biol **15**(9): 4843-4850.

Jonsson, Z. O., S. Jha, et al. (2004). "Rvb1p/Rvb2p recruit Arp5p and assemble a functional Ino80 chromatin remodeling complex." Mol Cell **16**(3): 465-477.

Joyce, E. F., M. Pedersen, et al. (2011). "Drosophila ATM and ATR have distinct activities in the regulation of meiotic DNA damage and repair." Journal of Cell Biology **195**(3): 359-367.

Joyce, E. F., S. N. Tanneti, et al. (2009). "Drosophila Hold'em Is Required for a Subset of Meiotic Crossovers and Interacts With the DNA Repair Endonuclease Complex Subunits MEI-9 and ERCC1." Genetics **181**(1): 335-340.

Kalocsay, M., N. J. Hiller, et al. (2009). "Chromosome-wide Rad51 Spreading and SUMO-H2A.Z-Dependent Chromosome Fixation in Response to a Persistent DNA Double-Strand Break." Molecular Cell **33**(3): 335-343.

Kashiwaba, S., K. Kitahashi, et al. (2010). "The mammalian INO80 complex is recruited to DNA damage sites in an ARP8 dependent manner." Biochem Biophys Res Commun **402**(4): 619-625.

Keeney, S., C. N. Giroux, et al. (1997). "Meiosis-specific DNA double-strand breaks are catalyzed by Spo11, a member of a widely conserved protein family." Cell **88**(3): 375-384.

Keeney, S. and N. Kleckner (1995). "Covalent protein-DNA complexes at the 5' strand termini of meiosis-specific double-strand breaks in yeast." Proc Natl Acad Sci U S A **92**(24): 11274-11278.

Khanna, K. K. and S. P. Jackson (2001). "DNA double-strand breaks: signaling, repair and the cancer connection." Nat Genet **27**(3): 247-254.

Kim, J. E., K. Minter-Dykhouse, et al. (2006). "Signaling networks controlled by the MRN complex and MDC1 during early DNA damage responses." Mol Carcinog **45**(6): 403-408.

Klovstad, M., U. Abdu, et al. (2005). "Drosophila brca2 is Required for Mitotic and Meiotic DNA Repair and Efficient Activation of the Meiotic Recombination Checkpoint." PLoS Genet **preprint**(2008): e31.

Klovstad, M., U. Abdu, et al. (2008). "Drosophila brca2 is required for mitotic and meiotic DNA repair and efficient activation of the meiotic recombination checkpoint." PLoS Genet **4**(2): e31.

Klymenko, T., B. Papp, et al. (2006). "A Polycomb group protein complex with sequence-specific DNA-binding and selective methyl-lysine-binding activities." Genes Dev **20**(9): 1110-1122.

Kobor, M. S., S. Venkatasubrahmanyam, et al. (2004). "A protein complex containing the conserved Swi2/Snf2-related ATPase Swr1p deposits histone variant H2A.Z into euchromatin." Plos Biology **2**(5): 587-599.

Kohl, K. P., C. D. Jones, et al. (2012). "Evolution of an MCM complex in flies that promotes meiotic crossovers by blocking BLM helicase." Science (New York, N Y) **338**(6112): 1363-1365.

Kotova, E., N. Lodhi, et al. (2011). "Drosophila histone H2A variant (H2Av) controls poly(ADP-ribose) polymerase 1 (PARP1) activation in chromatin." Proc Natl Acad Sci U S A **108**(15): 6205-6210.

Kracklauer, M. P., H. M. Wiora, et al. (2010). "The Drosophila SUN protein Spag4 cooperates with the coiled-coil protein Yuri Gagarin to maintain association of the basal body and spermatid nucleus." J Cell Sci. **123**(Pt 16): 2763-2772. doi: 2710.1242/jcs.066589. Epub 062010 Jul 066520.

Kusano, K., D. M. Johnson-Schlitz, et al. (2001). "Sterility of Drosophila with mutations in the Bloom syndrome gene--complementation by Ku70." Science **291**(5513): 2600-2602.

Kusch, T., L. Florens, et al. (2004). "Acetylation by Tip60 is required for selective histone variant exchange at DNA lesions." Science **306**(5704): 2084-2087.

Kuznetsov, S., M. Pellegrini, et al. (2007). "RAD51C deficiency in mice results in early prophase I arrest in males and sister chromatid separation at metaphase II in females." The Journal of cell biology **176**(5): 581-592.

Lake, C. M., J. K. Holsclaw, et al. (2013). "The development of a monoclonal antibody recognizing the Drosophila melanogaster phosphorylated histone H2A variant (gamma-H2AV)." G3 (Bethesda) **3**(9): 1539-1543.

Lake, C. M., R. J. Nielsen, et al. (2011). "The Drosophila zinc finger protein trade embargo is required for double strand break formation in meiosis." PLoS genetics **7**(2): e1002005.

Lallemand-Breitenbach, V. and H. de The (2010). "PML Nuclear Bodies." Cold Spring Harbor Perspectives in Biology **2**(5).

Lamarche, B. J., N. I. Orazio, et al. (2010). "The MRN complex in double-strand break repair and telomere maintenance." FEBS Lett **584**(17): 3682-3695.

Lamb, N. E., S. L. Sherman, et al. (2005). "Effect of meiotic recombination on the production of aneuploid gametes in humans." Cytogenet Genome Res **111**(3-4): 250-255.

Lange, J., J. Pan, et al. (2011). "ATM controls meiotic double-strand-break formation." Nature **479**(7372): 237-240.

Lantz, V., J. S. Chang, et al. (1994). "The Drosophila orb RNA-binding protein is required for the formation of the egg chamber and establishment of polarity." Genes & development **8**(5): 598-613.

LaRocque, J. R., B. Jaklevic, et al. (2007). "Drosophila ATR in double-strand break repair." Genetics **175**(3): 1023-1033.

Laurencon, A., A. Purdy, et al. (2003). "Phenotypic analysis of separation-of-function alleles of MEI-41, Drosophila ATM/ATR." Genetics **164**(2): 589-601.

Lee, J. H. and T. T. Paull (2005). "ATM activation by DNA double-strand breaks through the Mre11-Rad50-Nbs1 complex." Science **308**(5721): 551-554.

Lee, J. H. and T. T. Paull (2007). "Activation and regulation of ATM kinase activity in response to DNA double-strand breaks." Oncogene **26**(56): 7741-7748.

Lilly, M. A. and A. C. Spradling (1996). "The Drosophila endocycle is controlled by Cyclin E and lacks a checkpoint ensuring S-phase completion." Genes Dev. **10**(19): 2514-2526.

Lisby, M., U. H. Mortensen, et al. (2003). "Colocalization of multiple DNA double-strand breaks at a single Rad52 repair centre." Nat Cell Biol **5**(6): 572-577.

Lisby, M. and R. Rothstein (2004). "DNA damage checkpoint and repair centers." Current Opinion in Cell Biology **16**(3): 328-334.

Liu, H., J. K. Jang, et al. (2000). "Two genes required for meiotic recombination in Drosophila are expressed from a dicistronic message." Genetics **154**(4): 1735-1746.

Liu, H., J. K. Jang, et al. (2002). "mei-P22 encodes a chromosome-associated protein required for the initiation of meiotic recombination in Drosophila melanogaster." Genetics. **162**(1): 245-258.

Lohmiller, L. D., A. De Muyt, et al. (2008). "Cytological analysis of MRE11 protein during early meiotic prophase I in Arabidopsis and tomato." Chromosoma. **117**(3): 277-288. doi: 210.1007/s00412-00007-00147-z. Epub 02008 Feb 00422.

Lou, Z., K. Minter-Dykhouse, et al. (2006). "MDC1 maintains genomic stability by participating in the amplification of ATM-dependent DNA damage signals." Mol Cell **21**(2): 187-200.

Luo, G., M. S. Yao, et al. (1999). "Disruption of mRad50 causes embryonic stem cell lethality, abnormal embryonic development, and sensitivity to ionizing radiation." Proc Natl Acad Sci U S A **96**(13): 7376-7381.

Madigan, J. P., H. L. Chotkowski, et al. (2002). "DNA double-strand break-induced phosphorylation of Drosophila histone variant H2Av helps prevent radiation-induced apoptosis." Nucleic Acids Res **30**(17): 3698-3705.

Marechal, A. and L. Zou (2013). "DNA damage sensing by the ATM and ATR kinases." Cold Spring Harbor perspectives in biology **5**(9).

Margueron, R. and D. Reinberg (2010). "Chromatin structure and the inheritance of epigenetic information." Nat Rev Genet **11**(4): 285-296.

Mazin, A. V., A. A. Alexeev, et al. (2003). "A novel function of Rad54 protein. Stabilization of the Rad51 nucleoprotein filament." J Biol Chem **278**(16): 14029-14036.

McCaffrey, R., D. St Johnston, et al. (2006). "Drosophila mus301/spindle-C encodes a helicase with an essential role in double-strand DNA break repair and meiotic progression." Genetics **174**(3): 1273-1285.

McKim, K. S., J. B. Dahmus, et al. (1996). "Cloning of the Drosophila melanogaster meiotic recombination gene mei-218: a genetic and molecular analysis of interval 15E." Genetics. **144**(1): 215-228.

McKim, K. S., B. L. Green-Marroquin, et al. (1998). "Meiotic synapsis in the absence of recombination." Science. **279**(5352): 876-878.

McKim, K. S. and A. Hayashi-Hagihara (1998). "mei-W68 in Drosophila melanogaster encodes a Spo11 homolog: evidence that the mechanism for initiating meiotic recombination is conserved." Genes & Development **12**(18): 2932-2942.

McKim, K. S., J. K. Jang, et al. (2002). "Meiotic recombination and chromosome segregation in Drosophila females." Annu Rev Genet **36**: 205-232.

McKim, K. S., J. K. Jang, et al. (2000). "mei-41 is required for precocious anaphase in Drosophila females." Chromosoma **109**(1-2): 44-49.

McKim, K. S., E. F. Joyce, et al. (2009). "Cytological analysis of meiosis in fixed Drosophila ovaries." Methods in molecular biology (Clifton, N J) **558**: 197-216.

Mehrotra, S. and K. S. McKim (2006). "Temporal analysis of meiotic DNA double-strand break formation and repair in Drosophila females." PLoS Genet **2**(11): e200.

Metaxakis, A., S. Oehler, et al. (2005). "Minos as a genetic and genomic tool in Drosophila melanogaster." Genetics **171**(2): 571-581.

Miller, D. E., S. Takeo, et al. (2012). "A Whole-Chromosome Analysis of Meiotic Recombination in Drosophila melanogaster." G3 (Bethesda) **2**(2): 249-260.

Miller, J. and I. Stagljar (2004). "Using the yeast two-hybrid system to identify interacting proteins." Methods Mol Biol. **261**: 247-262.

Mimitou, E. P. and L. S. Symington (2008). "Sae2, Exo1 and Sgs1 collaborate in DNA double-strand break processing." Nature **455**(7214): 770-774.

Mimitou, E. P. and L. S. Symington (2009). "Nucleases and helicases take center stage in homologous recombination." Trends Biochem Sci **34**(5): 264-272.

Mimitou, E. P. and L. S. Symington (2011). "DNA end resection-Unraveling the tail." DNA Repair (Amst) **10**(3): 344-348.

Mirzoeva, O. K. and J. H. Petrini (2001). "DNA damage-dependent nuclear dynamics of the Mre11 complex." Mol Cell Biol **21**(1): 281-288.

Mizuguchi, G., X. Shen, et al. (2004). "ATP-driven exchange of histone H2AZ variant catalyzed by SWR1 chromatin remodeling complex." Science **303**(5656): 343-348.

Mladenov, E. and G. Iliakis (2011). "Induction and repair of DNA double strand breaks: the increasing spectrum of non-homologous end joining pathways." Mutat Res **711**(1-2): 61-72.

Moore, J. D., O. Yazgan, et al. (2007). "Diverse roles for histone H2A modifications in DNA damage response pathways in yeast." Genetics **176**(1): 15-25.

Moreau, S., J. R. Ferguson, et al. (1999). "The nuclease activity of Mre11 is required for meiosis but not for mating type switching, end joining, or telomere maintenance." Mol Cell Biol **19**(1): 556-566.

Morris, J. and R. Lehmann (1999). "Drosophila oogenesis: versatile spn doctors." Current biology : CB **9**(2): R55-58.

Morrison, A. J., J. Highland, et al. (2004). "INO80 and gamma-H2AX interaction links ATP-dependent chromatin remodeling to DNA damage repair." Cell **119**(6): 767-775.

Morrison, A. J. and X. Shen (2006). "Chromatin modifications in DNA repair." Results Probl Cell Differ **41**: 109-125.

Moynahan, M. E., A. J. Pierce, et al. (2001). "BRCA2 is required for homology-directed repair of chromosomal breaks." Mol Cell **7**(2): 263-272.

Nagai, S., K. Dubrana, et al. (2008). "Functional targeting of DNA damage to a nuclear pore-associated SUMO-dependent ubiquitin ligase." Science **322**(5901): 597-602.

Nakamura, A. J., V. A. Rao, et al. (2010). "The complexity of phosphorylated H2AX foci formation and DNA repair assembly at DNA double-strand breaks." Cell cycle (Georgetown, Tex) **9**(2): 389-397.

Nam, E. A. and D. Cortez (2011). "ATR signalling: more than meeting at the fork." Biochem J **436**(3): 527-536.

Neale, M. J., J. Pan, et al. (2005). "Endonucleolytic processing of covalent protein-linked DNA double-strand breaks." Nature **436**(7053): 1053-1057.
Neufeld, T. P., A. F. de la Cruz, et al. (1998). "Coordination of growth and cell division in the Drosophila wing." Cell **93**(7): 1183-1193.
Neumann, F. R., V. Dion, et al. (2012). "Targeted INO80 enhances subnuclear chromatin movement and ectopic homologous recombination." Genes Dev **26**(4): 369-383.
Ni, J.-Q., R. Zhou, et al. (2011). "A genome-scale shRNA resource for transgenic RNAi in Drosophila." Nature methods **8**(5): 405-407.
Nicolette, M. L., K. Lee, et al. (2010). "Mre11-Rad50-Xrs2 and Sae2 promote 5' strand resection of DNA double-strand breaks." Nature Structural & Molecular Biology **17**(12): 1478-1485.
Niu, H. Y., W. H. Chung, et al. (2010). "Mechanism of the ATP-dependent DNA end-resection machinery from Saccharomyces cerevisiae." Nature **467**(7311): 108-U143.
O'Driscoll, M. and P. A. Jeggo (2006). "The role of double-strand break repair - insights from human genetics." Nat Rev Genet **7**(1): 45-54.
Oikemus, S. R., J. Queiroz-Machado, et al. (2006). "Epigenetic telomere protection by Drosophila DNA damage response pathways." PLoS Genet **2**(5): e71.
Osman, F., J. Dixon, et al. (2003). "Generating crossovers by resolution of nicked Holliday junctions: a role for Mus81-Eme1 in meiosis." Mol Cell **12**(3): 761-774.
Oza, P., S. L. Jaspersen, et al. (2009). "Mechanisms that regulate localization of a DNA double-strand break to the nuclear periphery." Genes Dev **23**(8): 912-927.
Page, S. L. and R. S. Hawley (2001). "c(3)G encodes a Drosophila synaptonemal complex protein." Genes Dev **15**(23): 3130-3143.
Papamichos-Chronakis, M., J. E. Krebs, et al. (2006). "Interplay between Ino80 and Swr1 chromatin remodeling enzymes regulates cell cycle checkpoint adaptation in response to DNA damage." Genes Dev **20**(17): 2437-2449.
Papamichos-Chronakis, M. and C. L. Peterson (2008). "The Ino80 chromatin-remodeling enzyme regulates replisome function and stability." Nature structural & molecular biology **15**(4): 338-345.
Papamichos-Chronakis, M., S. Watanabe, et al. (2011). "Global Regulation of H2A.Z Localization by the INO80 Chromatin-Remodeling Enzyme Is Essential for Genome Integrity." Cell **144**(2): 200-213.
Paull, T. T. (2010). "Making the best of the loose ends: Mre11/Rad50 complexes and Sae2 promote DNA double-strand break resection." DNA Repair (Amst) **9**(12): 1283-1291.
Paull, T. T. and M. Gellert (1998). "The 3' to 5' exonuclease activity of Mre 11 facilitates repair of DNA double-strand breaks." Mol Cell **1**(7): 969-979.
Paull, T. T. and J. H. Lee (2005). "The Mre11/Rad50/Nbs1 complex and its role as a DNA double-strand break sensor for ATM." Cell Cycle **4**(6): 737-740.
Paull, T. T., E. P. Rogakou, et al. (2000). "A critical role for histone H2AX in recruitment of repair factors to nuclear foci after DNA damage." Curr Biol **10**(15): 886-895.

Pawelczak, K. S. and J. J. Turchi (2010). "Purification and characterization of exonuclease-free Artemis: Implications for DNA-PK-dependent processing of DNA termini in NHEJ-catalyzed DSB repair." DNA Repair (Amst) **9**(6): 670-677.

Plug, A. W., A. H. F. M. Peters, et al. (1998). "Changes in protein composition of meiotic nodules during mammalian meiosis." J Cell Sci **111**: 413-423.

Polo, S. E. and S. P. Jackson (2011). "Dynamics of DNA damage response proteins at DNA breaks: a focus on protein modifications." Genes & development **25**(5): 409-433.

Price, B. D. and A. D. D'Andrea (2013). "Chromatin remodeling at DNA double-strand breaks." Cell. **152**(6): 1344-1354. doi: 1310.1016/j.cell.2013.1302.1011.

Przewloka, M. R., W. Zhang, et al. (2007). "Molecular analysis of core kinetochore composition and assembly in Drosophila melanogaster." PLoS One **2**(5): e478.

Queiroz-Machado, J., J. Perdigao, et al. (2001). "tef: a mutation that causes telomere fusion and severe genome rearrangements in Drosophila melanogaster." Chromosoma **110**(1): 10-23.

Radford, S. J., E. Goley, et al. (2005). "Drosophila ERCC1 is required for a subset of MEI-9-dependent meiotic crossovers." Genetics. **170**(4): 1737-1745. Epub 2005 Jun 1738.

Raisner, R. M., P. D. Hartley, et al. "Histone Variant H2A.Z Marks the 5′ Ends of Both Active and Inactive Genes in Euchromatin." Cell. 2005 Oct 21;123(2):233-48.

Raynard, S., H. Niu, et al. (2008). "DNA double-strand break processing: the beginning of the end." Genes & development **22**(21): 2903-2907.

Razafsky, D. and D. Hodzic (2009). "Bringing KASH under the SUN: the many faces of nucleo-cytoskeletal connections." J Cell Biol. **186**(4): 461-472. doi: 410.1083/jcb.200906068. Epub 200902009 Aug 200906017.

Redon, C., D. Pilch, et al. (2002). "Histone H2A variants H2AX and H2AZ." Current Opinion in Genetics & Development **12**(2): 162-169.

Richardson, C. and M. Jasin (2000). "Frequent chromosomal translocations induced by DNA double-strand breaks." Nature **405**(6787): 697-700.

Riechmann, V. and A. Ephrussi (2001). "Axis formation during Drosophila oogenesis." Curr Opin Genet Dev **11**(4): 374-383.

Riemer, D., N. Stuurman, et al. (1995). "Expression of Drosophila lamin C is developmentally regulated: analogies with vertebrate A-type lamins." J Cell Sci. **108**(Pt 10): 3189-3198.

Robzyk, K., J. Recht, et al. (2000). "Rad6-dependent ubiquitination of histone H2B in yeast." Science **287**(5452): 501-504.

Rogakou, E. P., C. Boon, et al. (1999). "Megabase chromatin domains involved in DNA double-strand breaks in vivo." J Cell Biol **146**(5): 905-916.

Rogakou, E. P., D. R. Pilch, et al. (1998). "DNA double-stranded breaks induce histone H2AX phosphorylation on serine 139." J Biol Chem **273**(10): 5858-5868.

Rong, Y. S. and K. G. Golic (2003). "The homologous chromosome is an effective template for the repair of mitotic DNA double-strand breaks in Drosophila." Genetics. **165**(4): 1831-1842.

Rorth, P. (1998). "Gal4 in the Drosophila female germline." Mechanisms of development **78**(1-2): 113-118.
Rupnik, A., N. F. Lowndes, et al. (2010). "MRN and the race to the break." Chromosoma **119**(2): 115-135.
Saleh-Gohari, N. and T. Helleday (2004). "Conservative homologous recombination preferentially repairs DNA double-strand breaks in the S phase of the cell cycle in human cells." Nucleic acids research **32**(12): 3683-3688.
San Filippo, J., P. Sung, et al. (2008). "Mechanism of eukaryotic homologous recombination." Annu Rev Biochem **77**: 229-257.
Sanders, S. L., M. Portoso, et al. (2004). "Methylation of histone H4 lysine 20 controls recruitment of Crb2 to sites of DNA damage." Cell **119**(5): 603-614.
Sartori, A. A., C. Lukas, et al. (2007). "Human CtIP promotes DNA end resection." Nature **450**(7169): 509-514.
Schupbach, T. and E. Wieschaus (1991). "Female sterile mutations on the second chromosome of Drosophila melanogaster. II. Mutations blocking oogenesis or altering egg morphology." Genetics. **129**(4): 1119-1136.
Sekelsky, J. J., M. H. Brodsky, et al. (2000). "DNA repair in Drosophila: insights from the Drosophila genome sequence." J Cell Biol **150**(2): F31-36.
Sekelsky, J. J., M. H. Brodsky, et al. (2000). "DNA repair in Drosophila: insights from the Drosophila genome sequence." The Journal of cell biology **150**(2): F31-36.
Sekelsky, J. J., K. S. McKim, et al. (1995). "The Drosophila meiotic recombination gene mei-9 encodes a homologue of the yeast excision repair protein Rad1." Genetics **141**(2): 619-627.
Shareef, M. M., C. King, et al. (2001). "Drosophila heterochromatin protein 1 (HP1)/origin recognition complex (ORC) protein is associated with HP1 and ORC and functions in heterochromatin-induced silencing." Mol Biol Cell. **12**(6): 1671-1685.
Shen, X., G. Mizuguchi, et al. (2000). "A chromatin remodelling complex involved in transcription and DNA processing." Nature **406**(6795): 541-544.
Shen, X. T., H. Xiao, et al. (2003). "Modulation of ATP-dependent chromatin-remodeling complexes by inositol polyphosphates." Science **299**(5603): 112-114.
Shimada, K., Y. Oma, et al. (2008). "Ino80 chromatin remodeling complex promotes recovery of stalled replication forks." Current biology : CB **18**(8): 566-575.
Shinohara, A., H. Ogawa, et al. (1992). "Rad51 protein involved in repair and recombination in S. cerevisiae is a RecA-like protein." Cell **69**(3): 457-470.
Shroff, R., A. Arbel-Eden, et al. (2004). "Distribution and dynamics of chromatin modification induced by a defined DNA double-strand break." Curr Biol **14**(19): 1703-1711.
Sibon, O. C. M., A. Laurencon, et al. (1999). "The Drosophila ATM homologue Mei-41 has an essential checkpoint function at the midblastula transition." Current Biology **9**(6): 302-312.
Silva, E., S. Tiong, et al. (2004). "ATM is required for telomere maintenance and chromosome stability during Drosophila development." Curr Biol **14**(15): 1341-1347.

Sinha, M. and C. L. Peterson (2009). "Chromatin dynamics during repair of chromosomal DNA double-strand breaks." Epigenomics **1**(2): 371-385.

Smeenk, G. and H. van Attikum (2013). "The chromatin response to DNA breaks: leaving a mark on genome integrity." Annu Rev Biochem **82**: 55-80.

Sonam Mehrotra, R. Scott Hawley, et al. (2008). "Synapsis, Double-Strand Breaks, and Domains of Crossover Control in Drosophila Females." Recombination and MeiosisGenome Dynamics and Stability **Volume 2**: pp 125-151

Song, Y. H., G. Mirey, et al. (2004). "The Drosophila ATM ortholog, dATM, mediates the response to ionizing radiation and to spontaneous DNA damage during development." Curr Biol **14**(15): 1354-1359.

Soutoglou, E. and T. Misteli (2008). "Activation of the cellular DNA damage response in the absence of DNA lesions." Science **320**(5882): 1507-1510.

Spradling, A. C. (1993). "Developmental genetics of oogenesis." **The Development of Drosophila melanogasterCold Spring Harbor Laboratory Press, Cold Spring Harbor**: 1–70.

Staeva-Vieira, E., S. Yoo, et al. (2003). "An essential role of DmRad51/SpnA in DNA repair and meiotic checkpoint control." Embo J **22**(21): 5863-5874.

Stewart, G. S., B. Wang, et al. (2003). "MDC1 is a mediator of the mammalian DNA damage checkpoint." Nature **421**(6926): 961-966.

Stiff, T., C. Reis, et al. (2005). "Nbs1 is required for ATR-dependent phosphorylation events." Embo Journal **24**(1): 199-208.

Stracker, T. H., C. T. Carson, et al. (2002). "Adenovirus oncoproteins inactivate the Mre11-Rad50-NBS1 DNA repair complex." Nature **418**(6895): 348-352.

Stracker, T. H. and J. H. Petrini (2011). "The MRE11 complex: starting from the ends." Nat Rev Mol Cell Biol **12**(2): 90-103.

Stucki, M. and S. P. Jackson (2004). "MDC1/NFBD1: a key regulator of the DNA damage response in higher eukaryotes." DNA Repair (Amst) **3**(8-9): 953-957.

Sung, P. (1997). "Function of yeast Rad52 protein as a mediator between replication protein A and the Rad51 recombinase." J Biol Chem **272**(45): 28194-28197.

Sung, P. (1997). "Yeast Rad55 and Rad57 proteins form a heterodimer that functions with replication protein a to promote DNA strand exchange by Rad51 recombinase." Genes Dev **11**(9): 1111-1121.

Sung, P. and H. Klein (2006). "Mechanism of homologous recombination: mediators and helicases take on regulatory functions." Nat Rev Mol Cell Biol **7**(10): 739-750.

Sung, P. and D. L. Robberson (1995). "DNA strand exchange mediated by a RAD51-ssDNA nucleoprotein filament with polarity opposite to that of RecA." Cell **82**(3): 453-461.

Symington, L. S. (2002). "Role of RAD52 epistasis group genes in homologous recombination and double-strand break repair." Microbiol Mol Biol Rev **66**(4): 630-670, table of contents.

Taddei, A., G. Van Houwe, et al. (2009). "The functional importance of telomere clustering: global changes in gene expression result from SIR factor dispersion." Genome Res **19**(4): 611-625.

Tanneti, N. S., K. Landy, et al. (2011). "A pathway for synapsis initiation during zygotene in Drosophila oocytes." Current biology : CB **21**(21): 1852-1857.
Tearle, R. G. and C. Nusslein-Volhard (1987). Tubingen mutants and stock list. **66:** 209-269.
Technau, M. and S. Roth (2008). "The Drosophila KASH domain proteins Msp-300 and Klarsicht and the SUN domain protein Klaroid have no essential function during oogenesis." Fly (Austin). **2**(2): 82-91. Epub 2008 Mar 2001.
Trujillo, K. M. and P. Sung (2001). "DNA structure-specific nuclease activities in the Saccharomyces cerevisiae Rad50*Mre11 complex." J Biol Chem **276**(38): 35458-35464.
Trujillo, K. M., S. S. Yuan, et al. (1998). "Nuclease activities in a complex of human recombination and DNA repair factors Rad50, Mre11, and p95." J Biol Chem **273**(34): 21447-21450.
Tsukuda, T., A. B. Fleming, et al. (2005). "Chromatin remodelling at a DNA double-strand break site in Saccharomyces cerevisiae." Nature **438**(7066): 379-383.
Tsukuda, T., Y. C. Lo, et al. (2009). "INO80-dependent chromatin remodeling regulates early and late stages of mitotic homologous recombination." DNA Repair (Amst) **8**(3): 360-369.
Tsuzuki, T., Y. Fujii, et al. (1996). "Targeted disruption of the Rad51 gene leads to lethality in embryonic mice." Proc Natl Acad Sci U S A **93**(13): 6236-6240.
Usui, T., H. Ogawa, et al. (2001). "A DNA damage response pathway controlled by Tel1 and the Mre11 complex." Mol Cell **7**(6): 1255-1266.
Uziel, T., Y. Lerenthal, et al. (2003). "Requirement of the MRN complex for ATM activation by DNA damage." Embo J **22**(20): 5612-5621.
van Attikum, H., O. Fritsch, et al. (2007). "Distinct roles for SWR1 and INO80 chromatin remodeling complexes at chromosomal double-strand breaks." Embo Journal **26**(18): 4113-4125.
van Attikum, H., O. Fritsch, et al. (2004). "Recruitment of the INO80 complex by H2A phosphorylation links ATP-dependent chromatin remodeling with DNA double-strand break repair." Cell **119**(6): 777-788.
van den Bosch, M., R. T. Bree, et al. (2003). "The MRN complex: coordinating and mediating the response to broken chromosomes." EMBO Rep **4**(9): 844-849.
Vincent, J. A., T. J. Kwong, et al. (2008). "ATP-dependent chromatin remodeling shapes the DNA replication landscape." Nat Struct Mol Biol **15**(5): 477-484.
Wang, X. and J. E. Haber (2004). "Role of Saccharomyces single-stranded DNA-binding protein RPA in the strand invasion step of double-strand break repair." PLoS Biol **2**(1): 104-112.
Watanabe, S. and C. L. Peterson (2010). "The INO80 family of chromatin-remodeling enzymes: regulators of histone variant dynamics." Cold Spring Harb Symp Quant Biol **75**: 35-42.
Wei, D. S. and Y. S. Rong (2007). "A genetic screen for DNA double-strand break repair mutations in Drosophila." Genetics **177**(1): 63-77.
Weterings, E. and D. J. Chen (2008). "The endless tale of non-homologous end-joining." Cell Res **18**(1): 114-124.

Williams, G. J., S. P. Lees-Miller, et al. (2010). "Mre11-Rad50-Nbs1 conformations and the control of sensing, signaling, and effector responses at DNA double-strand breaks." DNA Repair (Amst) **9**(12): 1299-1306.

Williams, R. S., G. Moncalian, et al. (2008). "Mre11 dimers coordinate DNA end bridging and nuclease processing in double-strand-break repair." Cell **135**(1): 97-109.

Wu, L. and I. D. Hickson (2003). "The Bloom's syndrome helicase suppresses crossing over during homologous recombination." Nature **426**(6968): 870-874.

Wu, S., Y. Shi, et al. (2007). "A YY1-INO80 complex regulates genomic stability through homologous recombination-based repair." Nat Struct Mol Biol **14**(12): 1165-1172.

Wyatt, H. R., H. Liaw, et al. (2003). "Multiple roles for Saccharomyces cerevisiae histone H2A in telomere position tip effect, Spt phenotypes and double-strand-break repair." Genetics **164**(1): 47-64.

Xiao, Y. and D. T. Weaver (1997). "Conditional gene targeted deletion by Cre recombinase demonstrates the requirement for the double-strand break repair Mre11 protein in murine embryonic stem cells." Nucleic Acids Res **25**(15): 2985-2991.

Xu, X. and D. F. Stern (2003). "NFBD1/KIAA0170 is a chromatin-associated protein involved in DNA damage signaling pathways." J Biol Chem **278**(10): 8795-8803.

Yao, T., L. Song, et al. (2008). "Distinct modes of regulation of the Uch37 deubiquitinating enzyme in the proteasome and in the Ino80 chromatin-remodeling complex." Molecular Cell **31**(6): 909-917.

Yeung, P. L., N. G. Denissova, et al. (2012). "Promyelocytic leukemia nuclear bodies support a late step in DNA double-strand break repair by homologous recombination." J Cell Biochem **113**(5): 1787-1799.

Yildiz, O., H. Kearney, et al. (2004). "Mutational analysis of the Drosophila DNA repair and recombination gene mei-9." Genetics. **167**(1): 263-273.

Yildiz, O., S. Majumder, et al. (2002). "Drosophila MUS312 interacts with the nucleotide excision repair endonuclease MEI-9 to generate meiotic crossovers." Mol Cell **10**(6): 1503-1509.

Yonetani, Y., H. Hochegger, et al. (2005). "Differential and collaborative actions of Rad51 paralog proteins in cellular response to DNA damage." Nucleic Acids Res **33**(14): 4544-4552.

Yonetani, Y., H. Hochegger, et al. (2005). "Differential and collaborative actions of Rad51 paralog proteins in cellular response to DNA damage." Nucleic acids research **33**(14): 4544-4552.

Yoo, S. and B. D. McKee (2005). "Functional analysis of the Drosophila Rad51 gene (spn-A) in repair of DNA damage and meiotic chromosome segregation." DNA Repair (Amst) **4**(2): 231-242.

Youds, J. L. and S. J. Boulton (2011). "The choice in meiosis - defining the factors that influence crossover or non-crossover formation." Journal of Cell Science **124**(4): 501-513.

Zhang, H. Y., D. N. Roberts, et al. (2005). "Genome-wide dynamics of Htz1, a histone H2A variant that poises repressed/basal promoters for activation through histone loss." Cell **123**(2): 219-231.

Zhu, J., S. Petersen, et al. (2001). "Targeted disruption of the Nijmegen breakage syndrome gene NBS1 leads to early embryonic lethality in mice." Curr Biol **11**(2): 105-109.

Zhu, Z., W. H. Chung, et al. (2008). "Sgs1 helicase and two nucleases Dna2 and Exo1 resect DNA double-strand break ends." Cell **134**(6): 981-994.

Zickler, D. and N. Kleckner (1999). "Meiotic chromosomes: integrating structure and function." Annu Rev Genet **33**: 603-754.

Zlatanova, J. and A. Thakar (2008). "H2A.Z: View from the top." Structure **16**(2): 166-179.